

# IEA Annex 41, MOIST-ENG

## Subtask 1 – Modelling Principles and Common Exercises

Final Report

Monika Woloszyn  
Carsten Rode

*Draft – 23<sup>rd</sup> of July 2007*

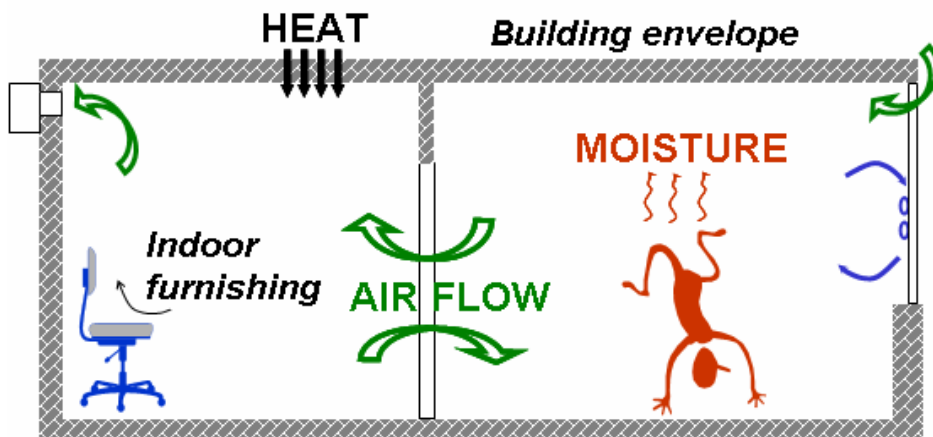


# Table of Contents

IEA Annex 41, MOIST-ENG	1
Subtask 1 – Modelling Principles and Common Exercises	1
1 Introduction	4
1.1 State of the art	4
1.2 Background and scope for the modelling subtask	4
2 Whole building HAM modelling – phenomena and granularity	7
2.1 Heat balances	7
2.1.1 Enthalpy flows	8
2.1.2 Convective heat flow	9
2.1.3 Radiation heat flow	10
2.1.4 Heat flow in materials and structures	12
2.1.5 Interfacial heat flow	13
2.2 Air balances	14
2.2.1 Air flow in rooms	14
2.2.2 Air flow through building envelopes	15
2.3 Moisture Balances	17
2.3.1 Moisture in air	18
2.3.2 Moisture in materials	19
2.3.3 Moisture transport	21
2.3.4 Interfacial moisture flow	23
2.4 Interactions	25
2.4.1 Physical phenomena	25
2.4.2 Interactions between physical elements of the building	28
2.5 Granularity and spatial discretization	28
2.6 Numerical methods for space and time discretization	32
2.6.1 Finite Difference Methods (FDM) / Finite Control Volume methods (FCV)	32
2.6.2 Finite Element Method (FEM)	35
2.6.3 Response factor method	37
3 State of the art of modelling	42
3.1 Analytical solution	42
3.1.1 Solution of CE1A – 0A	44
3.1.2 Solution of CE1A – 0B periodic state:	44
3.1.3 Solution of CE1A – 0B first days:	46
3.2 Simplified models	47
3.2.1 Introduction	47
3.2.2 Classification of simplified models	48
3.2.3 Definition of model parameters	51
3.3 WBHAM models (overview of models from CE)	53
3.3.1 General presentation	53
3.3.2 Introduction of different software	55
3.4 Airflow integration	72
3.4.1 Airflow problems presented within Annex 41	73
3.5 Advances in 3D airflow modelling	77
4 Common Exercises	79
4.0 Common Exercise 0 - BESTEST DIGEST - Whole building energy modelling	80
4.0.1 Introduction	80
4.0.2 Case description	80
4.0.3 Participants	81
4.0.4 Results	82

4.0.5	Discussion	85
4.0.6	Conclusions	86
4.1	Common Exercise 1 – Moisture balance of BESTEST building	87
4.1.1	Introduction	87
4.1.2	BESTEST Case as Common Exercise 1	87
4.1.3	Results	92
4.1.4	Conclusions to draw	96
4.1.5	General Conclusions	98
4.1.6	Appendices	98
4.2	Common Exercise 2 - Small climate chamber test	99
4.2.1	Introduction	99
4.2.2	Experimental and simulation setting	99
4.2.3	Comparison between simulation and experimental results	103
4.2.4	Conclusion	107
4.3	Common Exercise 3 – Test building with two parallel rooms	108
4.3.1	Introduction	108
4.3.2	Experimental investigations	108
4.3.3	Participating institutions and simulation tools	110
4.3.4	Results	110
4.3.5	Conclusion	123
4.4	Common Exercise 4 – Extension of Common Exercise 3	124
4.4.1	Introduction	124
4.4.2	Case description	124
4.4.3	Participants	125
4.4.4	Results and discussion	125
4.4.5	Original ideas	128
4.4.6	Conclusions	131
4.5	Common Exercise X	132
4.5.1	Introduction	132
4.5.2	The case	132
4.5.3	The exercise	133
4.5.4	Methodology applied	137
4.5.5	Reference Solution	140
4.5.6	Solutions introduced	147
4.5.7	Conclusions	149
5	Some indicators for Whole Building HAM Modelling	150
6	Challenges for the future	152
7	Conclusion and Perspectives	154
	References	155
	Addenda – digital edition	161

# 1 Introduction

Indoor air humidity is an important factor influencing air quality, energy consumption of buildings and the durability of building materials. Indoor air moisture depends on several factors, such as moisture sources (human presence and activity, equipment), airflow, sorption from/to solid materials and possible condensation. As all these phenomena are strongly interdependent, numerical predictions of indoor air humidity need to be integrated into combined heat-airflow simulation tools. Subtask 1 has set out to advance the development in modelling the integral heat, air and moisture transfer processes that take place in “whole buildings”.

## 1.1 State of the art

The past few decades have seen the development and professional use of tools which, for some of the processes or some of the building elements, describe their building physical conditions.

For instance, fairly comprehensive tools for transient building energy simulation have been well established for more than a decade. A list of such tools can be seen in [http://www.eere.doe.gov/buildings/tools\\_directory](http://www.eere.doe.gov/buildings/tools_directory). Such tools comprise the whole building with a granularity going from the suite of rooms that make up the building down to the individual building materials and individual parts and controls of the heating, ventilation and air-conditioning system. However, the building energy simulation tools are relatively poor tools to describe the moisture transfer processes in buildings.

Air flow simulation tools at building level, e.g. COMIS (Lawrence Berkeley National Laboratory, 2007), CONTAM (National Institute of Standards and Technology, 2007), or at room level, e.g. CFD codes like Fluent (Fluent 2007), STAR-CD (CD-adapco, 2007), make good descriptions of air exchange between the zones of a building and the outer environment. Some of them deal with airborne moisture transport, and even take into account moisture impact on the airflow. They also represent the heat transfer in the air and in the envelope. However most of them do not take into account the moisture flow between the air and porous surfaces.

Detailed, transient tools have been developed (e.g. in the era around IEA Annex 24 - Hens, 2002) for the combined heat, air and moisture transfer (HAM) within individual building components. The results of calculations with the building envelope HAM-tools may however be very dependent on the assumptions made about for instance the climatic boundary conditions. Many HAM-tools for building envelopes have fairly good procedures to represent the outdoor environmental exposures, e.g. from weather data files, but the indoor environment would often have to be assumed and specified by the user. However, it should also be realized that the collection of building elements themselves form one of the most important factors to determine the indoor climate, and thus there is a mutual link between the envelope and room conditions.

For building envelopes, detailed tools exist for the multidimensional flow of heat, as for instance around thermal bridges. In some cases, models also exist for predicting multidimensional air or moisture flows in envelope constructions (CHAMPS from Building Energy and Environmental Systems Laboratory at Syracuse University, 2007 and WUFI from Fraunhofer Institut für Bauphysik, 2007).

Thus, there has been a motivation to combine the capabilities of earlier tools in order to make it possible to describe all relevant hygrothermal processes in a composite building, i.e. to bring a holistic perspective to building physics modelling. This has been the outset ambition for Subtask 1 of IEA Annex 41.

## 1.2 Background and scope for the modelling subtask

Modelling of different physical aspects of buildings (Heat, Air and Moisture) has been a key element of Annex 41, involving most of the participants. A very large number of coupled phenomena were in the scope of the Annex. The physical processes and their state

variables (temperature, air pressure and moisture content) have immense influences on one another. Some examples:

- The air exchange of a building has an important effect on the energy consumption for thermally conditioning the building
- Air flow through building envelopes tremendously affects the moisture conditions
- Moisture conditions are strongly influenced by the temperature
- Condensation or evaporation of moisture involves a significant conversion of energy
- Thermal conditions within and around buildings incite air flow by stack effect

Of course such whole building models should take into account location and orientation of the building (climatic zone), various heating, ventilating and air conditioning systems, air in- or exfiltration, user behaviour (number of people, activities, moisture & heat production, window ventilation, etc.) and type of room (bathroom, living room, office, etc.). Management of the overall physical processes for the whole is a matter of not only being able to describe the conditions in the different building elements, but also to master the interfacial transfers and balances.

Therefore the initial objective of Subtask 1 - Modelling was to encourage the development and testing of new models that:

- Integrate several physical aspects of buildings (Heat, Air and Moisture).
- Operate on various levels of buildings: from porous materials, over composite constructions to whole buildings with their furnishing, systems and users
- Consider as well indoor as outdoor climatic conditions
- May adopt 1-, 2- and 3-dimensional aspects, or combinations, as appropriate

Objectives are met by theoretical analysis, computer model development, application of engineering tools (from MATLAB to CFD), Benchmarking and Common Exercises. Another important focus was put on parameter analysis and making considerations about which details are important (and which not).

However, it has not been the intention that the subtask and Annex per se should be developing a unique integral tool. The intention was that the Annex by its common authority should stimulate and be a concerting forum for the development among individual researchers of tools which would take as many of the integral aspects into account as possible. The developments could take place by making entirely new models and tools, or by extension of already existing tools, as for instance:

- Extending the existing building simulation tools (to account better for processes linked with the envelope), e.g. Rode & Grau, 2003.
- Extending the building component simulation tools, e.g. Holm et al., 2003
- A combination of both building simulation and building component simulation tools, e.g. Koronthalyova et al., 2004.

It is a long road to the full-fledged hygrothermal model for whole buildings, so it is natural that the path is taken in smaller steps. The ambition of the Subtask has been to always encourage researchers to take even such small steps, as long as they contributed to the progress of development. In practice, the work within Subtask 1 has been organised in two parts:

- common exercises, where all the willing participants simulated the same case, and the results were then compared.
- so-called "free papers", presenting the most recent developments of whole building HAM modelling.

It was a difficult task to gather the common experience from the four year project. The final structure of the present report can be divided into three main parts:

- general introduction on HAM physics and modelling (section 2)
- advances in the HAM modelling provided by contributors to subtask 1 (section3)
- reports from common exercises 4)

It is also impossible to talk about HAM modelling without experimental data for inputs and validation (scope of subtask 2); boundary conditions (subtask 3) and relevant applications (subtask 4). The present report is then strongly related to other subtasks reports of Annex 41.

## 2 Whole building HAM modelling – phenomena and granularity

In order to predict indoor environment and building energy consumption important heat and mass flows must be described. Mass flows concern air as a whole as well as some of its specific components, water vapour being one of them. For several applications water vapour should be treated separately. Indeed it is the unique ambient air component that can condensate at usual conditions, involving important latent energy. Vapour concentration in the air can also vary in some important proportions.

Water vapour balance should therefore include both, vapour and liquid forms, main phenomena being vapour sources, transport by the air, diffusion and adsorption in solids. Solid form of water (ice) may also appear in buildings causing mechanical damages.

It should also be stated that working at whole building level we can not go too deeply into the detail of each component. For example envelope parts are in general porous media with a complex structure. If the following we'll be using only macroscopic properties, such as apparent conduction, apparent density, which are in fact values averaged over a representative elementary volume, including both the solid matrix and the porous network.

The aim of this Chapter 2 is to introduce some principles of coupled Heat, Air and Moisture modelling in buildings without forming a comprehensive textbook on heat, air and mass transfers in buildings. It should give a general overview of physical phenomena, their interactions and main questions relevant for building modelling. It should help in understanding more in detail Chapters 3 and 4 where the work developed within the Annex is presented.

This chapter is structured in six sections. The first three present three conservation equations and main physical phenomena relevant for HAM modelling, namely heat, air and moisture. Then main interactions are described. Section five discusses issues related to the granularity of the description of the system and finally the most used numerical methods are introduced.

### 2.1 Heat balances

Energy behaviour of a building can be assessed by analysing energy balances from thermodynamics, taking into account the impact of thermal and mechanical energy.

Energy conservation equation in a very general control volume can be written then as the rate of thermal and mechanical energy that enters the volume ( $\dot{E}_{in}$  in [W]) minus the rate of thermal and mechanical energy that leaves the control volume ( $\dot{E}_{out}$  in [W]) plus the rate of thermal and mechanical energy generated in control volume ( $\dot{E}_{generated}$  in [W]) that must equal the rate of increase in the amount of energy stored in the control volume ( $E_{stored}$  in [J]):

$$\frac{dE_{stored}}{dt} = \dot{E}_{in} - \dot{E}_{out} + \dot{E}_{generated} \quad (2.1.1)$$

In most of the building applications kinetic and potential energy contributions can be neglected. Variation of energy of the control volume is then proportional to temperature variations ( $T$  in K), density ( $\rho$  in  $[\text{kg}\cdot\text{m}^{-3}]$ ) and specific heat ( $c$  in  $[\text{J}\cdot\text{kg}^{-1}\cdot\text{m}^{-3}]$ ) of the material composing the control volume [ $V$  in  $\text{m}^3$ ]. (2.1.1)

$$\frac{dE_{stored}}{dt} = c\rho V \frac{dT}{dt} \quad (2.1.2)$$

The rate of energy stored in the control volume is then equal to internal energy variations, proportional to the specific heat at constant volume ( $c_v$ ) for gases. However in buildings pressure changes are very small compare to total atmospheric pressure. Alternatively rate of energy stored in the control volume can be assumed equal to internal enthalpy variations, proportional to specific heat at constant pressure ( $c_p$ ) for gases. This last formulation is the most used in building modelling. Main advantage is that the numerical formulation of the problem is straightforward. Indeed, thermodynamics defines only rates of energy or enthalpy variations, and not the precise values. We have:

$$\text{- change in specific internal energy } u \text{ (J.kg}^{-1}\text{): } du = c_v dT \quad (2.1.3)$$

$$\text{- change in specific enthalpy } h \text{ (J.kg}^{-1}\text{): } dh = c_p dT \quad (2.1.4)$$

A reference state must be then chosen to start computations. As explained below, the energy fluxes associated with mass transfer are in general expressed as enthalpy fluxes. Then in the energy balance we have the enthalpy flow and enthalpy or internal energy for storage term as shown in Table 2.1.1.

Formulation	Energy storage	Mass flow	Required reference state
All enthalpy	Internal energy	Enthalpy	Energy and Enthalpy
Mixed	Enthalpy	Enthalpy	Enthalpy

Table 2.1.1. Energy and Enthalpy formulations for Energy balance

Both formulations are correct. However in case of a mixed formulation a great attention should be driven to the choice of reference states. They must respect thermodynamic relations, such as enthalpy definition and Mayer's relation ( $c_p - c_v = r$ ,  $r$  being perfect gas constant). The reference value of nil enthalpy is typically taken at 0°C for dry air and liquid water at 0°C for water vapour. Specific enthalpies read then:

$$\text{- for dry air : } h_{dry\_air} = c_{p,dry\_air} T[in \text{ } ^\circ C] \quad (2.1.5)$$

$$\text{- for water vapour : } h_{water\_vapour} = L_{v,0^\circ C} + c_{p,water\_vapour} T[in \text{ } ^\circ C] \quad (2.1.6)$$

where  $L_{v,0^\circ C}$  is the latent heat of vaporisation of  $H_2O$  at 0°C.

In the equation (2.1.1) the energy generation is in fact conversion of some other form of energy (chemical, electrical, etc.) into thermal energy. Some typical examples are exothermic chemical reaction in freshly erected concrete walls, human metabolism or heat generation in electrical appliances.

In buildings the rates of energy coming in or leaving the system are heat fluxes and energy fluxes due to mass flows.

Basically three heat transfer modes can be distinguished to describe heat transfers; they are all due to a temperature gradient. When a temperature gradient exists in a stationary medium, such as solid or immobile fluid, conduction heat transfer occurs. Convection refers to heat transfer between a solid surface and a mobile fluid and thermal radiation involves electromagnetic waves exchange between two surfaces.

### 2.1.1 Enthalpy flows

As some control volumes in buildings are open systems, there is a mass flow transporting energy into and out of the system. Mass flow is typically air and/or water in vapour or liquid state. Room volume with air flowing in and out is a perfect illustration. Mechanical work associated with a mass flow is done by pressure forces moving the fluid through system boundaries. For a unit mass the amount of work is equivalent to the product of pressure ( $p$ , [Pa]) and specific volume ( $v$ , [ $m^3 kg^{-1}$ ]). Therefore in practice specific enthalpy  $h$  replaces the specific internal energy  $u$  and work according to enthalpy definition:

$$h = u + \rho v \quad (2.1.7)$$

Energy fluxes due to mass flows are often referred to as enthalpy flows or fluxes and read:

$$\dot{E} = h \cdot \dot{m} \quad (2.1.8)$$

Where  $\dot{m}$  is mass flux in [kg/s] and  $h$  specific enthalpy given by (2.1.5) and (2.1.6).

### 2.1.2 Convective heat flow

Convection refers to heat transfer between a solid surface and a mobile fluid. The convective heat transfer processes for air are relevant in building applications as concerns conditions in the outdoor ambience, heat flow in rooms, as well as heat flow in cavities in building elements or even in pores in building materials.

Convective heat flow is composed of two physical processes: a dominant part, called advection, is due to bulk or gross motion of fluid particles and a complementary part is transferred by conduction. For convection, the Nusselt number ( $Nu$ ) indicates in dimensionless form the factor by which the heat flow is enhanced due to convection compared to a situation with conduction in still air.

$$Nu = \frac{h_c L}{\lambda} \quad (2.1.9)$$

Where  $h_c$  is the convection heat transfer coefficient  $W/(m^2K)$ ,  $\lambda$  is the thermal conductivity,  $W/(m \cdot K)$ , and  $L$  is a characteristic length, m.

The convection heat transfer coefficient has traditionally been determined empirically, based on some characteristic situations. It is highly dependent on air flow conditions whether caused by forced convection (some external force driving fluid motion) or natural convection. In natural convection the driving force is buoyancy induced by variations of air density in a volume. Density of air is temperature and moisture content dependent, however most simple correlations in the literature take into account temperature dependency only.

For buildings and air some simplified correlations for average values of convection coefficient for typical surfaces can be found in the literature. It is common usage to consider that indoors heat transfer is mainly due to natural convection and therefore  $h_c$  is temperature dependent, and outdoor the heat transfer is mainly due to forced convection and therefore  $h_c$  is wind velocity dependent for outdoors. For example equation (2.1.6) gives the outdoor  $h_c$  following Mac Adams (1954) and Table 2.1.2 gives some indications of the indoor walls.

$$h_c = 5.7 + 3.8V \quad (2.1.10)$$

where  $V$  is air velocity in [m/s].

Wall geometry	convection heat transfer coefficient for laminar flow [ $W \cdot m^{-2} \cdot K^{-1}$ ]	Characteristic dimension [m]
Vertical wall	$h_c = 1.78 \cdot  T_{surface} - T_{fluid} ^{0.25}$	
Horizontal wall heating upwards	$h_c = 1.32 \cdot \frac{ T_{surface} - T_{fluid} ^{0.25}}{L}$	L : wall width
Horizontal wall heating downwards	$h_c = 0.66 \cdot \frac{ T_{surface} - T_{fluid} ^{0.25}}{L}$	L : wall width

Table 2.1.2. Values of convection heat transfer coefficient for natural convection in air (Eygulent, 1997)

In the correlations from Table 2.1.2 both temperature surface and fluid values are in general unknown in building modelling. Use of such relations requires solving of systems of non-linear algebraic equations, which may slow down the convergence process and increase computational time. Therefore in many practical applications convection heat transfer coefficient is directly given as a constant value.

For outdoor convection, numerical implementation of equation (2.1.2) is straightforward, because outdoor air velocity (wind) is in general given in the weather file. The possible difficulty lies in the estimation of local wind velocities close to the building surfaces.

Once the convective heat transfer coefficient known, the density of the convection heat flow is calculated as:

$$\varphi_c = h_c (T_{surface} - T_{fluid}) \quad (2.1.11)$$

### 2.1.3 Radiation heat flow

Thermal radiation heat flow involves electromagnetic waves exchange between two surfaces, and requires no matter. Thermal radiation emitted by a surface is characterised by its spectral distribution (distribution over a large range of wavelengths) and directionality (spatial distribution). Both depend on surface temperature and properties.

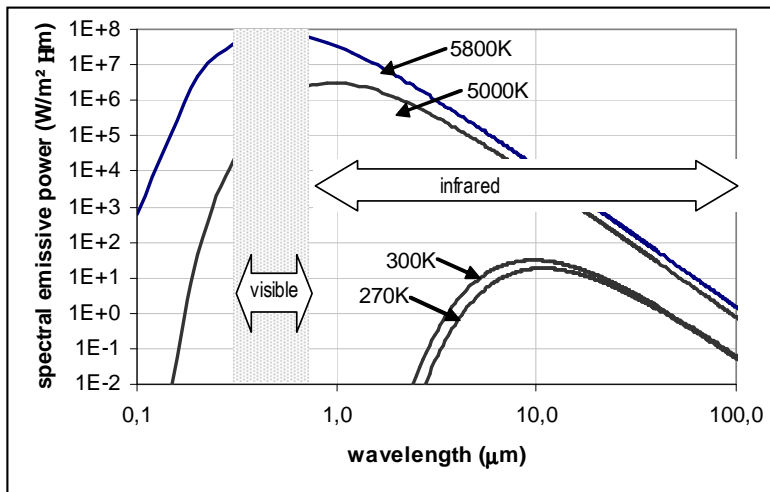


Figure 2.1.1. Spectral blackbody emissive power (Planck's law)

Ideal model for radiation is called "blackbody".

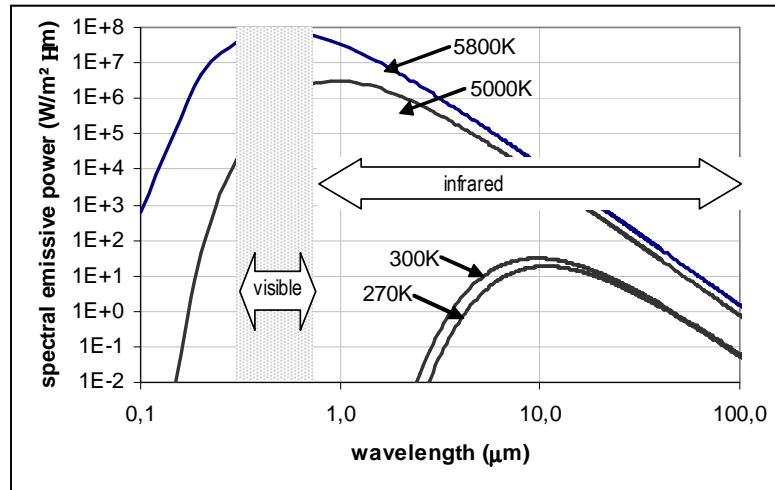


Figure 2.1.1 shows the spectral blackbody emissive power computed by Planck's law. In buildings application two wavelengths are of importance:

- so-called Short-Wave radiation, mostly concentrated in visible spectra, coming from very hot sources, in usual buildings it is exclusively solar radiation,
- so-called Long-Wave radiation, mostly concentrated in infrared spectra, coming from all surfaces at ambient temperature,

For whole building modelling surfaces are in general modelled as gray bodies, where surface properties do not depend on wavelength and radiation is diffuse.

Total radiation emitted by a gray surface is given by Stefan-Boltzmann law

$$E = \varepsilon \cdot \sigma \cdot T^4 \quad (2.1.12)$$

Where E is emissive power [W/m<sup>2</sup>],  $\varepsilon$  surface emissivity [-],  $\sigma$  Stefan-Boltzmann constant and T is surface temperature in [K]

The total irradiation coming on a semi-transparent medium can be either reflected, absorbed or transmitted, depending on surface reflectivity  $\alpha$ , absorptivity  $\rho$ , and transmissivity  $\tau$ . Energy conservation yields into:

$$\alpha + \rho + \tau = 1 \quad (2.1.13)$$

And Kirchoff's law for gray surfaces gives:

$$\alpha = \varepsilon \quad (2.1.14)$$

As real surfaces do not always behave as perfect gray bodies, sometimes a differentiation is made for short-wave and long-wave radiative properties.

Modelling radiation heat transfer in buildings is then mainly composed of modelling solar radiation coming on building surfaces and modelling infrared radiation exchanges between surfaces at ambient temperature.

The solar radiation is mainly short-wave radiation and is composed of beam and diffuse radiation. Outdoor solar radiation is given in weather file as boundary condition. Then taking into account building geometry, solar shadings and relative position of sun, solar irradiation on each building surface can be computed. Solar transmission through windows can also be

assessed, using transmittance properties of windows. The calculations can go from very simple ratio, to detailed computations of radiative exchanges inside the double-glazing. The radiation incoming inside the building must be integrated in the energy balance of the building. Different models are available. The simplest hypothesis is to assume that the whole transmitted sun flux is absorbed by the floor. It can also be distributed on different walls in the room, and some sophisticated tools are able to compute the detailed position of sun patch on the floor or wall.

Infrared radiation exchanges are relevant for both indoor and outdoor surfaces. The net radiative exchange between surfaces  $i$  and  $j$  is given by the following equation:

$$\phi_{ij} = S_i F_{ij} \sigma (T_i^4 - T_j^4) \quad (2.1.15)$$

Where  $F_{ij}$  is the view factor, defined as the fraction of radiation leaving  $i$  intercepted by  $j$ . View factor depends on shape and relative position of both surfaces. Indoor exchanges take place between indoor building surfaces, and outdoor exchanges between outdoor building surfaces and neighbourhood. In general ground and surroundings are assumed to be at the outdoor air temperature. Often the concept of "sky temperature" is introduced, to take into account long-wave radiation heat loss from the outdoor surfaces.

Several practical difficulties must be solved to implement radiation heat transfers in a whole building model. Radiation fluxes are proportional to temperatures power four, and therefore introduce non linear terms in heat balance equations. Moreover computations of view factors are rather time-consuming and need information not only on the size of each surface, but also on their topology – the relative position of all the surfaces.

Therefore in many practical applications the long wave radiation exchange is often linearised, and equation (2.1.15) is replaced by:

$$\phi_{ij} = S_i h_r (T_i - T_j) \quad (2.1.16)$$

Where  $h_r$  is radiation heat transfer coefficient in  $[W/m^2K]$ . Often the surface temperature  $T_j$  is replaced by the temperature of the ambient air. Then the radiation flux has a similar expression to convection flux, which facilitates numerical computations. Sometimes one global surface coefficient, including convection and radiation, is used.

#### 2.1.4 Heat flow in materials and structures

Heat transfer in solids is dominated by conduction, which is energy transport by molecular activity without any bulk motion. Energy conservation applied to a control volume in homogenous media gives the heat equation:

$$\rho \cdot c \cdot \frac{\partial T}{\partial t} = \text{div}(\lambda \cdot \text{grad}T) + \dot{q} \quad (2.1.17)$$

Where  $\rho$  is material density  $[kg/m^3]$ ,  $c$  specific heat capacity  $[J/kg.K]$ , and  $\dot{q}$  energy generation rate per unit volume  $[W/m^3]$

The thermal conductivity  $\lambda$   $[W/mK]$  is the transport property determining the rate of conduction heat transfer ( $\phi$  in  $W/m^2$ ) in still media:

$$\phi = -\lambda \cdot \text{grad}T \quad (2.1.18)$$

For constant and isotropic conductivity and no energy generation, equation (2.1.12) gives :

$$\frac{\partial T}{\partial t} = a \cdot \Delta T \quad (2.1.19)$$

Where  $a = \lambda / \rho c$  is the thermal diffusivity [ $m^2/s$ ]. It measures the ability of a material to conduct thermal energy relative to its ability to store thermal energy.  $\Delta$  is laplace operator, representing second space derivative. In cartesian coordinates reads

$$\Delta = \frac{\partial^2}{\partial x^2} + \frac{\partial^2}{\partial y^2} + \frac{\partial^2}{\partial z^2} .$$

Heat equation is very common partial differential equation, and many solving methods exist in the literature. For some simple cases (1-dimensionnal transfer, steady state) analytical solutions can be found. For more complex cases numerical computations using diverse techniques such as finite differences, control volumes, response factors or finite elements are helpful. As long as conductivity can be assumed constant, the equations are linear with temperature and the computations are straightforward. Main difficulties for building problems are coming from coupling the heat equation with mass transfers in porous media.

### 2.1.5 Interfacial heat flow

Interfacial heat flow is the flow at the boundary between two different elements. For buildings there are two main types of boundaries:

- a. between control volumes of similar type (interface between two materials in a multilayer wall)
- b. between control volumes of different type (interface between air and material)

In general the contact resistance between two control volumes of the similar type can be neglected, and a-type boundary for heat transfer without matter displacement can be written as continuity of temperature fields and heat fluxes between materials  $i$  and  $j$ :

$$-\lambda_i \frac{\partial T_i}{\partial n} \Big|_{surface} = -\lambda_j \frac{\partial T_j}{\partial n} \Big|_{surface} \quad (2.1.20)$$

$$T_i (surface) = T_j (surface)$$

For b-type boundary, three types of conditions are in general described:

1. Constant temperature  $T(surface, t) = T_s$
2. Constant surface flux  $-\lambda \frac{\partial T}{\partial n} \Big|_{surface} = \varphi_s$ , for adiabatic conditions this flux is nil.
3. Linear surface flux  $-\lambda \frac{\partial T}{\partial n} \Big|_{surface} = h_c (T_{fluid} - T_{surface})$

In practice the interfacial flows at b-type boundary may be a combination of different kinds of boundary conditions, as shown in Figure 2.1.2 .

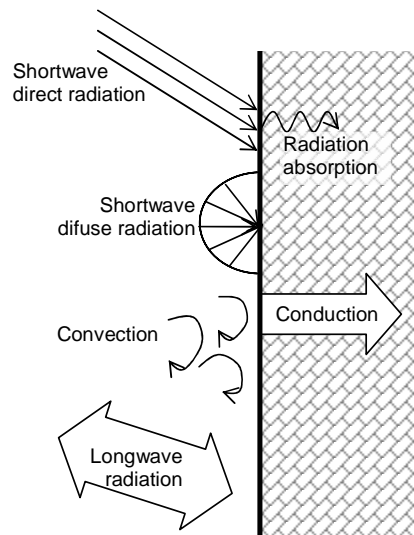


Figure 2.1.2: Wall with different heat fluxes

The correct treatment of the interfacial flows is a key point in successful modelling. Indeed, at the interfaces all heat transfer modes exist, and energy conservation yields into non-linear equations.

## 2.2 Air balances

Air flows in buildings involve significant transfers of energy and moisture. They can be assessed by analysing air mass and momentum conservation equations. General expression of mass balance, called also “continuity equation” reads:

$$\frac{\partial \rho}{\partial t} = -\text{div}(\rho \vec{v}) \quad (2.2.1)$$

Where  $\vec{v}$  is the velocity vector in (m/s) and  $\rho$  density ( $\text{kg/m}^3$ ). Mass conservation equation applied to a control volume can be also written as :

$$\frac{dm_{air}}{dt} = \dot{m}_{air,in} - \dot{m}_{air,out} \quad (2.2.2)$$

Where  $m$  is the mass in (kg). The conservation equation has the same form for both types of control volumes: situated in the air zone or in the envelope.

The momentum conservation equations, called also motion equation (derived from Newton’s second law) assumes that the variation of the momentum of a fluid cell is the sum of all forces applied on this fluid cell. The summation of forces include pressure forces, shear forces related to the viscosity and other forces, such as gravity.

The airflows are due to pressure differences driven by wind pressures, buoyancy forces or some mechanical devices such as fans. Buoyancy forces depend on the variations of air density, which is temperature and moisture content dependent.

General principles of airflow modelling are presented in the following. Some more details are given in “Airflow integration chapter”.

### 2.2.1 Air flow in rooms

Intra-room air flows are due to combined effect of buoyancy forces in non isothermal conditions (natural convection) and additional inter-zone pressure differences induced by

wind, fans, or global stack effect. Modelling of intra-room flows requires using an important number of control volumes for each room, and solving for energy, mass and momentum conservation equations in each control volume. This set of partial differential equations is known as Navier-Stokes equations. In general some additional considerations about turbulence influence and boundary layers must be added. Two powerful techniques exist to solve this problem: Computational Fluids Dynamics (CFD) and zonal models. Both are very specific and will not be further discussed here. Interested reader may refer to numerous positions in the literature, such as Versteeg and Malalasekera (1995) for fluid mechanics. Some specific issues on 3D modelling of moist air flows are discussed in chapter 3.

At whole building level the usual approach is to assume a perfectly mixed air zone. Then only inter-zone airflows should be represented. This is often done using "pressure network" modelling. In general one zone represents one room or a set of rooms with similar behaviour.

In pressure network model, one zone is assumed to have uniform characteristics. Each physical quantity of interest is then described by a node: air pressure, temperature, humidity and/or contaminant concentration nodes. The links between nodes represent the flows of modelled physical quantity. For air flows at each node the mass conservation equation (2.3.2) is solved. As in whole buildings airflow dynamics is very fast compare to energy and moisture balances, equation (2.3.2) is often solved in steady-state:

$$\dot{m}_{air,in} = \dot{m}_{air,out} \quad (2.2.3)$$

Usual ways of computing the air flows are given below.

## 2.2.2 Air flow through building envelopes

Inter-zone air flows are in fact flows through building envelope and interior partitions; they are due to pressure differences across openings. The openings may be voluntary, such as vents, ducts, or involuntary such as cracks. In some particular cases where walls are very air-permeable the air may flow through the entire wall.

The pressure difference can be intentionally imposed using ventilators or may occur due to wind pressure or buoyancy effect. For pressure-network type models three type of openings can be distinguished: small openings, large openings and eventually air flow through the mass of the wall. They are presented below.

### 2.2.2.1 Air flow through small openings

In pressure network "small opening" means that the air can flow only one-way, depending on pressure difference ( $P_j$  and  $P_i$ , in Pa, air pressures on both sides of the opening). The mass air flow can be written as:

$$\dot{m}_{air} = C_s \rho (P_i - P_j)^n \quad (2.2.4)$$

The flow coefficient  $C_s$  represents pressure drop through the opening, it depends on the size and type of opening, but also on the air velocity. The exponent  $n$  represents laminar or turbulent flow and in general equals 0.5 to 1.

Air pressure  $P$  corresponds to the pressure of the air zone at the location of the opening. In general hydrostatic distribution is supposed, allowing taking into account buoyancy driven natural ventilation.

$$P_i(z) = P_{i,reference\ level} - \rho(z) \cdot g \cdot z + C_D \frac{\rho \cdot v^2}{2} \quad (2.2.5)$$

Where  $g$  is gravity ( $m/s^2$ ),  $z$  the height above the reference level (m) and  $\rho$  the density of air in the zone ( $kg/m^3$ ). The last term describes wind dynamic pressure, with wind velocity  $v$  (m/s) and wind pressure coefficient  $C_D$ . For indoor air zones wind velocity is nil. In most of the models the density in each zone is assumed uniform, but some pressure-network based

tools (for example COMIS) allow using a temperature gradient in the room air, and therefore air density gradient.

We should also notice that in this type of models the phenomena on the air path are not represented. There is no impact of flow on local temperature or humidity distribution in the neighbourhood of the opening.

### 2.2.2.2 Air flow through large openings

In pressure network “large opening” means that the air can flow both ways inside the same opening, as shown in Figure 2.2.1. Typically they represent open doors and windows.

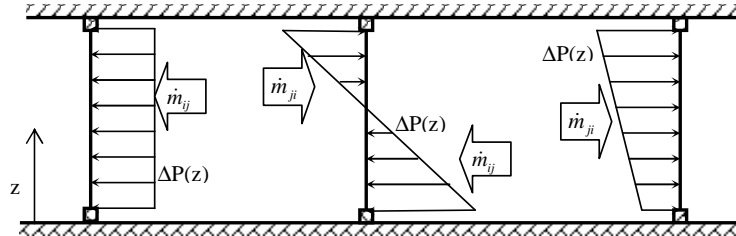


Figure 2.2.1. Different configurations of the airflow through large opening

Supposing that the pressure distribution is hydrostatic in both zones *i* and *j*, horizontal pressure gradient  $\Delta P(z)$  can be estimated:

$$\Delta P(z) = P_{i,reference\ level} - \rho_i(z) \cdot g \cdot z - P_{j,reference\ level} + \rho_j(z) \cdot g \cdot z \quad (2.2.6)$$

The most popular models representing mass and heat flow through an open door are based on Bernoulli equation and give the following expression for air velocity (*u*, m/s) in the aperture:

$$u(z) = \Delta P(z) \sqrt{\frac{2}{\rho |\Delta P(z)|}} \quad (2.2.7)$$

Where  $\Delta P(z)$  is the difference of total pressures on both sides of the opening, far enough from the opening to assume that the air velocity is equal to 0.  $\rho$  is the density of the transported air. The mass flow is then easy to obtain using the following integration:

$$\dot{m}_{ij} = C_s L \int_a^b u(z) \rho(z) dz \quad (2.2.8)$$

The integration bounds *a* and *b* correspond to the physical limits of the airflow and are either 0, *H* (total height of the opening) or *z<sub>n</sub>* (position of the neutral axis). This last value is the solution of the following equation:

$$\Delta P(z_n) = 0 \quad (2.2.9)$$

The effects of viscosity and flow contraction are taken into account in equation (2.2.8) using experimentally found flow coefficient *C<sub>s</sub>*.

In some cases analytical integration of equation (2.2.8) is possible, but several configurations have to be treated. In general this type of equations introduces non-linearities

with an ill-conditioned jacobian matrix. Often some special numerical methods must be used to avoid divergence problems.

Similar approach can be used to compute air flow through large horizontal openings (staircases) and for open windows. When one of the zones is the exterior climate, wind effect must be somehow represented.

### 2.2.2.3 Air flow through the envelope volume

Some air flows through the envelope may have a significant impact on the local thermo-hygric conditions within the envelope. These are namely flows through the entire wall surface for very air-permeable walls, local flow through cracks, or airflow through ventilated cavities in building envelope. From pressure network point of view the airflow can be computed using equation 2.3.4, adapted flow coefficient and eventually hydrostatic pressure distribution. However in coupled heat-air-moisture modelling local interactions between the three quantities can not be neglected. Some issues related to that topic were studied within the Annex 41 and are presented in chapter 3.

### 2.2.2.4 On computing airflows in HAM modelling

The equations in this section on air balances use gas pressure, density and mass flow.. Crucial question is what gas should be represented? Dry air? Humid air?

For Air only or Heat-Air modelling both choices are strictly equivalent. But for Heat-Air-Moisture problems the question is not trivial.

Humidity is one of the components of the ambient air and H<sub>2</sub>O participates in the total air pressure. Air density depends on temperature and relative humidity. Therefore the driving forces are the total pressure forces (total pressure is the sum of partial pressures of dry air and water vapour, see Equation (2.3.3)). It means that in Equations (2.2.4), (2.3.7) and (2.2.6) values of pressure and density refer to moist air. In balance Equations (2.2.2) and (2.2.8) mass flows, and therefore air density refer to dry air.

## 2.3 Moisture Balances

The equation for conservation of mass ( $m$ , kg) of water within a volume element can be written in a general form as:

$$\frac{dm_{moisture}}{dt} = \sum_{in} G_{vapour\ diffusion} + \sum_{in} G_{liquid} + \sum_{in} G_{convection} - \left( \sum_{out} G_{vapour\ diffusion} + \sum_{out} G_{liquid} + \sum_{out} G_{convection} \right) + \dot{m}_{source} \quad (2.3.1)$$

$$m_{moisture} = m_{liquid\ water} + m_{water\ vapour}$$

where

$m$  is mass of moisture, kg

$G$  is moisture flow over the surfaces of the volume element, kg/s

$m_{liquid\ water}$  in the second term of Equation (2.3.1) pertains to moisture in any kind of condensed of absorbed phase. For moisture in a porous material, the mass of water vapour in the pore is most likely to be negligible compared to mass in the absorbed or condensed phases. The opposite is the case for cavities in building assemblies and spaces in buildings, where the mass of vapour will most likely dominate over the mass of condensed moisture.

As well, there may be several many ways to interpret the terms on the right-hand side of the first term of Equation (2.3.1), depending on the size and type of the control volume. The control volume could be a part of an air zone in a building, or it could be a delimited part of a building material. The size of air spaces could vary considerably from being a whole room (or an collection of several rooms) in a multi-zone model of a building, down to just a few mm<sup>3</sup> or

cm<sup>3</sup> in CFD models. Likewise, for a building assembly, the volume may comprise a whole wall, or it could go down to the pore scale of a material. The most common modelling approaches for both air and material are described in the following.

### 2.3.1 Moisture in air

In air, the equation for conservation of moisture can be written in volume intensive form as (neglecting liquid flows):

$$\rho_{air} \frac{dx}{dt} = -\text{div}(g_{\text{vapour diffusion}} + g_{\text{convection}}) + \dot{\mu}_{\text{source}} \quad (2.3.2)$$

where

$\rho_{air}$  is dry density of air

$x$  is the humidity ratio, kg/kg

$g$  are moisture fluxes, kg/(m<sup>2</sup>s)

$\dot{\mu}$  is a volumetric moisture production rate kg/(m<sup>3</sup>s)

Water in the air is mainly present in vapour state. In some special situations it may occur as small liquid droplets: for example in humidifiers, or after a hot shower in a cold bathroom.

The moisture content of air can be indicated by the humidity ratio  $x$  (mass of water per mass of dry air, kg/kg), partial vapour pressure  $p$  (Pa), vapour concentration  $v$  (kg/m<sup>3</sup>), or dew point temperature (and other units...).

Atmospheric air pretty much follows the law of perfect gases, so this can be used to convert between the different units to describe moisture content of air. The water vapour molecule (H<sub>2</sub>O) has molecular mass  $M_{H_2O} = 0.01802$  kg/mole. Dry air mainly comprises of Nitrogen (N<sub>2</sub>, ~78 vol-%), Oxygen (O<sub>2</sub>, 21%), Argon (Ar, 0.9%) and carbon dioxide (CO<sub>2</sub>, 0.03%), which gives it a molecular mass of  $M_{\text{atmospheric air}} = 0.02896$  kg/mole.

Dalton's law tells us that the atmospheric pressure ( $P$ , Pa) is the sum of partial pressures of the constituents of the atmosphere – or in our representation, the sum of the partial pressures of water vapour and dry air:

$$P = p_{\text{water vapour}} + p_{\text{dry air}} \quad (2.3.3)$$

Incidentally this gives the following relations:

$$x = 0.622 \frac{p_{\text{water vapour}}}{P - p_{\text{water vapour}}} \quad (2.3.4)$$

$$v = \frac{p_{\text{water vapour}}}{R_{H_2O} \cdot T} \quad (2.3.5)$$

where

$R_{H_2O}$  is the gas constant for water vapour = 461.5 J/(kg·K)

$T$  is absolute temperature, K

The maximum amount of vapour in air is very strongly dependent on temperature. The ratio between the actual amount of moisture in an air volume compared to the maximum possible at the same temperature gives the definition of relative humidity,  $\phi$ . This could also from the ideal gas law be expressed as the ratio between the vapour pressure,  $p$ , and the saturation vapour pressure,  $p_s$ .

The air inside a building is generally in permanent movement. Therefore, water vapour flow into and out of a control volume is mainly due to advective mass transport by the air, and the diffusion flow can in large scale models be neglected.

The sources in the air volume are mainly due to human activity: respiration, transpiration, laundering and laundry drying, bathing, cooking, cleaning, and moisture release from some types of equipment.

In small scale models (e.g. such as in Computational Fluid Dynamics models, CFD) control volumes are very small and the diffusion term must be taken into account.

### 2.3.2 Moisture in materials

In materials, the equation for conservation of moisture can be written in volume intensive form as:

$$\rho_{mat} \frac{du}{dt} = -\text{div}(g_{vapour\ diffusion} + g_{liquid} + g_{convection}) + \dot{u}_{source} \quad (2.3.6)$$

where

$\rho_{mat}$  is dry density of the material

$u$  is the moisture content, kg/kg

Most building materials are porous materials which could be considered as being comprised of a solid matrix and pores filled with air. Moisture will be present in porous materials as water vapour in the air-filled pores, as adsorbed layers of water molecules on the internal pore wall surfaces, as capillary condensed liquid water in the fine pores, as bulk water in the coarse pores, and as water which may be physio-chemically bound in the material that constitutes the solid matrix. The moisture content of a material is indicated as the ratio of the weight of absorbed moisture to the dry weight of the material,  $u$  (kg/kg). Other units exist to indicate the moisture content which are typically based in the volume of the material.

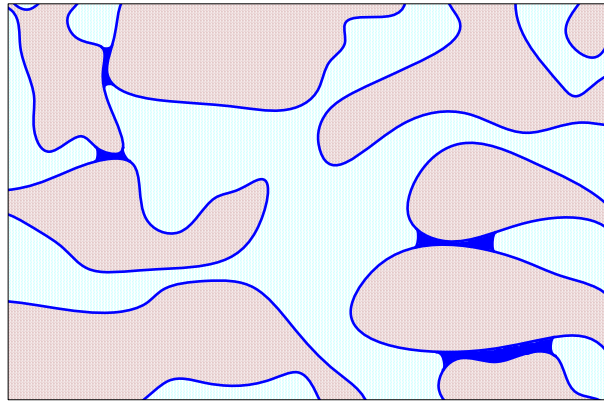


Figure 2.3.1 A partially water-filled pore system. Islands of water fill the smallest capillaries, and a surface film of adsorbed water cover the pore walls.

The amount of water, where and how it is deposited in the porous material depends on the moisture conditions in the surroundings of the material, and on the history of moisture accumulation in the material. When a material has been fully immersed in water it will be at its capillary saturation moisture content,  $u_{cap}$ . However, all pores will be filled with water, only when the water immersion test takes place under vacuum conditions, otherwise some air voids will be encapsulated within the material. The moisture content at total saturation is the vacuum saturation moisture content,  $u_{vac}$ . The temperature also has some impact on the equilibrium that exists between the amount of moisture absorbed in a material and the moisture content in surrounding air.

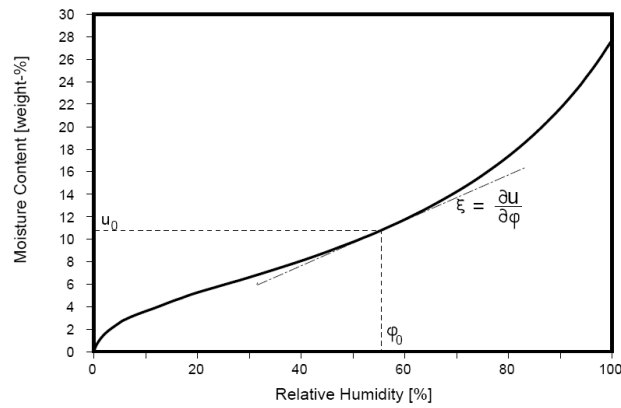


Figure 2.3.2 Sorption curve with indication of moisture capacity.

The equilibrium condition is expressed by some form of a retention curve that gives the relation between moisture content in the material and the moisture condition imposed on it by the surroundings. In the region of hygroscopic moisture uptake (for relative humidity less than 98%) the sorption curves (Figure 2.3.2) will be best suited to represent the equilibrium – they give the relation between relative humidity in the pore air, and equilibrium moisture content in the material. Of interest from the sorption curve is to know its slope, the so-called moisture capacity, as it tells how moisture needs to be absorbed (or released) by a material before it attains equilibrium with a new higher (or lower) relative humidity.

In the over-hygroscopic region, suction curves (Figure 2.3.3) may be better suited, as they give the relation between (the usually negative) hydraulic pressure of water contained within the material and moisture content. Thermodynamically, however, the two types of curves represent the same thing, as the Kelvin equation gives the relation between relative humidity ( $\varphi$ , -) in pore air, and the hydraulic pressure ( $P_h$ , Pa) of water in the pores. The term suction pressure ( $P_{suc}$ ) is introduced to indicate the absolute value of the negative hydraulic pore water pressure.

$$\ln(\varphi) = \ln\left(\frac{p}{p_s}\right) = \frac{P_h}{\rho_w \cdot R_{H_2O} \cdot T} = -\frac{2 \cdot \sigma \cdot \cos(\theta)}{\rho_w \cdot R_{H_2O} \cdot T \cdot r_k} \quad (2.3.7)$$

where

$\sigma$  is surface tension (N/m),

$\rho_w$  is the density of water (kg/m<sup>3</sup>)

$r_k$  is the pore radius (m)

$\theta$  is the contact angle (°) between the surface of capillary absorbed water and the pore walls (the contact angle is often taken to be 0°).

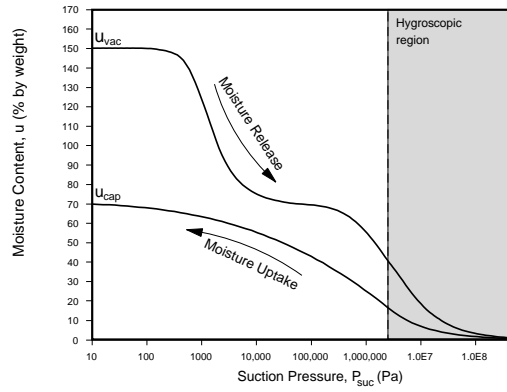


Figure 2.3.3 Suction curve with indication of the hygroscopic region (shaded area) and the hysteresis between water uptake and release.

Moisture retention curves typically exhibit some degree of hysteresis, such that one curve is followed during moisture uptake (absorption) and another is followed during moisture release (desorption). Scanning curves are followed during intermittent transitions between moisture uptake and release. Considering also the temperature dependency of moisture retention, the equilibrium between moisture content and relative humidity or hydraulic pressure could be represented to lie within a space in a three dimensional coordinate system, such as shown in Figure 2.3.4.

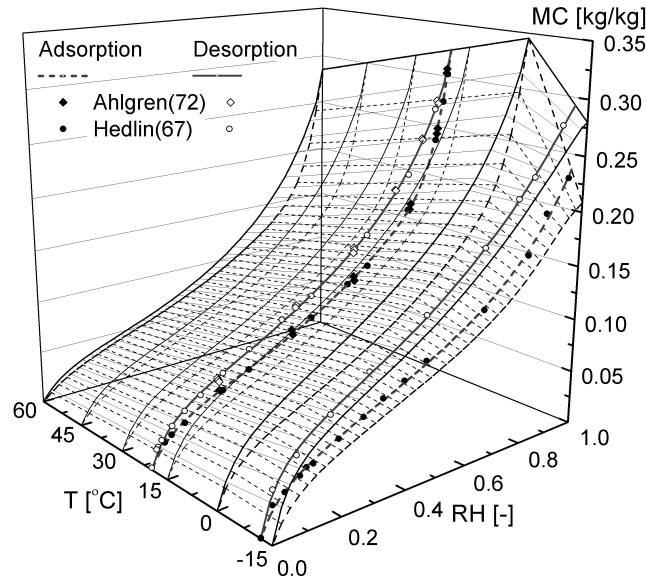


Figure 2.3.4 Sorption curve with hysteresis and temperature dependency.

**2.3.3 Moisture transport**

Moisture transport is in general caused by the following processes:

- Vapour : Diffusion
- Liquid: Capillary suction  
Darcy flow  
Surface diffusion
- Convective moisture flow

Several models to describe the vapour diffusion and liquid moisture flows can be found in literature and there is no consensus on what is the most pertinent driving potential. Many authors use partial vapour pressure, relative humidity, but also water content. Some of the most used models were discussed in IEA Annex 24.

Moisture sources exist, but hopefully should be minimal and could in many cases be minimized by practical precautions. Moisture sources may originate from some chemical reactions, construction moisture, leaks, and wind driven rain. A moisture source may also be negative (i.e. work as a moisture drain) such as in hardening of concrete.

### 2.3.3.1 Vapour diffusion

Vapour diffusion is governed by Fick's law, which in one-dimensional form looks:

$$g_{\text{vapour diffusion}} = -\delta \frac{\partial p}{\partial x} \quad (2.3.8)$$

where

$\delta$  is water vapour permeability, kg/(m·s·Pa)

The water vapour permeability is a function of the moisture content in the material. Moist materials normally have somewhat higher permeability than when they are dry, and this effect may be attributed to an enhancement by liquid transport on the microscopic scale in the finest pores and surface diffusion along the pore walls. In the beginning, when there is no continuous water phase in the pore system, this additional transport as such is not categorized as liquid moisture transport, but it is noted as an increase in the apparent water vapour permeability.

Vapour diffusion is a relatively slow mechanism compared to other moisture transport forms. However, when liquid and convective transports do not take place, vapour diffusion becomes the governing form of moisture transport and should certainly be considered. This would be the case for air tight materials in the hygroscopic regime, i.e. be the most common for materials in contact with indoor air. It should also be noted that for partially wetted materials, some of the finer areas of the pore system may be water filled and continuously connected so a liquid transport takes place through the material, while parallel and coarser pores may be open such that the vapour can diffuse in these pores. The vapour diffusion and liquid transport may be in opposite directions.

### 2.3.3.2 Liquid moisture transport

Liquid moisture transport is governed by Darcy's law, which in one-dimensional form looks:

$$g_{\text{liquid}} = -K \frac{\partial P_h}{\partial x} = K \frac{\partial P_{\text{suc}}}{\partial x} \quad (2.3.9)$$

where

$K$  is water permeability, kg/(m·s·Pa)

The hydraulic conductivity is a very strong function of moisture content. As more and bigger pores are being filled with water, the liquid moisture transport will be significantly enhanced. The moisture content where liquid transport ceases in a material that undergoes drying, is called the critical moisture content, and is the moisture content below which the liquid water is no longer continually connected through the material. However, liquid transport may still exist on the micro-scale in small, disconnected pores, where it may enhance the vapour diffusion that takes place in surrounding, larger pores (see Figure 2.3.4). Some transport may also take place in the film of liquid moisture that may be absorbed on the inner surfaces of the pore system – this phenomenon is also illustrated in Figure 2.3.4. Figure 2.3.5 shows how the water vapour permeability varies as a function of relative humidity for one particular material (aerated concrete). The enhancement of the apparent water vapour permeability is particularly pronounced in the relative humidity region above 50% RH.

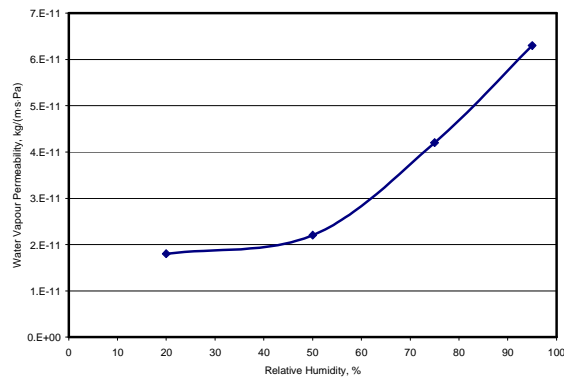


Figure 2.3.5 Water vapour permeability of aerated concrete (from: *Material Properties: A Compilation on Behalf of International Energy Agency, ECBCS, Annex 24*).

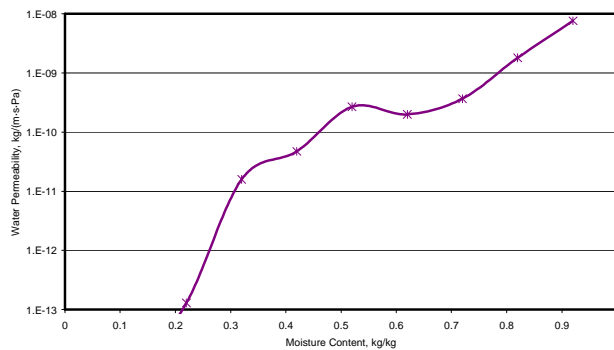


Figure 2.3.6 Water permeability of aerated concrete (recalculated after data from: *Material Properties: A Compilation on Behalf of International Energy Agency, ECBCS, Annex 24*).

### 2.3.3.3 Convective moisture transport

Convective moisture transport occurs when a flow of humid air is passing through a porous material or through cracks and joints in an assembly. The flow can be calculated as in Eq. (2.3.10).

$$g_{convection} = g_{air} \cdot x \quad (2.3.10)$$

where

$g_{air}$  is the air flux, kg/(m<sup>2</sup>·s)

When present, convective moisture flow will very often be a dominating moisture flow process. It should be minimized by preventing undesired air leaks in construction. However, convective moisture flow may also under some weather conditions be a significant way to dry out excess moisture from constructions, such as by outdoor ventilated cavities, and ventilated attics. The air flows,  $g_{air}$ , can be calculated as outlined in Section 2.2.2.

### 2.3.4 Interfacial moisture flow

To investigate whole buildings it is important to describe the rate of moisture transfer between building materials and air, which includes both transfer to the external climate and

internal transfers between interior surfaces of materials and furnishing materials and the room air.

The convective transfer between a surface and ambient air is:

$$g = \beta \cdot (v_a - v_{surface}) \quad (2.3.11)$$

Where  $\beta$  is the moisture transfer coefficient (m/s),  $v_a$  and  $v_{surface}$  is the vapour content in the ambient air and the surface layer (kg/m<sup>3</sup>)

There is a connection between the surface moisture transfer coefficient,  $\beta$  and the convective surface heat transfer coefficient  $\alpha_c$ . The relation is expressed by the Lewis formula for turbulent flows:

$$\beta = \frac{h_c}{\rho \cdot c_p} \quad (2.3.12)$$

where  $\rho$  is the density (kg/m<sup>3</sup>),  $c_p$  is the heat capacity of air (J/kg·K) and  $h_c$  is the convective surface heat transfer coefficient (W/m<sup>2</sup>·K).

However, for the internal transfers the velocities may not be fully turbulent so instead is used a general expression. Nusselt (1930) derived a more general form of the relationship, which also can be used for not fully turbulent flows.

$$\beta = \frac{D}{\lambda} \cdot \left( \frac{\lambda}{\rho \cdot c_p \cdot D} \right)^n \cdot h_c = \frac{D}{\lambda} \cdot (Le)^n \cdot h_c, \quad (2.3.13)$$

where  $\lambda$  is the thermal conductivity of air (W/m·K),  $D$  is the diffusivity (m<sup>2</sup>/s) and  $n$  is a number between 0 or 1. The coefficient  $n$  is 0 for laminar flows and 1 for fully turbulent flows.

Condensation on a surface will occur if the moisture content of the ambient air is greater than or equal to the saturation moisture content at the surface. If the surface temperature is  $T$  then:

$$g = \beta \cdot (v_a - v_s(T)) \quad (2.3.14)$$

where  $v_s(T)$  is the saturation vapour content (kg/m<sup>3</sup>) at temperature  $T$ .

A similar expression is given here for the surface evaporation:

$$g = \beta \cdot (v_s(T) - v_a) \quad (2.3.15)$$

Generally there are some relations between heat and moisture transfers. Similar to the thermal effusivity a moisture effusivity of a material can be derived. It describes the moisture buffer effect of a material or moisture accumulation ability. The moisture effusivity,  $b_m$  is a number that describe the ability of the material to absorb or release moisture and it can be calculated from standard material properties for the material:

$$b_m = \sqrt{\frac{\delta_p \cdot \rho_0 \cdot \frac{\partial u}{\partial \varphi}}{\rho_s}} \quad (2.3.16)$$

where  $\delta_p$  (kg/(m·s·Pa)) is the water vapour permeability,  $\rho_0$  (kg/m<sup>3</sup>) dry density of the material,  $u$  (kg/kg) moisture content,  $\varphi$  (-) relative humidity, and  $\rho_s$  (Pa) saturation vapour pressure.

To quantify the volume of material that will interact with the moisture content in the surrounding air a combined parameter for the penetration depth is commonly used. It comprises cycle time ( $t_p$ ), water vapour permeability ( $\delta_p$ ), saturation moisture content in the air (highly temperature dependant),  $p_s$  and the moisture capacity ( $\xi$ , slope of the sorption curve in the given RH range). The penetration depth,  $d_p$  gives the active layer of a construction and calculation of the depth were the surface exposure is reduced to e.g. 1% of that at the surface is found by:

$$d_{p,1\%} = 4.61 \sqrt{\frac{D \cdot t_p}{\pi}} \quad (2.3.17)$$

where

$$D = \frac{\delta_p \cdot p_s(T)}{\rho_0 \cdot \xi}$$

Here a sinusoidal moisture variation is assumed.

The method is strictly valid only for a semi-infinite (or “very thick”) material.

## 2.4 Interactions

### 2.4.1 Physical phenomena

Even if the basic conservation equations are fairly simple, their practical use is complex. The main reason is very strong interaction between heat and mass flows, involving many non linear terms.

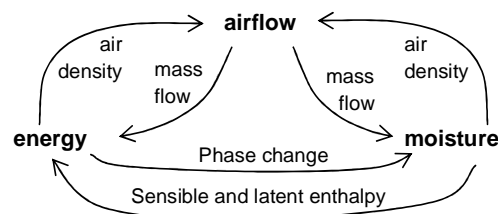


Figure 2.4.1. Main interactions between state variables

In several situations some of the interactions can be neglected in order to simplify numerical resolution.

Some of the most important interactions are explained in the following:

#### 2.4.1.1 Moisture conditions are temperature dependent

Together with calculation of moisture conditions in buildings and building components, it is necessary to know the thermal conditions of the same components, since the temperature determines the amount of vapour can be contained in the air, and thus the relative humidity, condensation risk, etc. For calculations of whole buildings, it will therefore be necessary to be able to predict the thermal conditions of indoor spaces, construction surfaces, as well as interstitially in building components.

#### 2.4.1.2 Moisture content influences material properties

As moisture replaces air in the small voids of a porous building material, the thermal conductivity of the material will increase. This is not only because water has a higher thermal conductivity (around 0.6 W/(m·K)) than still air (0.024 W/(m·K)), but also because even in a partially saturated material, water deposits such that it improves the thermal contact between the solid constituents of the material. For these reasons, even though water itself has a lower thermal conductivity than some dense building materials, e.g. concrete, the presence of

water in such materials will augment the thermal conductivity of the material. Obviously, for light weight materials, their thermal conductivity increases as moisture infiltrates into the large open voids, and settles on the fibres and pore walls.

Figure 2.4.2 shows how the thermal conductivity increases with moisture content for one particular material (aerated concrete).

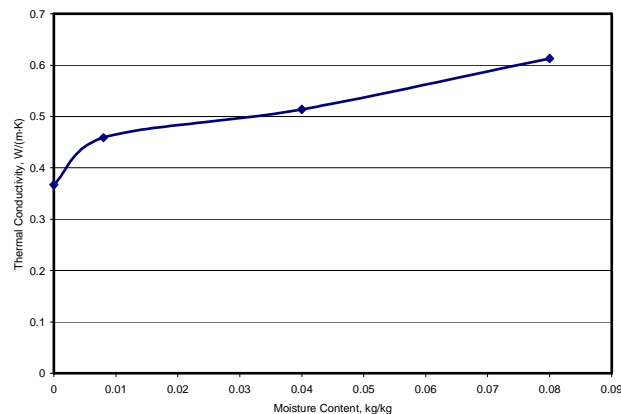


*Figure 2.4.2 Thermal conductivity of aerated concrete as a function of moisture content. Even though the material is not saturated at 8 % moisture content by weight, its thermal conductivity reaches about the same value as that of still water. (From: Material Properties: A Compilation on Behalf of International Energy Agency, ECBCS, Annex 24)*

The consequence for hygrothermal calculations of buildings is that thermal conductivity should be regarded as a function of moisture content. The thermal conductivity of ice is even higher (2.3 W/(m·K)) than that of water, which is worth considering under conditions where wet materials may also be frozen.

As the heat capacity of water is rather high, a significant contribution to the specific heat of materials is due to that of water absorbed in the material. Thus, it should be considered that wet materials have higher heat capacity.

#### 2.4.1.3 Latent heat flow

Another reason why moist materials appear to conduct heat better than dry materials could be the so-called *heat pipe* effect which is illustrated in Figure 2.4.3. Moisture is evaporated from the warm side of a large pore, transported across the pore as vapour, and then condenses on the opposite side. Heat is taken up for the evaporation, which is then released again where the condensation takes place. The heat of evaporation/condensation of water is  $2.45 \cdot 10^6$  J/kg at 20°C (at 0°C the value is  $2.5 \cdot 10^6$  J/kg, and at 100°C it is  $2.26 \cdot 10^6$  J/kg). The moisture is sucked back again as liquid through the surrounding small pores, so the process may continue to take place even in a steady state situation.

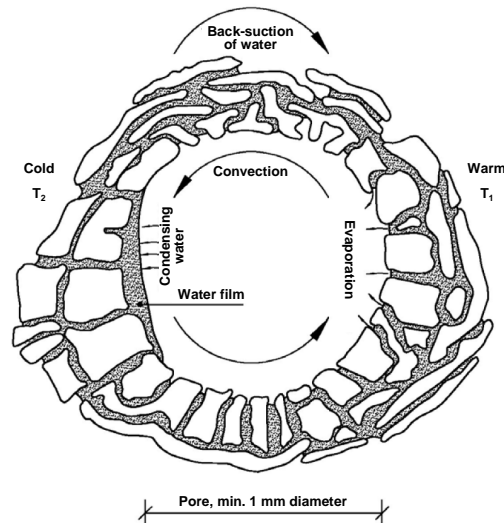


Figure 2.4.3 Local transfer of latent heat by evaporation and condensation within a large pore. (For copyright reasons, the graphical elements of this figure need to be redrawn before final publication – its origin is not well-known).

Another form of latent heat transport takes place on a macroscopic level when moisture evaporates from one side of a construction (the warm side), migrates through the construction as vapour, and condenses on the cold side. In this case, there will normally not be an immediate back-suction of the water, but the same process will work in the opposite way if/when the direction of the temperature gradient changes. The amount of heat involved can be calculated as the rate of diffusing vapour times the enthalpy of phase change. For vapour permeable materials with low thermal conductivity, e.g. mineral wool, the latent heat transport can be similar in magnitude to the heat conducted through the material in those periods when there are possibilities for significant vapour flows (Pedersen, 1990).

#### 2.4.1.4 Advection phenomena

It has been explained previously how air flow could be an important mechanism to carry heat and moisture with it, when it passes through building components and indoor spaces. Thus, if it is known that a convection air stream will be present in rooms or building components, this should certainly be considered in order to correctly estimate the associated heat and moisture flows. This will be calculated as outlined in Sections 2.1.2 and 2.3.3.3 using knowledge about air flows as calculated according to Section 2.2.

#### 2.4.1.5 Air flows are temperature and moisture content dependent

Thermal buoyancy is one of the important reasons for air flow in building components and in rooms. The reason is the strong temperature dependency of density of air, expressed by Equation (2.4.1). Of some importance is also that other fluid flow properties, e.g. viscosity or surface tension, are somewhat temperature dependent. Thus, in order to calculate air flows correctly, it is again important to have a good prediction of the thermal conditions in the rooms and components. In well insulated buildings, when the temperature gradients are small, moisture content influence on air density can be dominant, and concentration buoyancy driven flows may appear.

$$\rho_{\text{moist air}}(T, P_{\text{atm}}, w) = \frac{P_{\text{atm}}(1+x)}{(x \cdot R_{\text{H}_2\text{O}} + R_{\text{dry air}})T} \quad (2.4.1)$$

Where  $\rho_{moist\ air}$  is density of moist air,  $\text{kg/m}^3$ ;  $P_{atm}$  is atmospheric pressure, Pa;  $x$  is air humidity by mass,  $\text{kg/kg}$ ;  $T$  is absolute temperature, K; and  $R_{H_2O}$  and  $R_{dry\ air}$  are gas constants for water vapour and air, respectively,  $\text{J}/(\text{kg}\cdot\text{K})$

As it may appear from Equation (2.4.1), the density of moist air is lower than that of dry air. However, this does not mean that humid air will “separate” from dry air and seek to the top, it impacts only buoyancy forces of the bulk of air. The different molecular constituents of humid air remain well mixed.

Moisture retention curves are used as equations of state in transient moisture flow calculations to give the relationship between the potential driving the moisture transport and the continuity parameter (moisture content). If retention curves are not used directly, then they are represented indirectly via the way the moisture retention capacity influences moisture diffusivity. However, the retention curves are somewhat temperature dependent.

For instance for the sorption curve, this means that the equilibrium moisture content will be lower, if relative humidity is held constant as temperature increases. Or the equilibrium relative humidity will increase with temperature if the moisture content is held constant. This is illustrated in Figure 2.3.4.

#### 2.4.1.6 Freezing/thawing

It is well known that water/ice will freeze/thaw around  $0^\circ\text{C}$ . Thus, it is important to know the temperature in order to predict the state of water. However, it should be noted that the freezing point will be lowered if salts are dissolved in the water, or if the water is under suction (such as in a pore system). Water that is held in the fine pores of a partly saturated material freezes only at several degrees below the normal atmospheric freezing point.

Like for evaporation/condensation, there is also a transformation of enthalpy related to the freezing or thawing of water. The freezing/thawing enthalpy is  $334\text{ kJ/kg}$ .

### 2.4.2 Interactions between physical elements of the building

For calculation of the hygrothermal conditions of a building component it is necessary to know the boundary conditions very well. Some boundary conditions are given by the external environment, while others are formed by the indoor environment. Conversely, in order to calculate the hygrothermal conditions of an indoor environment, it is necessary to know the conditions of its boundaries, which are formed by the building components. Thus, it is necessary to calculate the conditions in rooms and building components simultaneously respecting the mutual influence between the various constituents of the building.

In such calculation, it is necessary to consider also other influencing factors, which apart from the outdoor climate, are for instance: users of buildings; systems for heating, cooling and ventilation; and materials used for indoor furnishing. Models that predict the hygrothermal conditions of whole buildings must consider all significant interactions between these constituents.

## 2.5 Granularity and spatial discretization

Following [Wikipedia] “granularity” is used here to measure of the size of the descriptions of components that make up a system – the “whole building”. The model of a building composed of large components can be called coarse-grained, and model composed of small components can be called fine-grained; here coarse and fine are the granularity of description of the system.

A fine-grained description of a system is a detailed, low-level model of it. A coarse-grained description is a model where some of this fine detail has been smoothed over or averaged out.

Granularity is related to the size of the control volume. In buildings a large panel of granularity is available (see Figure 2.5.1): from the simplest mono-zone modelling (whole building = one zone) to computational fluid dynamics (CFD) modelling, enabling detailed predictions of temperature, velocity and species concentration fields in one room. Intermediate approaches use multi-zone modelling, dividing the building, and even sometimes a room, in a few zones with different air characteristics. Similar classification can apply for granularity of envelope models: from simplest transfer functions, through 1D, 2D representation to 3D modelling using control volume or finite elements techniques. Four main granularity classes can be proposed:

- the very fine-grained models:
  - o Computational fluid dynamic (CFD) modelling of room air, which enables detailed calculations of temperature, velocity and concentration fields in a room. Typically a room is divided into thousands to millions control volumes and conservation equations are solved using control volume or finite elements techniques
  - o 3D models for the envelope, using control volume or finite elements techniques, with typical size of mesh between few mm<sup>3</sup> to a few cm<sup>3</sup>. In this approach heat and mass fluxes, as well as temperature and concentration fields in the envelope parts are computed, including singular points and 3D thermal bridges
- the fine-grained models:
  - o zonal models for air volumes, where each room air is subdivided into several control volumes (typically between ten and a few hundred). In this approach advective mass transfers between zones are very important and must be accurately represented. Zonal models can also be used to represent several adjacent rooms connected by openings
  - o 2D models for the envelope, using control volume or finite elements techniques, with typical size of mesh between few mm<sup>2</sup> to several cm<sup>2</sup>. In this approach heat and mass fluxes, as well as temperature and concentration fields in the envelope parts are computed, including thermal bridges or similar singular geometries
- the intermediate-grained models:
  - o multi-zone models for air volumes, where several rooms or groups of rooms are represented, each with different characteristics. Therefore heat and mass transfers must be modelled not only between indoor and outdoor environments but also between different zones inside one building. These transfers include transfers in walls but also air flows, that can be computed using for example pressure network modelling
  - o 1D models for the envelope, using control volume or finite elements techniques, with typical size of mesh between few mm to several cm. In this approach heat and mass fluxes, as well as temperature and concentration fields within the envelope parts are computed
- the coarse-grained models:
  - o mono-zone models for air volumes, where the whole building is represented as one perfectly mixed zone, that is same temperature and humidity are assumed for all rooms
  - o Transfer function models for the envelope, where dynamic heat and possibly mass fluxes are represented, without investigating conditions within the envelope

Certainly all four granularities have their advantages, but also their limitations, some of them are mentioned in Table 2.5.1 below.

**Table 2.5.1** *Main advantages, limitations and applications of different granularities in whole-building modelling*

Granularity	Advantages	Limitations	Applications
<b>Very Fine</b> Type CFD in air 3D fine mesh in envelopes	<ul style="list-style-type: none"> <li>- detailed representation of temperature, concentration and possibly velocity fields</li> <li>- represent stratification, details of cold bridges, weak points, etc.</li> </ul>	<ul style="list-style-type: none"> <li>- need detailed description of geometry (including air inlets, cracks etc),</li> <li>- very costly in terms of computing time,</li> </ul>	<ul style="list-style-type: none"> <li>- detailed investigations of coupled HAM transfers in some critical points (critical rooms, thermal bridges)</li> <li>- calculating some global properties as inputs for coarser models, such as surface coefficients</li> <li>- adapted for steady state or short-period dynamic computations</li> </ul>
<b>Fine</b> Zonal in air 2D mesh in envelopes	<ul style="list-style-type: none"> <li>- Good representation of non homogenous volumes,</li> <li>- Reasonable computing time</li> </ul>	<ul style="list-style-type: none"> <li>- Requires use of adapted empirical laws for critical points (driving flows for air, 3D effects for solids)</li> <li>- Air zonal modelling with fixed mesh not adapted for strongly changing driving flows</li> </ul>	<ul style="list-style-type: none"> <li>- detailed behaviour of one room or of a group of a few rooms, in dynamic conditions,</li> <li>- 2D computations of the envelope</li> </ul>
<b>Intermediate</b> multi-zone for air 1D mesh in envelopes	<ul style="list-style-type: none"> <li>- Relatively fast,</li> <li>- Can represent complex buildings, with thermally different zones (differences between north and south exposed, undergrounds and attics, differentially controlled heating or ventilation systems...)</li> </ul>	<ul style="list-style-type: none"> <li>- Can not represent non-uniformity of air characteristics in one room,</li> <li>- can not represent thermal bridges...</li> </ul>	<ul style="list-style-type: none"> <li>- adapted to whole-building dynamics, (including annual) computations of energy and mean indoor climate</li> </ul>
<b>Coarse</b> 1 zone for air transfer functions for the envelope	<ul style="list-style-type: none"> <li>- fast,</li> <li>- give good estimation of energy use for simple buildings</li> </ul>	<ul style="list-style-type: none"> <li>- not adapted to complex buildings</li> <li>- unable to asses conditions within the envelope parts</li> </ul>	<ul style="list-style-type: none"> <li>- adapted to dynamic simulations of energy and mean indoor climate in simple buildings or in a single room</li> </ul>

There are no models "better" or "worse", there are only models better adapted to a given situation. Finely grained models are not "better" than coarsely grained. It means that the most important part of modelling is to consider: (1) what are the information (outputs) needed from the model, (2) what are the available information (inputs) and (3) what can eventual constraints (computational time) and then to chose the most adapted tools. For example some moisture problems in dwellings are caused by condensation or high relative humidity at cold surfaces. To investigate this type of problems a detailed study of temperature and moisture content in the air room is needed. Condensation or mould growth occur in general locally and depend on local temperatures but also on local air flows. Therefore "very-finely" or "finely" grained models should be used.

In previous pages and in Table 2.5.1 some parallel is dressed between granularity for indoor air and for envelope parts. However in practice simulation tools are not always associating similar levels of granularity, as shows Table 2.5.2. For example often very fine envelope simulations tools use coarse approach for air volume. Some reasons can be explained by historical developments of simulation tools. In the past researches were mainly concentrated on either indoor air or envelope. As result some very fine and sophisticated tools were proposed separately for both specific applications. For example Fluent or StarCD can represent finely room air, but at the origin they had only a very simple vision of the envelope. Similarly finely and very-finely grained tools as CHAMPS, DELPHIN and WUFI were originally developed to analyse transfers within envelope parts and were associated with coarsely-grained mono-zone air models, or even with given air characteristics. Of course, for some specific applications such associations are relevant. However they must be used with care. As whole building simulation field is still under active development, probably in near future some of the blanks in Table 2.5.2 will be filling in.

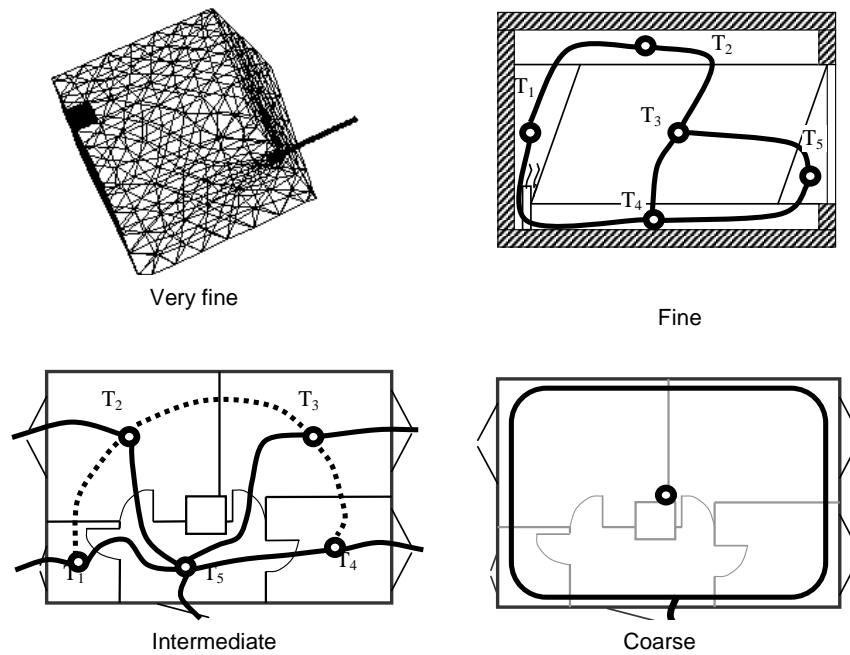


Figure 2.5.1 Levels of granularity for room air

Table 2.5.2 Typical associations of model granularities

Air \ Envelope	coarse	intermediate	fine	very fine
Coarse	<b>X</b>	<b>X</b>		<b>X</b>
Intermediate	<b>X</b>	<b>X</b>	<b>X</b>	
Fine		<b>X</b>		
Very fine		<b>X</b>		<b>X</b>

As a final remark it must be stressed that even if the granularity is related to the complexity of the model, it is not its only indicator. Granularity here is relevant to the space-scale, but not to the level of detail of physical phenomena. For example 1D model for envelope, using finite element or control volume technique, is classified here as intermediately-grained. If this model represents coupled HAM transfers, including liquid transport, hysteresis in sorption isotherm, temperature and relative humidity dependence of material properties, its computational time can be similar to CFD computations, and the model can be justly categorized as “very complex” or “advanced” model, in terms of represented physical processes.

## 2.6 Numerical methods for space and time discretization

### 2.6.1 Finite Difference Methods (FDM) / Finite Control Volume methods (FCV)

Finite Difference Methods are widely used for calculation of problems of the diffusion type (e.g. for heat conduction, vapour, liquid or air flow problems). These problems may be governed by a partial differential equation such as:

$$\frac{\partial P}{\partial t} = D \frac{\partial^2 P}{\partial x^2} \quad (2.6.1)$$

Where

$P$  is a potential driving the flow

$D$  is a diffusivity,  $m^2/s$

The principle for the calculation with the Finite Difference Method is to transform the differential equation into a difference equation. A wall, in which the transient  $P$ -profile is to be determined, is divided into a number of *grid points*. The principle is shown in Figure 2.6.1. The grid points are numbered by the index  $i$ .

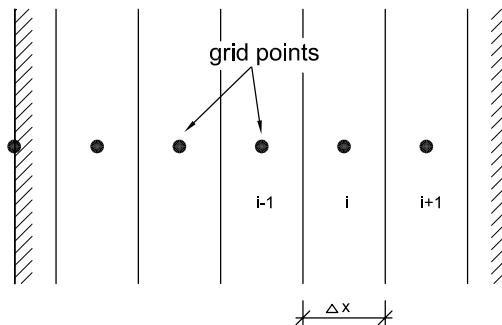


Figure 2.6.1 Wall in which the grid points are inserted at a distance of  $\Delta x$ .  $i$  is an index for the discretized space coordinate.

The finite difference equation can be written in several forms depending on which approximation will be used. Some programs use the explicit finite difference method. Then the finite difference approximation can be written in the following form:

$$\frac{P_i^{j+1} - P_i^j}{\Delta t} = D \frac{(P_{i+1}^j - P_i^j) + (P_{i-1}^j - P_i^j)}{\Delta x^2} \quad (2.6.2)$$

Here, the time step  $\Delta t$  is the difference between the time levels  $j$  and  $j+1$ .

Equation (2.6.2) can be rearranged, and the Fourier number  $Fo = D \cdot \Delta t / \Delta x^2$  inserted to achieve the following form of the equation:

$$P_i^{j+1} = Fo \cdot P_{i-1}^j + (1 - 2Fo) \cdot P_i^j + Fo \cdot P_{i+1}^j \quad (2.6.3)$$

Equation (2.6.3) represents a very easy formula for forward calculation of new values (time index  $j+1$ ) of  $P$  based on values from a previous or initial time step ( $j$ ). However, it has the drawback that in order to provide stable calculation results,  $Fo$  must not be larger than 0.5.

Thus the largest permissible time step  $\Delta t$  is  $\frac{(\Delta x)^2}{2D}$ . This may lead to slow calculations.

It is possible to use new values of the potential  $P$  on the right-hand side of Equation (2.6.2), in which case after some new sorting of the terms it may look:

$$-F_0 \cdot P_{i-1}^{j+1} + (1+2F_0) \cdot P_i^{j+1} - F_0 \cdot P_{i+1}^{j+1} = P_i^j \quad (2.6.4)$$

This equation can only be solved if it is done synchronously with all similar equations for the whole calculation domain ( $i = 1..n$ ). However, this is possible by solving a set of equations like (2.6.4). This is called an implicit method.

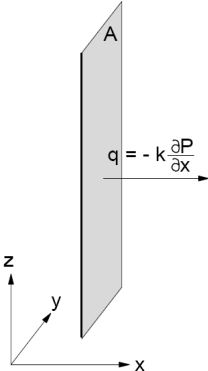
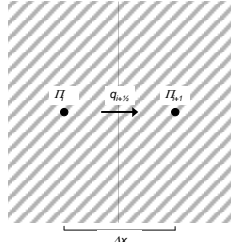
The implicit method requires slightly more computational effort than solving  $n$  equations like (2.6.3), but the advantage is the implicit method has no stability problems with large time steps, so the calculation may proceed faster in time.

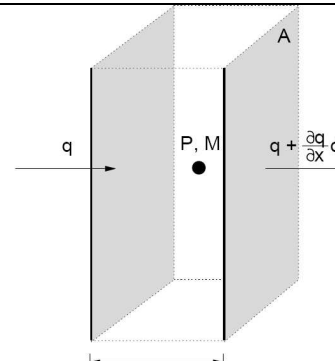
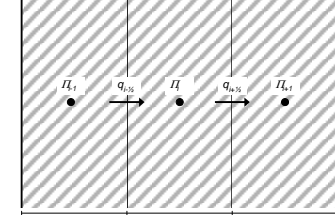
Combination forms exist between the explicit and implicit schemes. E.g., if Equation (2.6.2) is written as:

$$\frac{P_i^{j+1} - P_i^j}{\Delta t} = D \left( 0.5 \frac{(P_{i+1}^j - P_i^j) + (P_{i-1}^j - P_i^j)}{\Delta x^2} + 0.5 \frac{(P_{i+1}^{j+1} - P_i^{j+1}) + (P_{i-1}^{j+1} - P_i^{j+1})}{\Delta x^2} \right) \quad (2.6.5)$$

we have the form which is used in Crank-Nicolson's method. Like the implicit method, it requires an equation system to be solved for all control volumes. Crank-Nicolson's method has a smaller truncation error (see below) as it makes an average between the explicit and implicit approximations, and it is therefore in principle more accurate. However, the gained accuracy is obtained at an increased computational effort, since more elementary algebraic operations are needed in each calculation step. As well, other sophisticated time integrated schemes have been developed such as the Runge-Kutta method, predictor-corrector methods, or multi-step procedures such as the Adams methods.

Another way of reaching some almost similar equations is to use the so-called Finite Control Volume method. However, the FCV-method incurs some conceptual advantages in setting up the numerical scheme for a new problem. As the name says, Finite Control Volumes is about book keeping or control of flows into and out of a certain discrete volume. The difference between what enters and what leaves a volume, will accumulate in the volume. The FCV-method can be understood as being set up by three types of equations:

<p>1a. <b>The transport equation</b> (differential form): One-dimensional flux of the matter in question (e.g. heat, air or moisture) through a geometrical plane in a material or in a fluid is governed by transport equation like:</p> $q = -k \frac{\partial P}{\partial x} \quad (2.6.6)$ <p>Where  <math>q</math> is flux  <math>k</math> is a conductivity/permeability</p>	
<p>1b. The discretized form of the transport equation is an approximation which looks:</p> $q_{i+1/2} \approx -k \frac{P_{i+1} - P_i}{\Delta x} \quad (2.6.7)$ <p>In addition to this, it may be possible to add a source or sink term to the right hand side of the continuity equation.</p>	

<p>2a. <b>The continuity equation</b> (differential form)                  Control is kept with the balance of "substance" <math>M</math> (energy or mass):</p> $\frac{\partial M}{\partial t} = -\frac{\partial q}{\partial x} \quad (2.6.8)$ <p>A basic assumption in the discretized form of the continuity equation is that everything is "well-mixed" within the volume, e.g. that a temperature in a node point, which may be located centrally in the volume, is representative for conditions in the whole volume.</p>	
<p>2b. The discretized form of the continuity equation looks:</p> $\frac{M_i^{j+1} - M_i^j}{\Delta t} = -\frac{q_{i+1/2} - q_{i-1/2}}{\Delta x} = k \frac{P_{i-1} - 2P_i + P_{i+1}}{(\Delta x)^2} \quad (2.6.9)$	
<p>3. <b>Equation of state</b>                  Since the transport equation uses the potential <math>P</math> to drive the transport, and the continuity equation keeps control of the "substance" <math>M</math>, it is necessary for the further calculations to relate changes of <math>M</math> to changes of <math>P</math>. This is done by the continuity equation.                  For heat transport, the heat capacity explain how the quantities change in relation to each other:</p> $\partial T = \frac{\partial H}{c} \Rightarrow T^{j+1} \approx T^j + \frac{H^{j+1} - H^j}{c} \quad (2.6.10)$	
<p>For moisture transport, the moisture retention curves are used to relate changes in moisture content to changes in liquid or vapour pressures (possibly via the relative humidity).</p>	

Also the finite control volume method can take an explicit or implicit form depending on the time level with which the driving potential is inserted in the transport equations.

The explanations above have not presented the possibility that the geometrical grid, i.e.  $\Delta x$ , could vary such the grid points do not have to be equidistant. And  $\Delta t$  could vary such as to concentrate the computational effort in periods when rapid changes place. Also the material properties such as conductivity/permeability and equations of state may be values or functions that could be evaluated locally at the actual conditions. In this way, the finite difference and control volume methods offer great flexibility for developers to model such conditions that may be at hand.

The above explanations also assume the transports to be one-dimensional. However, the method could be expanded to work in two- or three-dimensional orthogonal coordinate systems as well. Although it would in principle be possible (and has been done) to extend the finite difference/control volume methods also to free-form geometry, this is somewhat cumbersome, and is not normal practice of use of these methods.

2.6.1.1 Numerical errors

As a result of approximating the differential terms with finite differences the Finite Difference and Finite Control Volume methods will give solutions that deviate from the exact solution of the PDE. This difference is called the *discretization* or *truncation error*. The important thing is that the error decreases as  $\Delta u$  (i.e.  $\Delta t$  and  $\Delta x$ ) tend to zero, that is the discretization error is some  $O[(\Delta u)^n]$ -function, where the exponent  $n$  is the order of the error. Precision is higher for higher  $n$ .

Another requirement of a good numerical method is that the discretization error does not increase from one iteration in time to another, i.e. that the method must be *stable*, as discussed already about the explicit finite difference method.

Finally, computers are not able to give exact representations of the results of finite difference equations. Any result that has more digits than can be retained by the computer (most real numbers) is subject to a *round-off error*. Round-off errors will accumulate if the results of the calculations are generated on the basis of results from earlier time steps or iterations of the same calculations. While small space and time discretizations decrease the discretization errors, they also increase the total number of computations needed, and thus, may cause round-off errors to add up.

## 2.6.2 Finite Element Method (FEM)

Finite Element Methods (FEM) represent an efficient and flexible way to solve partial differential equations in many engineering problems. The flexibility mainly comes through the method's ability to find solutions for unstructured grids, meaning that very good approximations can be achieved even for many multidimensional problems, where the physical geometry to be modelled, or the desired numerical mesh, do not have a rectangular/orthogonal shape. This makes it easier to concentrate the computational effort in those loci where the main interest is, and thus overall, to get a more optimal spending of the computational resources.

Finite Element Methods offer the same flexibility to cope with non-linear phenomena, e.g. when the material properties are functions of the variables to be calculated, as do the Finite Difference and Control Volume Methods.

The price is that Finite Elements can be a little more mathematically involving to develop and set up, than FDM/FCV methods. However, because of the strong power and generality of Finite Element Methods, we see today a number of general purpose Finite Element tools which have flexibility to also model combined Heat, Air and Moisture problems (COMSOL, 2007; COSMOS, 2007; ABAQUS, 2007). These tools are often marketed with a "MultiPhysics" label, indicating their wide range of applicability. As such, the tools may also be suitable for modelling of fluid flow problems (CFD).

However, while FEM has for a long time been the dominating numerical method to calculate problems in structural engineering, it is still not the most common method used in building physics. Examples where FEM has been used in building physics are presented by van Schijndel, 200x; Janssen, 2002; Fitsum... The general conception is however, that FEM is becoming more common as a numerical modelling method for building physics applications – not least due to the advent of the commercial tools.

While FEM modelling is being used and developed for modelling of building components and objects that surround buildings, e.g. the soil volume, it has still not been used (and may not be used...?) to model the whole building completely with FEM. However, there are examples of research (e.g. Fitsum, 2007, van Schijndel, 200x) where FEM models for the building envelope are coupled to the modelling of zone balances carried out in other tools, e.g. by setting up the complete balance equations for indoor rooms regarding their use, conditioning and interaction with other environments.

### 2.6.2.1 Numerical paradigm of FEM – a very brief introduction

Finite Element Methods make use of a technique to find so-called weak form solutions (or general solutions) to the governing partial differential equations. For a transient heat conduction problem in two dimensions, the governing partial differential equation can be written as:

$$\rho c \frac{\partial T}{\partial t} - \nabla^T \lambda \nabla T = 0 \quad (2.6.11)$$

The weak formulation of this PDE is found by making use of Galerkin weighted residual method to obtain an approximate solution as the solution which minimizes the spatial integral:

$$\int_V M \left[ \rho c \frac{\partial T}{\partial t} - \nabla^T \lambda \nabla T \right] \partial V = 0 \quad (2.6.12)$$

Where  $V$  is a volume representing the calculation domain of interest, and  $M$  is some weight function.

Applying the divergence theorem (Gauss) yields:

$$\int_V \left[ M \rho c \frac{\partial T}{\partial t} - \nabla^T (M \lambda \nabla T) \right] \partial V + \int_S M \mathbf{n}^T \lambda \nabla T \partial S = 0 \quad (2.6.13)$$

Where  $S$  is the surface of  $V$ , and  $n$  is a normal vector to  $S$ .

(Also add some more info on boundary conditions...)

In numerical calculation, the calculation domain  $V$  is subdivided into a number of volume elements  $V^e$ , and the temperature is approximated by interpolation relations:

$$T = \mathbf{N} \mathbf{T}^e \quad (2.6.14)$$

Where the vector  $N$  contains an interpolation function, and  $T^e$  contains the discrete node point values of temperature values. In one-dimensional calculations,  $T^e$  represent node points at the beginning and end of the linear segments that form the elements. In multidimensional calculations,  $T^e$  are located in the vertices of planar elements which typically have either a triangular or quadrangular shape, and thus can give good approximation to many free forms.

This means that Equation (2.6.13) could be represented entirely by the discrete node points and solved for all elements.

Like for the FDM and FEM methods, it is possible to solve (2.6.14) using explicit or implicit formulations (or even combinations thereof). An example of a numerical mesh for FEM calculation of the soil volumes below and around a basement is shown in Figure 2.6.2.

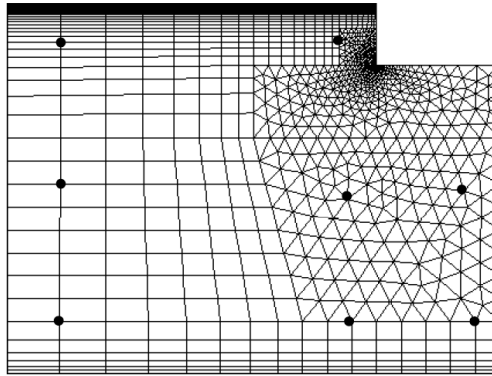


Figure 2.6.2 example of a numerical mesh for FEM calculation of the soil volumes below and around a basement (from Janssen, 2002).

*The above is an attempt by a person (CAR) who is not skilled in FEM to write just "two pages" about the principle of the method. It is not entirely whole and correct. We need*

*someone with skills in FEM to amend it or to write an entirely new, short and appropriate text about FEM.*

*The following text is from <http://www.u-aizu.ac.jp/~niki/feminstr/introfem/introfem.pdf> - it is not acceptable to use this text directly in our report!*

*Alternatively, there is also an appropriate description in Hans Janssen's doctoral thesis (2002)...*

The finite element method (FEM) is a numerical technique for solving problems which are described by partial differential equations or can be formulated as functional minimization. A domain of interest is represented as an assembly of *finite elements*. Approximating functions in finite elements are determined in terms of nodal values of a physical field which is sought. A continuous physical problem is transformed into a discretized finite element problem with unknown nodal values.

For a linear problem a system of linear algebraic equations should be solved. Values inside finite elements can be recovered using nodal values. Two features of the FEM are worth to be mentioned:

Piece-wise approximation of physical fields on finite elements provides good precision even with simple approximating functions (increasing the number of elements we can achieve any precision).

Locality of approximation leads to sparse equation systems for a discretized problem. This helps to solve problems with very large number of nodal unknowns.

How the FEM works

To summarize in general terms how the finite element method works we list main steps of the finite element solution procedure below.

1. *Discretize the continuum.* The first step is to divide a solution region into finite elements. The finite element mesh is typically generated by a pre-processor program. The description of mesh consists of several arrays main of which are nodal coordinates and element connectivities.
2. *Select interpolation functions.* Interpolation functions are used to interpolate the field variables over the element. Often, polynomials are selected as interpolation functions. The degree of the polynomial depends on the number of nodes assigned to the element.
3. *Find the element properties.* The matrix equation for the finite element should be established which relates the nodal values of the unknown function to other parameters. For this task different approaches can be used; the most convenient are: the variational approach and the Galerkin method.
4. *Assemble the element equations.* To find the global equation system for the whole solution region we must assemble all the element equations. In other words we must combine local element equations for all elements used for discretization. Element connectivities are used for the assembly process. Before solution, boundary conditions (which are not accounted in element equations) should be imposed.
5. *Solve the global equation system.* The finite element global equation system is typically sparse, symmetric and positive definite. Direct and iterative methods can be used for solution. The nodal values of the sought function are produced as a result of the solution.
6. *Compute additional results.* In many cases we need to calculate additional parameters. For example, in mechanical problems strains and stresses are of interest in addition to displacements, which are obtained after solution of the global equation system.

### 2.6.3 Response factor method

Response factor methods, also called transfer functions, are used especially in some computer programs to solve problems of transient heat conduction and to calculate the thermal condition and energy consumption of buildings (e.g. EnergyPlus, 2007 and

TRNSYS, 2007). Response factor methods will be described here as a method for calculation of heat transfer, although in principle it could be used equally for other diffusive type of flows.

Compared to the finite difference method, the big advantage of the response factor method is that the calculation time is rather short because it is necessary to calculate the response factors of a wall only once. Calculation of the response factors requires some effort of the computer program in the beginning of the calculation, but once this has been done, the rest of the calculations can be rather quick. In the following will be described only the basic principles of the response factor method. Reference is made to the literature, e.g. Hittle, D.C., 1981, for further explanation.

For a wall with constant thermo-physical properties it is possible to use the *superposition principle* to solve the general heat conduction equation. Together with *time series*, the superposition principle constitutes a fundamental element of the response factor method, and thus, it is important with a solid understanding of these two concepts.

### 2.6.3.1 Superposition principle

Linearity and invariability are conditions for any superposition method. By *linearity* is understood that a physical system can be presented by a set of linear algebraic equation such that a certain action on the system, and the system's response on the action, are proportional. By *invariability* is understood that a certain action on the system will result always in the same response of the system. The *superposition principle* can be summarized as follows: "When a system is exposed to a number of actions, each of these actions work independently of the others, and the total change is the sum of the effects of the individual actions".

The linearity requirement means that the response factor method is not as well suited to calculate moisture flow processes, which in some case have a strongly non-linear character.

To cast more light on the concept, the following hypothetical example will be given of a one-dimensional wall initially at the uniform temperature  $T_0$ . The temperature of the outer wall surface is instantly raised by one degree over  $T_0$ . This will result in a time dependent heat flow through the inner wall surface. The example is illustrated in (2.6.3).

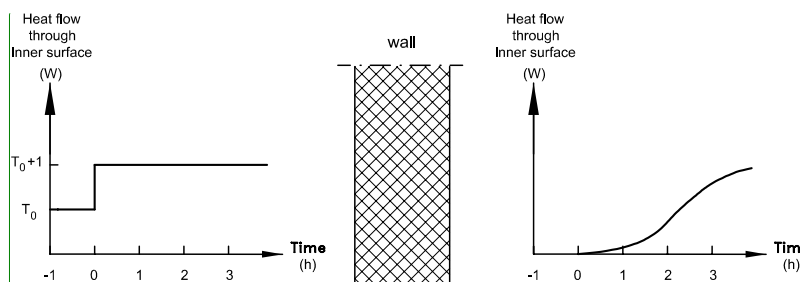


Figure 2.6.3 Wall with a uniformly distributed temperature  $T_0$ , where the outer surface temperature is suddenly, at time 0, raised by one degree causing a (delayed) heat flow through the inner surface.

If the outer wall surface temperature had been increased by two degrees, instead of only one, the heat flow through the inner surface would have been doubled. The variation of the heat flow with time can also be indicated as the wall's response on the given impact.

### 2.6.3.2 Time Series

In the previous example was used a constant temperature increase of one degree. In practice, it will be necessary to describe the variation of the outer temperature as a continuous function. Mitalas, G.P. et al., 1967, and Stephenson, D.G. et al., 1967 improved the method by introducing overlapping triangular pulses. As a unit pulse is used a triangle with the height, one degree, and the width, two time intervals (e.g. two hours).

**Commentaire :** This and the following drawings on the response factor method are from Jørgen Erik Christensen's lic.techn. thesis. His permission should be granted, or new similar figures be made.

Hereafter, the principle is to describe the continuous function by giving the functional values of advancing time intervals as a time series, see Figure 2.6.4. Every step on the time series is represented by a triangular pulse centred in the actual point in time, and with a width of two times the time step that is used for the calculations. The approximation is a linear interpolation between the individual points in time, and the precision depends on the size of the time interval. By using the approximation shown in Figure 2.6.4, it is possible to calculate even rather complex influences since the time series follow the cumulative and distributed laws, whereby they can be added, subtracted, multiplied and divided. Therefore, it is adequate to calculate the system's response on just one unit triangular pulse, and then it will be possible to calculate the response on any other influence.

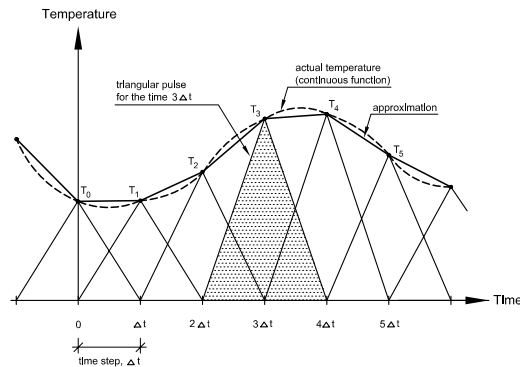


Figure 2.6.4 Time series of triangular pulses approximating a continuous function.

### 2.6.3.3 Response Factors

An example of a wall will be given to illustrate the use of the superposition principle. The wall is shown schematically in Figure 2.6.5 with a left-hand boundary (surface 1), and a right-hand boundary (surface 2). There are four variables of interest: Two surface temperatures, and two heat flows through these surfaces. Thus, of interest is a system with two driving forces (temperatures) and two flows (the heat flows).

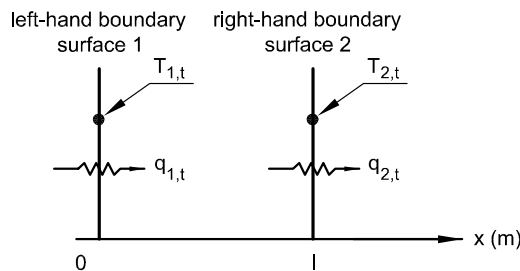


Figure 2.6.5 Wall with four variables of interest: Two wall surface temperatures and two heat flows.

If the temperature at the left-hand boundary is changed, this will have an impact on the heat flow through both boundaries. Likewise goes for the right-hand boundary, but the effects don't have to be the same unless the wall is symmetric. To explain the development of the response factor superposition technique, it will be beneficial to regard the heat flow on each side of the wall as a sum of heat flows caused by temperature variations on the same and the opposite sides.

By observing Figure 2.6.6, the principles for superposition can be seen. A unit triangular pulse with the height one degree is imposed on both surfaces at time 0, Figure 2.6.6A. These influences give rise to increases in the heat flows on the same sides as they are imposed, Figure 2.6.6B. In addition, they cause heat flows on the opposite sides of the wall

as shown in Figure 2.6.6C. The magnitude of these heat flows at time intervals  $\Delta t$  are the response factors. They will be ascribed as follows:

- X For the heat flow through the left-hand boundary resulting from a temperature pulse on the left-hand boundary.
- Y For the heat flow through boundary opposite the temperature pulse.
- Z For the heat flow through the right-hand boundary resulting from a temperature pulse on the right-hand boundary.

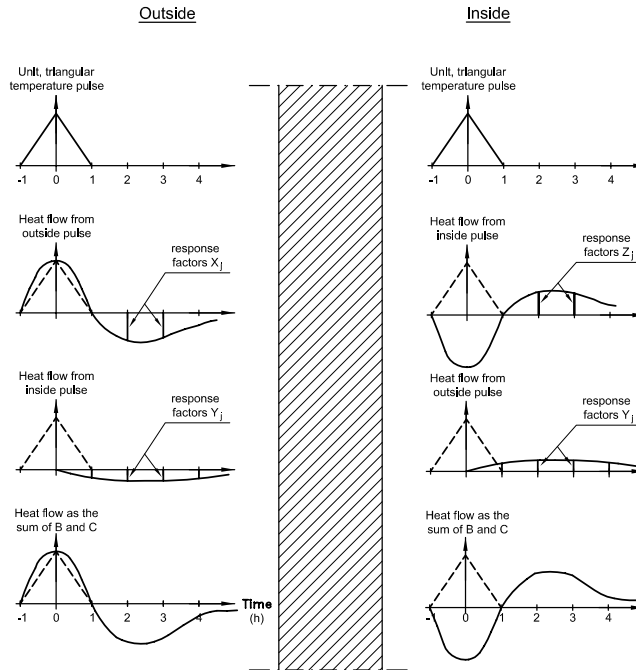


Figure 2.6.6 Schematic illustration of heat flows by use of the superposition principle.

The idea of adding these heat flows can be summarized as follows:

1. The continuous temperature function in Figure 2.6.4 is replaced by a time series of triangular pulses for the temperature. This is done both at the left-hand and the right-hand boundary.
2. The heat flows from every pulse on either side is determined by increasing the response from a unit pulse by the height of the actual temperature pulse.
3. Finally, the increased flows from all the temperature pulses on both sides are added up. Theoretically, a temperature pulse has an effect for a long time, but in practice it will die out after a limited number of time steps.

Mathematically, the three steps can be written as follows:

Heat flow through left-hand boundary:

$$q_{1,t} = \sum_{j=0}^{\infty} T_{1,t-j\Delta t} \cdot X_j - \sum_{j=0}^{\infty} T_{2,t-j\Delta t} \cdot Y_j \tag{2.6.15}$$

Heat flow through right-hand boundary:

$$q_{2,t} = \sum_{j=0}^{\infty} T_{1,t-j\Delta t} \cdot Y_j - \sum_{j=0}^{\infty} T_{2,t-j\Delta t} \cdot Z_j \tag{2.6.16}$$

where	$X_j$	Indicates for the times $j \cdot \Delta t$ , the sequence of response factors that are heat flows over the left-hand boundary resulting from a unit triangular temperature pulse on the left-hand boundary for the time $t = 0$ ( $j = 0, 1, 2, \dots$ ).
	$Y_j$	Indicates for the times $j \cdot \Delta t$ , the sequence of response factors that are heat flows over the opposite boundary resulting from a unit triangular temperature pulse on the left-hand boundary for the time $t = 0$ ( $j = 0, 1, 2, \dots$ ).
	$Z_j$	same as $X_j$ if the wall were symmetric. Otherwise the definition is similar to that of $X_j$ when the word <i>left</i> is replaced with <i>right</i> .
	$t$	is time
	$\Delta t$	is the size of the time interval. The unit triangular pulse has the duration $2 \cdot \Delta t$ .
	$q_1$	is the heat flow through the left-hand boundary.
	$q_2$	is the heat flow through the right-hand boundary.
	$T_1$	is the temperature on the left-hand boundary.
	$T_2$	is the temperature on the right-hand boundary.

#### 2.6.3.4 Further on the response factor / transfer function method

It is usually not possible in standard use of the response factor / transfer function method to predict the hygrothermal conditions in points within a wall assembly. There are two calculation methods already available in a program like EnergyPlus for hygrothermal response of wall assemblies: Conduction transfer functions (CTF) for thermal transfer, and the effective moisture penetration depth model (EMPD – see Eq. (2.3.17) and text before it) for hygric buffering calculation.

In case of moisture transfer the EMPD is used since characteristic times are usually too long for using moisture transfer functions. The EMPD concept assumes that a thin layer close to the wall surface behaves dynamically and exchanges moisture with the air domain when exposed to cyclic air moisture pulses. For short periods where the cyclic integral of the total moisture adsorption and desorption is near zero (i.e. there is no net moisture storage), the EMPD concept can be a reasonable approximation of reality. The EMPD model assumes no spatial distribution of moisture content across the thickness of the solid; rather, a thin layer of uniform moisture content is assumed to represent the total moisture content of the solid. For constructions with considerable interstitial moisture accumulation, or under conditions where the moisture transport properties exhibit strong moisture content dependency, the EMPD approach may be considered less suitable.

### 3 State of the art of modelling

This chapter intends to highlight some of the analytical and modelling work that has been provided by contributors to Subtask 1. Subsections 3.1, 3.2, 3.4 and 3.5 represent some derivation and review type of work which has been provided by particular members of the Annex. Subsection 3.3 gives an overview of the models that have been used and presented, and adapted or possibly/redeveloped during the course of the Annex. It starts with a rather simple case, where an analytical solution could be provided, then presents simplified modelling approaches. Next (subsection 3.3) whole building simulation tools dealing with moisture are presented, followed by a discussion of the possibilities of airflow integration, and finally the advanced 3D modelling of moist air flows is introduced.

#### 3.1 Analytical solution

By Thomas Bednar and Carl-Eric Hagentoft

To develop a benchmark example which can be solved analytically the following scenario has been defined. The analytical solution takes as a reference the building which has been analyzed in Common Exercise 1, CE1 (see Section 4.1). That building is a simple rectangular house with no inner walls, and it is in general very simply configured.

As the ventilation rate and the outdoor climate are constant and the moisture production is periodic the resulting indoor climate and the moisture content of the construction will reach a periodic state after a long time. The solution for the periodic state can be calculated with Fourier analyses without any additional assumptions. For the development of the indoor concentration for the first days a solution could be found by neglecting the air volume as a moisture capacity. This is a good approximation only if the moisture buffering of the construction is much larger than the air volume. The material parameters for the construction are therefore chosen to represent such a situation.

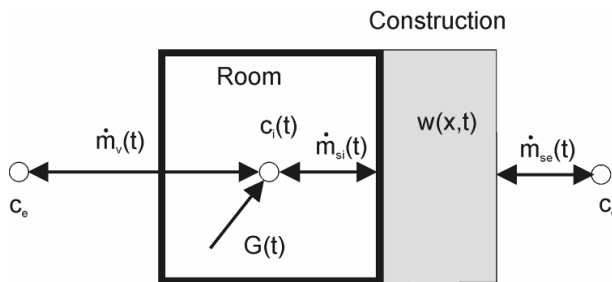


Figure 3.1.1 Mass flow network for CE 1A

The following equations summarize the mathematical formulation of the problem. In the following sections the equations will be solved without moisture transfer to the construction (CE 1A – 0A) and afterwards with moisture buffering in the construction (CE 1A – 0B).

Water vapour is assumed to be an ideal gas

$$p = c \cdot R \cdot T \quad R = 461.5 \frac{\text{J}}{\text{kg} \cdot \text{K}} \quad (3.1.1)$$

The mass flow of moisture through ventilation is calculated from the difference of absolute humidity and the ventilation rate

$$\dot{m}_v(t) = n \cdot V \cdot (c_e - c_i) = R_a \cdot (c_e - c_i) \quad (3.1.2)$$

and the moisture exchange with the construction is

$$\dot{m}_{si}(t) = A \cdot \beta_{Ti} \cdot R \cdot T \cdot (c_i - c) = A \cdot \beta_{Ti} \cdot (c_i - c). \quad (3.1.3)$$

The balance equation for the room, regarding the room volume gives

$$\dot{m}_v + G - \dot{m}_{si} = V \frac{\partial c_i}{\partial t}. \quad (3.1.4)$$

The basic equation for the moisture transfer in the construction is calculated from the balance equation together with Fick's law of diffusion. The sorption isotherm is assumed to be a linear function of the relative humidity.

$$\frac{\partial w}{\partial t} = \delta_c \cdot \frac{\partial c}{\partial x} \quad w = \zeta \cdot \varphi = \frac{\zeta}{c_{sat}} \cdot c \quad (3.1.5)$$

The coupling between room air and construction moisture is done by the following boundary condition

$$\beta_{Ti} \cdot (c_i - c(0, t)) = -\delta_c \left. \frac{\partial c}{\partial x} \right|_{x=0} \quad (3.1.6)$$

$$\beta_{Te} \cdot (c_e - c(L, t)) = \delta_c \left. \frac{\partial c}{\partial x} \right|_{x=L} \quad (3.1.7)$$

Volume and surface area of the room are

$$V = 6 \cdot 8 \cdot 2.7 \text{ m}^3 = 129.6 \text{ m}^3$$

$$A = 6 \cdot 2.7 \cdot 2 + 8 \cdot 2.7 \cdot 2 + 6 \cdot 8 \cdot 2 \text{ m}^2 = 171.6 \text{ m}^2$$

The thickness of the wall is

$$L = 0.15 \text{ m}$$

The air change rate is assumed to be constant

$$n = 0.5 \text{ h}^{-1}$$

and the moisture production inside the room is generated with a square pulse

$$G(t) = \begin{cases} G_0 & 09:00 - 17:00 \\ 0 & 17:00 - 09:00 \end{cases} = G_0 \cdot \sum_{m=0}^{\infty} u(t - (9h + m \cdot 24h)) - u(t - (17h + m \cdot 24h))$$

where  $u(t)$  is the step function,  $G_0 = 0.5 \text{ kg/h}$  and  $m$  is an integer from 0 to  $\infty$ .

The temperature and outdoor conditions are

$$\vartheta_e = \vartheta_i(t) = \vartheta(x, t) = 20^\circ\text{C} \quad p_{sat}(\vartheta_e) = 2342 \text{ Pa}$$

$$\varphi_e(t) = \varphi_i(t) = \varphi(x, 0) = 0.3 \quad c_e = 5.193 \text{ gm}^{-3}.$$

The moisture transfer coefficient is set to the standard value for indoor conditions

$$\beta_{Ti} = \frac{1}{5 \cdot 10^7} \frac{\text{kg}}{\text{m}^2 \text{s Pa}}$$

and the outer surface is considered as vapour tight

$$\beta_{Te} = 0 \frac{\text{kg}}{\text{m}^2 \text{s Pa}}$$

The vapour permeability, moisture capacity and density for the construction material (aerated concrete) is

$$\delta_p = 3 \cdot 10^{-11} \frac{\text{kg}}{\text{m s Pa}} \quad \frac{dw}{d\phi} = 42.965 \frac{\text{kg}}{\text{m}^3} \quad \rho = 650 \frac{\text{kg}}{\text{m}^3}$$

According to Equation (3.1.5) the vapour permeability for the moisture concentration is needed. The conversion is calculated with

$$\delta_c = \delta_p \cdot R \cdot T \quad (3.1.8)$$

### 3.1.1 Solution of CE1A – 0A

Exercise 0A is the simplest case. Assuming no interaction with the construction the balance equation becomes the simple form of the following equation

$$\dot{m}_v + G = V \frac{\partial c_i}{\partial t} \quad (3.1.9)$$

The general solution of such a balance equation together with an initial moisture content  $c_{i0}$  at time  $t_0$  is

$$c_i(t) = c_e + \frac{G}{n \cdot V} + \left( c_{i0} - c_e - \frac{G}{n \cdot V} \right) \cdot e^{-n(t-t_0)} \quad t \geq t_0 \quad (3.1.10)$$

The time schedule of the moisture production can be divided into a period 1 (17:00-09:00) with a duration of  $\tau_1 = 16\text{h}$  without moisture production and a period 2 (09:00-17:00) with a duration of  $\tau_2 = 8\text{h}$  with moisture production.

In the periodic state the absolute humidity at the end of period 2 equals the initial absolute humidity of period 1. This leads to the following equation to calculate the initial moisture content of period 1.

$$c_i(\tau_2) = c_e + \left( c_e + \frac{G_0}{n \cdot V} + \left( c_{i0} - c_e - \frac{G_0}{n \cdot V} \right) \cdot e^{-n \cdot \tau_1} - c_e \right) \cdot e^{-n \cdot \tau_2} = c_{i0} \quad (3.1.11)$$

$$c_{i0} = \left( 1 - e^{-n(\tau_1 + \tau_2)} \right)^{-1} \cdot \left( c_e + \left( \frac{G_0}{n \cdot V} - \left( c_e + \frac{G_0}{n \cdot V} \right) \cdot e^{-n \cdot \tau_1} \right) \cdot e^{-n \cdot \tau_2} \right)$$

The resulting daily average of the indoor relative humidity in the periodic state for this case is

$$\bar{c}_i = c_e + \frac{\bar{G}}{R_a} = 7.765 \text{ gm}^{-3}$$

$$\bar{\phi}_i = 44.86\%$$

### 3.1.2 Solution of CE1A – 0B periodic state:

The solution of the problem for the periodic state can be found with the help of Fourier analyses.

$$c_i = \operatorname{Re} \sum_k \hat{c}_{i,k} e^{ikt \frac{2\pi}{t_p}} \quad (3.1.12)$$

$$k=0$$

$$\hat{c}_{i,0} = c_e + \frac{\bar{G}}{Ra0}$$

$$Ra0 = R_a + A \frac{1}{\frac{1}{\beta_{Ti}} + \frac{L}{\delta_c} + \frac{1}{\beta_{Te}}} \quad (3.1.13)$$

$$k>0$$

$$\hat{c}_{i,k} = \frac{\hat{G}_k}{R_a + A \delta_c m M_{11} + iVk \frac{2\pi}{t_p}} \quad (3.1.14)$$

$$\hat{G}_k = \frac{2 \cdot G_0}{\pi \cdot k} \cdot \sin \frac{k \cdot \pi}{3} \quad (3.1.15)$$

$$M_{11} = \left( \frac{\beta_{Ti} \cdot \beta_{Te}}{\delta_c m} \cosh mL + \beta_{Ti} \sinh mL \right) \cdot \frac{1}{X} \quad (3.1.16)$$

$$X = (\beta_{Ti} + \beta_{Te}) \cosh mL + \left( \frac{\beta_{Ti} \cdot \beta_{Te}}{\delta_c m} + \delta_c m \right) \sinh mL \quad (3.1.17)$$

$$m = (1+i) \sqrt{\frac{\pi k}{a t_p}} \quad (3.1.18)$$

The resulting daily average of the indoor relative humidity in the periodic state is the same as in case 0A as the outer surface is vapour tight.

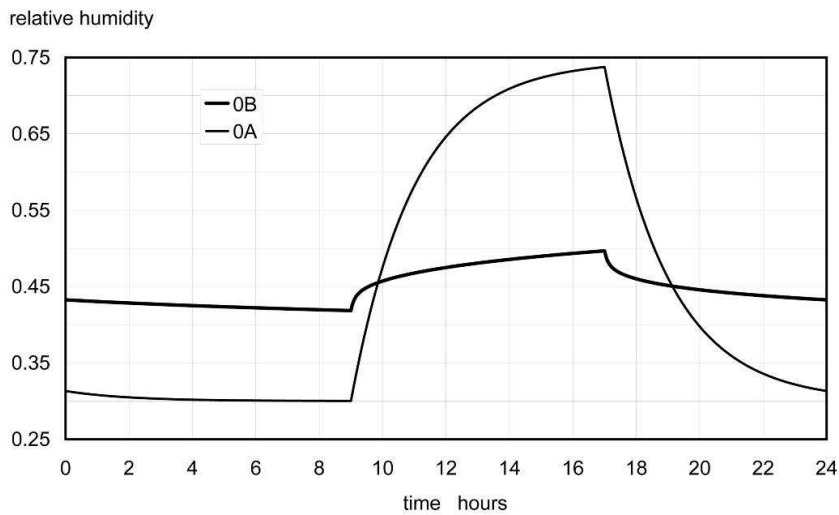


Figure 3.1.2 Solution for the periodic state for CE 1A -0A and 0B

### 3.1.3 Solution of CE1A – 0B first days:

It is possible to find a solution for CE 1A – 0B for the first days if one neglects the influence of the air volume and assumes an infinite construction. The mass balance of the room is reduced to the following form.

$$\dot{m}_v + G - \dot{m}_{si} = 0$$

In Figure 3.1.3 the influence of the air volume on the moisture content of the room is presented. Due to the chosen material parameters the buffer capacity of the construction is much higher than the air volume.

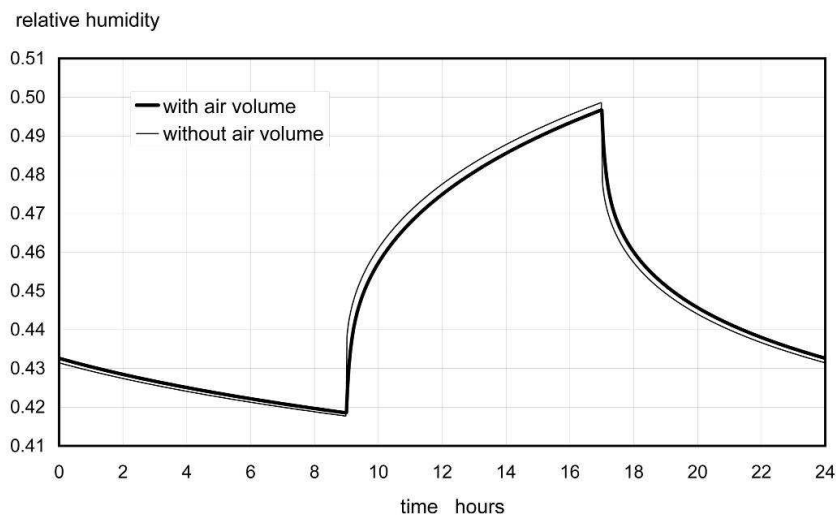


Figure 3.1.3 Solution for the periodic state for CE 1A -0B with and without the buffering effect of the air volume

By using these assumptions one can find the solution by summing up single steps of the moisture production.

$$c(x,t) = c_e + \sum_n c_n(x,t) \quad (3.1.19)$$

$$y \geq 0 \quad c_n(t) = \frac{G_{0,n}}{R_a} \cdot \left( 1 - \left( 1 - \frac{d_s}{d_2} \right) \cdot e^y \cdot \operatorname{erfc}(\sqrt{y}) \right) \quad (3.1.20)$$

$$y < 0 \quad c_n(t) = 0 \quad (3.1.21)$$

where

$$y = \frac{a_c \cdot (t - t_{0,n})}{d_2^2}, \quad d_2 = d_s + \frac{A \cdot \delta_c}{Ra}, \quad d_s = \frac{\delta_c}{\beta_T}, \quad a_c = \frac{\delta_c \cdot c_{\text{sat}}}{\zeta} \quad (3.1.22)$$

and the times  $t_{0,n}$  and the step height  $G_{0,n}$  are presented in Table 3.1.1.

Table 3.1.1 Parameters for the different steps

	0	1	2m m=1..∞	2m+1 m=1..∞
$t_{0,n}$	9	17	9+24*m	17+24*m
$G_{0,n}$	+G <sub>0</sub>	-G <sub>0</sub>	+G <sub>0</sub>	-G <sub>0</sub>

relative humidity

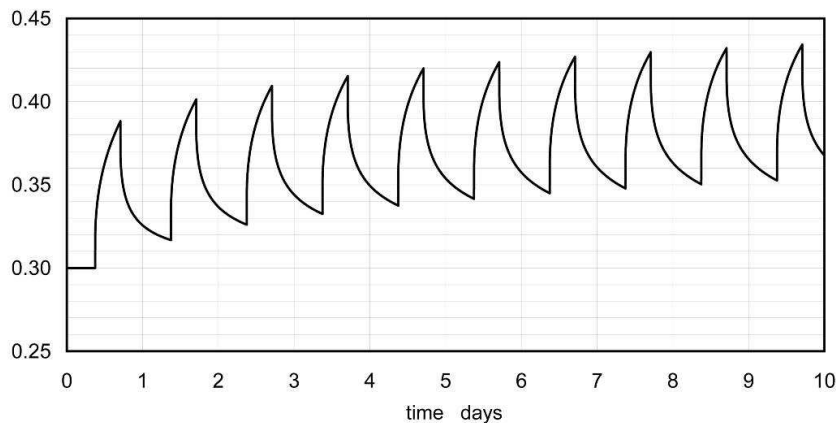


Figure 3.1.4 Solution for CE 1A – 0B during the first days

## 3.2 Simplified models

By Arnold Janssens

### 3.2.1 Introduction

Today different numerical models are available to describe the transient water vapour balance of a room and predict indoor humidity. A typical room moisture balance includes water vapour production by moisture sources (humans, plants,...), convective water vapour transfer with infiltration and ventilation air, and water vapour exchange with the building

fabric and furniture. The water vapour exchange between room air and surrounding materials (walls and furniture) is governed by three physical processes: the transfer of water vapour between the air and the material surface, the moisture transfer within the material and the moisture storage within the material.

A full and coupled calculation of the impact of water vapour storage on the indoor climate is complicated. The detailed knowledge of geometry and properties of many indoor materials is needed, such as building materials, wall and floor finishing, furniture and even books and other hygroscopic objects. This information is often not available. Therefore the moisture exchange between the air and surrounding materials may be modelled in a simplified way.

Although simplified models describe only part of the complex physical reality, they may help in understanding the phenomena involved. For some applications they can give a proper assessment of the indoor humidity dynamics in buildings.

These simplified indoor humidity models are the ones incorporated in the commercial thermal and ventilation building simulation codes, e.g. TRNSYS, EnergyPlus and CONTAM. The main focus of these models is to predict the temperature fluctuations, energy demands or air change rates of individual rooms. As a result the water vapour exchange with surrounding materials is described in a simplified way.

### 3.2.2 Classification of simplified models

#### 3.2.2.1 Governing equations

All simplified models have one basic simplification in common, namely that the air in a room is well mixed, such that the room conditions (temperature, humidity, air pressure) are equal in the whole zone. This is a common assumption for so-called multi-zone models.

Equation (3.2.1) gives the non-steady-state moisture balance for the indoor air in a room, in terms of the partial pressure of water vapour.

$$\dot{M}_p + \dot{M}_{sys} + \frac{\dot{V}_a}{R_v T_i} (p_e - p_i) = \frac{V}{R_v T_i} \frac{dp_i}{dt} + \sum_j A_j \beta_j (p_i - p_{s,j}) \quad (3.2.1)$$

The left-hand side contains all moisture sources: indoor vapour production  $M_p$  (kg/s), vapour addition by the HVAC-system  $M_{sys}$  (kg/s) and vapour gains by ventilation and infiltration. The right hand side contains the terms describing the vapour storage in the air, and the convective vapour transfer from the air to the interior surfaces of the enclosure walls. The balance may be further completed by considering interzonal airflow from adjacent rooms (not taken into account here).

Further symbols are:  $p_i$  and  $p_e$  for the partial water vapour pressures of the indoor and outside air (Pa),  $R_v$  the gas constant for water vapour (462 J/kg/K),  $T_i$  the indoor air temperature (K),  $\dot{V}_a$  the volume flow rate of outside air (m<sup>3</sup>/s),  $V$  the room volume (m<sup>3</sup>),  $A_j$  the area of the interior surface of wall  $j$  (m<sup>2</sup>),  $\beta_j$  the convective surface film coefficient for vapour transfer (s/m) and  $p_{s,j}$  the vapour pressure at the interior surface of wall  $j$  (Pa).

This latter variable couples the enclosure moisture balance to the moisture conservation equations of the walls and materials surrounding the enclosure. Equation (3.2.2) describes the mass balance equation for 1D-transfer and storage of water vapour in a wall with porous building materials:

$$\frac{\partial}{\partial x} \left[ \delta(\varphi) \frac{\partial p}{\partial x} \right] = \frac{\partial w}{\partial t} = \rho \xi(\varphi) \frac{\partial}{\partial t} \left[ \frac{p}{p_{sat}(\theta)} \right] \quad (3.2.2)$$

where  $\delta$  is the vapour permeability (s),  $\varphi$  the relative humidity (-),  $w$  the moisture content by volume (kg/m<sup>3</sup>),  $\rho \xi$  the moisture capacity in terms of relative humidity, derived from the material sorption isotherm (kg/m<sup>3</sup>) and  $p_{sat}(\theta)$  the water vapour pressure at saturation at

temperature  $\theta$ . Vapour transfer and storage properties are typically a function of ambient humidity.

Finally the boundary condition at the interior material surface is:

$$\beta_i \cdot (p_i - p_s) = -\delta(\varphi) \left. \frac{\partial p}{\partial x} \right|_s \quad (3.2.3)$$

### 3.2.2.2 Effective Moisture Penetration Depth Model

The EMPD model is a simplified lumped approach to simulate surface moisture adsorption and desorption (Karagiozis and Gu 2004). This approach is also called the lumped parameter approach (Hens 2005) or buffer storage humidity model (Abadie et al. 2005).

In the EMPD approach, Equation (3.2.2) and (3.2.3) are solved by assuming that only a thin layer near the interior surface interacts with the indoor air (the so-called sorption-active layer or humidity buffer), see Figure 3.2.1. This implies that water vapour diffusion between inside and outside through exterior walls is neglected. The thin layer absorbs and releases moisture to the room air when exposed to cyclic air humidity variations. Temperature and vapour pressure are assumed to vary linearly in that layer (Hens 1991).

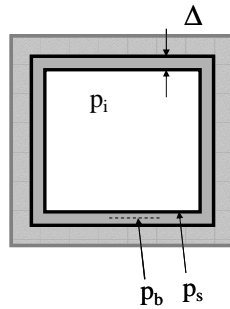


Figure 3.2.1 Representation of the humidity buffering layer.

The depth  $\Delta$  of the sorption-active layer is related to the effective moisture penetration depth EMPD associated with the period of typical fluctuations in the vapour pressure at the wall surface (Cunningham 2003):

$$EMPD = \sqrt{\frac{\delta \cdot p_{sat}(\theta) \cdot T}{\rho \xi \cdot \pi}} \quad (3.2.4)$$

In Equation (3.2.4)  $T$  is the period of the cyclic variation (s). For porous building materials the effective penetration depth for moisture exchange is typically in the order of millimetres for daily variations and in the order of centimetres for yearly fluctuations. It can be shown that 95% of the moisture exchange between the wall and the wall surface occurs in a region of 3 times EMPD near the wall surface.

In the assumption that the wall-air interaction occurs in a humidity buffering layer with thickness  $\Delta$  and linearly varying temperature and vapour pressure, then the equations (3.2.2) and (3.2.3) are reduced to a single equation:

$$\frac{p_i - p_b}{\frac{1}{\beta_i} + Z_b} = \rho \xi(\varphi_b) \Delta \frac{d}{dt} \left[ \frac{p_b}{p_{sat}(\theta_b)} \right] \quad (3.2.5)$$

Here  $p_b$  is the average vapour pressure in the humidity buffering layer (Pa) and  $Z_b$  is the diffusion resistance between the surface and the moisture storage center of the layer (m/s).

The calculation of indoor humidity as a function of time now requires the numerical solution of the set of ordinary differential equations (3.2.1) and (3.2.5).

In the more complete approach Equation (3.2.5) is applied to all wall surfaces. The number of equations to be solved per room is  $j+1$ , with  $j$  the number of humidity buffering surfaces. Non-isothermal conditions are assumed: the temperature that appears in Equation (3.2.5) follows from the solution of the energy conservation equations for the individual walls. The moisture capacity of the intervening layer is a function of the relative humidity of the layer. This more complete approach is used in the computer code EnergyPlus (EnergyPlus 2005).

In a more simple approach Equation (3.2.5) is applied to a single humidity buffering layer with properties representative of the average moisture storage properties of all room surrounding surfaces. Isothermal conditions are assumed when solving the buffering layer mass balance: the temperature of the humidity buffering layer is constant in time. Also the moisture capacity is constant and independent of the layer humidity. This approach is used in the computer codes TRNSYS and Clim2000.

With a single humidity buffering layer with constant properties, the equations (3.2.1) and (3.2.5) may also be solved analytically, as Hens (2005) shows. The solution assumes constant ventilation flow and vapour production rates.

It is clear that a representation of moisture adsorption by a single sorption active layer can model only moisture variations with a single well-defined cycle, e.g. daily fluctuations. To overcome this limitation, the EMPD-approach has been elaborated further in the TRNSYS and Clim2000 codes by dividing the humidity buffer into a surface layer and a deep layer (Abadie et al. 2005, Woloszyn et al. 2005). With this representation both short-term exchanges (between the air and the surface buffer) and mid-term exchanges (using the deep buffer) can be modelled.

### 3.2.2.3 Effective capacitance model

The previous approach is further simplified by assuming that the thermal and humidity conditions in the humidity buffering layer are the same as in the room air, and so the moisture capacities of walls, furniture and room air are combined into a single room moisture capacity (the so-called effective capacitance or air mass multiplier).

Hence the vapour pressure of the wall layer is eliminated from Equation (3.2.1), and the set of 2 equations reduces to a single differential equation, Equation (3.2.6). This simplest approach is also incorporated in most building simulation codes (effective capacitance humidity model). The factor on the right hand side is then treated as a constant capacitance, independent of temperature.

$$\dot{M}_p + \dot{M}_{sys} + \frac{\dot{V}_a}{R_v T_i} (\rho_e - \rho_i) = C \frac{d\rho_i}{dt} \quad (3.2.6)$$

with:

$$C = \frac{V}{R_v T_i} + \frac{(A\rho\xi\Delta)_{eq}}{\rho_{sat}(\theta_i)} \quad (3.2.7)$$

In this equation  $(A\rho\xi\Delta)_{eq}$  represents the equivalent moisture capacity of the room (kg). In order to improve the effective capacitance model Janssen and Roels (2005) introduce a time dependent capacitance given in Equation (3.2.8) in stead of the constant value defined in Equation (3.2.7). This adapted model gives a more reliable prediction of indoor humidity variations in case of a repeated step change in vapour production.

$$C = \frac{V}{R_v T_i} + 2 \frac{t - t_{rev}}{\Delta t_p} \frac{(A\rho\xi\Delta)_{eq}}{\rho_{sat}(\theta_i)} \quad (3.2.8)$$

with  $t_{rev}$  the time point of the most recent production reversal, and  $\Delta t_p$  the time interval of the moisture production phase concerned (Figure 3.2.2).

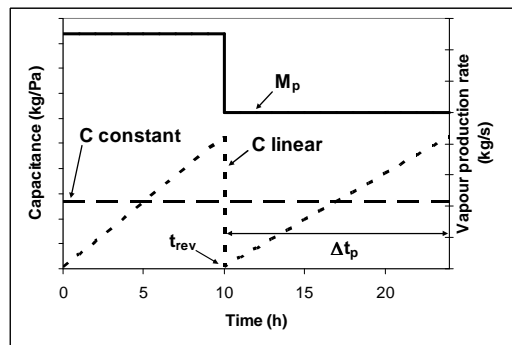


Figure 3.2.2 Proposal for a time dependent capacitance, in line with the moisture production phases, as an alternative to the effective capacitance model.

#### 3.2.2.4 Harmonic analysis

The governing equations may also be solved analytically by means of harmonic signal analysis. In order to apply this methodology, the boundary conditions (outside vapour pressure, vapour production rate) should be decomposed into an average and harmonics of first and higher order by Fourier transform. A constant ventilation flow rate, constant vapour production rate and isothermal conditions are assumed, and this limits the applicability of harmonic analysis.

This methodology is described more in detail by Hens (1991, 2005) and Hokoi (2005).

### 3.2.3 Definition of model parameters

#### 3.2.3.1 Humidity buffering layer

One of the problems with simplified models is to correctly evaluate the model parameters based on the materials that compose the envelope and that are in contact with the room air. Janssens et al. (2005) and Abadie et al. (2005) give some guidance on the choice of the buffering layer thickness  $\Delta$  to be used in the simplified humidity models. They compare simulations of the humidity variation in a room with homogeneous walls in aerated concrete. The comparison shows a good agreement between predictions with the simplified EMPD-model and a HAM-model when the buffering layer thickness is taken equal to the effective moisture penetration depth defined in Equation (3.2.4). The diffusion resistance  $Z_b$  in Equation (3.2.5) is equal to half the diffusion resistance of the buffering layer.

Figure 3.2.3 makes this more clear: it shows a comparison between periodic state solutions of the indoor humidity variation predicted with the simplified models described above, and a state-of-the-art HAM-model (Janssens et al. 2005). The simplified models are the EMPD-model and the EC-model (effective capacitance). In these two models the diffusion resistance and moisture capacity of the humidity buffer are taken constant and evaluated at average indoor humidity conditions. The HAM-model takes the dependency of moisture properties with relative humidity into account.

The humidity variation predicted by the EMPD-model is very sensitive to the proper choice of the buffering layer thickness. Figure 3.2.4 shows this by comparing the previous simulation results to calculations where the buffering layer thickness is taken double and half the value of the EMPD of the wall material. Clearly the humidity variation is underestimated, respectively overestimated, when the model parameters are not properly defined.

In case the humidity absorbing walls are not homogeneous but multi-layered, the model parameters should be calculated from the properties of the finishing layers and one or more of the layers behind. If the thickness of a wall finishing  $d_1$  is larger than its effective moisture penetration depth  $EMPD_1$ , then the influence of other layers is not taken into account. If its thickness is smaller (for instance a wall paper), then the whole finishing layer is considered sorption active and the effective moisture penetration depth of the layer behind is added

(Hens 2005). The model parameters in Equation (3.2.5) are calculated as follows (suffix 1 refers to the wall finishing, 2 to the layer behind):

$EMPD_1 > d_1$ :

$$\rho \xi \Delta = \rho \xi_1 d_1 + \rho \xi_2 EMPD_2 \quad (3.2.9)$$

$$Z_b = 0.5(Z_1 + EMPD_2 / \delta_2) \quad (3.2.10)$$

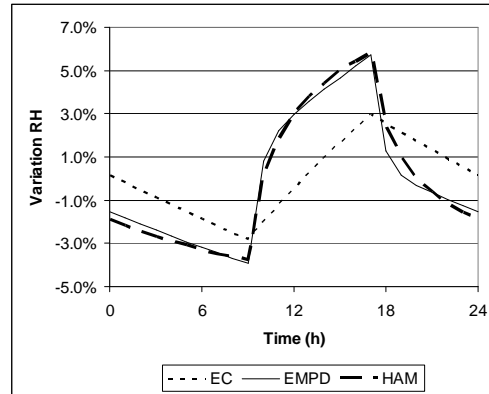


Figure 3.2.3 Periodic state solution of three models: relative humidity variation around the daily average for effective capacitance model (EC), effective penetration depth model (EMPD) and HAM-model.

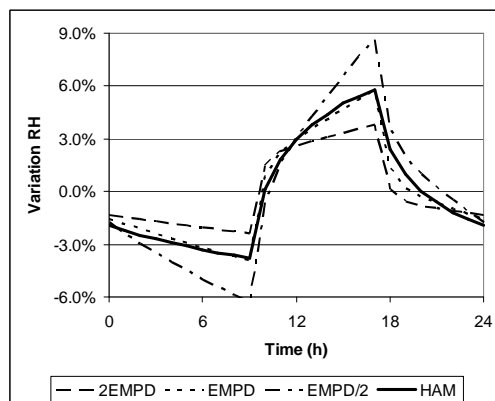


Figure 3.2.4 Periodic state solution of two models: relative humidity variation around the daily average. The figure shows the sensitivity of the EMPD-model to the choice of the buffering layer thickness  $\Delta$

### 3.2.3.2 Effective air capacitance

The hygric inertia of a room is the result of the combination of hygroscopic finishing materials and objects (furniture, books) present in the room, each characterized by a buffering layer thickness and volumetric moisture capacity. The influence of these different materials may be aggregated into a single equivalent moisture capacity of the room  $(A\rho\xi\Delta)_{eq}$ , applied in Equation 7 to calculate the effective room capacitance  $C$ :

$$(A\rho\xi\Delta)_{eq} = \sum A_i\rho\xi_i\Delta_i \quad (3.2.11)$$

As Figure 3.2.3 shows, the effective capacitance model gives a reasonable estimate of indoor humidity variations. However, this simple model is not able to predict the initial fast response of indoor humidity to changes in moisture production, compared to the HAM- and EMPD-model.

Ramos et al. (2005) and Janssen and Roels (2007) propose an alternative method to define the effective capacitance of a room based on measurements of the Moisture Buffer Value of finishing materials according to the Nordtest-protocol. The Moisture Buffer Value (MBV, unit: g/(m<sup>2</sup>·%RH)) indicates the amount of moisture uptake or release by a material when it is exposed to repeated daily variations in relative humidity between two given levels. When the moisture uptake from beginning to end of the exposure to high relative humidity is reported per open surface area and per % RH variation, the result is the MBV (Rode et al. 2005). The moisture uptake of a single object may be characterized similarly per % RH variation as MBV' (g/%RH).

With known Moisture Buffer Values of materials present in a room, the equivalent moisture capacity is given in Equation (2.3.14). The factor 10 appears in the equation to convert units kg/m<sup>2</sup> to g/(m<sup>2</sup>·%).

$$(A\rho\xi\Delta)_{eq} = 0.1 \cdot \left( \sum_{surfaces} A_i MBV_i + \sum_{objects} MBV'_i \right) \quad (3.2.12)$$

The equations 11 and 12 are obviously equivalent. The MBV of a material relates physically to its vapour permeability and hygroscopic moisture capacity. In absence of direct MBV-measurements and if certain requirements are fulfilled (Roels et al. 2005) its value may be calculated directly from Equation (3.2.13), with EMPD defined for a 24h cycle.

$$MBV \approx 10 \cdot \rho\xi \cdot EMPD \quad (3.2.13)$$

The MBV is derived from a measuring protocol where the material is exposed to a moisture loading cycle of 24 h. For this reason, the room moisture capacity derived from Equation (3.2.12) gives reasonable results only for modelling 24 h moisture production regimes (Janssen and Roels 2007).

### 3.3 WBHAM models (overview of models from CE)

By Monika Woloszyn

#### 3.3.1 General presentation

As stated before, it has not been the intention that the subtask and Annex per se should be developing a unique integral tool. The intention was that the Annex by its common authority should stimulate and be a concerting forum for the development among individual researchers of tools which would take as many of the integral aspects into account as possible. The developments could take place by making entirely new models and tools (Tariku et al, 2006), or by extension of already existing tools, as for instance:

- Extending the existing building simulation tools (to account better for processes linked with the envelope), e.g. Rode & Grau, 2003.
- Extending the building component simulation tools, e.g. Holm et al., 2003
- A combination of both building simulation and building component simulation tools, e.g. Koronthalyova et al., 2004.

Therefore several engineering tools were under development during Annex 41 period, improving their capacities to represent coupled heat-air and moisture response of buildings. Some of them are well known building energy simulation software, such as TRNSYS and EnergyPlus, some have more proprietary use, such as PowerDomus, Clim2000 and Spark. They are all able to simulate energy behaviour of a building and of simple heating and

ventilating systems in dynamic conditions. All of them calculate also moisture level in the indoor air and can account for vapour storage in hygroscopic materials. This last phenomenon is modelled either using simple lumped models or using a detailed description of the heat and mass transfer phenomena in the building envelope. In the last case, moisture level in building elements can also be assessed using the simulation tool.

All 16 models presented in this section were used in at least one of the Common Exercises of the Annex, and some improvements were made to them during the project duration. First a brief introduction is given for all the models. Then their main features are contrasted in 10 tables. Evidently, it is impossible to give a full description of 16 simulation tools in a limited number of pages. The aim of this section is to give a general overview of main features, focusing more on moisture modelling and on the interactions between Heat Air and Moisture.

It must also be stated that some of the models are under active development. Therefore between the moments of writing the report and using the information some more or less important improvements can be made.

Table A gives the origin of the tool and main institutions working with it in Annex 41. It can be seen that ten tools are used by developers (HAMLab, Spark...) and six remaining by other institutions (IDA-ICE, TRNSYS...). Five are commercially available, and also five are freeware. Four are only research tools and two personal products. Ten, meaning majority, of the tools originate from energy simulation, four from envelope simulations, and two latest were directly developed as whole building simulation heat-air-moisture tools.

Table B gives a first overview of WBHAM models implemented in the tool. Most of them can simulate a multi-zone building and heat and mass transfer in the envelope. Of course all multi-zone tools can represent mono-zone building. Four tools represent 1-dimensional heat transfer in the envelope (1D H), seven 1-dimensional heat and moisture transfer in the envelope (1D HM) and two 1-dimensional heat, air and moisture transfer in the envelope (1D HAM). Finally only 3 tools can deal with multi-dimensional coupled transfers at building level (2D HAM and 3D HAM). Furniture effect on indoor relative humidity and temperature is not represented as such, but can be approximated as interior building envelope. Some tools use lumped approach. Also, with 3 exceptions the tools can represent most of the typical HVAC systems. However in most of the tools the systems are represented in a rather simplified way, where the action of the system on the indoor conditions is represented without a detailed description of the HVAC element itself.

Main elements of heat model are contrasted in Table C. "Standard" window model means use of standard coefficients, such as U (heat loss), g (solar gain) and SC (shading coefficient). Such model allows also for calculations of heat gains according to the position of sun. "Detailed" window model means that the heat transfer is modelled including convection and radiation between and inside the glazing, etc. Some information are also given on the way how the solar gain are treated. Also wall models are briefly described in this table, and especially if they are treated in 1 or 2 dimensions, and what is the main numerical method used (finite control volume – FCV, finite element method – FEM or transfer function, as described in the previous chapter). Also principles of computing convection and long-wave radiation are presented in this table.

Table D details main characteristics of moisture models. Twelve tools include vapour diffusion through the envelope, seven also liquid diffusion. Moist air diffusion through the envelope, which is one-dimensional air flow through very permeable constructions excluding cracks, can be simulated by five tools (two more will be available soon), and hysteresis effect of sorption isotherm only by one tool. Also a rather large variety of driving potentials for moisture flow can be seen in Table D. For example vapour pressure [Pa] is used in seven tools, moisture content [ $\text{kg}_{\text{vap}}/\text{kg}_{\text{dry\_material}}$ ] also in seven, relative humidity [-] in four and vapour density [ $\text{kg}_{\text{vap}}/\text{m}^3$ ] in two, some tools using more than one. Moreover suction pressure [Pa], Temperature [°C] and volumetric content [ $\text{m}^3.\text{m}^{-3}$ ] are also used.

Table E depicts main characteristics of the airflow models 7 tools. Six have only lumped representation of the indoor air, eight are able to use pressure network to represent more accurately inter-zonal flows and different ventilation systems and one tool is a zonal model, where several control volumes are used to describe one room. Most of the multi-zone model and the zonal model include wind and buoyancy effect, also one-way flow through the cracks in the envelope and indoor partitions, as well as cross-flow through large openings. In most

of the “lumped” models ventilation and infiltration flows can be defined by user and added to energy and moisture balances of the indoor air. Also some tools can be coupled with airflow simulation tools, such as COMIS or CFD to enhance their modelling capacities.

Main couplings between Heat, Air and Moisture models are represented in Table F. Of course all tools represent both latent and sensitive contributions of internal sources. Latent heat due to vapour transfer and to condensation/evaporation process is taken into account in most of the codes, however in most of them it is either in the envelope or in the HVAC system. Only seven tools are able to take both into account. Also most of the multi-zone models can take into account the impact of both humidity and temperature on air density and therefore on buoyancy. Some tools can also represent moisture and temperature impact on some of the material properties.

Numerical methods are contrasted in table G. Some of the simulation tools use an external solver, such as for example Matlab for HAMLab, HAM-Tools and HAMFitPlus. Explicit and implicit methods, as well as constant or variable time-step methods are almost equally distributed. In the envelopes ten tools use Finite Control Volume (FCV) method, four transfer function and three Finite Element Method (FEM). If a mesh is used, it is the same for all transfer process (Heat, Air and Moisture). Moreover in most of the cases (eleven tools) all equations are simultaneously solved ensuring full coupling between different flows.

All the tools can use variable inputs from weather files, however not all the information are used. From table H it can be seen that only five tools are able to deal with wind driven rain and but eight with heat and moisture transfer through the ground. Wind impact on outdoor convection and on infiltrations is rather often represented (twelve tools), as well as the solar shadings from close neighbourhood (eleven tools).

Then some specific features, not described in the first tables are mentioned in table I. It can be seen that several tools include daylight calculations, air quality predictions with CO<sub>2</sub> and VOC calculations, comfort indices and also CAD (Computer-Aided Design) capabilities. Also the new developments encouraged by Annex 41 are described. Fourteen out of sixteen tools were, and are still being, improved during the Annex duration. New developments include mainly enhancement of moisture calculations for energy tools, and improvements of heat and air models in envelope tools, all aiming to improve Whole Building Heat Air and Moisture simulation capabilities.

Finally in table J interested reader can find the main references to the detailed presentation of each tool, its validation and examples of application.

### **3.3.2 Introduction of different software**

#### **3.3.2.1 BSim**

Rode and Grau (2004) present the program BSim2000, which is a computational design tool for analysis of indoor climate, energy consumption and daylight performance of building, developed in Denmark by the Danish Building Research Institute. The core of the system is a common building data model shared by the design tools, and a common database with typical building materials, constructions, windows and doors. The software can represent a multi-zone building with heat gains, solar radiation through windows (with shadings), heating, cooling, ventilation and infiltration, steady state moisture balance, condensation risks. A new transient moisture model for the whole building - its indoor climate and its enclosure - was also developed as an extension of BSim2000. Simultaneously, calculations of transient moisture conditions are carried out for all interior and exterior constructions of the building using full model for humidity balance for zone air and a model for vapour diffusion in the constructions. Also furnishing may be considered as interior building constructions that face the same zone on both sides. BSim has a fairly accurate, yet efficient numerical implementation. Another advantage is that moisture calculations are implemented in an energy simulation tool which is very common in use by building designers/ consultants in Denmark and a few other places. One of the limitations is that liquid moisture transfer in constructions is not yet represented.

### 3.3.2.2 Clim2000

CLIM2000 simulation environment is being developed by Electricité de France (Bonneau et al, 1993). An important advantage of CLIM2000 is its open structure, allowing combinations of existing components with elements created by the user. CLIM2000's library is still growing, but many models exist. A lot of work has been done to validate energy models representing building envelopes (Lomas et al. 1997, Moinard et al. 1998).

The heat modelling includes the enthalpy transported by air flow, the energy sources (internal loads, heating system), the heat transfer through the envelope and eventually latent heat due to moisture changes. The airflow system is based on the popular pressure network model, where nodes represent pressures in each zone and the connections are the flow paths. The air paths include different elements, such as air leakage, ventilation and the coupling of two rooms through an open door model, including cross-flow. Pressure network model in Clim2000 is adapted to represent the moist airflow, introducing air density dependence on moisture as well as on temperature. Moisture balance of the indoor air is also represented including airborne transport, sources, condensation/evaporation and buffering effect of materials, using hygroscopic buffer model by Duforestel and Dalicieux (1994). The comprehensive energy - moisture - airflow Clim2000 model is well adapted to study different situations when moisture impact on energy or airflow can not be neglected. Based on coupled energy - airflow models, it can predict as well energy needs and air flows and can be applied to a large sample of real situations.

The software is implemented in Unix environment with a graphical interface, pre-processor is also available on PC platform. The models are well documented and new modules can be easily added by user. However up to now, Clim2000 software is not commercially available. Also moisture transfer through the walls is not yet included.

### 3.3.2.3 DELPHIN4

The numerical simulation program DELPHIN4 has been developed at the Dresden University of Technology (TUD) to support research in the field of transport processes in porous building materials. DELPHIN4 is based on the software DIM1-3 (1987-1999) developed by the same group. The computer code allows a close-to-reality simulation of the hygrothermal behaviour of building components, i.e. their performance analysis under transient climatic boundary conditions and considering moisture and temperature depended material functions. The software is used to support the development of building materials with optimised physical properties, to design new constructional details with better hygrothermal performance, to evaluate retrofitting measures of old buildings and to investigate the reasons for moisture-related damages. The DELPHIN4 program allows a user-friendly data handling by pre- and post-processing tools. A graphical representation of the analysed constructional detail and its discretisation can be automatically generated. The assignment of material properties and boundary conditions runs interactively. The included material database represents the current research results in material modelling. Up to now the calculation of coupled heat, moisture and air transport through building materials is possible. Modules for salt transport and crystallisation, CFD-calculation in cavities, VOC transport and storage in the material, coupling with TRNSYS are in development and are actually used for scientific purposes. The new integrated room model allows the calculation of the indoor climate in a simplified room as boundary conditions for 1 and 2D-wall details.

### 3.3.2.4 EnergyPlus

A new building energy simulation program, known as EnergyPlus, was first released in April 2001. Building on the capabilities and features of BLAST and DOE-2, EnergyPlus includes many simulation features that have not been available together in a mainstream building energy simulation program. EnergyPlus comprises completely new code written in Fortran 90. It is primarily a simulation engine—with a relatively simple user interface, which does not allow the user to input building geometry graphically. More complete interfaces are available from independent third-party developers. Some key capabilities of simulation engine include variable time steps, configurable modular systems integrated with heat balance-based zone simulation, multiple comfort models, daylighting and advanced fenestration, multi-zone

airflow, displacement ventilation, flexible system modelling, and photovoltaic and solar thermal simulation.

EnergyPlus is a very strong whole building energy model including moisture balance. Moisture sorption by building materials is represented by EMPD model. The ventilation module in early versions of Energyplus was based on COMIS, later versions now include a more complete Air Network model which allows natural ventilation and mechanical systems to interact more fully. Third parties are actively encouraged to develop new modules for EnergyPlus, either by new code written in Fortran or by integration of modules developed in SPARK.

### 3.3.2.5 ESP-r

ESP-r (Clarke 1985) is a modelling system for the assessment of the environmental and energy performance of buildings. It is capable of modelling the heat, power and fluid flows within combined building and plant systems when subjected to control actions. The package comprises a number of interrelating program modules addressing project management, simulation, results analysis and client report generation. In use, the spaces comprising the building are defined in terms of geometry, construction and usage profiles. HVAC systems may then be defined in terms of their comprising components and networks added to explicitly represent air, moisture and power flow-paths. The defined system is then subjected to simulation processing against user-specified control definitions and climate. The problem definition exercise is achieved interactively and with the aid of pre-existing databases offering standard construction materials, glazing systems, event profiles and plant components. The process of problem definition, simulation and results analysis is coordinated by a central Project Manager which supports the importing/exporting of building geometry from/to CAD packages and other simulation environments, e.g. for lighting simulation or time series analysis.

### 3.3.2.6 NPI

NPI is a 1D heat and moisture transport model for a system of structures with ideally mixed and time variably ventilated indoor air space. It was developed at the Institute of Construction and Architecture of Slovak Academy of Sciences and is applied in case studies connected mainly with a diagnostics of moisture induced damage problems. NPI involves also the dependency of material parameters on moisture content but it does not take into account sorption curve hysteresis and air flow through the structures. In the former version of NPI two types of indoor structure were coupled simultaneously with the indoor air. It was changed with the aim to enable coupling with more types of hygroscopic structures/surfaces and not to enlarge the computation time: the current version of NPI does not couple all indoor structures with the indoor air simultaneously but it gradually couples the indoor space only with the one type of structure and afterwards the resulting indoor air RH course is calculated as the weighted mean of the previously calculated indoor air RH courses.

### 3.3.2.7 Coupling ESP-r and NPI

An original way of computing whole building energy behaviour is to integrate several simulation tools. Koronthylova et al 2004 present coupling of NPI and ESP-r. The model created by the coupling of these two independent existing computer tools allows for the simulation of:

- Whole building heat and air transfer (not considering hygric inertia and complex moisture transfer in structures).
- Zone heat and moisture transfer in the adjacent building structures (1D) linked with the air and moisture balance in the zone.
- Zone air flows

The coupling between the tools was realised by the following subsequent steps algorithm realised in each calculation time (hourly) interval at different levels:

- The whole building level - simulation of the 3D heat and air transfer consisting of the modelling of radiation and conduction transfer, together with the air and moisture flows balance of a zone, without hygric inertia (ESP-r).

- Zone level - simulation of heat and moisture transfer in the adjacent envelope structures (1D) linked with the air and moisture balance of the zone (NPI).

Post-processing or coupling of the ESP-r and NPI enables to exploit the capabilities of the both particular tools.

### 3.3.2.8 IDA-ICE

IDA Indoor Climate and Energy (IDA ICE) a tool for building simulation of energy consumption, the indoor air quality and thermal comfort was presented by Kalamees (2004). IDA ICE is commercially available and marketed by the Swedish company EQUA Simulation AB (<http://www.equa.se>). IDA, on which IDA ICE is based, is a general-purpose simulation environment, which consists of the translator, solver, and modeler, developed in Sweden by the Royal Institute of Technology in Stockholm (KTH) and the Swedish Institute of Applied Mathematics (ITM). The mathematical models of the IDA ICE, written in the Neutral Model Format (NMF) have been developed at the Royal Institute of Technology in Stockholm and at the Helsinki University of Technology. IDA ICE covers a large range of phenomena, such as the integrated airflow network and thermal models, CO<sub>2</sub> and moisture calculation, vertical temperature gradients and daylight predictions. To calculate moisture transfer in IDA ICE, the common wall model RCWall should be replaced with HAMWall, developed by Kurnitski and Vuolle (2000). The moisture transfer is modelled by one moisture-transfer potential, the humidity by volume. The liquid water transport is not modelled and hysteresis is not taken into account. Many different cases in whole building heat air and moisture transport can be simulated with IDA ICE, however for comprehensive moisture simulations the computational time is rather high compare to only energy simulations and the interface is not very "user-friendly".

### 3.3.2.9 HAMFitPlus

HAMFitPlus is newly developed during the Annex 41 project by Fitsum Tariku (Concordia University, Canada). This whole building hygrothermal simulation tool is used to assess the durability, indoor conditions (occupant comfort) and also energy efficiency of a building in an integrated manner. It comprises two primary models: Building envelope and indoor models. The building envelope model is developed based on a set of partial differential equations (PDEs) that govern the heat, air and moisture transfer across building envelope components. These nonlinear and coupled PDEs are simultaneously solved for temperature and relative humidity distributions using a finite-element based software called COMSOL Multiphysics (formerly called FEMLAB) and MatLab. This model can be used as a stand alone for simulating HAM transfer in building envelope components, or might be coupled with the indoor model to create the whole building hygrothermal model. The indoor model is used to predict the indoor temperature and relative humidity of a zone taking into account the indoor heat and moisture generations, HVAC system, and dynamic HAM interaction with building envelope components. The heat and moisture balance equations for a zone are solved for the indoor temperature and relative humidity using Simulink and MatLab. In the single zone the indoor air is assumed to be well mixed and uniform inside the room, and consequently, represented by a single node. In multi-zone simulations, the air-exchange between different zones is calculated by coupling with COMIS. The building envelope and indoor models are coupled to form the whole building hygrothermal on Simulink development platform.

### 3.3.2.10 HAMLab

A new integrated heat, air and moisture (HAM) modelling toolkit in MATLAB named HAMLab, developed by the Technical University of Eindhoven (Netherlands), was presented by Van Schijndel (2005). The model based on ELAN, a computer model for building energy design and an analogue hygrothermal model, was implemented in a Building Physics Toolbox in MATLAB (Schijndel and de Wit 1999) and was named WaVo. A major recent improvement is the development of WaVo model in Simulink (HAMBBase) (Wit 2004). The implemented numerical model consists of a continuous part for the HVAC system and the indoor climate, solved with a variable time step and a discrete part, solved with a time step of one hour for the external climate. HAM responses of building constructions and internal/external airflow were modelled and simulated with COMSOL, an environment for

modelling simulations of partial differential equations (PDE). Combining MATLAB/Simulink modelling toolkit with COMSOL allows comprehensive modelling of a room with 2D/3D HAM transport in constructions or 2D airflow. It should be noted that HAMLab models are available for free from the web site and the simulation environment is open - it is relatively easy to integrate new models that are based on ODEs and/or PDEs. MatLab / SimuLink / COMSOL combination provides a powerful & flexible simulation environment, but full 3D HAM models require a lot of computer memory.

#### 3.3.2.11 HAM-Tools

HAM-Tools, presented by Sasic Kalagasidis (2004), is a modular building simulation software, developed in Sweden by Chalmers University of Technology in collaboration with Technical University of Denmark. The main objective of this tool is to obtain simulations of transfer processes related to building physics, i.e. heat and mass transport in buildings and building components in operating conditions. Using the graphical programming language Simulink and Matlab numerical solvers, the code is developed as a library of predefined calculation procedures (modules) where each supports the calculation of the HAM transfer processes in a building part or an interacting system. Simulation modules are grouped according to their functionality into five sub-systems: Constructions, Zones, Systems, Helpers and Gains. The model solves heat air and mass balance equation in an air zone (supposed fully mixed) and in building enclosure, considering air, vapour and liquid transport in one dimension. By combining different modules such as a single-layer wall in a multi-layer wall, a couple of different walls in a zone, several zones in a building, and finally together with climatic load and HVAC equipment, it is possible to build a house as a system. It should be noticed that HAM-Tools has a user friendly interface and can be downloaded as a freeware, and was successfully used by other participants of the annex. The software is an open source, new modules can be easily added by users, and moreover they are free of charge and can be downloaded from internet. As a disadvantage, some calculations can be slow due to the graphical interface, granularity, complexity, flexibility in modelling.

#### 3.3.2.12 PowerDomus

In PowerDomus (Mendes et al., 2003b) heat and moisture transfer in walls are solved simultaneously according to the method developed by Mendes et al. (2002). The use of this method avoids numerical oscillations, since it keeps the discrete equations strongly coupled between themselves, preventing the occurrence of physically unrealistic behaviour when time step is increased and producing a numerically stable method, which is very suitable to be used in building yearly energy simulation programs. Integrated simulation of HVAC systems can be performed for both direct and indirect expansion systems. Different levels of calculation complexity are available (with or without moisture transfers, constant or variable material hygrothermal properties, vapour pressure or moisture content driving potentials...). In total there are 7 levels of HAM models inserted into the program. Graphical interface allows a rapid learning of the programs and makes it a valuable tool for building energy simulation teaching. 2 other programs have been developed during the annex and are being integrated into PowerDomus:

- ViewFactor-LST for numerical and exact calculation of view factors, considering openings and obstructions for any geometry;
- Vitreous-LST for accurate calculation of the combined heat transfer through triple-double- and single-glazing systems;

However, the possibility of airflows between zones is not available yet and simulation time may become high according to the complexity of the building and required accuracy.

#### 3.3.2.13 SPARK

The non-uniform behaviour of the air inside a room, which is important in comfort analysis, can be evaluated by zonal models such as these implemented in SPARK solver. While not as finegrained as CFD simulation, they do give useful information about temperature and moisture distributions that is not available from lumped parameter models. Therefore, we have developed a tool, called SimSPARK, to automatically build dynamic zonal simulations of a building zone. Its model library includes different models to describe heat and moisture

transfers across the building zone envelope, with two of them taking into account moisture adsorption/desorption by building materials. The resulting set of non-linear coupled equations is solved simultaneously by the object-oriented simulation environment, SPARK (Simulation Problem Analysis and Research Kernel). To make easier the development of a zonal model to predict temperature and moisture fields in a building, the latter was divided into two different domains: the indoor air and the building envelope. The zonal model is therefore composed of two different sub-models that correspond to the two domains in that the building was divided.

SimSPARK is suited to parametric studies and complex problems, program oriented object, user free inputs and can be linked to other simulation tools like EnergyPlus. It has also a powerful solver which uses several numerical methods. However, for multilayer walls, time simulation becomes long due to the high number of variables.

#### 3.3.2.14 TRNSYS

TRNSYS (TRAnSient SYStems Simulation) program is a well known building energy simulation tool. It is a transient systems simulation program with a modular structure. It recognizes a system description language in which the user specifies the components that constitute the system and the manner in which they are connected. Some other tools (COMIS, Matlab/Simulink, etc.) can be directly linked to the software. The TRNSYS library includes many of the components commonly found in thermal and electrical energy systems, as well as component routines to handle input of weather data or other time-dependent forcing functions and output of simulation results. The modular nature of TRNSYS gives the program good flexibility, and facilitates the addition to the program of mathematical models not included in the standard TRNSYS library.

Main applications include: solar systems (solar thermal and photovoltaic systems), low energy buildings and HVAC systems, renewable energy systems, cogeneration, fuel cells. It allows also for predictions of the indoor relative humidity, including some buffering effect of materials, using the penetration depth model. Some limitations are implied by the fact that the model can be used only once, so it is difficult to assess the buffering effect in different construction-types. During the Annex work, a new module for moisture buffering was developed by Kwiatkowski et al. 2007 and integrated into TRNSYS.

#### 3.3.2.15 TRNSYS ITT

The software TRNSYS ITT is a tool for building simulation that is based on the framework of TRNSYS 14.1. The wall-model in type 56 (type for a multi zone building) is replaced by a new one (type 158). The new type has the performance for the coupled heat- and moisture transfer in the envelope. Diffusion, liquid water transport, phase changing and icing are taken into account. The heat and moisture fields in the envelope were simultaneously solved with the whole system (building and HVAC-systems). In contrast to the original type 56 the new type 158 is a geometrical model and it is possible to represent realistic rooms and zones (with shading and long wave radiation). A visual interface for the input of the geometrical data is available. An advantage of the software is the possibility of using all the TRNSYS efficiency like integration of a windows library or coupling to MatLab/Simulink. The program is developed for research in the field of enhancement of the components of the heating and ventilation systems and the coupling with CFD programs via a PVM (parallel virtual machine).

#### 3.3.2.16 Wufi +

Holm et al. (2004) describe a holistic model called WUFI-Plus [Holm et al. 2003] based on the hygrothermal envelope calculation model WUFI [Künzel 1994]. The hygrothermal behaviour of the building envelope affects the overall performance of a building. WUFI-Plus is a working combinations of both models, heat and moisture transfer in the building envelope and also whole building simulation tools for energy calculations. It takes into account moisture sources and sinks inside a room, input from the envelope due to capillary action, diffusion and vapour ab- and desorption as a response to the exterior and interior climate conditions as well as the well-known thermal parameters. The coupled heat and mass transfer for vapour diffusion, liquid flow and thermal transport in the envelope parts is a

strong feature of the model. A stable and efficient numerical solver had to be designed for the solution of the coupled and strongly non-linear equations. Indeed, the conductive heat flux and the enthalpy flux by vapour diffusion with phase changes in the energy equation are strongly depending on the moisture fields. The vapour flux is simultaneously governed by the temperature and moisture field due to the exponential changes of the saturation vapour pressure with temperature. By way of well documented field experiments the new model was also validated. Models like WUFI-Plus can help to improve energy simulations because latent heat loads and their temporal pattern can be calculated more accurately. At the same time the determination of indoor air and surface conditions in a building becomes more reliable. This is very important to assess indoor air comfort and hygiene. Post processing models for the determination of mould growth [Sedlbauer 2001] or corrosion risks rely on accurate results of the transient temperature and humidity conditions. The same holds for the design of HVAC systems in heritage buildings or museums [Harriman et al. 2001] where the humidity buffering capacity of the envelope and furniture helps to control temperature and humidity fluctuations.

#### 3.3.2.17 Xam

A heat and moisture simulation program Xam is being developed by IWAMAE. It calculates the annual variations of temperature and humidity in a house and the energy for heating/cooling. The numerical model depends on the simultaneous heat and moisture (humidity ratio) transport in porous 1D wall. The main feature of Xam is the graphical interface of the software. User can set and modify the properties, wall construction and weather condition, etc. Room planning is defined by another program called Marble, which was made by same author in 1996. It has also additional function for simple estimation of hygrothermal properties in 1D wall. User can get the information about the sensitivity of the properties of material on the temperature and humidity variations.

The heat and moisture variations are calculated by the explicit finite difference method. It has an automatic function to avoid the divergence. If the solution shows a sign of small divergence, program goes back to the past step and recalculates with smaller time interval automatically.

In a room space, the temperature and moisture are uniform, inter-room heat and moisture flows due to air flows are calculated. In the latest version, the air flow is defined by user and is constant. In the future version, the air flow will be calculated by the mass balance model.

Table A. General information about the software

Name	Developer	Main user in Annex 41	Availability	Origin	Possibility of adding new components	Remarks
<b>BSim</b>	Danish Building Research Institute (Denmark)	Technical University of Denmark	Commercial program	Energy	No	
<b>Clim2000 3.2.0</b>	EDF (Electricité de France)	Centre de Thermique de Lyon - CETHL, (France)	Research program, not commercially available	Energy	Yes	Core program on Unix workstations
<b>DELPHIN 4.5</b>	TU Dresden, (Germany)	TU Dresden	Research program, commercial version available	Envelope	No	
<b>EnergyPlus v1.2.1</b>	Department of Energy (USA)	University College London, (UK)	Freeware	Energy	Yes	
<b>ESP-r</b>		ICA SAS	Freeware	Energy	Yes	
<b>NPI</b>	ICA SAS (Slovakia)	ICA SAS	Research program	Envelope	Yes	
<b>IDA-ICE</b>	EQUA Simulation AB, (Sweden)	Tallinn University of Technology, (Estonia)	Commercial program	Energy	Yes	The code is open
<b>HAMFitPlus</b>	Concordia University, (Canada)	Concordia University,	Personal Research program (F. Tariku)	HAM whole building	Yes	Requires Matlab/ Simulink and Comsol
<b>HAMLab (Heat Air &amp; Moisture Laboratory)</b>	Eindhoven University of Technology (Netherlands)	Eindhoven University of Technology	Freeware	Energy	Yes	Requires Matlab/ Simulink and Comsol
<b>HAM-Tools</b>	Chalmers University of Technology (Sweden)	Chalmers University of Technology, CETHIL	Freeware	HAM whole building	Yes	Requires Matlab/ Simulink
<b>PowerDomus</b>	LST at the Pontifical Catholic University of Parana - PUCPR, (Brazil)	PUCPR	Not ready for distribution	Envelope	No	
<b>SPARK 2.01</b>	LEPTAB, University of La Rochelle (France)	LEPTAB	Freeware	Energy	Yes	Possible couplings with EnergyPlus
<b>TRNSYS 16.00</b>	University of Wisconsin, Madison, (USA)	University of Gent (Belgium) PUCPR, CETHIL	Commercial program	Energy	Yes	Possible coupling with COMIS
<b>TRNSYS ITT</b>	Solar Energy Lab (University of Wisconsin), TU Dresden, (Germany)	TU Dresden, Germany	Research program	Energy	Yes	All features of TRNSYS available
<b>WUFI-Plus</b>	Fraunhofer-Institut für Bauphysik, (Germany)	Fraunhofer-Institut für Bauphysik	Commercial program	Envelope	Yes	
<b>Xam</b>	Kinki University, Japan	Kinki University, Japan	Personal product by A. Iwamae	Energy	No	Personal use by the author

Table B. General features of whole building Heat Air Moisture models

Name	Granularity	Envelope	Air	Furniture	HVAC Systems
<b>BSim</b>	multi-zone, capable of zonal model	1D HM, air flow through envelope under development	Interzonal flows (including cross flow through large openings), natural and mechanical ventilation	approximated as interior bldg. envelopes	Most of the typical systems
<b>Clim2000</b>	multi-zone, capable of zonal HA model	1D H, vapour diff. through envelope under development	Interzonal flows (including cross flow through large openings), natural and mechanical ventilation	Lumped model for moisture buffering (rendering+furniture)	Most of the typical systems, with detailed representation of some systems
<b>DELPHIN</b>	1 zone	1/2D HAM	1 well mixed volume	No	No
<b>EnergyPlus</b>	multi-zone	1D H	Interzonal flows (including cross flow through large openings), natural and mechanical ventilation	approximated as interior bldg. envelopes	Some of the typical systems, with capabilities of detailed representation of most systems & controllers
<b>ESP-r</b>	multi-zone	1D H	Interzonal flows, natural and mechanical ventilation	No	Most of the typical systems, with detailed representation of systems
<b>NPI</b>	1 zone	1D HM	1 well mixed volume	Yes	No
<b>IDA-ICE</b>	multi-zone	1D HAM	Interzonal flows (including cross flow through large openings), natural and mechanical ventilation	For moisture buffering: approximated as interior building. envelope	Most of the typical systems, with detailed representation. Possibility to create own systems
<b>HAMFitPlus</b>	multi-zone	1/2D HAM	Single zone: Well mixed zone Multi-zone: Coupled with COMIS	approximated as interior bldg. envelopes	Some of the typical systems
<b>HAMLab</b>	multi-zone, capable of CFD	standard 1D HM capable of 1/2/3D HAM	Interzonal flows, (including cross flow through large openings), natural and mechanical ventilation, CFD capabilities,	one parameter for all moisture storage in each zone	Some of the typical systems, with capabilities of detailed representation of some systems & controllers
<b>HAM-Tools</b>	multi-zone	1D HAM	Well mixed volumes, interzonal flows, natural and mechanical ventilation	approximated as interior bldg. envelopes	Most of the typical systems, 2D and 3D floor heating systems
<b>PowerDomus</b>	multi-zone	1D HM, air flow through envelope under development	Well mixed volumes, natural and mechanical ventilation. Possible link with COMIS is under analysis.	approximated as interior bldg. envelopes	Most of the typical systems, with detailed representation of systems
<b>SPARK</b>	zonal model	1D HM	Zonal, represents airflows in one room and intra-rooms, including ventilation	approximated as interior bldg. envelopes	Some of the typical systems, including solar DEC
<b>TRNSYS</b>	multi-zone	1D H	Interzonal flows, ventilation, extensions possible using COMIS	Lumped model for moisture buffering (rendering+furniture)	Most of the typical systems, including many solar components, with detailed representation of systems
<b>TRNSYS ITT</b>	multi-zone	1D HM	well mixed zone, zonal model or interactive coupling with CFD available	Lumped models for heat and moisture buffering	all of the TRNSYS modules
<b>WUFI-Plus</b>	1 zone	1D HM	1 well mixed zone	approximated as interior bldg. envelopes	Most of the typical systems, including heat recovering
<b>Xam</b>	1 zone	1D HM	1 well mixed zone	No	hourly schedule of H&M gain/sink

Table C. Some details of the energy model

Name	Windows	Walls	Indoor Interfaces
<b>BSim</b>	Standard or detailed available solar gains can be calculated in detail for all surfaces	1D H, FCV, mesh defined by user ventilated cavities	Combined constant coefficient for convection and LV radiation, optional separated calculations
<b>Clim2000</b>	Standard and detailed available solar gains on the floor	1D H, FCV, mesh defined by user	Combined constant coefficient for convection and LV radiation, optional separated calculations with constant and temperature-dependent convection and view factors for LV radiation
<b>DELPHIN</b>	No	2D HM, FCV, mesh defined by user	Combined constant coefficient for convection and LV radiation
<b>EnergyPlus</b>	Standard or detailed available solar gains calculated in detail for all surfaces	1D H, Transfer functions	Separated calculations with constant or temperature-dependent convection and view factors for LV radiation
<b>ESP-r</b>	Detailed model, solar gains are calculated from angle dependent glass properties	1D H, FCV, mesh defined by user	Separated calculations with constant or temperature-dependent convection and view factors for LW radiation
<b>NPI</b>	No	1D HM, FCV, mesh defined by user	Combined constant coefficient for radiation and convection
<b>IDA-ICE</b>	Standard and detailed available. Distributed solar gains.	1D HAM, FCV, mesh defined by user	Separated calculations with temperature and slope-dependent convection and view factors for LW radiation
<b>HAMFitPlus</b>	Standard, solar gains: uniformly distributed	1/2D HAM, FEM, mesh defined by user	Combined constant coefficient for convection and LV radiation
<b>HAMLab</b>	Standard or detailed available solar gains	1D H, Transfer functions, capable of 1/2/3D HAM using FCV	Separated calculations with convection and integrating sphere approximation for LW radiation
<b>HAM-Tools</b>	Standard, gains distributed by user or calculated (the first bounce only)	1D HAM, FCV, mesh defined by user	Combined constant coefficient for convection and radiation or separated calculations with constant or temperature dependent convection and exact view factors for LW radiation
<b>PowerDomus</b>	Standard and detailed. Solar gain on the floor.	1D HM, FCV, mesh defined by user. Possible extension with 3D HM model through the ground	Separated calculations with constant and temperature-dependent convection. The program ViewFactor-LST is being integrated to get precise values of view factors, considering obstructions for LW calculation.
<b>SPARK</b>	Standard or detailed available, Detailed solar gains for all surfaces	1D HM, FCV, mesh defined by user	Separated calculations for convection and LV radiation (fictitious enclosure method)
<b>TRNSYS</b>	Standard or detailed available, solar gains can be distributed	1D H, Transfer functions	Combined constant coefficient for radiation and convection or separated calculations with temperature-dependent convection
<b>TRNSYS ITT</b>	Embedding of the WINDOW5 library possible	1D HM, FEM, mesh defined by the program	Separated calculations with constant or temperature-dependent convection (or delivered by CFD) and with view factors for LV radiation
<b>WUFI-Plus</b>	Standard, with solar gains	1D HM, FCV, mesh defined by user (coarse, medium, fine)	Combined constant coefficient for radiation and convection
<b>Xam</b>	Standard, solar gains: divided on the floor and the space	1D H, Transfer functions	Combined constant coefficient for radiation and convection

Table D. Main characteristics of moisture models

Name	Lumped	Diffusion through the envelope			Hysteresis	Driving potentials for moisture transfer
		Vapour	Liquid	Moist air		
<b>BSim</b>	No	Yes	No	Under development	Yes	vapour pressure [Pa]
<b>Clim2000</b>	Duforestel & Dalicieux	Under development	No	No	No	Moisture content [ $\text{kg}_{\text{vap}}/\text{kg}_{\text{dry\_air}}$ ] for airborne flow; vapour density for buffering effect [ $\text{kg}_{\text{vap}}/\text{m}^3$ ] and vapour pressure [Pa] for 1D HM envelope under development
<b>DELPHIN</b>	No	Yes	Yes	Yes	No	Vapour pressure [Pa] for vapour diffusion, moisture content [ $\text{kg}_{\text{vap}}/\text{kg}_{\text{dry\_material}}$ ] or water pressure [Pa] (choice between the 2 models) for liquid water
<b>EnergyPlus</b>	EMPD	No	No	No	No	Relative humidity [-]
<b>ESP-r</b>	-	No	No	No	No	Relative humidity [-]
<b>NPI</b>	No	Yes	Yes	No	No	Relative humidity [-]
<b>IDA-ICE</b>		Yes	No	Yes	No	Vapour density [ $\text{kg}_{\text{vap}}/\text{m}^3$ ]
<b>HAMFitPlus</b>	No	Yes	Yes	Yes	No	Relative humidity [-]
<b>HAMLab</b>	transmittance & admittance	Yes	No	Yes	No	Vapour pressure [Pa]
<b>HAM-Tools</b>	No	Yes	Yes	Yes	No	Vapour pressure [Pa] for vapour flow, suction pressure [Pa] for liquid flow and moist air pressure for air flow [Pa]
<b>PowerDomus</b>	No	Yes	Yes	Under development	No	Temperature and volumetric content [ $\text{m}^3 \cdot \text{m}^{-3}$ ] or vapour pressure [Pa] (choice between different models)
<b>SPARK</b>	No	Yes	Yes	No	No	Moisture content [ $\text{kg}_{\text{vap}}/\text{kg}_{\text{dry\_material}}$ ] and Temperature
<b>TRNSYS</b>	- capacitance - "buffer storage"	No	no	No	No	Moisture content [ $\text{kg}_{\text{vap}}/\text{kg}_{\text{dry\_material}}$ ]
<b>TRNSYS ITT</b>	No	Yes	Yes	No	No	Vapour pressure [Pa] for diffusion, water content [ $\text{kg}_{\text{vap}}/\text{kg}_{\text{dry\_material}}$ ] for liquid transport
<b>WUFI-Plus</b>	No	Yes	Yes	No	No	Vapour pressure [Pa] and moisture content [ $\text{kg}_{\text{vap}}/\text{kg}_{\text{dry\_material}}$ ]
<b>Xam</b>	No	Yes	No	No	No	Moisture content [ $\text{kg}_{\text{vap}}/\text{kg}_{\text{dry\_air}}$ ]

*Table E. Main characteristics of the airflow models*

<b>Name</b>	<b>Air network</b>	<b>Included effects</b>	<b>Airflow between zones</b>	<b>Airflow through the wall</b>	<b>Possible extensions</b>
<b>BSim</b>	Pressure network	Buoyancy and wind effects			
<b>Clim2000</b>	Pressure network	Buoyancy effect	1 way ex/infiltrations cross-flow in large openings	No	
<b>DELPHIN</b>	Lumped	-	No	1D/2D flow + crack flow (flow path model)	
<b>EnergyPlus</b>	Pressure network	Buoyancy and wind effects, plus pressure effects of mechanical system on natural flows	1 way ex/infiltrations cross-flow in large openings	No	
<b>ESP-r</b>	Pressure network	Buoyancy and wind effects	1 way ex/infiltrations	No	
<b>NPI</b>	Lumped	-	No	No	
<b>IDA-ICE</b>	Pressure network	Buoyancy and wind effects	1 way ex/infiltrations cross-flow in large openings	1D flow	
<b>HAMFitPlus</b>	Lumped, capable of pressure network	Buoyancy and wind effects	1 way ex/infiltrations cross-flow in large openings	Capable of 1D/2D flow in porous media and cracks (flow path model)	CFD
<b>HAMLab</b>	Lumped, capable of pressure network	Capable of buoyancy and wind effects	Capable of 1 way ex/infiltrations	Capable of 2D/3D flow in cracks and porous media	CFD with COMSOL
<b>HAM-Tools</b>	Lumped or pressure network	Buoyancy and wind effects, effects of ventilation systems	1 way ex/infiltrations cross-flow in large openings	1D flow	Airflow model can be used stand-alone application
<b>PowerDomus</b>	Lumped	Buoyancy and wind effects	No	1D flow under development	
<b>SPARK</b>	Intra-room pressure network	Buoyancy and wind effects, also empirical laws for jets and plumes	1 way ex/infiltrations cross-flow in large openings	No	
<b>TRNSYS</b>	Lumped	-	Possible defined by user	No	Coupling possible with Comis
<b>TRNSYS ITT</b>	Pressure network by Type157 (based on COMIS)	Capable of buoyancy, wind effects and detailed simulation of ventilation systems	1 way ex/infiltrations cross-flow in large openings	No	CFD (Fluent, PNS)
<b>WUFI-Plus</b>	Lumped	-	No	Infiltration in cracks	
<b>Xam</b>	Lumped	-	Possible defined by user	No	

Table F. Main couplings between Heat-Air and Moisture models

Name	Latent heat	Airflow	Material properties depending on temperature	Material properties depending relative humidity
<b>BSim</b>	In envelopes			
<b>Clim2000</b>	In HVAC systems	T & RH impact on air density and airflow	None	None
<b>DELPHIN</b>	In envelopes	-	thermal conductivity and vapour diffusivity	Yes
<b>EnergyPlus</b>	In HVAC systems	T & RH impact on air density and airflow	None	None
<b>ESP-r</b>	In HVAC systems	T impact on air density and airflow	Thermal conductivity	None
<b>NPI</b>	In envelopes	-	water vapour permeability + moisture diffusivity	water vapour permeability; moisture diffusivity + thermal conductivity (using sorption isotherm)
<b>IDA-ICE</b>	In envelopes In HVAC systems	T & RH impact on air density and airflow	By default: no	water vapour permeability
<b>HAMFitPlus</b>	In envelopes In HVAC systems	T & RH impact on air density and airflow	Only vapour permeability	Yes
<b>HAMLab</b>	Capable of latent heat in envelopes And in HVAC-systems	T & RH impact on air density and airflow	Possible using COMSOL	Possible using COMSOL
<b>HAM-Tools</b>	In envelopes In HVAC systems	T & RH impact on air density and airflow	All	All
<b>PowerDomus</b>	In envelopes In HVAC systems	T & RH impact on air density and airflow	Possible	All properties by means of specific tables
<b>SPARK</b>	In envelopes In HVAC systems	T & RH impact on air density and airflow	Conductivity, Cp for phase change materials	Transport coefficients
<b>TRNSYS</b>	In HVAC systems	T & RH impact on air density and airflow (in COMIS)	No	No
<b>TRNSYS ITT</b>	In envelopes and HVAC systems	T & RH impact on air density and airflow	Yes	Yes
<b>WUFI-Plus</b>	In envelopes	T & RH impact on air density and airflow	None	Water vapour permeability, Thermal conductivity, Liquid, transp. coef. , Heat capacity
<b>Xam</b>	In envelopes In HVAC systems	T & HR impact on air density and airflow	No	No

Table G. Numerical methods used in the tools

Name	Transfer in building elements	Time integration	Coupling	External solver
<b>BSim</b>	FCV (HM), mesh can be user defined, typical size : few cm per CV	Implicit, constant time-step	Intermittently between the different types of flow	
<b>Clim2000</b>	FCV (H), mesh is user defined, typical size : few cm per CV	Implicit, variable time-step	All the equations solved simultaneously if convergence problem appear an iterative block method can be used	ESACAP
<b>DELPHIN</b>	FCV (HM) typical mesh size: (1D 100...200 Elements / 2D <10.000 elements)	Variable time-step	All the equations solved simultaneously	CVODE Solver
<b>EnergyPlus</b>	Transfer function for heat transfer	Constant time-step		
<b>ESP-r</b>	FCV (H), maximum 24 volumes per element	Can be chosen: explicit, implicit or Crank Nicholson, constant time step	All the equations solved simultaneously	
<b>NPI</b>	FCV (HM), same mesh for heat and moisture, about 1mm size	Implicit (Crank Nicholson), constant time-step	All the equations solved simultaneously	
<b>IDA-ICE</b>	FCV (HAM), mesh can be defined by user, same mesh for heat, air and moisture	variable time-step	All the equations solved simultaneously	yes
<b>HAMFitPlus</b>	FEM (HAM), mesh can be defined by user, typical size: 1 to 5 mm per element	Explicit, variable time-step	Separate solving for indoor air and envelope with periodical coupling	MATLAB COMSOL
<b>HAMLab</b>	Transfer function for heat transfer Capable of FEM (HAM)	Combinations of implicit, explicit, constant time-step, capable of variable time-step	Different solutions for heat and moisture or air and envelope	MATLAB
<b>HAM-Tools</b>	FCV (HM), mesh can be defined by user, no limits in number of elements Typical size: 1cm per CV, 0.0001 mm at contact surfaces when liquid flow is present.	Explicit, Variable time-step,	All the equations solved simultaneously	Standard ODE solvers included in MATLAB
<b>PowerDomus</b>	FCV (HM), mesh can be user defined typical mesh size: 1 volume/mm	Implicit, constant time-step from 1s to 24h is user defined	All the equations solved simultaneously (MTDMA – MultiTriDiagonal Matrix Algorithm)	
<b>SPARK</b>	FCV (HM), mesh can be user defined typical	Implicit, variable time step	All the equations solved simultaneously	
<b>TRNSYS</b>	Transfer function for heat transfer	Constant time-step	All the equations solved simultaneously	
<b>TRNSYS ITT</b>	FEM (HM), user defined mesh size, typical mesh size: 50 layers for each wall (distributed with a nonlinear function)	A combination of implicit and explicit methods with variable time-step	All the equations solved simultaneously	
<b>WUFI-Plus</b>	FCV (HM), expanding and contracting mesh	Implicit, constant time-step	All the equations solved simultaneously	
<b>Xam</b>	Transfer function	Explicit, Constant time-step, capable of variable time-step	all the equations solved simultaneously	

When ESP-r + NPI are coupled, results of energy simulations (as indoor air temperature, calculated by ESP-r) are used as inputs for NPI calculation

Table H. Representation of outdoor boundary condition

Name	Wind driven rain	Wind	Neighbourhood	Ground
<b>BSim</b>	No	Impact on outdoor convection Impact on infiltrations		Simple representation HM possible
<b>Clim2000</b>	No	Impact on outdoor convection Capable of impact on infiltrations	No	No
<b>DELPHIN</b>	Yes	No	No	No
<b>EnergyPlus</b>	No	Impact on outdoor convection Impact on infiltrations	Shadows for solar radiation	Heat transfer
<b>ESP-r</b>	No	Impact on outdoor convection Impact on infiltrations	Shadows for solar radiation	Heat transfer
<b>NPI</b>	No	No	No	No
<b>IDA-ICE</b>	No	Impact on infiltrations and on outdoor convection	Shadows for solar radiation	Heat transfer
<b>HAMFitPlus</b>	Yes	Impact on outdoor convection Impact on infiltrations	Shadows for solar radiation Adjustable coefficients for Wind profile, Wind-driven rain load	Heat and moisture transfer
<b>HAMLab</b>	Capable of	Capable of wind impact on infiltration/ventilation	Shadows for solar radiation Local pressure coefficients for wind,	Heat transfer
<b>HAM-Tools</b>	Possible with simplified models	Impact on outdoor convection Impact on infiltrations	Shadows for solar radiation Local pressure coefficients for wind, local temperature for radiation	Heat and moisture transfer
<b>PowerDomus</b>	No	Impact on outdoor convection Impact on infiltrations	Shadows for solar radiation	Heat and moisture transfer
<b>SPARK</b>	No	No	Shadows for solar radiation	Heat and moisture transfer
<b>TRNSYS</b>	No	No, In Comis impact on infiltrations available	Shadows for solar radiation	Heat (ground temperature as a boundary)
<b>TRNSYS ITT</b>	No	Impact on outdoor surface coefficients (heat and moisture) Impact on air flow network (Type 157)	Shadows for solar radiation	1 D - Heat and moisture transfer
<b>WUFI-Plus</b>	Yes	Impact on outdoor convection Impact on infiltrations	Shadows for solar radiation (simplified)	Simple representation with adjusted T&RH
<b>Xam</b>	No	No	Shadows for solar radiation	Calculated as a very thick wall

Table I. Specific characteristics and new developments

Name	Special features	New developments for Annex 41
<b>BSim</b>	Solar distributions; Daylight; PhotoVoltaics; Bldg. regulations compliance check; Import of CAD geometry (semi-automatic)	Model for outdoor ventilated cavities Model for 1D airflow through envelopes
<b>Clim2000</b>	Heat-air zonal models; Simple daylight calculations	1D HM model for the envelope is being developed
<b>DELPHIN</b>		A room lumped model added to the DELPHIN 4 for simulations of CE
<b>EnergyPlus</b>		A new module for EnergyPlus is under development and testing. This comprises of a 1D HAM model applied to the envelope
<b>ESP-r</b>	Daylight level at an arbitrary room location; Comfort indices (PPD, PMV...) CO <sub>2</sub> calculations... ; Possible coupling with CFD	coupling ESP-r with NPI
<b>NPI</b>		Coupling ESP-r with NPI; Water vapour permeability dependence on moisture, Improvement of the numerical methods
<b>IDA-ICE</b>	Daylight level at an arbitrary room location; Thermal bridges and furniture; Comfort indices (PPD, PMV...), CO <sub>2</sub> calculations Air temperature stratification in displacement ventilation; Total energy cost based on time-dependent prices.	
<b>HAMFitPlus</b>	Coupling with COMIS for energy and indoor humidity calculations of multi-zone buildings	Newly developed
<b>HAMLab</b>	Combining MATLAB/Simulink modelling toolkit with COMSOL allows comprehensive modelling of a room with 2D/3D HAM transport in constructions and 2D airflow	Wind/thermal induced ventilation modelling D HAM Construction modelling encouraged, 3D HA Zone modelling Sensitivity & uncertainty modelling
<b>HAM-Tools</b>	Transfer of VOCs (volatile organic compounds) Coupled HAM and VOC transfer in building envelopes	long-wave radiation heat exchange between internal surfaces using exact view factors
<b>PowerDomus</b>	3-D building display and 2-D surface plan display HVAC air-side and water-side system diagramming PMV and PPD, thermal loads statistics, integrated fluxes Visualization of Sun path; 1-minute time intervals for schedules	Vapour pressure based model for moisture transport was included Central HVAC system model, graphical interface, convective heat transfer correlations; Integration of detailed calculation of view factors and heat transfer through complex glazings;
<b>SPARK</b>	Comfort indices, earth to air heat exchanger, heating floor	Multi-layers walls
<b>TRNSYS</b>	Comfort indices, many HVAC systems including solar components,	Development of detailed moisture transfer envelope component
<b>TRNSYS ITT</b>	Coupling with CFD (ParallelNS, Fluent) by using a PVM (parallel virtual machine) as managing platform	general enhancement of the tool
<b>WUFI-Plus</b>	Generating of building geometry, 3D-view of building, CO <sub>2</sub> calculations, Database support, Seasonal definition of daily pattern of design conditions, occupancy and equipment	Optional outer climate of measured data, Optimising of numerical methods
<b>Xam</b>	Auto-recalculation function for anti-divergence	Coupling with CFD results for air movement in the room (commercial code STREAM)

Table J. References

Name	Web site	Detailed presentation of the tool	Validation	Examples of application
<b>BSim</b>	www.bsim.dk	Rode and Grau, 2004 <sup>a</sup> Rode, 2004.	Rode and Peuhkuri, 2006. Lengsfeld, 2006.	Rode and Peuhkuri, 2006. Lengsfeld, 2006.
<b>Clim2000</b>	-	Duforestel and Dalicieux. 1994. Woloszyn et al. 2004.	Plathner and Woloszyn, 2002. Lomas, K.J. et al. 1997.	Woloszyn et al. 2005 Woloszyn et al. 2000
<b>DELPHIN</b>	www.bauklimatik.-dresden.de	Grunewald, 1996 Grunewald. 2000.	Häupl et al. 2004	Grunewald et al. 2006 Häupl and Fechner, 2003
<b>EnergyPlus</b>	www.energy-plus.org	Crawley et al. 2004 Crawley et al. 2000	Henninger et al 2004 Witte et al 2004	Hong et al 2003 Ridley et al 2004
<b>ESP-r</b>	www.esru.strath.ac.uk	Clarke, 1985 Koronthályová et al. 2004a	Koronthályová, 2006	
<b>NPI</b>	-	Koronthályová et al. 2004b	Koronthályová et al. 2006	Koronthályová, 1998
<b>IDA-ICE</b>	http://www.equa.se	Sahlin et al. 2004 Sahlin, 1996 Kurnitski, and Vuolle, 2000.	Achermann. 2000. Kropf and Zweifel, Kurnitski and Vuolle, 2000.	Kurnitski et al. 2007
<b>HAMFitPlus</b>	-	PhD Thesis (In progress)	In progress	Tariku et al. 2006
<b>HAMLab</b>	http://sts.bwk.tue.nl/hamlab/	Schijndel, 2007. Wit, 2006.	Schijndel, 2007. Wit, 2006.	Schijndel, 2007. Wit, 2006.
<b>HAM-Tools</b>	www.ibpt.org	Sasic Kalagasidis, 2004b.	Hagentoft et al. 2004. Sasic Kalagasidis, 2004a.	Sasic Kalagasidis et al. 2005. Sasic Kalagasidis, 2007a and b.
<b>PowerDomus</b>	www.pucpr.br/LST	Mendes et al., 2002 Mendes and Philippi, 2004 Mendes and Philippi, 2005 Mendes et al. 2003b Mendes et al., 2005a Barbosa and Mendes, 2007	Abadie and Mendes, 2006 Akinyemi and Mendes, 2007 Mendes et al. 2003	Mendes et al. 2003 Mendes et al. 2005b Santos and Mendes, 2006
<b>SPARK</b>	http://gundog.lbl.gov/		Wurtz et al. 2006 Mora et al. 2004	Wurtz et al. 2005 Mendoca et al. 2005
<b>TRNSYS</b>	sel.me.wisc.edu/trnsys/	Klein et al. 2004 Crawley et al. 2005	Voit et al. 1994	Breesch. 2006
<b>TRNSYS ITT</b>	www.tu-dresden.de	Perschke, 2000. Klein et al. 2004	Lengsfeld, 2006	Perschke and Meinhold 2007
<b>WUFI-Plus</b>	www.wufi.de	Holm 2003	Lengsfeld, 2006	Holm 2003
<b>Xam</b>	-	Iwamae et al., 1999 Iwamae, 2004	Not yet	none

### 3.4 Airflow integration

By Angela Sasic Kalagesidis

Flow of air in buildings is governed by wind, differences in temperature between air zones and by mechanical ventilation systems. The differences in pressure thereby induced, force the air to move through openings and leakages in a building envelope and cause the air to circulate within a single zone. As a result, the modelling of air flow in buildings assumes the following calculation tasks:

- Wind-induced air pressure field around and inside a building
- Temperature-induced air pressure field inside a building
- Pressure field inside a building, caused by mechanical ventilation systems
- Flow of air through a ventilation system and through openings, cracks, air permeable materials and constructions in a building envelope

Each of these tasks represents a complex flow problem that is not straightforwardly measured or simulated.

The main difficulty with measurements is in the problem separation and localization; the flow is caused by several driving forces at the same time, it is often spread over large air volumes or hidden inside a building envelope where it takes complex flow paths, and, due to very small (almost negligible) inertia, all changes in boundary conditions are promptly propagated throughout the entire system. This latter is particularly associated to the measurements taken in field, whereas it can be much better controlled in laboratory conditions. Large number of possible flow geometries and the deviations of these due to the differences in workmanship, make the results of flow measurements as merely quantitative data. A statistical approach is obviously needed here, but it implies a considerable amount of work. The initiative of AIVC<sup>1</sup> centre on collecting the data on air flow characteristics of leakages and penetrations in a building envelope and on wind pressure coefficients into a publicly available catalogue is therefore particularly useful (AIVC, Technical notes). Unfortunately, the number of attempts in this direction has not been changed much since the first work carried out in the nineties.

The difficulties associated with modelling of convective flow fields have led to the development of specialized computational tools, the so-called computational fluid dynamics (CFD) tools<sup>2</sup>. CFD simulations provide credible solutions for some of the air flow problems in buildings, such as airflow patterns around high-rise buildings (ref. to B. Blocken's report, 2005?), or airflow rates through selected assemblies and leakages in timber-framed constructions (ref. to B. Mattsson's thesis, 2007). Direct application of CFD tools for whole building HAM simulations is attractive but also difficult. There are several reasons for this: CFD simulations normally investigate flow problems expressed in seconds and hours, as opposed to months and years needed in building simulations, demanding high computational capacity and user expertise. In addition, the moisture storage in walls, which is essential for whole building simulations, is poorly described there. It is quite possible that some future releases of commercial CFD tools will include this phenomenon as well. Some possibilities for applying CFD simulations in practice are seen through the integration with building simulation tools. Meanwhile, the results of CFD simulations can be used as complementary investigations for building simulations, for testing, for example, assumptions on boundary conditions or on the flow pattern inside an air zone.

Consequently, when integrating the air flow into the hygrothermal calculations for buildings, a variety of assumptions has to be made. The assumptions regard, for example, external boundary conditions in terms of a presupposed wind speed and wind pressure coefficients, a homogeneity of air enclosed in a zone, positions of leakage paths in a building envelope and the flow characteristics of these. The uncertainties thereby introduced, suggest that the results of air flow simulations should be taken with caution. This can be somewhat compensated by the detailed parametric and sensitivity analyses. A set of operating

---

<sup>1</sup> Air ventilation and infiltration centre

<sup>2</sup> CFD (computational fluid dynamics) is a term used for numerical solutions of the governing equations which describe the fluid flow: conservation equations for mass, momentum (described by Navier-Stokes equations) and energy.

scenarios that can be identified by these tests, lead to a better understanding of the problem and, at the same time, may increase the confidence in the results.

### 3.4.1 Airflow problems presented within Annex 41

#### 3.4.1.1 Space ventilation

All exercises that are enclosed in Subtask 1 consider a simple airflow problem, the space ventilation by outdoor air with a constant (CE 1-3) or a variable (CE 4) airflow rate. The solutions provided by the participating models are based on the assumption of a well-mixed air. In that case, the conservation equations of heat and moisture for the air read:

$$\begin{aligned}\rho c_a \frac{\partial \theta_m}{\partial t} &= \sum_i S_i \\ \rho \frac{\partial x_m}{\partial t} &= \sum_j M_j\end{aligned}\quad (3.4.1)$$

where  $S_i$  and  $M_j$  denote heat and moisture gains from walls, ventilation or other sources.

When the airflow is known, as is the case here, the ventilation heat and moisture gains are readily defined as:

$$\begin{aligned}S_{vent} &= n_v \rho c_a V (\theta_{out} - \theta_m) \\ M_{vent} &= n_v \rho V (x_{out} - x_m)\end{aligned}\quad (3.4.2)$$

This simplification was purposely introduced to decrease the number of sources of disagreement between the solutions. Based on this, in the two exercises where the measured data were provided (CE 2 and 3), the erroneous values on airflow rates were discovered by calculations (reference to the report on CE 2 and CE 3). In both cases, the walls were vapour-tight and the indoor air humidity was influenced by ventilation only. Results of calculations were in a very good agreement, while the measured data appeared displaced. Additional measurements confirmed that the airflow data had been indeed erroneous.

#### 3.4.1.2 Air filtration through a building envelope

Temperature and pressure gradients across walls' boundaries may lead to the onset of air convection inside air permeable materials and cavities, or to the air filtration through the wall. Depending on the magnitude and direction of the air flow, the convective transport of heat and moisture, induced in this manner, may become a dominant transfer mechanism in comparison to the heat conduction and vapour diffusion. This influence is described by the additional convective terms in the heat and vapour transfer equations for a wall:

$$\begin{aligned}q &= -\lambda \nabla \theta + c_a m_a \theta \\ m_v &= -\delta \nabla p + m_a x\end{aligned}\quad (3.4.3)$$

Air filtration is rarely one-dimensional (1D), but a two- or three-dimensional (2D, 3D) phenomenon. The flow equations (3.4.3) are still valid, except that the number of terms in their developed form increases due to the derivation over additional directions. Consequently, the time needed for the numerical solution will be greatly increased.

The convective terms may require another space-discretization techniques and numerical solver than those used for the diffusive problems, which additionally complicates the numerical model. The true difficulty appears where the pressure difference that governs the flow is unknown. This is a common case when the air filtration is caused by wind or by temperature differences. In such cases, the pressure inside a house has to be found in an iterative way to satisfy the conservation equation of mass balance for air:

**Commentaire :** Add units  $J/m^3$ , respectively  $kg/m^3$

**Commentaire :** The units for S and M are not consistent between Eq. (3.4.1) and Eq. (3.4.2)

**Commentaire :** The symbol for air flux should be made consistent with previous definitions

$$\sum_k m_{a,k} A_k = 0 \quad (3.4.4)$$

Equation (3.4.4) is valid for so-called one-node zone models, based on the assumption about a well-mixed air inside a zone. The more detailed model for the air inside a zone is discussed hereafter.

Heat and moisture, brought to a space by air infiltration, appear as additional sources in the balance equation (3.4.1):

$$\begin{aligned} S_{fil} &= c_a m_a A_{fil} (\theta_{fil} - \theta_{in}) \\ M_{fil} &= m_a A_{fil} (x_{fil} - x_{in}) \end{aligned} \quad (3.4.5)$$

The temperature and the moisture ratio at the air outlet from the wall,  $\theta_{fil}$  and  $x_{fil}$ , are found from the coupled balance equations for the air space (see equations (3.4.1)) and for the wall.

Examples of modelling the HAM response of a building in the presence of the air filtration through a building envelope are presented in the following two studies: Sasic, 2007 and Schijndel, 2007. The main modelling principles are outlined below.

*Hygrothermal response of a house with dynamical insulation in the roof. Case study: test house from CE 1.*

(A. Sasic Kalagasidis, 2007)

This work concerns the thermal efficiency of a dynamical insulation and the hygrothermal response of a building in relation to the air-tightness of a building envelope. The study is carried out for the test house from CE 1, where some additional details are introduced for the airflow calculations: the exposure of the house to the wind, the air-tightness of the construction and the flow characteristics of the dynamical insulation and the fan. Temperature and moisture distribution in walls and the dynamical insulation are studied using the 1D approach and the indoor air is assumed well-mixed (the one-node model). The pressure field inside the house is governed by the fan and by temperature and wind-induced pressure differences.

*Impact of airflow through a 2D envelope, a case study*

(J. van Schindjel, 2007)

The study also concerns the test house from CE 1. The geometry of the house and the materials are the same as in the original case, except that the whole construction is air permeable. The accidental air infiltration or ex-filtration through the building envelope is governed by wind-induced pressure differences. During the air infiltration, the wall becomes drier and colder. Opposite to that, the air ex-filtration warms up the wall and causes moisture accumulation inside it. The hygrothermal response of the construction is studied using the 2D approach, while the indoor air is modelled as well mixed. Results are given for the following test cases: without air movement through the construction, with air infiltration and with air ex-filtration.

#### 3.4.1.3 Air flow between zones

Air flow through leakages in a building envelope, usually considered as uncontrolled or unintentional ventilation, has actually both positive and negative effects. The positive effects are seen in improved overall ventilation of a building in the cases where regular ventilation is not sufficient. The negative effects are found in additional heating or cooling losses thereby induced, and in disturbances created in operation of mechanical ventilation systems. When the moisture balance is of interest, the uncontrolled ventilation has, again, both positive and negative effects. In cold and moderate climates, it helps in reducing the moisture content indoors. Conversely, in hot and humid climates, the outside air is a source of moisture. Thus, a simple design rule can be established: whenever a humid air enters a zone with a lower temperature, a special attention has to be paid on the increased moisture content in that zone.

The size and distribution of air leakages (and openings) determine not only the inflow of outdoor air into a building, but also the movement of indoor air between air zones and its outflow from a building. In cold and moderate climates, the indoor air appears as a moisture source when passing from a warmer to a colder zone. Therefore, it is important to have in mind that the above established rule applies also on the outflow of air from a building. The critical parts of a building are those exposed to internal over-pressure, such as ceilings and attics, because it is where the indoor air leaves the building. The moisture deposit from the air increases the moisture content in such parts of a building construction and sometimes even leads to severe moisture damages.

The modelling of air flow between zones and the moisture damages in a building construction caused in that way, are presented in the following two studies: Hens, 2006 and Sasic and Mattsson, 2005.

*Impact of adventitious ventilation on the moisture performance of roofs in moderate climates*  
*H. Hens*

Simple steady-state analyses are presented for a case where uncontrolled ventilation has a negative impact on the moisture performance of a roof. The following three conditions are needed for the occurrence of such a problem: the air-tightness of a building envelope is poor, a part of uncontrolled ventilation air leaves the building by ex-filtration through the roof, and the ventilation of a building is moderate enough to create a larger vapour excess between the indoor and outdoor air. Results, referred to a two-story building in a moderate climate, are proven by field observations.

*Modelling of moisture conditions in a cold attic space*

*A. Sasic Kalagasidis, B. Mattsson. 2005. Paper presented at the 26<sup>th</sup> AIVC conference.*

This study presents results from numerical investigations of the impact of wind and air infiltration from a living space on the moisture conditions in a cold attic. The role of attic ventilation is analyzed by comparing the ventilated with unventilated attics, with and without air infiltration from inside the dwelling. Air infiltration rates are modelled by taking into account the pressure distribution around and inside the building as a whole. The simulations are performed using a commercial CFD tool for attic ventilation rates and a building simulation tool for air infiltration rates through the attic floor and the hygrothermal states in the attic.

#### 3.4.1.4 Cavity ventilation

Building envelope components often contain outdoor ventilated cavities, or spaces such as attics or crawl spaces could be seen as specialized variations of ventilated cavities.

However, the ventilation in such cavities is not very often calculated in building simulation tools, since the constructions are normally represented by the one-dimensional flow that passes perpendicular to the plane of the constructions, whereas the cavity ventilation is parallel to the constructions. Stovall and Karagiozis (2004) present a detailed CFD analysis of the air flow pattern in a cavity, whereas Grau and Rode present a simple model to approximate in one-dimensional calculations perpendicular to the wall, the hygrothermal effect of cavity ventilation.

*CFD analysis of a ventilated brick cavity*

*T. Stovall, A. Karagiozis, 2004*

The inclusion of a ventilated air space within a brick cladding wall system has been shown to improve the moisture transport of the wall assembly. A parametric analysis using a commercial CFD model was constructed to investigate the influence of weather variables, including wind speed, insolation and outdoor air temperature for brick rain screen wall configurations. The configurations included multiple cavity depths and vent sizes. All models were based on a single-story building height with wind perpendicular to the wall. The results were used to develop a number of correlations intended to supplement the accuracy of transient hygrothermal models.

*A model for air flow in ventilated cavities implemented in a tool for whole-building hygrothermal analysis*

*K. Grau and C. Rode, 2006*

A model for calculating air flows in ventilated cavities has been implemented in a whole-building hygrothermal simulation tool. The ventilated cavity is modelled as another hygroscopic material in the sequence of layers that form the multilayered structure. However, the material is chosen such that it has some, but only a rather limited hygroscopic capacity and diffusion resistance. However, this material is just used as a dummy layer to hold the properties of the air that is passing through the cavity. The air flow is driven by an air pressure difference between inlet and outlet, which is caused by wind induced air pressure differences between the loci for inlet and outlet to the cavity, and stack effect.

#### 3.4.1.5 Air convection within a zone

The assumption of a well-mixed air in a zone or in an air cavity is often used in building simulations. The air volume is treated as homogeneous and the air circulation, caused by temperature and concentration gradients within it, or by mechanical devices, is neglected. The zone is treated as a one capacity node and all walls attached to it experience the same boundary conditions. Accordingly, the modelling procedure is considerably simplified and the simulation time is shorter.

In reality, the air is never perfectly mixed. HAM models based on the well-mixed air assumption may lead to erroneous results in situations where regions with low air circulation are present, such as in corners or spaces behind furniture. This is because the wall partitions, which are well-flushed with air, experience at least one order of magnitude larger surface transfer coefficients than those in a hidden position, and, due to the non-homogeneities of the distribution of air, other gradients that govern the transfer. As a result, only a part of the wall appears active in the HAM transfer investigated, while the other part is practically inactive.

Models based on fine spatial discretization of an air volume and on the detailed conservation equations of mass, momentum and energy in the air are needed for such problems. The conservation equations get the following generalized form:

$$\frac{\partial(\Phi)}{\partial t} + \bar{v} \cdot \nabla(\Phi) = \nabla(D_{\Phi} \nabla \Phi) + \sum S_{\Phi} \quad (3.4.6)$$

where  $\Phi$  represents any of the entities: temperature of air, density, momentum or humidity ratio. In contrast to Equation (3.4.1), convection and diffusion transport mechanisms are accounted for in Equation (3.4.6).

The papers presented below give some examples of the modelling of a convective flow field in buildings. The study of Steskens and Schijndel (2006) is limited to coupled heat and air problems. The study of Steeman et. al (2006) is focused on a coupled moisture and air problem under isothermal conditions.

#### *Towards full 3D HAM modelling of a room using COMSOL. Air volume and airtight construction HA modelling Steskens and Schijndel (2006)*

The work considers a 3D airflow field and a temperature distribution in a full-scale enclosure with a radiator. The results, showing the influence of the thermal jet projected from the radiator on the airflow field, are given for a steady state and transient conditions. The steady-state flow patterns are evaluated by the numerical and experimental results found in literature. The analysis is made using a commercial modelling package. The simultaneous modelling of transfer processes in the air zone and the building envelope, together with the interface that takes care about the data exchange between the domains, are seen as the main advantages of the software used. Large computational time is, among other modelling details, seen as a disadvantage.

#### *3D CFD analysis on the validity of the "well mixed air" assumption made in traditional HAM models*

*H.J. Steeman, A. Janssens, M. de Paepe*

The analysis of the validity of the "well mixed air" assumption is carried out for the test cases based on the isothermal test case given in CE 1B. The 3D airflow field is calculated by

commercial CFD software, extended with a wall model for moisture buffering. The average indoor relative humidity, calculated for different locations of a moisture source in the room and for different ventilation strategies, is compared to the result of the one-node model. According to the results, the “well mixed air” assumption can only be used for a case with a uniform moisture source and mixing ventilation. In all other cases the moisture contents in the walls can show steep gradients and local increased values due to local moisture sources.

#### Nomenclature

... should be common for the whole report.

### **3.5 Advances in 3D airflow modelling**

By Michel de Paepe

In the past few years CFD (Computational Fluid Dynamics) has been playing an increasingly important role in building design, following its continuing development for over a quarter of a century. CFD calculations can provide information with great detail in order to ameliorate comfort, indoor air quality, safety and energy-efficient building design. The areas in building design where CFD has been used are widespread : HVAC-design, ventilation design, fire and smoke control, wind comfort,...

A good overview of recent developments is given by Z. Zhai (Zhai 2006). It is interesting to note that whole building heat air and moisture modelling is not appearing in this overview. Most of the existing tools can represent water vapour diffusion and transport in the air, however they do not take into account mass transfer at the interface of the air and the building envelope.

Hohota et al. (2004) adapted the air flow equations in the Fluent CFD code, in order to represent vapour condensation on cold surfaces. This was done by adding source and sink terms to energy and mass balance equations for each cell of computational domain that is in contact with a solid surface. As soon as the surface temperature drops under the dew point of the inside air, liquid occurs on the surface. Vapour pressure against the surface remains at the saturation value as long as the surface is moist. Latent heat released during the condensation process is injected to the energy network. The comparison with the experimental work showed that the numerical model was able to predict correctly the regions where condensation appeared. This was confirmed as long as vapour injection in the inlet was kept homogenous and stable (Hohota, 2003).

Moisture transfer modelling in porous materials coupled with air flow modelling with CFD was done by Erriguible et al (2005). This model uses the commercial CFD code Fluent to generate vapour fluxes at the boundary of a porous and couples it to a vapour transfer model for porous materials. The model is validated with an example of drying wood. This method uses an external coupling of CFD and a porous material model.

Most of building materials are porous materials and they interact with indoor air by absorbing or releasing moisture. Existing CFD tools focus on air flow movement and are able to model heat transfer in solids. Solvers are also available for gas flows through porous materials. Some extended modelling was needed in order to include both heat and moisture transfer in CFD codes. During the Annex 41 several approaches were formulated in order to solve coupled mass transfer in air and building envelopes.

Hedegaard et al. (2004) proposed a method using existing diffusion equations in the CFD code mainly because it is a method where no programming of user defined functions is needed. As diffusion is computed only in fluid domains, the walls need to be defined as fluids. The building envelope was therefore modelled as immobile fluids with ordinary building material characteristics as material properties. This enables modelling of moisture diffusion within the walls.

Steeman et al. (2005) programmed a user defined function using the penetration depth model in order to describe moisture transfer in the building envelop. The main advantage of this approach is a better flexibility of the model.

This model was further expanded by using user defined scalars in Fluent containing the mass transfer equations in the solid porous material. This way the solver of the CFD code can be used to solve the mass transfer in the material. This model was successfully validated in Subtask 2, Modelling Exercise.

Neal et al programmed a moisture transfer model in Matlab and made an external coupling with Fluent in order to solve heat and mass transfer in air and porous materials. This approach was also validated with the Subtask 2, Modelling Exercise.

CFD has proven to be a useful tool to get detailed information of air flows in buildings and over building components. It also provides the users with local values of heat and mass transfer coefficient which can be used in whole building simulation programs.

In spite of the important advances in this field, two major limits are still imposed for such a detailed approach. One is the computational time: even if the computing power is rising significantly every year, annual simulations of whole building using CFD are still far beyond computer capabilities.

The second and very important limit consists in the problem of validation. Such detailed tools require very detailed description of the room (geometry and material properties) and a very experienced user in order to provide realistic results.

## 4 Common Exercises

The purpose of the common exercises being part of Subtask 1 of the Annex has been to test the current possibilities to use modelling as a means to predict the integrated hygrothermal behaviour of buildings and to stimulate new development in this area. This could be done either by clever use of already existing models, or by new modelling, where models were developed either from scratch or as extensions to already existing models which have some of the desired performances.

The following Common Exercises (CE) have been carried out as part of Subtask 1 of Annex 41:

- Common Exercise 0 (CE0). Validation of thermal aspects of the employed models. This was done by repeating the building energy simulation test BESTEST of IEA SHC Task 12 & ECBCS Annex 21 (Judkoff and Neymark, 1995).
- Common Exercise 1 (CE1). Expanding on CE0 and the BESTEST case by adding considerations about moisture interactions between building constructions and indoor climate.
- Common Exercise 2. This CE has been based on experimental data from climate chamber tests carried out at Tohoku University, Japan (the tests are of similar nature as those reported in Mitamura et. al 2004. Detailed measurements of boundary conditions, as well as of indoor conditions in several points were performed. This exercise was designed to test whole building HAM models but can also be used to validate detailed airflow codes (such as CFD for instance).
- Common Exercise 3. This exercise has been based on a double climatic chamber test carried out by the Fraunhofer Institut für Bauphysik, Germany (a somewhat similar test is mentioned in the paper by Holm et al., 2003). Here two identical chambers have been run with different cladding materials, and the experimental results were to be replicated by modeling.
- Common Exercise 4 - an extension of CE3. The exercise was based on the same two real test rooms from CE3. The intention of this common exercise was to show that an appropriate management of the indoor moisture reduces the building's energy consumption.
- Common Exercise "X". This was an exercise with data from a real life row house located in Belgium. The case is well documented and gradually more issues from the study of the house have been dealt with as the Annex progressed (therefore the name of the Exercise "X"). The objective of Common Exercise X was to simulate the air flow and hygrothermal conditions within a real house.

Besides testing existing modelling possibilities and stimulating new developments, common exercises provide elements of validation of whole building hygrothermal simulation tools. All three elements required by Judkoff and Neymark (1995) for code validation have been included in common exercises from Annex 41:

- analytical verification (CE1 and CEX),
- empirical validation vs. experimental data (CE2 and CE3),
- finally comparative testing, which is the heart of all the common exercises.

More details about common exercises are given in the following.

## 4.0 Common Exercise 0 - BESTEST DIGEST - Whole building energy modelling

By Monika Woloszyn, CETHIL, France

### 4.0.1 Introduction

In order to start rapidly with Subtask 1 efficient work, Common Exercise 0 (some of BESTEST cases) was suggested during the take-off meeting in November 2003. Common Exercise 0 was therefore proposed in April 2007, and the first draft of results was presented in May 2004 in Zurich. The purpose was to provide comparison between different modelling results for energy simulations. Along with the file containing numerical results from the study, a report on the program and modelling choices was filled in by the participants. These reports documented the first state-of-art of models that can be used for whole building heat, air and moisture transfer simulations.

### 4.0.2 Case description

For the purpose of Annex 41, four cases were chosen from the original BESTEST procedure, adapted for whole building approach (see Table 1). The four cases are indicated by their BESTEST code "600" for a building made of lightweight construction, "900" for a heavyweight building. Possibly the code "FF" indicates a building under free floating thermal conditions without heating or cooling systems. These four cases were chosen because they represent well the whole building approach, according to the scope of Annex 41, without focusing too much on some very specific issues such as solar shading or transfers to the ground.

Table 4.0.1. 4 cases tested as Common Exercise 0.

Case	Building structure	Heating and cooling
600 FF	plasterboard, insulation, wood	None
600	plasterboard, insulation, wood	Heating if $T_{int} < 20^{\circ}\text{C}$ , Cooling if $T_{int} > 27^{\circ}\text{C}$
900 FF	concrete, insulation, wood	None
900	concrete, insulation, wood	Heating if $T_{int} < 20^{\circ}\text{C}$ , Cooling if $T_{int} > 27^{\circ}\text{C}$

Common Exercise 0 study the IEA BESTEST building mentioned previously in some former IEA projects: IEA SHC Task 21 & ECBCS Annex 21. The IEA BESTEST building today is also referenced in ASHRAE Standard 140 (ASHRAE, 2004). The building is superficial, so no measurement data exist. The building, presented in Figure 4.0.1, has a very simple structure with two windows facing south, constant ventilation of 0.5 air change per hour and constant internal gains of 200 W of sensible heat. The weather file is from Denver (altitude: 1609 m, latitude: 39.8° north, longitude: 104.9° west) characterized by high temperature amplitudes and important solar radiation. All the data can be found in Judkoff and Neymark, 1995.

The participants run 1 year simulations and provided the following hourly results:

- indoor air temperatures,
- incident total solar radiation (diffuse and direct) on 5 faces of the building ( $\text{kWh/m}^2$ ),
- solar radiation transmitted through the windows ( $\text{kWh/m}^2$ ).
- hourly heating and cooling load (MWh) (Cases 600 and 900).

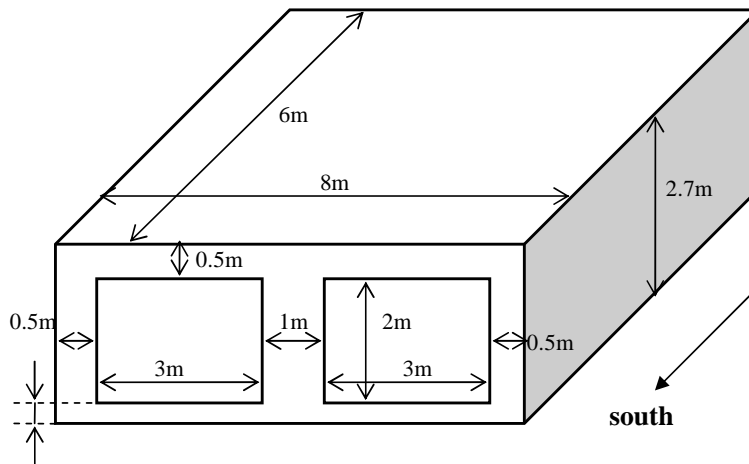


Figure 4.0.1. BESTEST base case building.

#### 4.0.3 Participants

13 sets of results were collected coming from 11 institutions from 9 countries using 10 different programs (see Table 4.0.2).

Table 4.0.2. Participants of Common Exercise 0

Institution	Country	Software
TUW	Austria	ESP-r
KUL	Belgium	ESP-r (2 results)
KUL	Belgium	TRNSYS
DTU	Denmark	BSim2002
TTU	Estonia	IDA ICE
CETHIL	France	TRNSYS
CETHIL	France	Clim2000
FHG	Germany	Wufi+
TUD	Germany	ITT DELPHIN
TUE	Netherlands	HAMLab
CTH	Sweden	HAMTool
ORNL	USA	EnergyPlus

The programs participating in CE0 are both public domain and commercial softwares, and their common feature is continuous development of physical models.

For numerical resolution, different solution methods are used, such as explicit and implicit algorithms, or response factor type methods. Both fixed and auto-adaptative time steps were equally represented. Some differences in the results can be expected because of the differences in the reconstruction of outdoor climate from meteorological data. Some programs use linear interpolation while the others assume that the climate remains constant over the sampling interval.

The used energy models include following features:

- outdoor heat transfer, including convection and radiation, using global exchange coefficients in most of the cases,
- indoor heat transfer including convection and long wave radiation (all except one), however different methods are used to compute the heat transfer: constant coefficients, detailed computations, linearization or not...
- perfect mixing of the air zone is assumed in all the cases,
- 1D heat transfer is assumed in envelope parts,

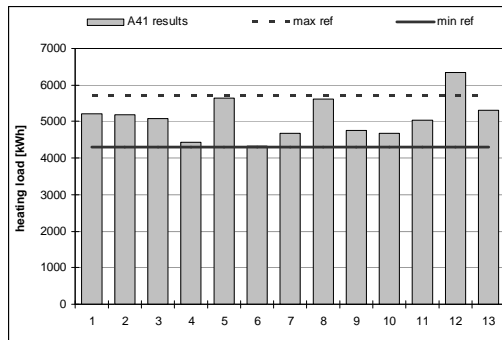
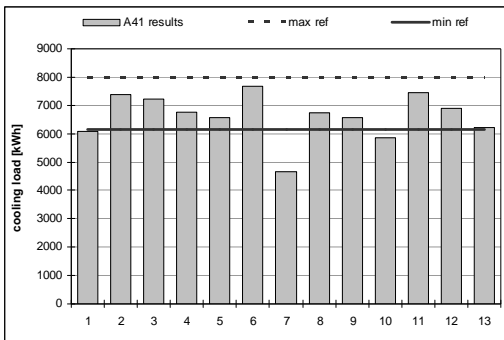
- some differences can be seen in the treatment of windows and solar gains: transmitted radiation distribution can be fixed by user or calculated as a function of solar position, also different possibilities are used to calculate the shortwave radiation transmitted through the windows,
- heating and cooling system represented is in general “perfect”: no dynamics, purely convective, controlled by air temperature.

All models used include moisture in the balance of the air zone, but at the time of executing CE0 only a few programs represent moisture transfer through the envelope. More detailed description of the tools can be found in previous chapter of this report and appendix X.

**4.0.4 Results**

In the following charts the main results of the exercise are given as annual values or as time-dependent plot during one day. The 13 sets of results from participating institutions are given in anonymous form and contrasted with previous results from Annex 21. The minimum and maximum reference values in Figure 4.0.2 - Figure 4.0.8 are taken as indications from the original BESTEST report (Judkoff and Neymark, 1995). They represent the minimum and maximum results out of eight most representative energy calculation tools chosen at the end of Annex 21. The aim of this range is to help in diagnosing eventual errors. However it should be stressed that results situated within these minimum and maximum range do not guarantee the validity of the simulation tool. On the opposite, the results out of the range are not a proof of any errors in the model. Whole building simulations, even if only energy is of interest are complex, and there are many ways of establishing correct models. Moreover the results of Annex 21 are only virtual; no measurements were performed on those cases.

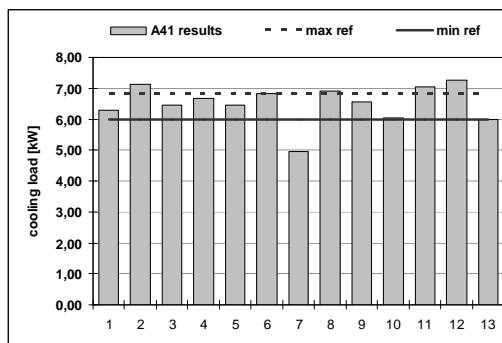
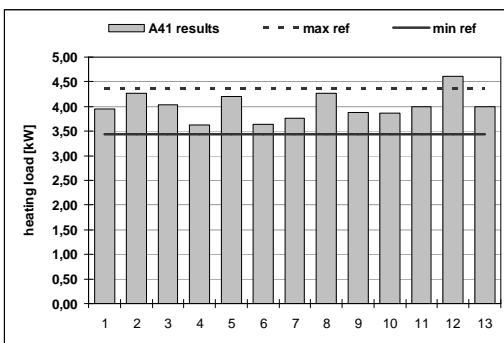
**4.0.4.1 Cases with heating and cooling (600 and 900)**



heating

cooling

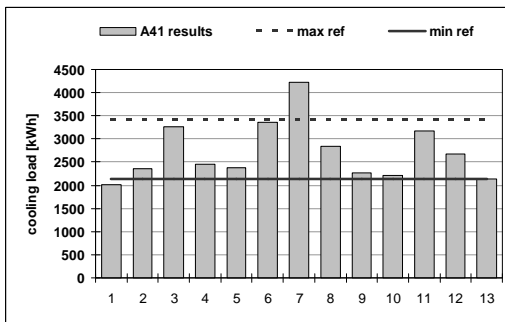
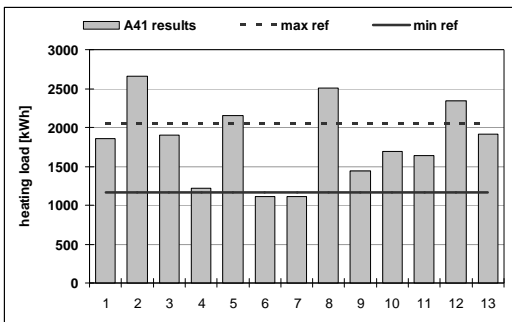
Figure 4.0.2. Annual interior heating and cooling loads for lightweight structure (Case 600).



heating

Cooling

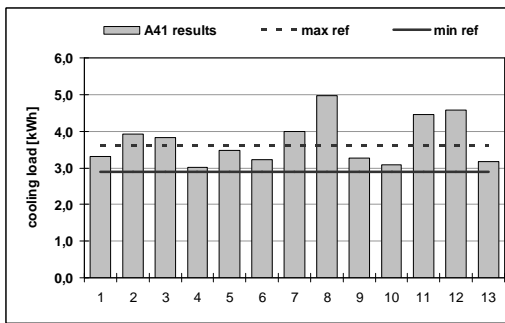
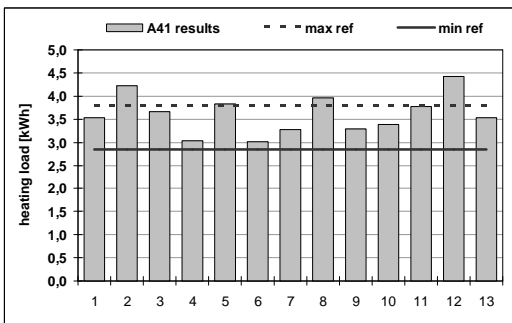
Figure 4.0.3. Maximum peak load for heating and cooling for lightweight structure (Case 600).



heating

cooling

Figure 4.0.4. Annual interior heating and cooling loads for heavyweight structure (Case 900).

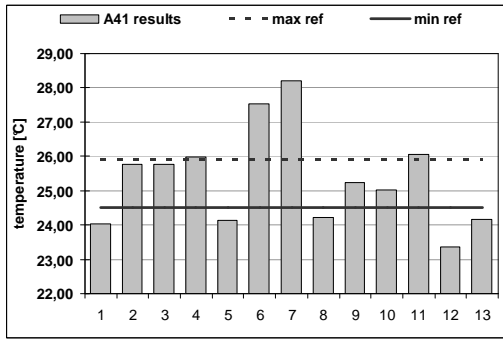
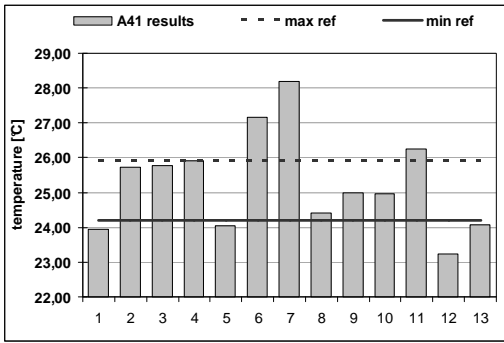


Heating

cooling

Figure 4.0.5. Maximum peak load for heating and cooling for heavyweight structure (Case 900).

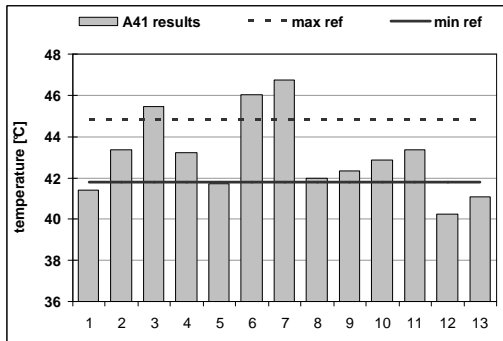
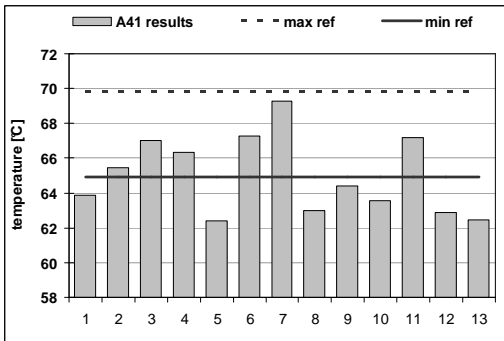
4.0.4.2 Cases without heating and cooling systems



lightweight structure (Case 600FF)

heavyweight structure (Case 900FF)

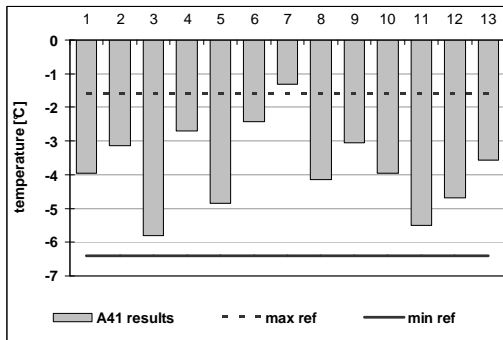
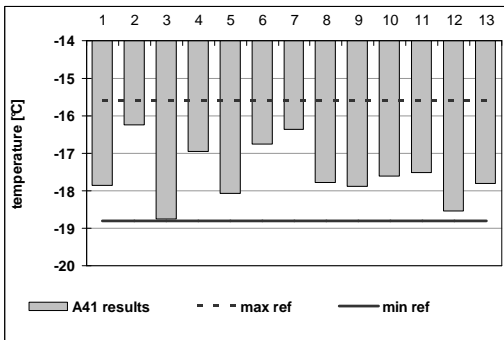
Figure 4.0.6. Mean annual temperature for both light- and heavy-weight structures



lightweight structure (Case 600FF)

heavyweight structure (Case 900FF)

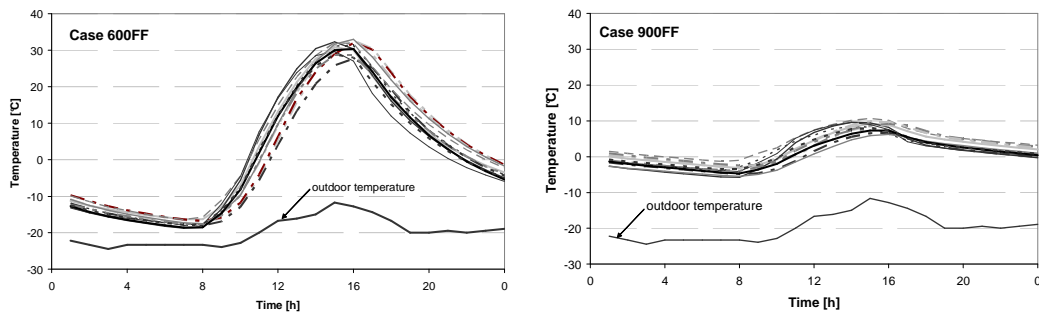
Figure 4.0.7. Maximum annual temperature for both light- and heavy-weight structures



lightweight structure (Case 600FF)

heavyweight structure (Case 900FF)

Figure 4.0.8. Minimum annual temperature for both light- and heavy-weight structures



*lightweight structure (Case 600FF)*

*heavyweight structure (Case 900FF)*

Figure 4.0.9. Temperature evolution for both light- and heavy-weight structures on Jan. 4<sup>th</sup>

#### 4.0.5 Discussion

Despite the differences, similar trends were found by all the participants in the CE0 and as shown in Figure 4.0.2 - Figure 4.0.9. Much higher energy use, as well as higher peak loads and larger temperature amplitude were found for the lightweight structure than for the heavyweight structure. For example Figure 4.0.9 shows that daily temperature evolution was found very similar by all of the tools with amplitude of almost 50°C for the lightweight structure and less than 15°C for the heavyweight structure.

Globally better agreement between codes was found for cooling (vs heating) loads. The dispersion of results was less for 600 than for 900 (see Figure 4.0.2 and Figure 4.0.3), but the opposite was true while there was no heating or cooling systems. In case 900FF the “crowd” of results was more compact than in the case 600FF.

Similar spread of several degrees between different sets of results can be seen for both one day data (Figure 4.0.9) and for the averages and extreme values (Figure 4.0.6 - Figure 4.0.8). Wide distribution in energy loads is shown in Figure 4.0.2 - Figure 4.0.5. However, as confusing as it may appear, with few exceptions the results are situated within the reference limits from the original BESTEST cases. Some more remarks can be formulated:

- several tools seem to overestimate the peak loads especially for heavyweight structure (Figure 4.0.4),
- concerning the free floating cases, some tools are more than 1°C “out of the band” for both the maximum and the annual average temperature (Figure 4.0.6 - Figure 4.0.8),
- each tool gives a very similar mean temperature for both types of structures (Figure 4.0.6).

More differences were found for maximum and average temperature than for minimum, when the impact of solar radiation is limited. Therefore the inconsistency could be partly due to the variations in calculations of solar gains through windows.

In order to explain better some of the differences, calculations of the incident solar radiation were also contrasted between the tools and can be seen in Figure 4.0.10. Predictably the smallest differences can be seen for the roof (horizontal surface), as well as for north façade, exposed mainly to the diffuse radiation. Differences are much higher for east, west and south walls, and therefore for solar gains of the building (window is exposed to the south). A comparison between these results and the reference computations from annex 21 is given in table 3. While the mean values are very similar, standard deviation is higher for the results from Annex 41.

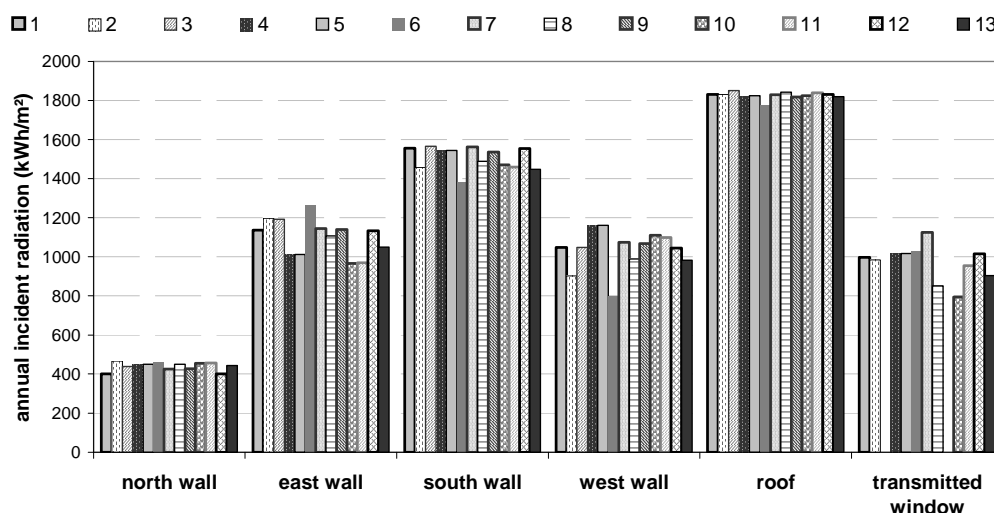


Figure 4.0.10. Annual radiation computed on different surfaces.

Table 4.0.3 Annual radiation computed on different surfaces. Comparison between mean values and standard deviations computed both by the reference tools in Annex 21 and in the present Annex.

	Annex 41		Annex 21	
	mean	st. dev.	mean	st. dev.
north wall	424	53	429	33
east wall	1 081	109	1080	94
south wall	1 495	88	1490	40
west wall	1 035	117	1018	82
roof	1 827	19	1827	13

These differences in solar radiation computations may be a reason for some of the deviations in the energy calculations. It should be pointed out that a thorough checking of the energy simulations was done by some of the participants, improving short and long wave radiations calculations, not represented in these results.

**4.0.6 Conclusions**

As intended the Common Exercise 0 stimulated some improvement of existing programs. New developments concerned the “H” (Heat) part of HAM-models, and specially radiation heat transfer calculations. Both short wave radiation (computation of incident solar radiation and heat gains through the windows) and long wave intra-zone exchanges were enhanced in some programs. As heat, air and moisture closely interact with each other in a building, a correct description of energy behaviour is needed before assessing whole building moisture performance.

The deviation of results within a reasonable range gives also some more confidence in energy models and provides a valuable reference case for some future sensitivity study on the impact of moisture on energy loads.

## **4.1 Common Exercise 1 – Moisture balance of BESTEST building**

Carsten Rode, Ruut Peuhkuri and Lone H. Mortensen

*Technical University of Denmark (DTU)*

### **4.1.1 Introduction**

This report summarizes some of the modelling exercises executed as a part of the International Energy Agency project, ECBCS, Annex 41. These exercises were given and answered during a period from August 2004 to May 2005. We thank all the institutions involved in the exercises for all the valuable work done and the plenum of Annex 41 participants for discussions during the working meetings in Glasgow 2004 and Montreal 2005. A total of 16 institutions from 13 countries contributed to the exercise.

#### **4.1.1.1 Annex 41: MOIST-ENG**

An important part of the IEA Annex 41 is about modelling the integral heat, air and moisture transfer processes that take place in “whole buildings”. Such modelling deals with all most relevant elements of buildings: The indoor air, the building envelope, the inside constructions, furnishing and systems. These building elements interact with each other and they are influenced by the use of the building, the building services, and the outside climate. IEA Annex 41 aims to reach new modelling possibilities in integral building simulation, and to document these. This report documents some new simulation tests used in IEA Annex 41 and elaborates about the challenges brought by these exercises.

#### **4.1.1.2 Common Exercises in Subtask 1**

The purpose of the common exercises being part of Subtask 1 of the Annex is to test the current possibilities to use modelling as a means to predict the integrated hygrothermal behaviour of buildings and to stimulate new development in this area. This could be done either by clever use of already existing models, or by new modelling, where models are developed either from scratch or as extensions to already existing models, which have some of the desired performances. Generally, the models used are either hygrothermal models for components of the building envelope that are expanded with models for indoor air volumes and by making provision for simultaneous calculation of several building components – e.g. Holm et al., 2003. Alternatively, building energy simulation models, which already have capabilities for making thermal analysis of whole buildings, are expanded with models for transient moisture transport in the building components - e.g. Rode & Grau, 2003.

Besides testing existing modelling possibilities and stimulating new developments, common exercises provide elements of validation of whole building hygrothermal simulation tools. All three elements required by Judkoff and Neymark (1995) for code validation will be included in common exercises from Annex 41:

- analytical verification,
- empirical validation vs experimental data,
- finally comparative testing, which is the heart of all the common exercises.

### **4.1.2 BESTEST Case as Common Exercise 1**

These exercises analyse the IEA BESTEST building mentioned previously in some former IEA projects: IEA SHC Task 21 & ECBCS Annex 21. The IEA BESTEST building today is also referenced in ASHRAE Standard 140 (ASHRAE, 2004). The building is shown in Figure 4.1.1. The building is superficial, so no measurement data exist. The main advantage of BESTEST cases is their “whole building” approach in the energy field.

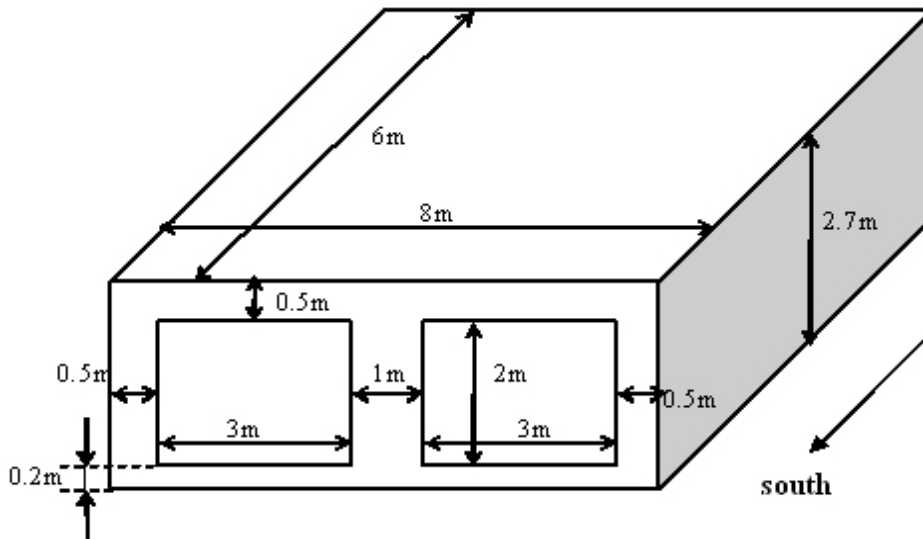


Figure 4.1.1 BESTEST case building.

The Common Exercises in IEA Annex 41 have had more than 15 participants, and it has seemed clear to define some consensus solutions based on where the “crowd” of results was lying. Along with the file containing numerical results from the study, the participants filled in a report about the program and modelling choices. In Appendix C, these reports document the first state-of-art of models that can simulate whole building heat, air and moisture transfer.

#### 4.1.2.1 CE 1 Hygrothermal building simulation

The BESTEST cases serve to provide comparison between different modelling results. For the thermal analyses in CE0 four cases were chosen from the original BESTEST procedure. Common Exercise 1 expands on Common Exercise 0 by adding some analysis of the indoor and building envelope moisture conditions for the BESTEST building used in CE0.

The original plan for CE1 was to add the moisture problem parts directly onto the problem from CE0. However, the first results of the Common Exercise 1 showed, that the original case had too many uncertainties even within the thermal calculation, e.g. the presentation of the material data, window models etc. Therefore, a step back was taken with Common Exercise 1A (an analytical case) and Common Exercise 1B (a more “realistic”, numerical case). The constructions were made monolithic, the material data were given as constant values (CE1A) or as functions (CE1B) and the solar gain through windows was modelled simplified. An overview of these variants is given in Table 4.1.1, and Table 4.1.2 shows some modelling details and parameter variations.

For all cases there is an internal moisture gain of 500 g/h from 9:00 - 17:00 every day. The air change rate is always 0.5 ach. The heating and cooling control for all the non-isothermal cases keeps the indoor temperature between 20 and 27°C with an infinite capacity. The system is a 100% convective air system and the thermostat is on air temperature.

The exercise texts for all 3 cases are found in Appendix A.

Table 4.1.1 Overview of variations of Common Exercise 1.		
<b>CE1</b> <i>Numerical cases in principle like in CE0. Natural climate</i>	<b>CE1A</b> <i>Monolithic walls with simple material properties. Const. climate.</i>	<b>CE1B</b> <i>Monolithic walls with realistic properties. Natural climate</i>
600_0A <i>Analytical</i> , Vapour tight surfaces	0A <i>Analytical</i> Vapour tight surfaces	$T_{\text{indoor}} 20^{\circ}\text{C}$ , no external radiation
600_0B <i>Analytical</i> , Vapour open surfaces	0B <i>Analytical</i> , Vapour open surfaces	$T_{\text{indoor}} 20 - 27^{\circ}\text{C}$ , no external radiation
600_Open <i>Numerical</i> , Vapour open surfaces		$T_{\text{indoor}} 20 - 27^{\circ}\text{C}$ ,
600 Paint&VR <i>Numerical</i> , Painted surfaces		
Case 900_Open <i>Numerical</i> Vapour open surfaces		

Table 4.1.2 Conditions and properties for the different variations of Common Exercise 1

1	1 CE 1	1 CE (analytical)	1A 1 CE 1B ("realistic")
2	2 <b>constant or varying indoor T</b>	2 <b>constant indoor T</b>	2 <b>constant or varying indoor T</b>
3 <b>Location</b>	3 Denver	3 No location	3 Copenhagen
4 <b>Constructions</b>	4 A variety of realistic sandwich constructions	4 Monolithic cellular concrete (d=0.15m)	4 Monolithic cellular concrete (d=0.15m)
5			
6 <b>Windows</b>	5 $U= 3W/m^2K$ , $g=0.787$ (normal incidence). Free choice of modeling	5 No windows	5 $U= 3W/m^2K$ , $g=1.0$ (all incidences)
7 <b>Indoor boundaries</b>	6 Free choice or a given constant R and Z, floor faces wet ground at 10°C	6 Case 0A: vapour tight surface; Case 0B: a given constant Z	6 Given constant values for R and Z
8 <b>Outdoor boundaries</b>	7 Free choice or a given constant R and Z	7 Vapour tight surface, floor faces outdoor air	7 Given constant values for R and Z, floor faces outdoor air
9 <b>Thermal conductivity</b>	8 Free choice of using moisture dependent values or not	8 A given constant	8 A given constant
10 <b>Vapour permeability</b>	9 Free choice of using catalogue values	9 A given constant, only vapour transfer	9 A given function of RH, only vapour transfer
11 <b>Sorption isotherm</b>	10 Free choice of using hysteresis or not	10 A given linear mean value, no hysteresis	10 A given function of RH, only absorption
12 <b>Internal heat gain (no heat gain for constant T=20°C)</b>	11 200 W (100% sensible; 60% radiative, 40% convective; always)	11 No gain	11 800 W (100% convective; 0% latent; every day 9:00-17:00)
13 <b>Solar gain and radiative properties</b>	12 given emissivity and absorption of materials	12 No gain	12 Cases 1 and 2 without, case 3 with a gain

## 4.1.2.2 Participating institutions and simulation tools

Table 4.1.3 shows the used simulation codes. Some of the institutions have used the same code for all the exercises – with or without modifications from case to case – while others have used 2 different codes or have not taken part in a single exercise.

Table 4.1.3 An overview of the participating institutions and the used simulation tools.

1 Simulation tool used for the exercise					
2 Institution	1 Country	1 CE 1	1 CE 1A	1 CE 1B	
3 CETHIL	2 France	2 Clim2000	2 -	2 -	
4 CTH	3 Sweden	3 HAM-Tools	3 HAM-Tools	3 HAM-Tools	
5 DTU	4 Denmark	4 BSim	4 BSim	4 BSim	
6 FhG	5 Germany	5 Wufi+	5 Wufi+	5 Wufi+	
7 KIU	6 Japan	6 Xam	6 Xam	6 Xam	
8 KYU	7 Japan	7 Original code	7 Original code	7 Original code	
9 ORNL	8 USA	8 EnergyPlus	8 -	8 -	
10 PUCPR	9 Brazil	9 -	9 PowerDomus	9 PowerDomus	
11 SAS	10 Slovakia	10 Esp-r + Wufi + NPI	10 NPI	10 Esp-r + NPI	
12 TTU	11 Estonia	11 IDA ICE	11 IDA ICE	11 IDA ICE	
13 TUD	12 Germany	12 TRNSYS ITT	12 DELPHIN TRNSYS ITT	12 DELPHIN TRNSYS ITT	
14 TUE	13 Netherlands	13 HAMLab	13 HAMBase	13 HAMLab	
15 TUW	14 Austria	14 HAM-VIE	14 HAM-VIE	14 HAM-VIE	
16 UCL	15 UK	15 EnergyPlus	15 EnergyPlus	15 EnergyPlus	
			16 Canute_beta		
17 UG	16 Belgium	16 (analytical)	17 TRNSYS	16 1DHAV+	
				17 TRNSYS 16	
18 ULR	17 France	17 -	18 TRNSYS	18 -	
			19 SPARK		

Description of the models is found in Appendix C, which is the collection of the participants' reports from their methodology of solving Common Exercise 1, and in the Subtask 1 main report's chapter on Whole Building HAM models used and developed in Annex 41. Some main characteristics of the used models are discussed in the following:

The models used and developed typically have one or several already existing models as starting points. For instance it has been quite common to start with a tool for whole building thermal analysis, such as some commercial Building Energy Simulation software which has been extended with models for moisture and possibly air transport in building envelopes. Another common approach has been to take as a starting point an existing model for transient heat, air and moisture transport which has been extended to comprise the whole building. Furthermore, some model approaches have been to develop new models in the form of toolboxes for instance for MATLAB, Simulink or FEMLAB (COMSOL Multiphysics), or new system analysis tools for TRNSYS. Finally for some developments, part of the modelling has taken place in commercial CFD code where the results were used in combination with results from other tools.

The extent of detail to which the components, such as HVAC systems and windows, have been modelled depends rather much on the history of the models. If the new developments are based on previously existing building energy simulation tools, these models typically already have some descriptions of HVAC systems, windows etc.

Numerically, the different models have been based on Finite Control Volumes (Finite Differences), Finite Element Methods, or Response factor methods. This implies some differences with respect to for instance how well the models can cope with non-linear phenomena and how well they manage geometry that does not fit in orthogonal cartesian networks.

Most models are 1D but with possible coupling to 2D models. For moisture, around half of the models are based on some lumped model, where the moisture capacity of walls is represented in a buffer layer at the effective depth of moisture penetration for daily cycles.

For moisture, some models considered only vapour diffusion, while others also dealt with liquid moisture transfer. Many models neglect hysteresis in the retention curves, while some models have some representation of it. Calculating moisture transfer, most of the integrated models also consider conversion of latent heat, and thereby have an improved modelling of the heat transfer processes when compared to traditional building energy simulation tools.

For airflow between zones, most models apply a lumped volume approach, but about half of the models have some possibility to make pressure network calculations. Most models consider some form of infiltration/exfiltration air flow in building envelopes.

### 4.1.3 Results

In the following charts a snap-shot of the exercise results is given. The results are given as values during one day. The results are presented anonymously.

#### 4.1.3.1 Original CE1

“CE1” is the original case of an exercise for simulations which also included moisture exchange. It was posed with a relatively high degree of freedom for modelling a realistic building, based on the descriptions for thermal BESTEST cases. Figure 4.1.2 and Figure 4.1.3 show results from the analytical calculations of variation of RH during 24 hours for the simplified cases, while Figure 4.1.4 shows the result as indoor RH during a single day (July 27) for the case with numerical simulations of the building with open, light-weight structures. To give an idea about the ability of the models to calculate conditions of the constructions, relative humidity in a roof construction for the light-weight construction without vapour retarder is shown in Figure 4.1.5.

For the analytical cases, just one day was studied which represent the conditions after quasi-steady conditions have been attained.

The numerical calculations were run for as many years as it was necessary to achieve quasi-steady conditions. The results were reported for the last year of calculation. An overall comparison of the calculated mean annual indoor relative humidity for the numerical cases is given in Figure 4.1.6. The annual heat demand is shown in Figure 4.1.7.

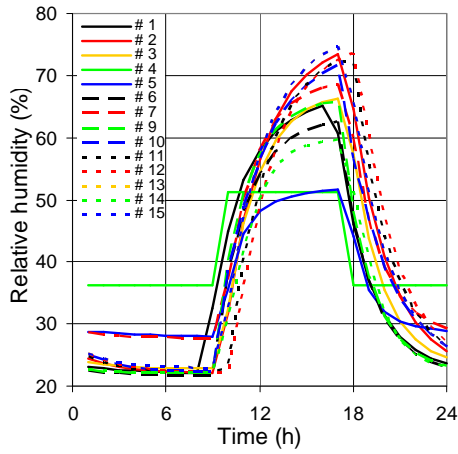


Figure 4.1.2 CE1, Case 600\_0A. Analytical test. Constant indoor and outdoor temperature. Construction surfaces are vapour tight.

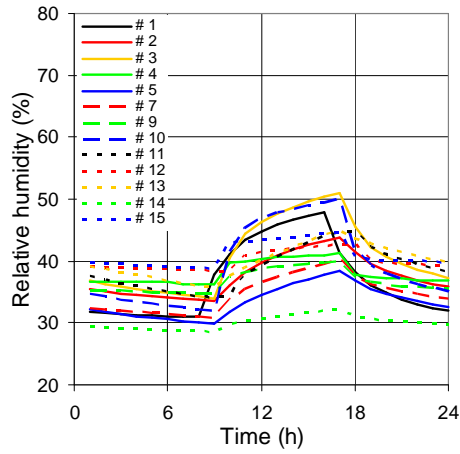


Figure 4.1.3 CE1, Case 600\_0B. Analytical test. Constant indoor and outdoor temperature. Construction surfaces are open. Same Constructions as in Case 600\_Open.

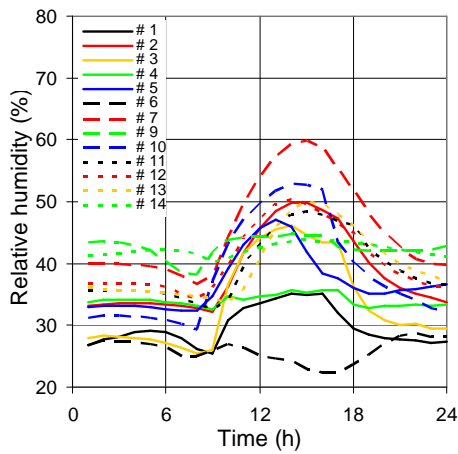


Figure 4.1.4 CE1, Case 600\_Open. Indoor RH. Lightweight structure with wood based interior wall claddings and cellulose insulation, open construction. Denver weather.

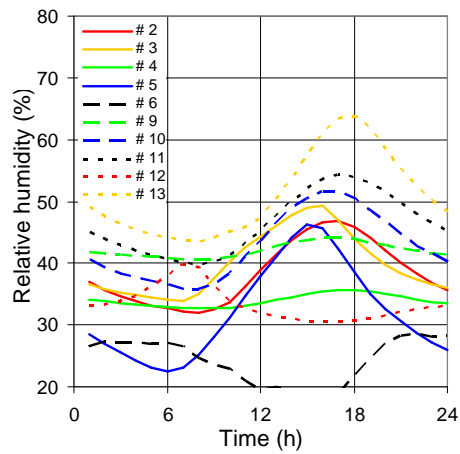


Figure 4.1.5 CE1, Case 600\_Open. Relative humidity in the roof construction. Constructions as in Case 600\_Open.

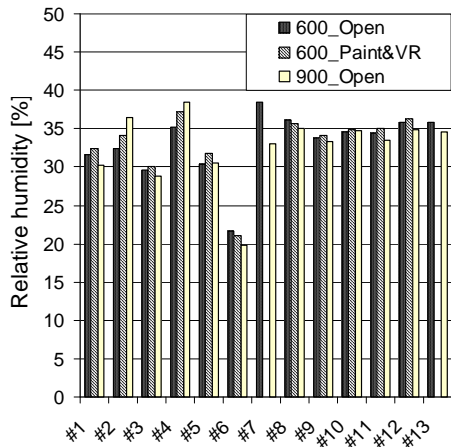


Figure 4.1.6 CE1, numerical cases. Comparison of annual mean indoor relative humidity.

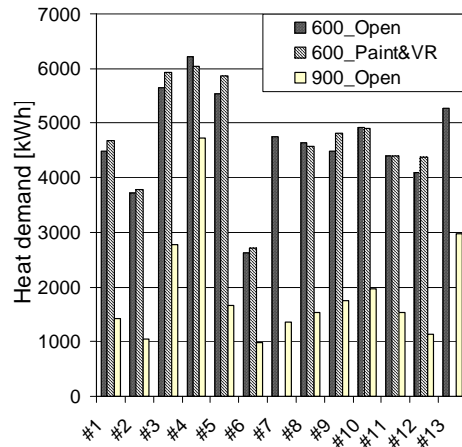


Figure 4.1.7 CE1, numerical cases. Comparison of annual heat demand.

4.1.3.2 CE 1A Analytical cases

This exercise applies the simplest conditions in terms of material properties and boundary conditions and uses properties which facilitate the possibility to solve the case analytically. Compared to the original CE1, the following changes were made: Constructions are made of monolithic aerated concrete with constant/linear properties. Tight membranes on the outside, and in case 0A also on the inside, prevent loss of vapour from the building by transport all the way through the walls. The exposure is completely isothermal, i.e. the same temperature outside as inside the building. The building has no windows. The initial conditions are given.

The calculations were run for as many days as it was necessary to achieve quasi-steady conditions. The results were reported for the last day of calculation.

It was possible also to solve the cases by using numerical tools. The numerical results are shown in Figure 4.1.8 and Figure 4.1.9, together with the analytical consensus solution prepared by Dr. Thomas Bednar, TUW and Prof. Carl-Eric Hagentoft, CTH. This solution is also found in Appendix B.

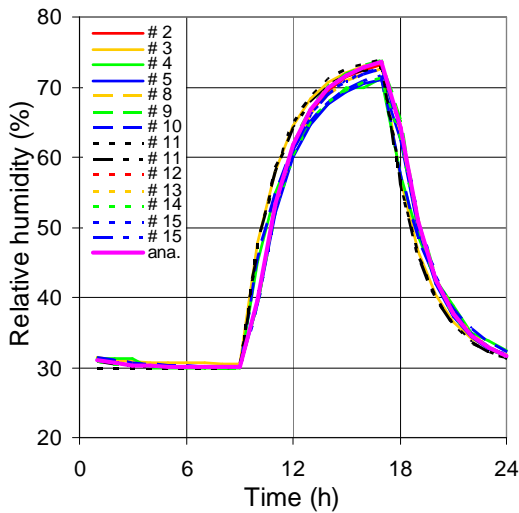


Figure 4.1.8 CE 1A, Case 0A. Analytical test. Isothermal exposure. Construction surfaces are tight. The results are here given as the numerical results compared with the analytical consensus

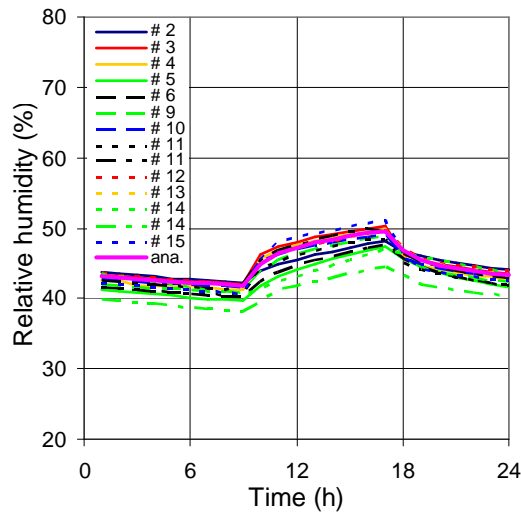


Figure 4.1.9 CE 1A, Case 0B. Analytical test. Isothermal exposure. Construction surfaces are open. The results are here given as the numerical results compared with the analytical consensus

solution of the indoor RH. The main deviation is due to the way the hourly values are given: either as mean values for an hour or as actual values.

4.1.3.3 CE1B "Realistic" cases

This exercise is the second part of the revised CE 1: the constructions are more simple than in CE1 and a more humid location, which is also close to sea level, is chosen: Copenhagen. All the envelope constructions are made of monolithic aerated concrete and face outdoor air. There are no coatings or membranes on any sides, not even at the roof. The results are again given as the indoor relative humidity (Figure 4.1.10, Figure 4.1.12 and Figure 4.1.13). Also an example on the needed cooling load (Figure 4.1.11) and the resulting solar gain in the room are given (Figure 4.1.15). Furthermore, the relative humidity on the top of the roof is shown in Figure 4.1.14.

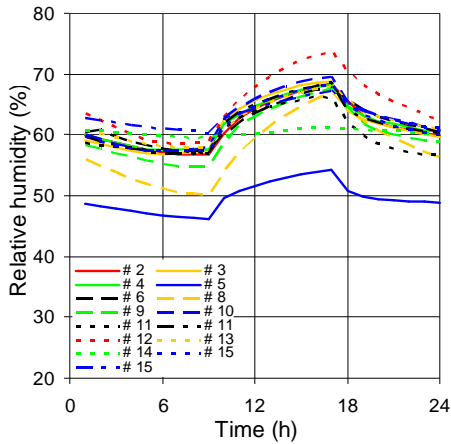


Figure 4.1.10 CE1B, Case 1 "20°C, no external radiation", case with constant indoor temperature and no solar radiation is used to reveal deviations in moisture calculations.

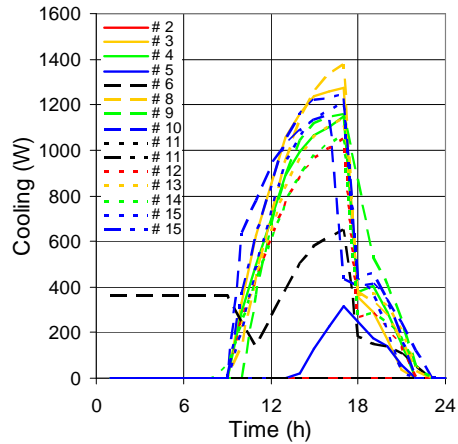


Figure 4.1.11 Internal cooling load for CE1B, Case 1 "20°C, no external radiation".

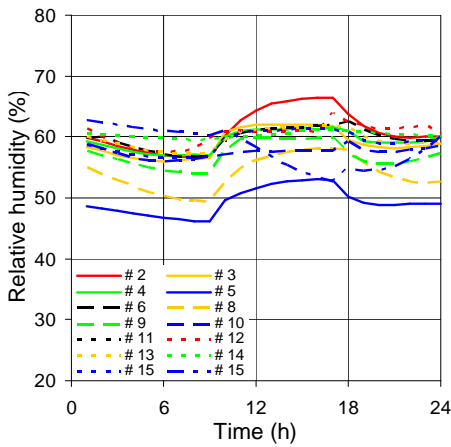


Figure 4.1.12 CE1B, Case 2 temp. range "20 to 27°C, no external radiation", which is a more realistic case but still without solar and long wave radiation.

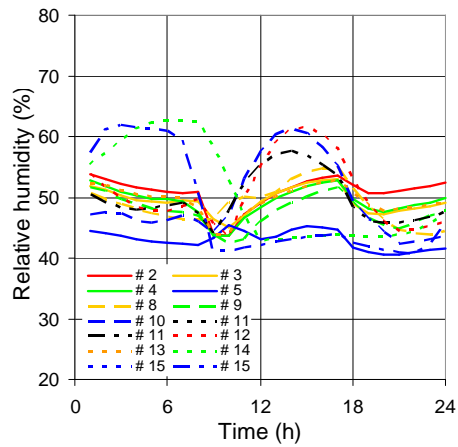


Figure 4.1.13 CE1B, Case 3 temp. range "20 to 27°C", now with solar and long wave radiation through the windows and on the external opaque surfaces.

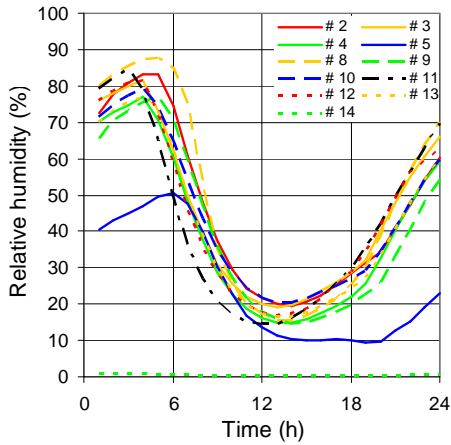


Figure 4.1.14 CE1B, Case 3 temp. range “20 to 27°C”. Relative humidity in the top of the roof.

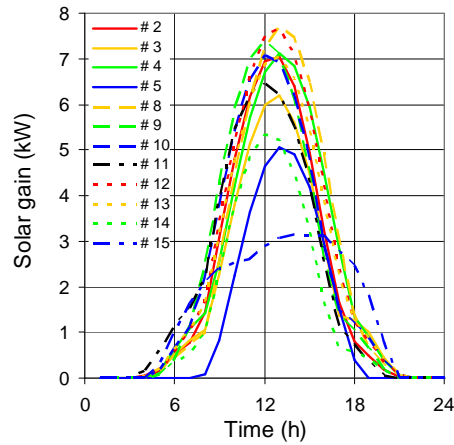


Figure 4.1.15 CE1B, Case 3, temp. range “20 to 27°C”, solar gain through window. The model includes solar and long wave radiation.

Hitherto it has been chosen to present the moisture variations in the room in relative humidity. The moisture variation could also have been represented as vapour pressures, which are independent of the temperature determination but the numbers are harder to relate. A vapour pressure representation is illustrated in Figure 4.1.16, which is comparable to Figure 4.1.12. Based on the figures it is clear that some of the deviations are due to differences in the thermal simulation but this cannot explain all the deviations in the solutions since some of those are also present in the vapour pressure representation. The problems of the thermal simulation are also seen indirectly from the comparison of Figure 4.1.10 and Figure 4.1.12 by the fact that some models are within the big crowd of solutions in Figure 4.1.10 but when the thermal conditions are allowed to change during the day the results in Figure 4.1.12 gives significant deviations from the “average” solution.

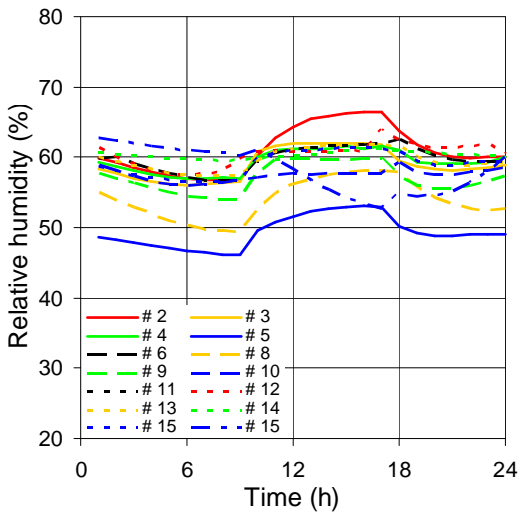


Figure 4.1.16 CE1B, Case 2 temp. range “20 to 27°C, no external radiation”, which is a more realistic case but still without solar and long wave radiation.

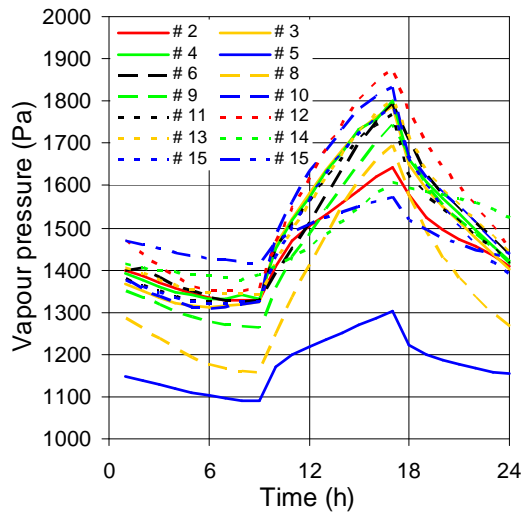


Figure 4.1.17 CE1B, Case 2 temp. range “20 to 27°C, no external radiation”, which is a more realistic case but still without solar and long wave radiation.

**4.1.4 Conclusions to draw**

The Common Exercise 1 stimulated some developments of different software as well as some original use of existing programs. Some energy models were improved in more moisture oriented programs, and moisture modelling was enhanced in more energy oriented tools.

They also showed that there is a need for some consensus data concerning heat and moisture properties of the materials.

In the following, the experience from these hygrothermal exercises is discussed more detailed. Attention is paid both to the new achievements and to the problems that occurred. Also issues for future work are stated.

#### 4.1.4.1 Improving thermal aspects

As intended, the Common Exercise 1 stimulated some improvement of existing programs. New developments concerned specially radiation heat transfer calculations. Both short wave radiation (computation of incident solar radiation and heat gains through the windows) and long wave intra-zone exchanges were enhanced in some programs. As heat, air and moisture closely interact with each other in a building, a correct description of energy behaviour is needed before assessing whole building moisture performance.

The deviation of results within a reasonable range gives also some more confidence in energy models and provides a valuable reference case for some future sensitivity study on the impact of moisture on energy loads.

#### 4.1.4.2 Improving hygrothermal aspects

The results from the original case (CE1) were rather disappointing: The deviation between the used models was large even for the simple isothermal case 600\_0A where the constructions were "hidden by" a vapour tight membrane. A study of the achieved indoor temperature showed that there was not agreement in the way the models calculated the thermal conditions, either. However, one should be reminded that this was first attempt ever of trying to compare the results of this kind of models with the moisture.

If the purpose of using such whole building hygrothermal simulations was to predict the resulting indoor humidity in a given building, the result would be up to a factor 2 different within the used simulation models, as shown in Figure 4.1.4. It was concluded after plenary presentation of these results that the exercise should be redesigned to be significantly simpler to avoid deviation due to factors that are not central for the hygrothermal modelling itself.

The first part of the revised exercise (CE1A), the very simplified isothermal case with tight and open indoor surfaces, showed a good agreement among both the analytical solutions and the numerical calculations. These results gave an increased belief that it was possible to predict the indoor RH with a whole building hygrothermal calculation. However, in this case some important building elements like windows were neglected.

The second and the more realistic part of the revised exercise (CE1B) illustrated again the complexity of the whole building hygrothermal modelling: Some deviations were significant. The differences in the thermal calculation could not explain the deviation as it was present also for the case with constant indoor temperature ("20°C, no external radiation"): Figure 4.1.11 shows a variety of cooling loads needed for keeping the temperature constant. A comparison of the solar gain calculated by the different models showed some unexpected variation: The gains differed although the exercise was posed with specification that the windows were 100% transparent (Figure 4.1.15).

#### 4.1.4.3 Further work

The experience from the Common Exercises so far tells that we are not finished with them yet. There is a need to execute more cases, possibly as a comparison with measurement data. Some other aspects have to be considered as well, e.g. adding furniture and considering the air flows.

The actual challenge in whole building Heat Air and Moisture modelling is to ensure a good balance between the many different physical phenomena which interact on each other, rather than to develop models that focus too much on mainly one phenomenon. For example in most of the existing programs if moisture is well modelled then the energy model is rather simple, or if energy is rather well calculated then moisture behaviour is treated in a simplified way, if not neglected.

Another issue that will be considered in Annex 41 modelling activity is the relative importance of the different phenomena and their interactions. Sensitivity analysis and the future common exercises should help to answer the fundamental question when and which interactions can be neglected and in which cases they must be represented.

#### 4.1.5 General Conclusions

The Common Exercise 1 executed as a part of the Annex 41 Subtask 1: Modelling illustrated the complexity of the whole building hygrothermal modelling: It was possible to find a consensus among the solutions with different calculation models only for an extremely simple isothermal case: monolithic building without windows and no contact to ground.

On the other hand, these results also underline the importance of this type of exercises: The existing codes are "tested" for their suitability for the whole building hygrothermal simulation and the new ones are created, including upgrading and developing the existing codes to be able to handle also the moisture calculation.

#### 4.1.6 Appendices

**Appendix A:** Exercise texts

**Appendix B:** The analytical consensus solution prepared by Dr. Thomas Bednar, TUW and Prof. Carl-Eric Hagentoft, CTH (**This is actually Section 0 of this report**)

**Appendix C:** Collection of individual reports

[CE 1](#)

[CE1A](#)

[CE1B](#)

## 4.2 Common Exercise 2 - Small climate chamber test

**ANNEX 41 – Subtask 1**  
**Common Exercise 2**  
 (Whole building heat and moisture analysis)

### “Small chamber test (THU test room) in the climate chamber”

By

<sup>1</sup> Hiroshi YOSHINO, Tohoku University, Japan

<sup>2</sup> Teruaki MITAMURA, Ashikaga Institute of Technology, Japan

<sup>3</sup> Ken-ichi HASEGAWA, Akita Prefectural University, Japan

#### 4.2.1 Introduction

In order to design the residential spaces for indoor humidity control, it is important to investigate the influence of ventilation rate and volume rate of the hygrothermal materials. This would become available data for indoor environmental design.

The objective of this common exercise is to simulate the small chamber (called “THU test room”) which is located in the climate chamber. Experiments for this small chamber started in autumn, 2005. Two kinds of experiments have been carried out. One is for ventilation rate (Case 1-1 to 1-3). Another is for the quantity and locations of the hygrothermal materials (Case 2-1 to 2-6). As moisture buffering material served gypsum boards (the same gypsum board of the round robin test from Subtask 2 was used). In the following the information about the small chamber (THU test room) and boundary conditions are described.

#### 4.2.2 Experimental and simulation setting

##### 4.2.2.1 General Information

Each experiment consists of a preconditioning period followed by 6 hours of humidification and 12 hours without humidification. Variations of indoor temperature and humidity are evaluated during the 6 + 12 hours. The quantity of humidification water is about 20 g/h. Experimental setting for the relationship between the moisture buffering effect and ventilation rate is shown in Table 4.2.1. Experimental setting for the relationship between the moisture buffering effect and quantity of the materials is shown in Table 4.2.2. For all experimental cases, ambient condition of the test chamber was 20 °C and 50 %RH.

Table 4.2.1 Experiments for ventilation rate

	Target of ventilation rate [1/h]	Hygrothermal materials	Remarks
Case 1-1	none	3 sides of walls, ceiling, floor	Reference data
Case 1-2	1.0		Usual condition
Case 1-3	5.0		Opening windows

**Table 4.2.2** Experiments for volume rate quantity and locations of the hygrothermal materials

	Hygrothermal materials	Target of ventilation rate [1/h]	Remarks
Case 2-1	all walls, ceiling, floor	1.0	Same as Case 1-2
Case 2-2	floor		
Case 2-3	one side of walls		
Case 2-4	3 sides of walls		
Case 2-5	ceiling		
Case 2-6	none		Reference data

#### 4.2.2.2 Test Method

##### Shape of the test Chamber

A schematic view of the test chamber is shown in Figure 4.2.1. The test chamber is located in the climate room at the Akita Prefectural University. In the climate room, it is possible to control indoor temperature ranging from 10 °C to 40 °C and also humidity from 30 %RH to 90%RH. This test chamber imitates a half size of a residential room in a house. The internal volume of the test chamber is 4.60 m<sup>3</sup> and its area of interior surface is 16.62 m<sup>2</sup>. The walls, ceiling and floor of the chamber consist of inside construction panels (12.5 mm of gypsum board) and outside insulation material (100 mm of polystyrene). In order to keep vapour- and airtight conditions in the chamber, an aluminium sheet is installed between the polystyrene and the gypsum board. The inlet and outlet for mechanical ventilation are located at the bottom and top of two opposite walls respectively. A small wind tunnel is connected with the outlet of the chamber to measure the ventilation rate accurately.

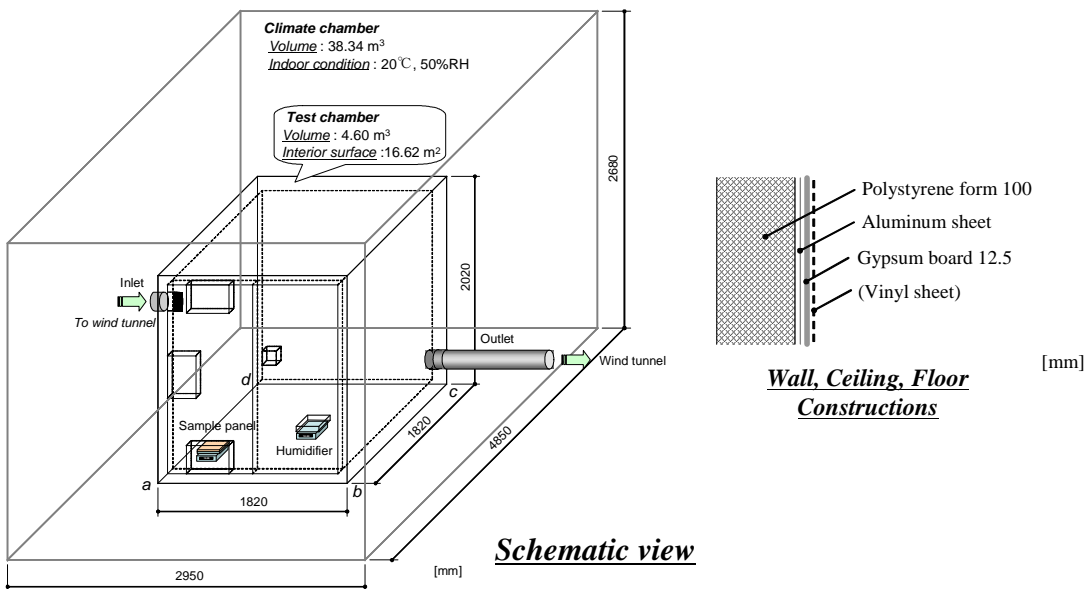


Figure 4.2.1 Schematic view of the test chamber and of the construction

##### Constructions

Wall, ceiling and floor constructions are shown in Figure 4.2.1. Material properties are shown in Table 4.2.3. The gypsum board on the walls, ceiling and floor is covered with the vinyl sheet according to the experimental cases (see Table 4.2.1 and Table 4.2.2) in order to prevent absorbing and desorbing moisture from the surface. On the front door gypsum board is not installed in any experimental cases.

Table 4.2.3 Material property

Materials	Thickness [m]	Density [kg/m <sup>3</sup> ]	Porosity [m <sup>3</sup> /m <sup>3</sup> ]	C <sub>p</sub> [J/kgK]	Lambda_dry [W/mK]	μ <sub>dry</sub> [-]	W <sub>80</sub> [kg/m <sup>3</sup> ]	W <sub>f</sub> [kg/m <sup>3</sup> ]	A <sub>f</sub> [kg/m <sup>2</sup> √s]
Outdoor surface									
Polystyrene	0.1	30	0.95	1500	0.04	50	0	0	0
Aluminium sheet	0.0001					2E+8	0	0	0
Gypsum board	0.0125	850	0.65	850	0.2	8.3	6.3	400	0.3
Vinyl sheet*	0.0002					1605	0	0	0

\*:M. Kumar KUMARAN, IEA ANNEX24 Heat, Air and Moisture Transfer Through New and Retrofitted Insulated Envelope Parts (Hamtie) Final Report Volume 3 TASK 3: MATERIAL PROPERTIES

### Internal Gains and schedules

Humidification took place by evaporating moisture from two water reservoirs (size: 340\*230 (W\*D) [mm]) that were heated by an electric heating element. The tray with the water reservoirs was weighed by another electric balance to measure the quantities of humidification water. The target moisture production rate was about 20 g/h. Experimental schedule is shown in Figure 4.2.2.

Actually, the moisture production rate was slightly different in each experimental case. And sensible heat was simultaneously generated by the water reservoirs. So data set of moisture production rate and water temperature was provided for simulation inputs. Alternatively the average values shown in Table 4.2.4 could be used as constant values.

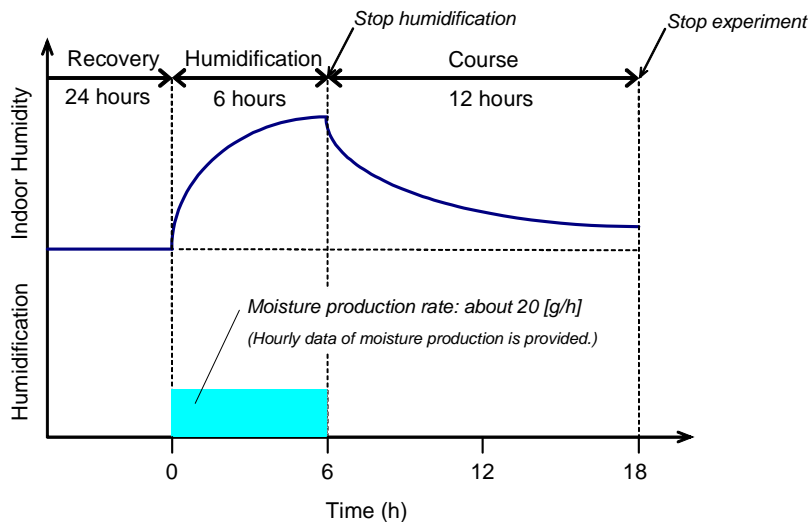


Figure 4.2.2 Experimental Schedule

Table 4.2.4 Average moisture production rate

	Moisture production rate [g/h]	Average water temperature [°C]
Case 1-1	17.8	29.0
Case 1-2	= Case 2-1	
Case 1-3	19.3	28.2
Case 2-1	21.7	29.4
Case 2-2	16.1	29.2
Case 2-3	18.6	28.4
Case 2-4	17.5	28.7
Case 2-5	17.0	28.3
Case 2-6	16.3	28.8

#### Ventilation rate and ambient conditions

Actually, the ventilation rate, ambient temperature and humidity were slightly different in each experimental case. If it is impossible to read these data file in the program, the average values shown in Table 4.2.5 was used as constant values.

Table 4.2.5 Average ventilation rate, ambient temperature and humidity

	Ventilation rate [1/h]	Ambient temp. [°C]	Humidity [%RH]
Case 1-1	–	20.4	49.5
Case 1-2	= Case 2-1		
Case 1-3	3.30	20.5	48.6
Case 2-1	0.66	20.5	51.3
Case 2-2	0.62	20.6	50.7
Case 2-3	0.78	20.6	50.7
Case 2-4	0.71	20.5	51.3
Case 2-5	0.62	20.5	49.7
Case 2-6	0.64	20.5	51.1

#### 4.2.2.3 Measurement Values for Simulation

Experimental data set for boundary conditions is provided as the following list.

- Indoor air temperature around the inlet and outlet
- Indoor air humidity around the inlet and outlet
- Inside and outside surface temperature (all walls, ceiling and floor)
- Ambient air temperature and humidity
- Water temperature of the water reservoir
- Weight change of the water reservoir (amount of moisture production)

#### 4.2.2.4 Comparison between Simulation and Measurement

Experimental data set for comparison between simulation and measurement is provided as the following list.

- Indoor air temperature
  - at 0.9 [m] height of the floor level (centre, around the surrounding walls)
  - at 0.1 [m] height of the floor level (only centre of the test chamber)
  - at 1.7 [m] height of the floor level (only centre of the test chamber)
- Indoor air humidity
  - at 0.9 [m] height of the floor level (centre, around the surrounding walls)
  - at 0.1 [m] height of the floor level (only centre of the test chamber)
  - at 1.7 [m] height of the floor level (only centre of the test chamber)

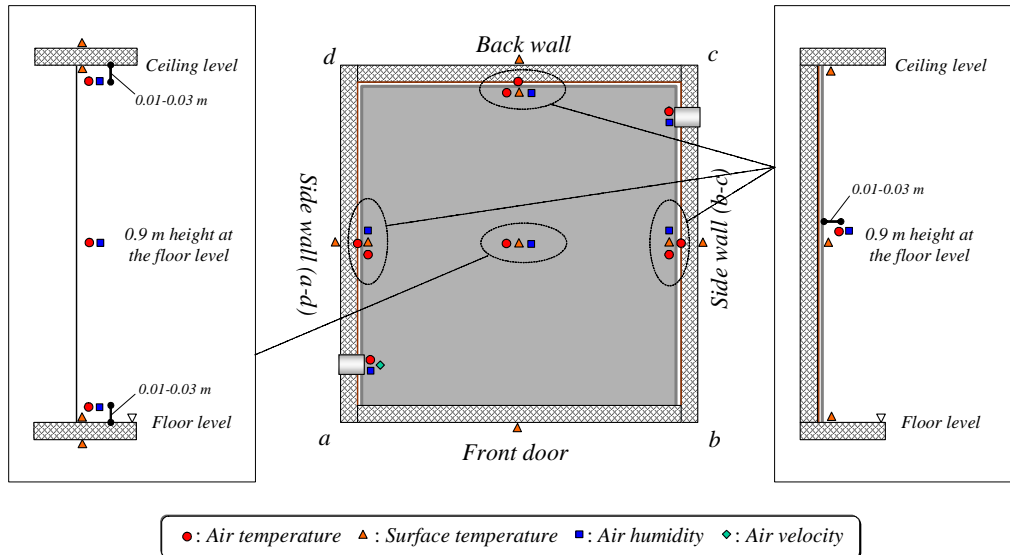


Figure 4.2.3 Measurement points

#### 4.2.2.5 Output Requirements

For each cases;

- Indoor air temperature [°C]
- Indoor air humidity (relative humidity [%] and absolute humidity [g/kg])

#### 4.2.3 Comparison between simulation and experimental results

##### 4.2.3.1 Simulation programs

Program and participants of the common exercise are shown in Table 4.2.6. Five participants submitted the simulation results by six programs. All cases were reported by all the programs, except for "XAM-CE2 x STREAM v5", which participated only in case 2.6.

Table 4.2.6 Program name and participants

	Institutions	Country	Program name
1	KIU	Japan	XAM-CE2
2	KIU	Japan	XAM-CE2 x STREAM v5 (STD model, ANK model)
3	Concordia	Canada	HAMFitPlus (COMSOL + MatLab + Simulink)
4	CSTB-CETHIL	France	HAM-Tools
5	CTH	Sweden	HAM-Tools
6	CETHIL	France	TRNSYS16.0
7	CETHIL	France	CLIM2000

**Commentaire :** "STD" and "ANK" should be explained

##### 4.2.3.2 Results

The comparison between measured and simulated data is given in the following figures. For all 8 cases indoor air temperatures and absolute humidities are plotted. Absolute humidity was chosen to represent moisture, because it is independent from temperatures.

In all the cases there was a rise of approximately 1.5-2°C in the air temperature, due to vapour production. It was correctly represented by all the models except one, which assumed almost isothermal conditions. As the power used to heat the water in the reservoirs was not known, the participant did not want to "guess" the value of heat source. Only for case 2-6 there was a

**Commentaire :** it would be useful to state here which values of RH and AH and T were used for comparison with the models (values measured in the center of the testcell ?)

misunderstanding of input values for temperature which explains the differences between the measured and the simulated data even at the initialisation.

Concerning moisture the spread was much larger:

0. Comparing only simulated results:

- a very good agreement was found between all the tools in cases 2-6 (no hygroscopic surfaces) and 1-3 (high ventilation rate),
- a large spread (over 2g/kg) was found in case 1-1 (no ventilation)
- the spread in the computed results was approximately 1 – 1.5g/kg in cases 2-1, 2-2, 2-3, 2-4, 2-5, (medium ventilation rate and some hygroscopic surfaces)

It indicates that the main difference between models is coming from the way the moisture exchange between air and hygroscopic surfaces is modelled in the simulation tools.

1. Comparing experimental vs. simulated results. Experimental data are higher than simulated values in all the cases. Moreover:

- Experimental values agree well with simulated values in cases 1-3 (high ventilation), 2-3 (one hygroscopic surface on the wall) and 2-6 (no hygroscopic surfaces).
- The simulation tools underestimate the peak absolute humidity by approximately 1g/kg in cases 2-1 (five hygroscopic surfaces), 2-4 (three hygroscopic surfaces on the wall) and 2-5 (one hygroscopic surface on the ceiling)
- The simulation tools underestimate the peak absolute humidity by approximately 2g/kg in cases 1-1 (five hygroscopic surfaces and no ventilation) and 2-2 (one hygroscopic surface on the floor)

The agreement is better when the impact of moisture buffering is lower (high ventilation and no hygroscopic surfaces). The biggest differences occur in cases with no ventilation and with hygroscopic surface lying on the floor. It may indicate that besides moisture adsorption on hygroscopic surfaces there is some stratification of the indoor air. Indeed with no ventilation the air is very quiet in the test chamber, so there is no mixing. Moreover water vapour is lighter than dry air, so it has tendency to go up, and therefore disadvantages the situation when the hygroscopic material is on the floor.

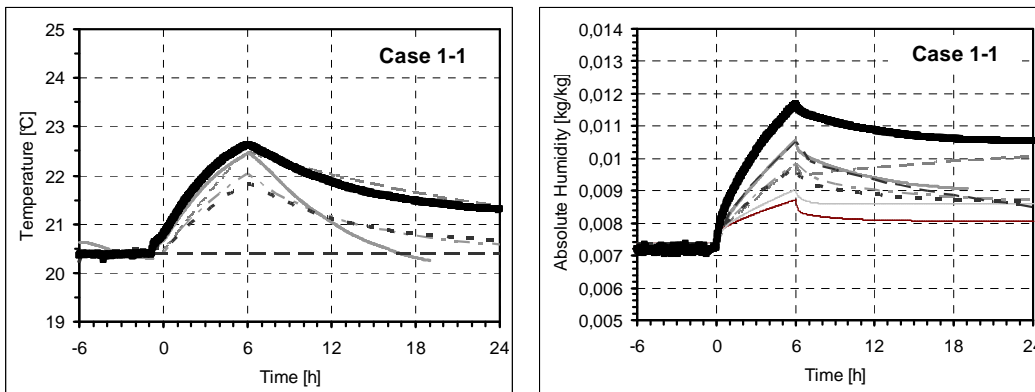


Figure 4.2.4 Comparison between measured values and simulation results (Case 1-1)

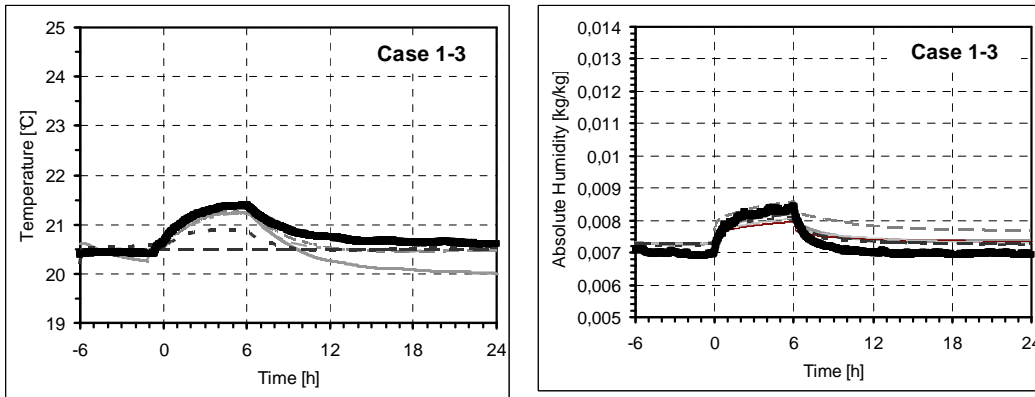


Figure 4.2.5 Comparison between measured values and simulation results (Case 1-3)

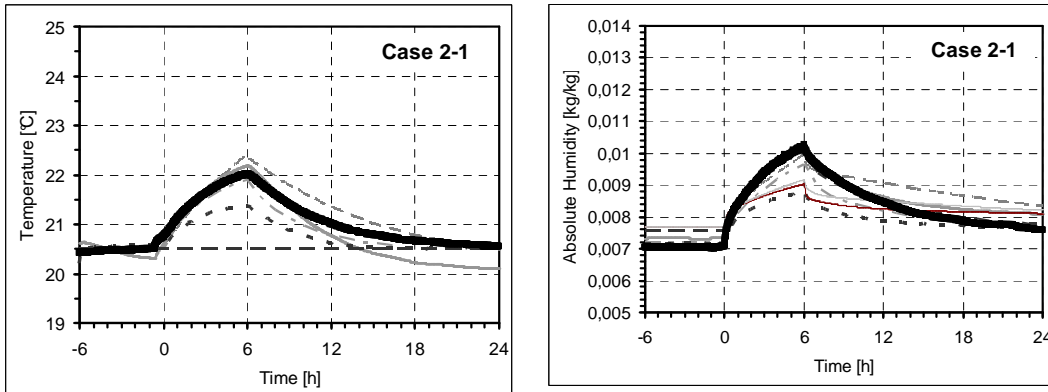


Figure 4.2.6 Comparison between measured values and simulation results (Case 2-1)

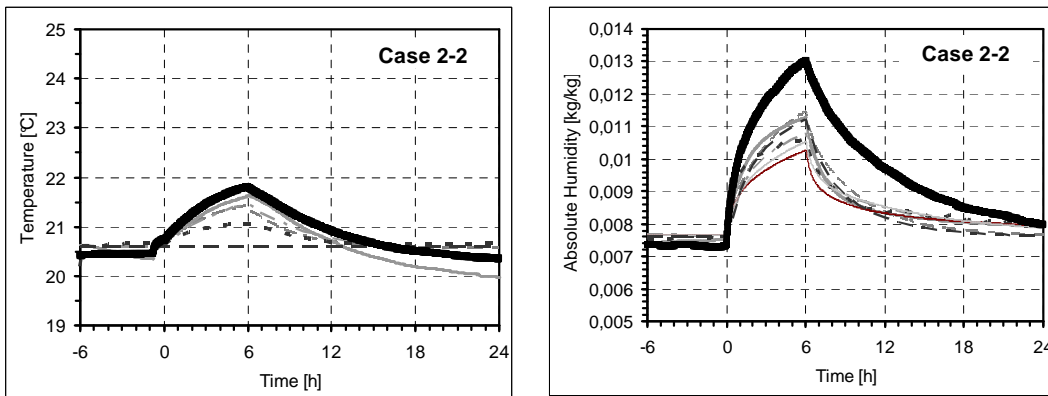


Figure 4.2.7 Comparison between measured values and simulation results (Case 2-2)

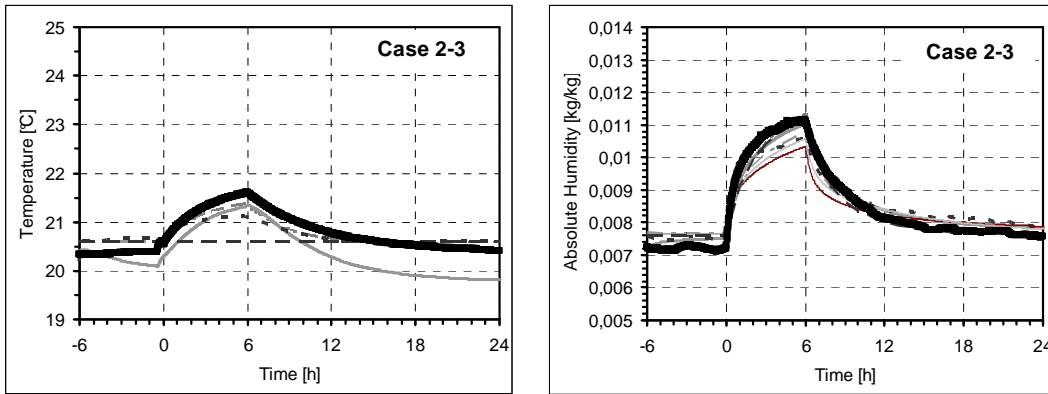


Figure 4.2.8 Comparison between measured values and simulation results (Case 2-3)

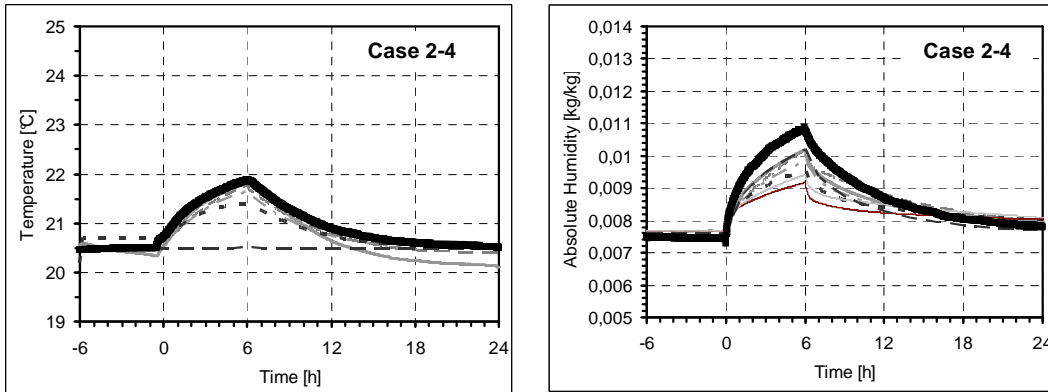


Figure 4.2.9 Comparison between measured values and simulation results (Case 2-4)

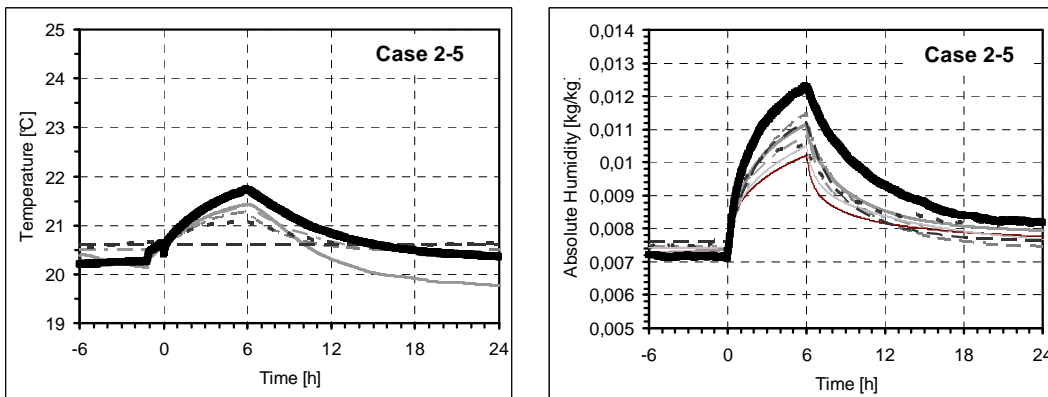


Figure 4.2.10 Comparison between measured values and simulation results (Case 2-5)

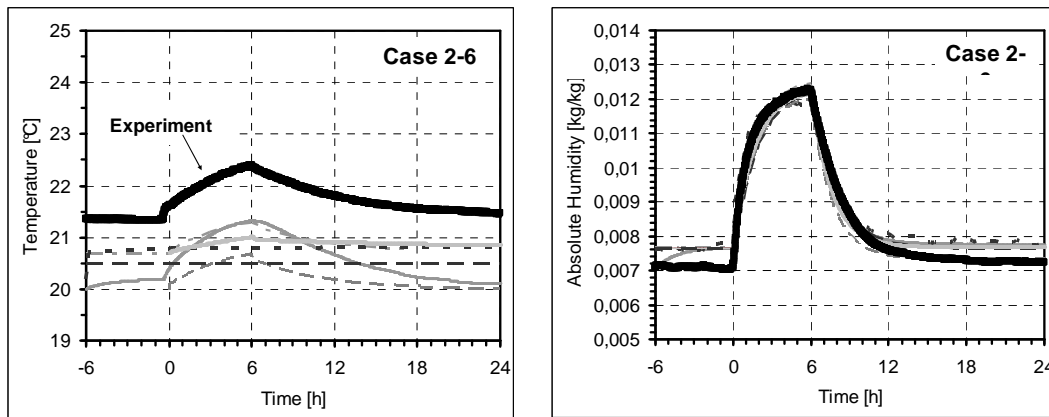


Figure 4.2.11 Comparison between measured values and simulation results (Case 2-6)

#### 4.2.4 Conclusion

Simulation results of humidity in Case 1-3, Case 2-3 and Case 2-6 indicated comparative good agreement with the experimental value. For features of simulation programs, simulated humidity by the XAM-CE2 and HAMFitPlus were similar and larger than that of other programs. The reasons of differences between the experiment and simulation would be a measurement error and an influence of distribution of indoor temperature and humidity, but these are not cleared.

### 4.3 Common Exercise 3 – Test building with two parallel rooms

## Annex 41 – Subtask 1

### Summary Report of Common Exercise 3 (Whole building heat and moisture analysis)

by  
Kristin Lengsfeld

#### 4.3.1 Introduction

Well-balanced conditions of thermal, moisture and air quality are very important in buildings because an imbalance of these factors could have significant influences on the construction and the inhabitants. The focus is the influence of different materials on the fluctuation of relative humidity specifically humidity peaks. In lieu of complicated and expensive laboratory testing several different software tools have been developed to estimate the indoor environmental conditions of buildings. In context of the Common Exercise 3 (CE 3) several software tools were used to point out how models can simulate the hygrothermal indoor climate conditions. For a successful application of such software tools a validation in comparison to measurement results are essential. Therefore for the common exercise two identical rooms were used to measure the moisture buffering capacity of several interior finish systems at the free field investigation area in Holzkirchen (Germany). The intention of the Common Exercise 3 is to point out how good the simulation tools are to calculate the indoor climate behaviour under real conditions with different areas of moisture buffering materials. Additionally the results of the validations show where further developments are necessary. In the following the results of the laboratory tests and simulation results of Common Exercise 3 are described.

#### 4.3.2 Experimental investigations

In context of the project Annex 41 – MOIST-ENG measurements of the moisture buffering effects have been carried out in two identical experimental rooms (Figure 4.3.1) at the free field investigation area in Holzkirchen.

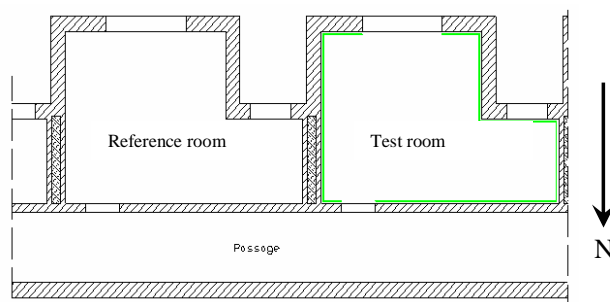


Figure 4.3.1: Ground plan of the two experimental rooms.

In the following the left room is defined as reference room, which has a traditional internal painted gypsum plaster as wall and ceiling surface. The test room is identical to the reference room as regard to geometry and dimensions. The difference in comparison to the reference room is that the wall and ceiling surfaces are covered with aluminium foil to prevent the sorption of the surfaces. The floor in both rooms is covered with a PVC floor covering, which is also supposed as inert from the hygrothermal point of view. The volume of each room is approx. 50 m<sup>3</sup> and the total surface of the room (without floor, window and door) is approx. 67 m<sup>2</sup>.

The indoor air temperature of the test rooms was held at 20 °C. One essential parameter influencing the indoor conditions is the air change due to infiltration via joints or other leakage. The natural air change rate was reduced in both rooms by masking surface defects. A ventilation system is installed in both rooms providing a constant air change. The air change rates during operation of the ventilation

system were determined by tracer gas measurements. The air change rate for the reference room is  $n = 0.63 \text{ h}^{-1}$  and for the test room is  $n = 0.66 \text{ h}^{-1}$ .

To achieve a realistic assessment of the course of relative humidity with regard to the moisture buffering effect, 2.4 kg of water is introduced by an ultrasonic evaporator into each room per day, which simulates the equivalent amount for a household of three persons [Hartmann et al. 2001]. To differentiate short- and long-term moisture buffering of surrounding surfaces, a practically orientated daily repeated moisture production cycle is chosen, whose peaks show a short but high intensity in the morning and a larger but moderate intensity in the evening. Thus, the moisture profile [Ellinger 2004] (Fig. 2) shows two peaks, one in the morning from 6 a.m. to 8 a.m. and in the afternoon from 4 p.m. until 10 p.m. These peaks simulate taking showers, washing, cooking and the presence of human beings. The moisture is generated according to the profile which is shown in Fig. 2 by using ultrasonic evaporators controlled by a clock timer.

To record room climatic conditions, temperature and humidity sensors are installed in the test rooms. The temperature of the wall surfaces, temperature layering in the middle of the rooms as well as relative humidity in the rooms are determined. The energy consumption of the heating system is measured by a power meter. The temperature and humidity in the centre of the room is considered for the evaluation of the following tests. Measured data were constantly recorded by means of a data acquisition system, are stored in a data base and then evaluated.

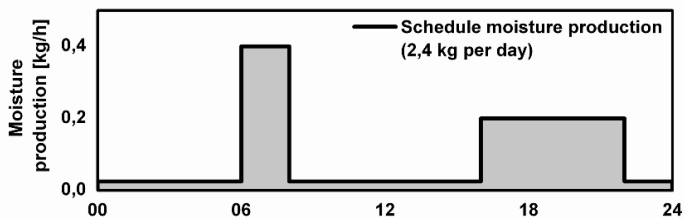


Figure 4.3.2: Course of the daily humidity generation in the two test rooms.

Additional to the measurements of the moisture buffering effects of the tested materials, experiments were made with and without a heating system and solar radiation through the window.

#### 4.3.2.1 Schedule of versions

In regarding to the calculations for the validation different versions are considered. In the test and reference room the hygrothermal climate conditions measured continuously. The different versions which were made are listed in Table 4.3.1 and Table 4.3.2. For Step 1 the test room is only covered with aluminium foil on the walls and the ceiling. The second step is with gypsum boards on the walls and the third step with gypsum boards on the walls and the ceiling in the test room. Parallel to these experiments the climate conditions in the reference room with painted gypsum plaster on the walls and the ceiling are measured. The additional measurements with and without heating system and solar radiation are combined in Step 4 (Table 4.3.2).

Table 4.3.1 Schedule of versions

	Step 1	Step 2	Step 3
<b>Time</b>	17.01. - 02.02.2005	14.02. - 20.03.2006	27.03. - 22.04.2006
<b>Reference room</b>	painted gypsum plaster	painted gypsum plaster	painted gypsum plaster
<b>Test room</b>	aluminium foil	gypsum boards on the walls	gypsum boards on the walls and ceiling
<b>Temperature and moisture load</b>	20 °C / 2.4 kg/d	20 °C / 2.4 kg/d	20 °C / 2.4 kg/d
<b>Outdoor climate</b>	Holzkirchen	Holzkirchen	Holzkirchen

Table 4.3.2 Step 4

	Date	Heating system	Moisture load	Outdoor climate
Reference room	10.1. – 23.1.2006	on	2.4 kg/d	Holzkirchen
	15.2. – 24.2.2006	off		
Test room	23.1. – 8.2.2006	on		
	8.2. – 15.2.2006	off		

All other information about the experiments are attached in appendix A.

#### 4.3.3 Participating institutions and simulation tools

Table 4.3.3 shows the institutions that are participated to the common exercise and the used simulation code. The description of the models is found in the collection of the reports (appendix B).

Table 4.3.3 An overview of the participating institutions and the used simulation tools.

		Step 1	Step 2	Step 3	Step 4
CETHIL	France	Clim2000			
CON	Canada	HAMFitPlus (COMSOL + MatLab + Simulink)			
CTH	Sweden	HAM-Tools			
DTU	Denmark	BSim, Version 4,5,7,7			
FhG	Germany	Raummodell 1.0 pro	WUFI <sup>®</sup> -Plus Version 1.0.1.24		
PUCPR	Brazil	Power Domus 1.0, TRNSYS 15.3			
SAS	Slovakia	ESP-r, NPI			
TUD	Germany	TRNSYS-ITT			
TUE	Netherlands	HAMLab			
TTU	Estonia	IDA Indoor Climate and Energy (IDA ICE) Version: 3.0 Build 14			
TUW	Austria				
UG	Belgium	TRNSYS 16.00.0036			

#### 4.3.4 Results

In the following the results of the calculations of the validation are shown exemplary for few days during the period of measurements. The main focus here is the course of the relative humidity. The heating power in the rooms is shown only for the reference room because the sensor in the test room was broken. The complete data of the measurements and the calculations are available on CD.

##### 4.3.4.1 Step 1

During the first testing phase the walls and the ceiling were covered with aluminium foil in the test room and through this no absorption and desorption of the surfaces was possible. The boundary conditions in the reference room are for all three steps the same. There are always painted gypsum plaster on the walls and the ceiling. The aim of Step 1 in the test room was to calculate the indoor climate without sorptive surface and only with the air change rate. The results of the measurement and the calculations of thirteen different simulation tools are shown in Figure 4.3.3 on the top for the test room and on the bottom for the reference room for two exemplary days. The main influence to the indoor climate in the test room is the air change rate. The measured air change rate is  $0.66 \text{ h}^{-1}$  in the test room. In comparison of the calculated relative humidity to the measured the spreading of the results are in the range of the tolerance. The spreading of the results in the reference room, where moisture buffering behaviour over the painted gypsum plaster is possible, is higher than in the test room. The required heating power for the heating to  $20 \text{ °C}$  is shown in Figure 4.3.4, but only for the reference room because the sensor in the test room was broken. The calculation of the heating power in the reference room shows big differences to the measurements.

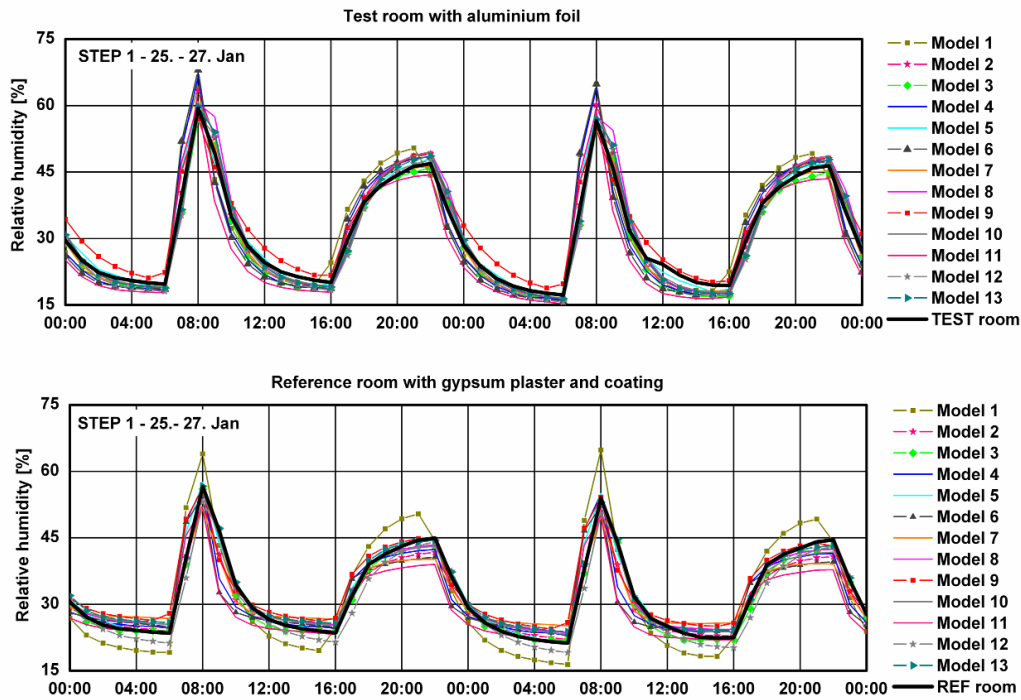


Figure 4.3.3: Courses of the measured and calculated relative humidity in the period of 25<sup>th</sup> to 27<sup>th</sup> January.

top: Test room with aluminium foil on the walls and the ceiling.  
 bottom: Reference room with painted gypsum plaster on the walls and the ceiling.

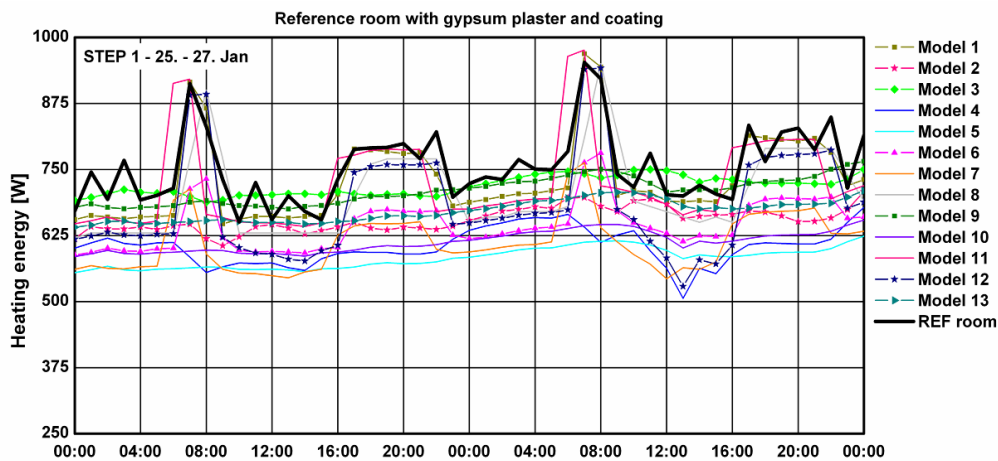


Figure 4.3.4: Course of the heating power in the reference room in the period of 25<sup>th</sup> to 27<sup>th</sup> January.

4.3.4.2 Step 2

The second step is with gypsum boards on the walls in the test room. The area of the sorptive surface is circa 45 m<sup>2</sup>. In this step the moisture buffering effect of the uncoated gypsum boards is in evidence. The courses of the measured and calculated indoor relative humidity are shown in Figure 4.3.5 on the top for the test room and on the bottom for the reference room. The courses of the heating power in the reference room are shown in Figure 4.3.6.

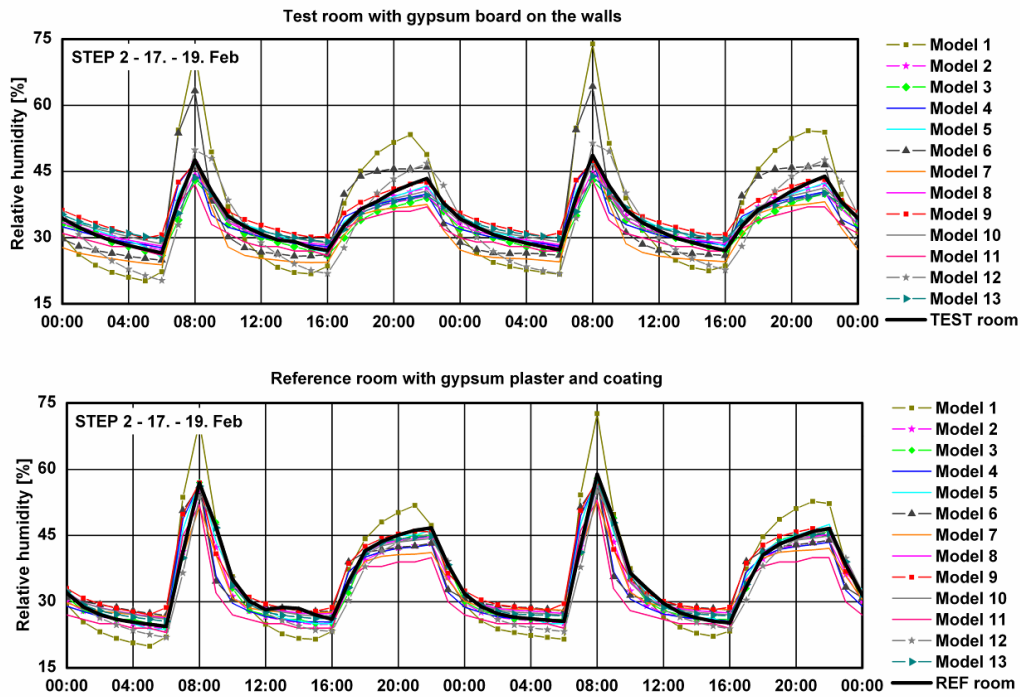


Figure 4.3.5: Courses of the measured and calculated relative humidity in the period of 17<sup>th</sup> to 19<sup>th</sup> February.

top: Test room with gypsum boards on the walls.  
 bottom: Reference room with painted gypsum plaster on the walls and the ceiling.

The spreading of the results in this case with the gypsum boards on the walls is high. The variations of the RH during the moisture peak in the morning is between -5 % and approx. +30 % from the measured data. Many of the simulation tools have difficulty modelling the moisture buffering effect of the uncoated gypsum boards in this step. The results in the reference room look better because the gypsum plaster is covered with a tight coating and therefore the moisture buffering effect is not so high as with uncovered gypsum boards.

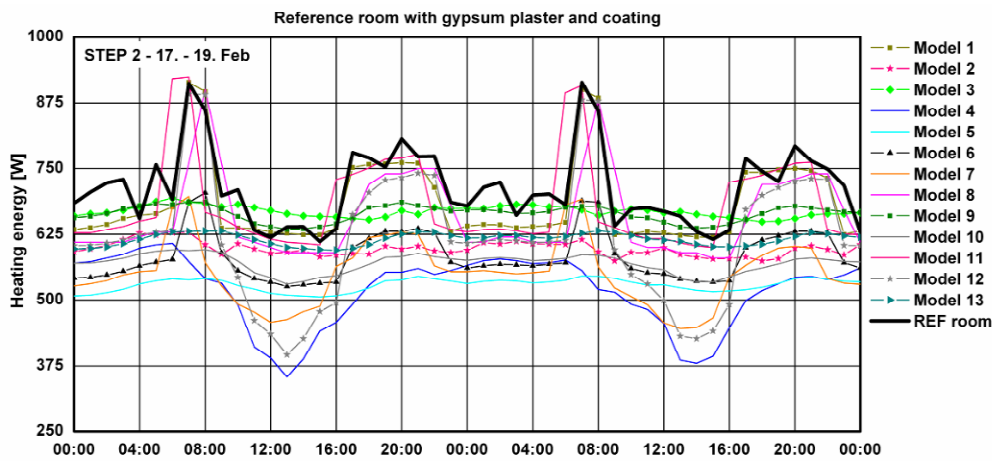


Figure 4.3.6: Course of the heating power in the reference room in the period of 17<sup>th</sup> to 19<sup>th</sup> February.

The calculation of the heating power in the reference room shows the same problem as in Step 1 and 2. The spreading between the measurements and the calculated results are very high and only a few models can simulate the higher heat energy consumption during the moisture production phases.

#### 4.3.4.3 Step 3

Step 3 is almost the same as Step 2 but for this experiment gypsum boards are installed on the walls and the ceiling. The sorptive surface in the test room is circa 67 m<sup>2</sup>. The results of Step 3 are shown in Figure 4.3.7 for two exemplary days on the top for the test room and on the bottom for the reference room. This step is the direct comparison between the moisture buffering effects of uncoated gypsum boards and painted gypsum plaster because the sorptive surface of the materials are comparable in both rooms. The courses of the heating power are shown in Figure 4.3.8 for the reference room. The results of Step 3 show almost the same spreading as in Step 2. It was not easy to model the moisture buffering effect and the heating power with the simulation tools used.

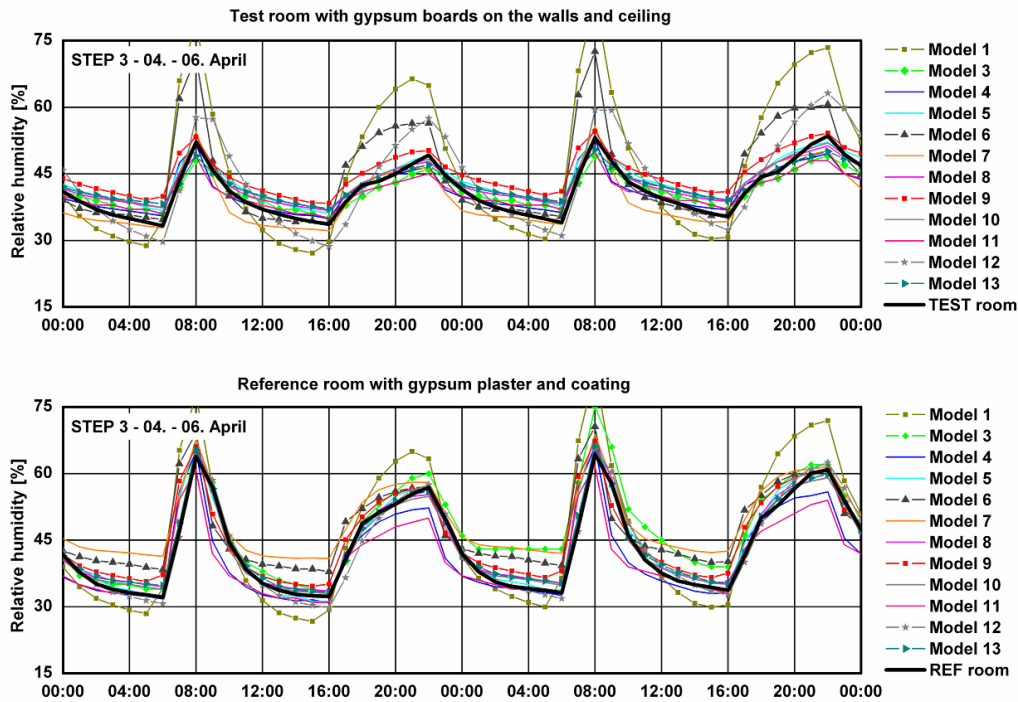


Figure 4.3.7: Courses of the measured and calculated relative humidity in the period of 04<sup>th</sup> to 06<sup>th</sup> April.

top: Test room with gypsum boards on the walls and the ceiling.

bottom: Reference room with painted gypsum plaster on the walls and the ceiling.

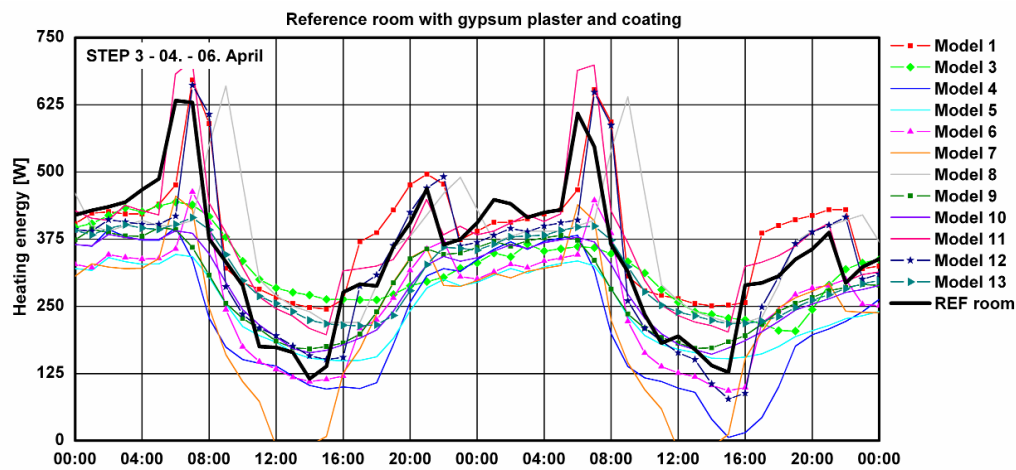


Figure 4.3.8: Course of the heating power in the reference room in the period of 04<sup>th</sup> to 06<sup>th</sup> April.

#### 4.3.4.4 Step 4

In Step 4 the influence of solar radiation through the windows are considered and additionally the indoor climate conditions are measured with and without a heating system. During this experimental phase the test room is empty and only covered with aluminium foil. These calculations were made only from four participants of the CE 3.

In Figure 4.3.9 the courses of the indoor temperature are shown on the top for the test room and on the bottom for the reference room but for different periods.

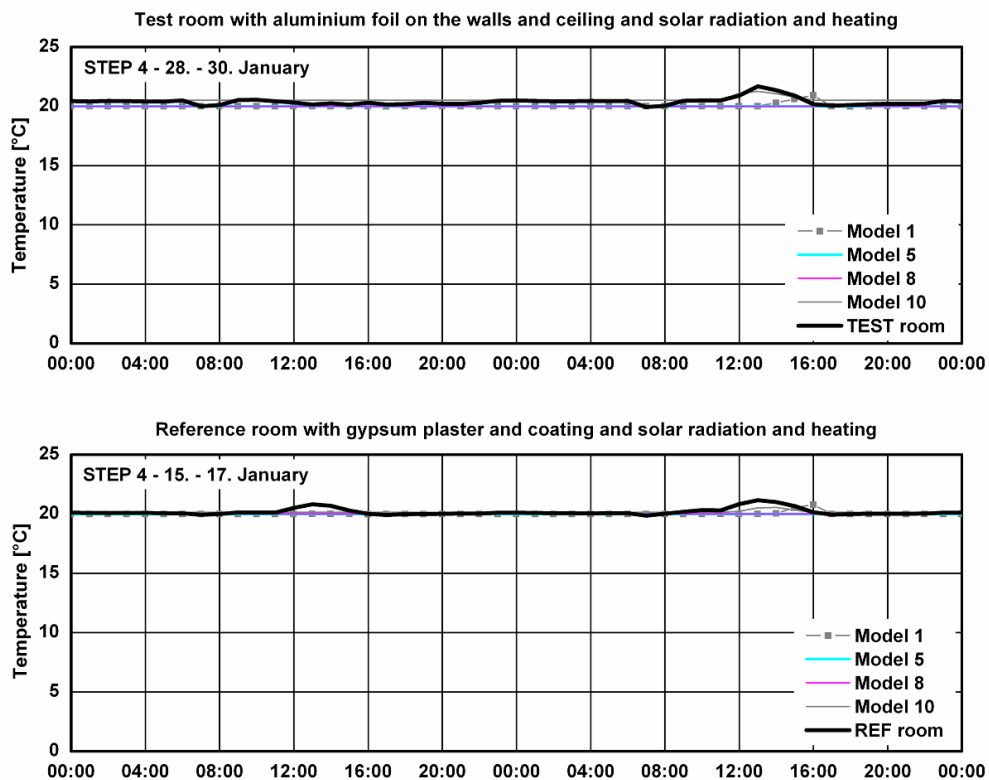


Figure 4.3.9: Courses of indoor temperature inclusive solar radiation and heating system.  
 top: In the period of 28<sup>th</sup> to 30<sup>th</sup> January in the test room.  
 bottom: In the period of 15<sup>th</sup> to 17<sup>th</sup> January in the reference room.

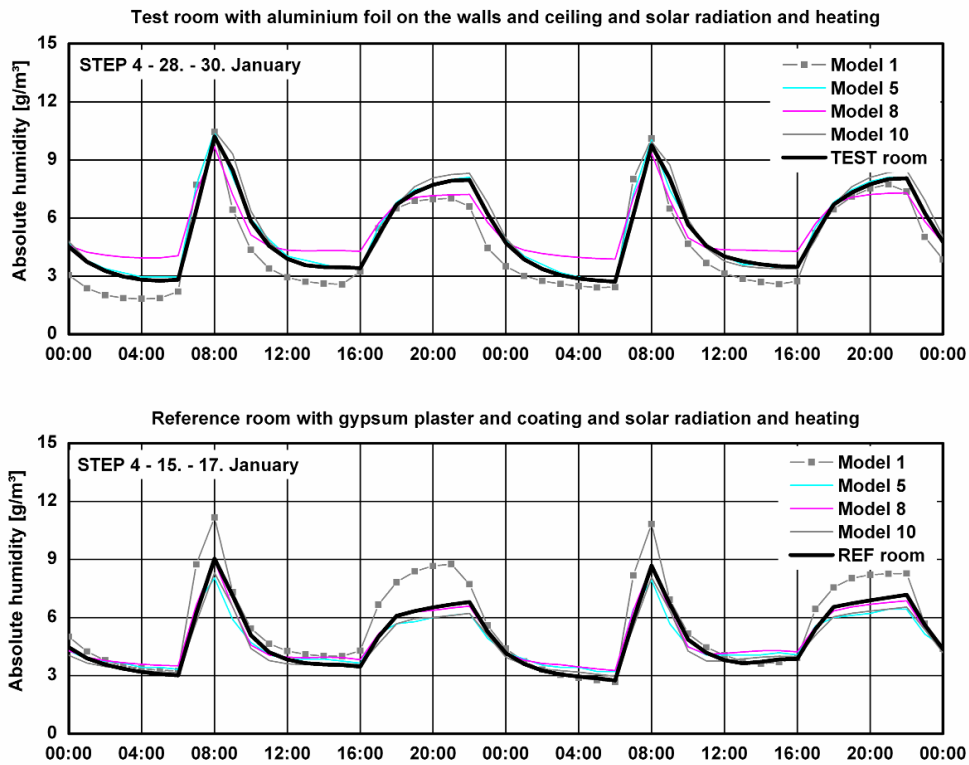


Figure 4.3.10: Courses of absolute humidity inclusive solar radiation and heating system.

top: In the period of 28<sup>th</sup> to 30<sup>th</sup> January in the test room.

bottom: In the period of 15<sup>th</sup> to 17<sup>th</sup> January in the reference room.

In Figure 4.3.10 the courses of the absolute humidity in the two experimental rooms are shown. During this testing phase the heating system is running and results of the heating power in the reference room is shown in Figure 4.3.11.

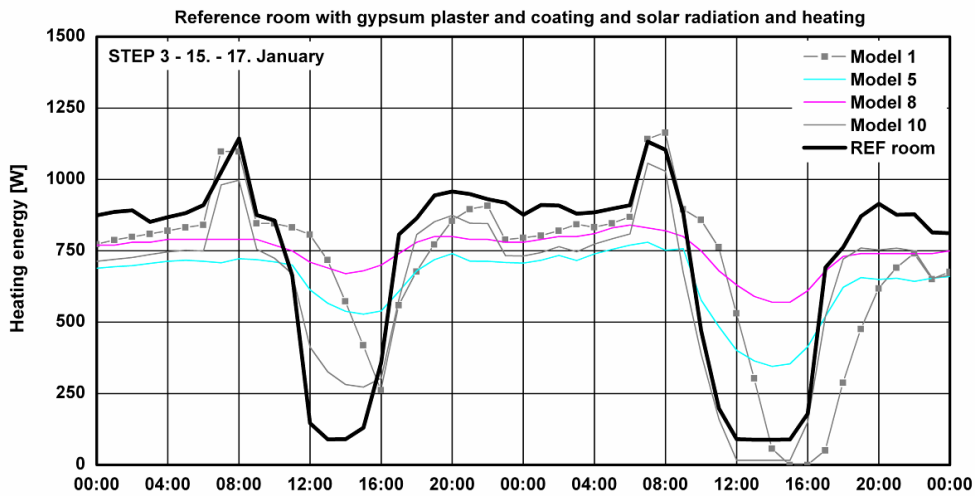


Figure 4.3.11: Courses of the heating power in the period of 15<sup>th</sup> – 17<sup>th</sup> January in the reference room.

During the second testing phase of Step 4 the heating system is switched off. The results of the measurements and the calculation are shown in Figure 4.3.12 and Figure 4.3.13. Figure 4.3.12 shows the indoor temperature and Figure 4.3.13 the absolute humidity in the rooms.

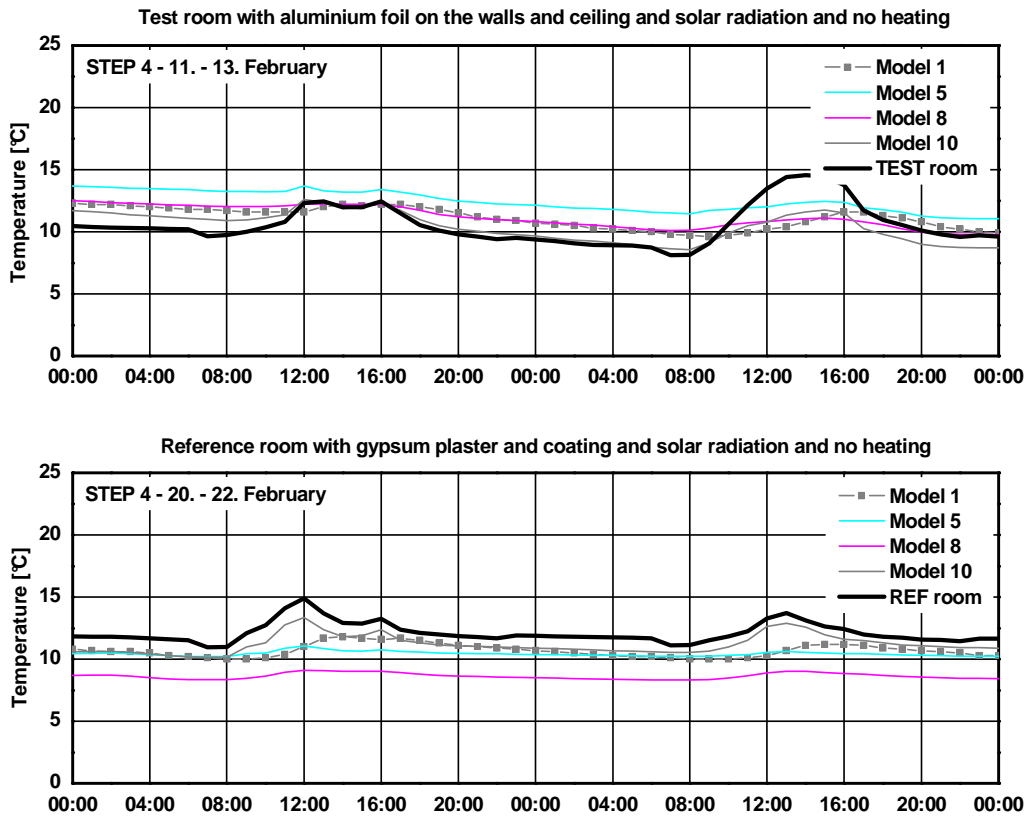


Figure 4.3.12: Courses of indoor temperature inclusive solar radiation and no heating system.

top: In the period of 11<sup>th</sup> to 13<sup>th</sup> February in the test room.

bottom: In the period of 20<sup>th</sup> to 22<sup>th</sup> February in the reference room.

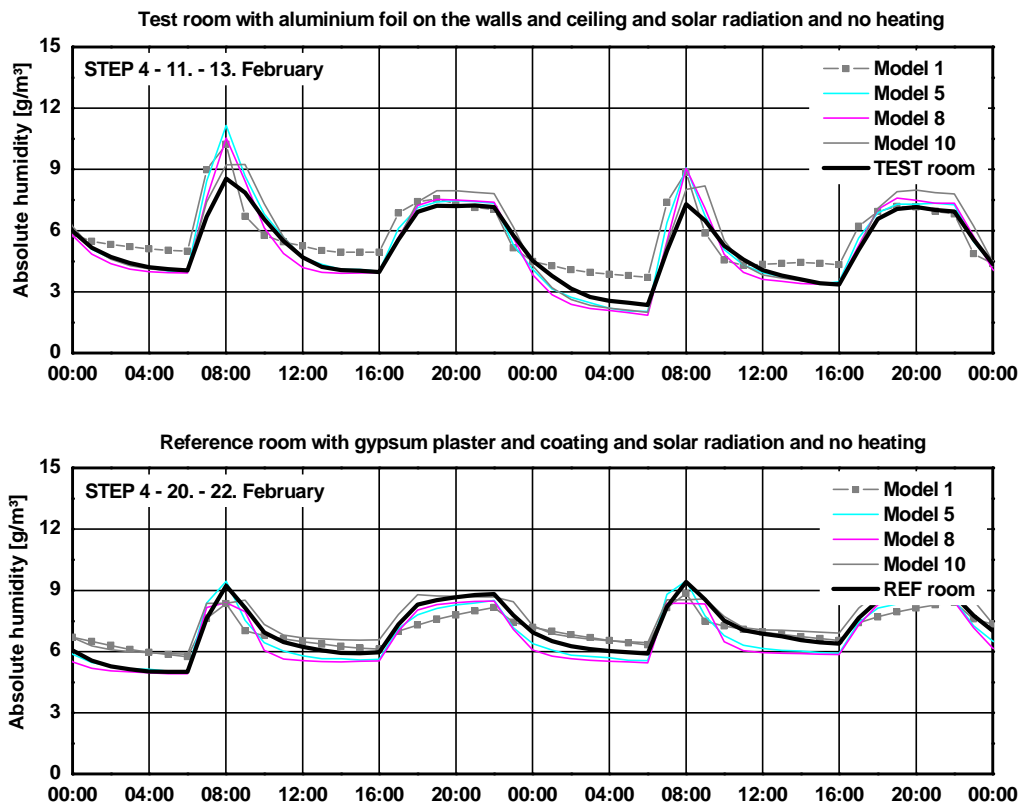


Figure 4.3.13: Courses of absolute humidity inclusive solar radiation and no heating system.

top: In the period of 11<sup>th</sup> to 13<sup>th</sup> February in the test room.

bottom: In the period of 20<sup>th</sup> to 22<sup>th</sup> February in the reference room.

#### 4.3.4.5 Statistical analysis of the results

Additional to the simulation results statistical analyses were made with the point of view to the descriptive statistics. For all analyses the whole periods of the different steps are considered.

Figure 4.3.14 and Figure 4.3.15 show the results of the statistical analyses of Step 1 in the test room with aluminium foil and in the reference room with painted gypsum plaster of the relative humidity. The period of this step run over 16 days. For the calculation of the median, 25 % and 75 % percentiles and the maximum and minimum values all data of the period were used. For the first step only with aluminium foil on the walls and the ceiling the variations of the medians and percentiles of Step 1 shows good agreements to the measurement which is the first plot in the diagram in Figure 4.3.14. In Figure 4.3.16 the statistical analysis of the heating power in the reference room is shown. The spreading of the results is very high.

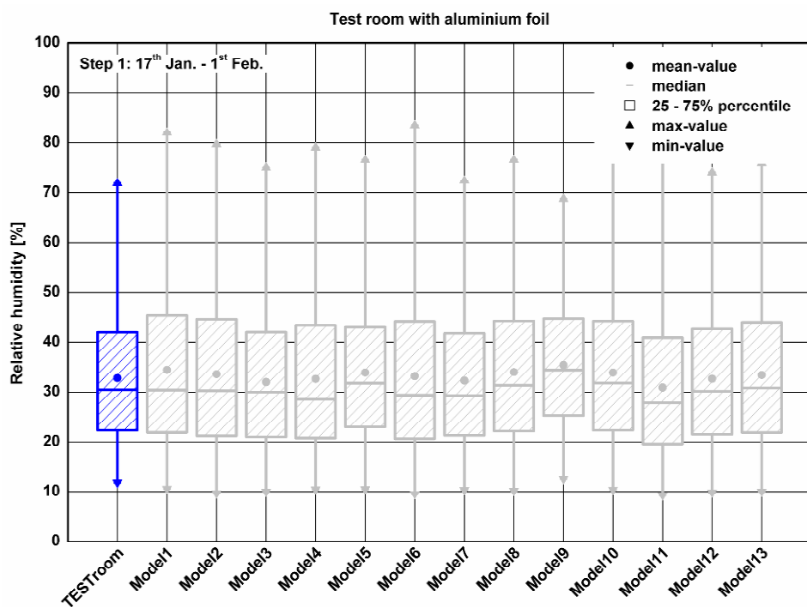


Figure 4.3.14: Statistical analysis of the results of the relative humidity in the test room with aluminium foil over a period of 16 days.

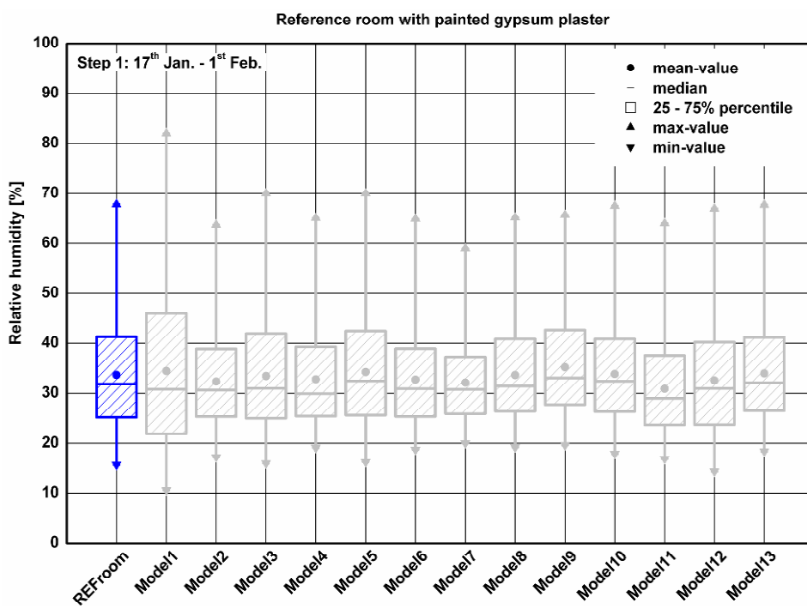


Figure 4.3.15: Statistical analysis of the results of the relative humidity in the reference room with painted gypsum plaster over a period of 16 days.

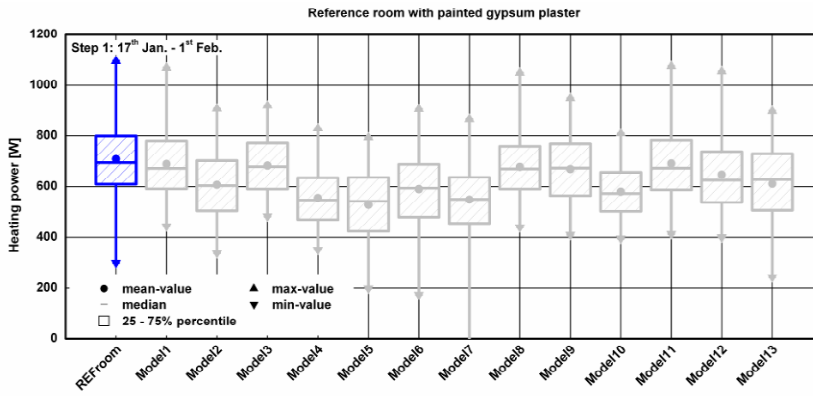


Figure 4.3.16: Statistical analysis of the results of the heating power in the reference room with painted gypsum plaster over a period of 16 days.

The same statistical analyses were done for Step 2, the test room with gypsum boards on the walls and the reference room with painted gypsum plaster on the walls and the ceiling. Figure 4.3.17 and Figure 4.3.18 show the medians, 25 % and 75 % percentiles and the minimum and maximum values over a period of 34 days. The results of the measurements are the first plot in the diagram. In this case the variation between the simulations and the measurements are partly higher. In Figure 4.3.19 the statistical analysis of the heating power in the reference room is shown. The most models have big problems to calculate the heating power in the room correctly.

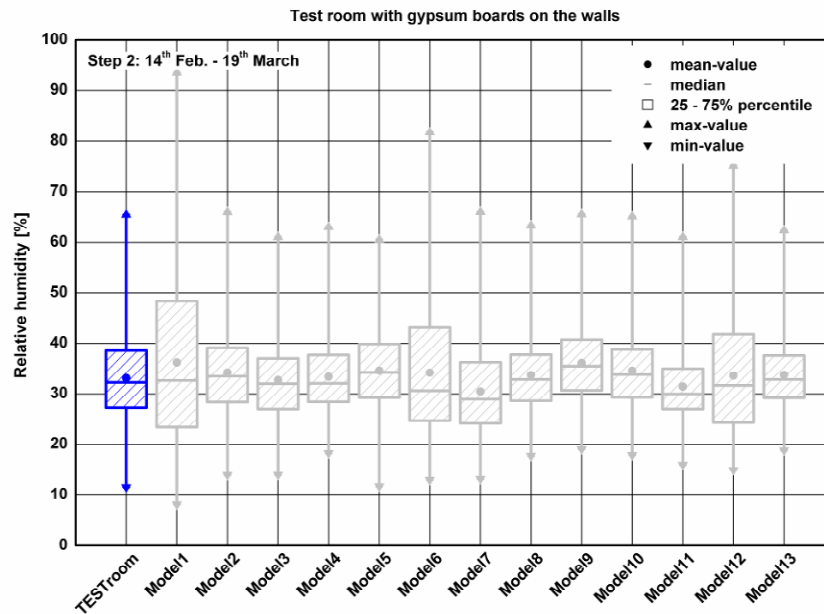


Figure 4.3.17: Statistical analysis of the results of the relative humidity in the test room with gypsum boards on the walls over a period of 34 days.

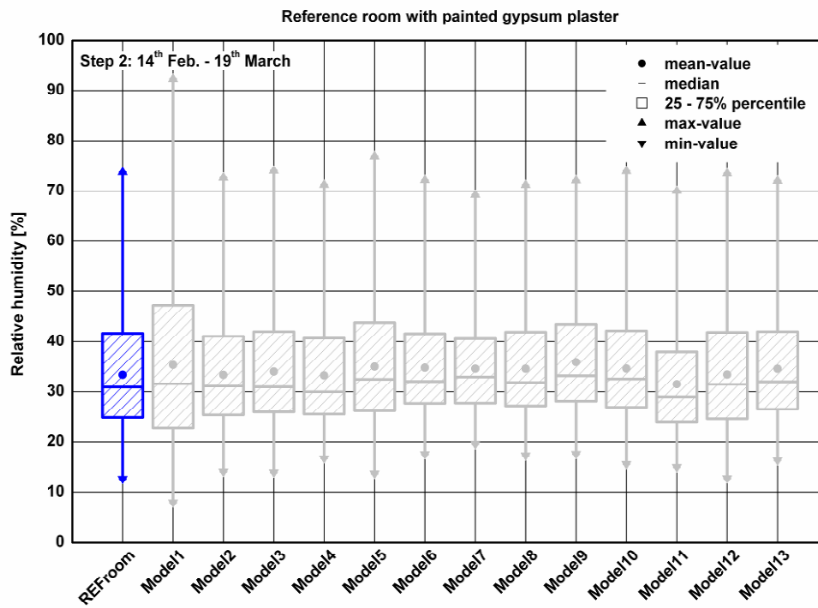


Figure 4.3.18: Statistical analysis of the results of the relative humidity in the reference room with painted gypsum plaster over a period of 34 days.

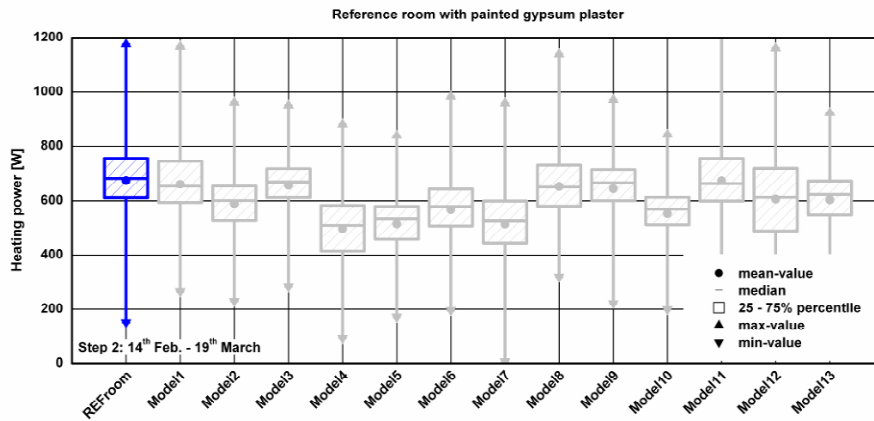


Figure 4.3.19: Statistical analysis of the results of the heating power in the reference room with painted gypsum plaster over a period of 34 days.

The results of the relative humidity for Step 3 with gypsum boards on the walls and the ceiling in the test room are shown in Figure 4.3.20. Figure 4.3.21 shows the result of the relative humidity in the reference room. The analyses comprised the results over a period of 26 days. The results of the descriptive statistic show similar results as for Step 2 also for the heating power in the reference room which are shown in Figure 4.3.22. Three models point out a higher deviation as the other models and the measurements.

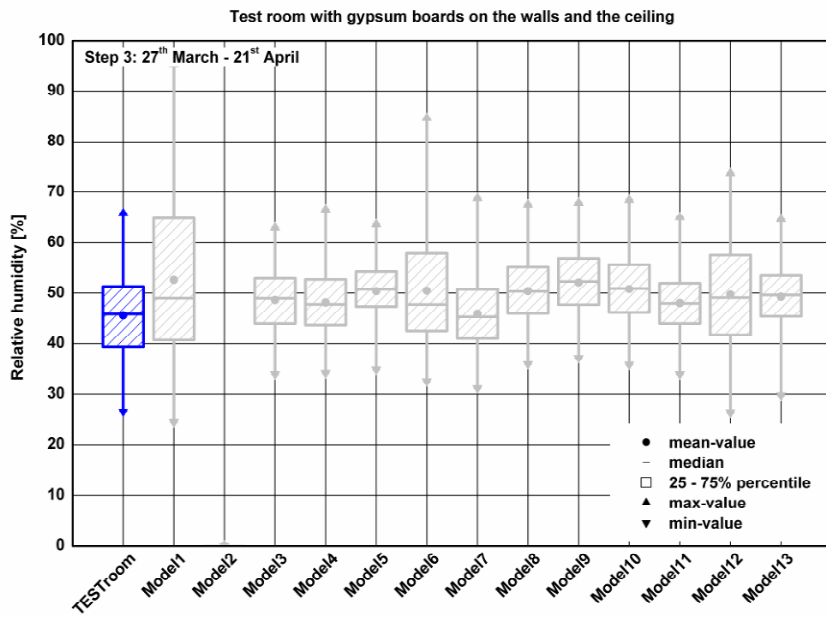


Figure 4.3.20: Statistical analysis of the results of the relative humidity in the test room with gypsum boards on the walls and the ceiling over a period of 26 days.

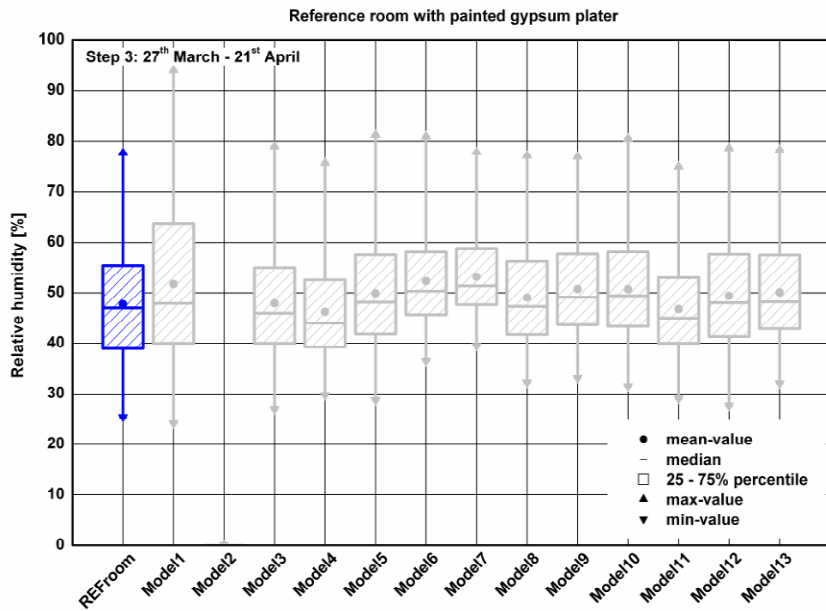


Figure 4.3.21: Statistical analysis of the results of the relative humidity in the reference room with painted gypsum plater over a period of 26 days.

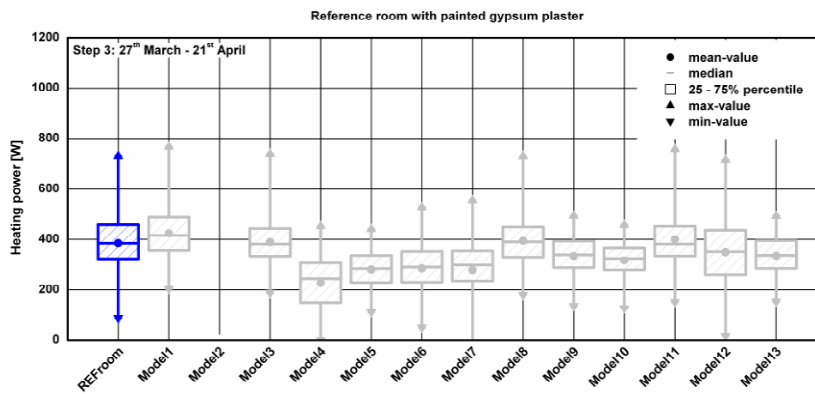


Figure 4.3.22: Statistical analysis of the results of the heating power in the reference room with painted gypsum plaster over a period of 26 days.

#### 4.3.5 Conclusion

To properly assess hygrothermal indoor climate conditions in interiors comprising several materials with complex experiments are needed. It is possible however to estimate the climate conditions in buildings using simulation tools expressly developed for this purpose. In context of the IEA-Annex 41 project experimental investigations and a common exercise (CE 3) for the validation of software tools has been carried out.

With the aid of experimental investigations which are carried out at the outdoor test site of the Fraunhofer-Institute of Building Physics in Holzkirchen to determine the moisture buffering effect of interior wall coverings of gypsum boards in comparison to a commercial painted interior plaster. The influences of materials with regard to the buffering behaviour were assessed by investigations in two identical test rooms under defined boundary conditions. The indoor climate in both rooms was constantly measured. The investigations showed that all variations with gypsum boards had a better moisture buffering effect than the traditional painted interior gypsum plaster. Whereas the untreated gypsum boards on the walls or on the walls and ceiling reduced humidity peaks by 40 % in comparison to the moisture buffering of an interior gypsum plaster. Additionally to the first three steps of experiments an extra step has been carried out. The Step 4 include two testing phases. Both with solar radiation into the rooms and the first phase with a heating system and the second phase without a heating system.

All results of the experimental investigations were used for the validation of newly developed simulation tools which were developed within context of the IEA-Annex 41 project. The validation was been made by thirteen participants with different simulation tools. For the results of Step 1 to Step 3 statistical analyses were made to point out how good are the simulation tools are and where are the problems for the calculation of the indoor climate. All the models could calculate the indoor RH within a correlation of minimum 97 % inside the test room with no sorptive surfaces inside. But with gypsum boards which have a good moisture buffering behaviours most of the models have difficulty in modelling the indoor RH correctly. The results show a correlation between the measurement and the simulation partly of circa 80 %. But if the buffering behaviour is not so distinctive the agreement with the measured results are better and the correlation increase to minimum 92 %. The agreement of the results of Step 4 are very different. If the heating system is running and solar radiation into the room is possible the spreading of the results are not to high. But at the results without a heating system only one model can simulate the indoor temperature in a correct way. The simulation of the absolute humidity is for one model a problem.

## 4.4 Common Exercise 4 – Extension of Common Exercise 3

### Moisture management for reducing energy consumption

By Monika Woloszyn, CETHIL, France

#### 4.4.1 Introduction

The intention of this common exercise was to show that appropriate management of indoor moisture reduces a building's energy consumption. The possibilities of combining a relative humidity sensitive (RHS) ventilation system and moisture buffering capacity of materials were investigated. The objective was to reduce energy consumption and improve the indoor climate. The target values of the indoor-air relative humidity were between 40% and 50%, as proposed by prEN 15251 for class A buildings.

This common exercise was launched in summer 2007 and results were presented in October 2007 in Lyon.

#### 4.4.2 Case description

The exercise is based on two real test rooms which are located at the outdoor testing site of the Fraunhofer-Institute of building physics in Holzkirchen and were used in Common Exercise 3 (CE3). The building, material properties, external and internal climates as boundary conditions, as well as moisture release were those from CE3 Steps 1, 2 and 3. There was no solar radiation transmission through the windows and indoor air temperature was kept constant at 20°C. The original characteristics of the ventilation system and of indoor materials, as used in CE3, can be seen in Table 4.4.1.

Table 4.4.1. Type of finishing materials from CE3

Room	Step 1	Step 2	Step 3
Reference (ach = 0.63 h <sup>-1</sup> )	Gypsum plaster + paint	Gypsum plaster + paint	Gypsum plaster + paint
Test (ach = 0.66 h <sup>-1</sup> )	Aluminium foil	Gypsum board on walls	Gypsum board on walls + ceiling

In some configurations constant airflow ventilation system was replaced by a relative humidity sensitive (RHS) exhaust (where the airflow is controlled by relative humidity). Such a system adapts the airflow to changes in the indoor relative humidity (RH), as shown in Figure 4.4.1 with RH1 = 25%, Q1 = 10 m<sup>3</sup>/h, RH2 = 60%, Q2 = 40 m<sup>3</sup>/h.

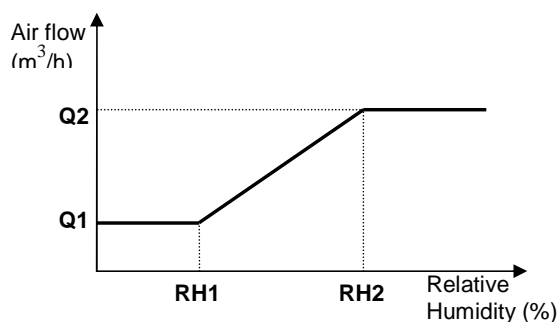


Figure 4.4.1. Relative humidity sensitive ventilation system

The participants were asked to perform five simulations changing the ventilation system and moisture-buffering capacity of the envelope (see Table 4.4.3):

- Run A: the original case from CE3, with constant ventilation

- Run B: using original finishing materials and the RHS ventilation system
- Run C: using original finishing materials and a RHS ventilation system with maximum and minimum airflow values modified by the participants
- Run D: using the original RHS ventilation system from run B, but changing the moisture-buffering capacity of materials by using different material properties and different surfaces
- Run E: combining both - the ventilation and the materials - in order to reduce the energy consumption and to improve indoor RH.

The simulations were run for a simulation period from January to April covering cold and mild periods.

#### 4.4.3 Participants

Six sets of results were collected, contributed from six institutions from six countries using five different simulation tools (see Table 4.4.2).

*Table 4.4.2. Participants of Common Exercise 4*

Institution	Country	Simulation tool
UG	Belgium	TRNSYS 16
TUT	Estonia	IDA ICE
CETHIL	France	Clim2000
TUE	Netherlands	HAMLab
CTH	Sweden	HAM Tools
PUCPR	Brazil	TRNSYS 15

All the simulation tools used in CE4 have already been tested in some other common exercises. All were whole building tools, with well developed energy and ventilation models, described more in detail in the previous chapter. Three tools can represent coupled heat and mass transfers in the envelope (IDA ICE, HAMLab and HAM Tools) and two use simplified models to represent the buffering effect of hygroscopic materials.

In one set of results, the constant ventilation rate proposed by the participant was very different from the other five tools. Therefore only five sets of results are included in the following comparison.

*Table 4.4.3. Sets of results for different runs of CE4*

Ventilation	Constant	RHS CE4	Proposed by participant	RHS CE4	Proposed by participant
Indoor materials	CE3	CE3	CE3	Proposed by participant	Proposed by participant
<i>Run</i>	<i>A</i>	<i>B</i>	<i>C</i>	<i>D</i>	<i>E</i>
Step 1 17/01-02/02	CTH, CETHIL, UG, PUCPR	TUE, CTH, CETHIL, UG, PUCPR	TUE, UG, PUCPR	TUE, CETHIL, UG,	TUE, UG
Step 2 14/02-19/03	CTH, UG, PUCPR	TUE, CTH, UG, PUCPR	TUE, UG, PUCPR	TUE, CTH, CETHIL, UG	TUE, UG
Step 3 28/03-21/04	CTH, UG, PUCPR	TUE, CTH, UG, PUCPR	TUE, UG	TUE, CTH, UG CETHIL, PUCPR	TUE, UG

#### 4.4.4 Results and discussion

The participants calculated hourly average temperatures, heating energy, relative humidity, ventilation flow, as well as vapour flow between air and construction. The results are presented for a typical cold week (24th to 31st of January) and a typical mild week (1st to 7th of April); see Figure 4.4.2. As the

computed indoor temperature was exactly equal 20°C for all codes, the relative humidity was used for comparative purposes.

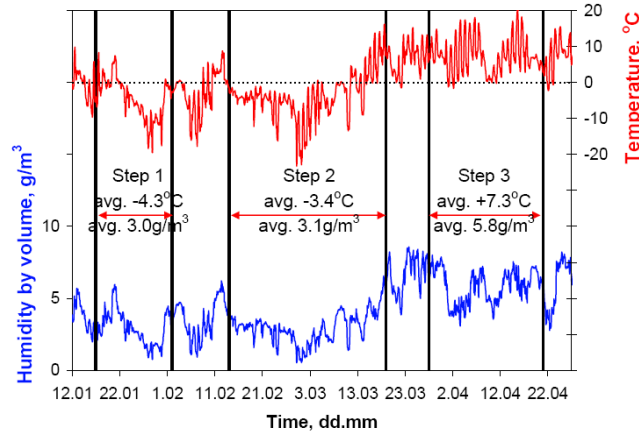


Figure 4.4.2. Outdoor conditions for all 3 steps.

4.4.4.1 Impact on indoor climate

Daily evolution of indoor RH for both ventilation systems in a room with no hygroscopic surfaces (test room of Step 1) is presented in Figure 4.4.3. Clearly, the amplitude of RH variations is smaller for RHS ventilation. Figure 4.4.4 provides more details about the statistical distribution of RH. It is noticeable that maximum values are similar for both systems. However, the mean and average values, as well as minimum values are higher for RHS system. Minimum values are over 20% RH for RHS system and go as low as 10% in the case of constant ventilation.

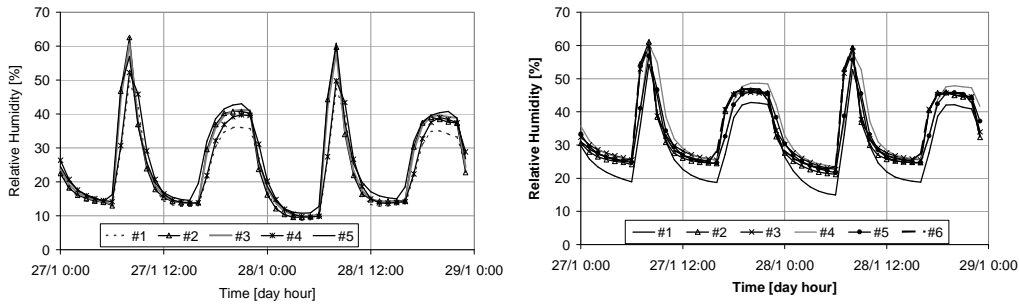


Figure 4.4.3. Indoor relative humidity as computed by all participants.  
 (a) Constant ventilation rate  
 (b) RHS ventilation

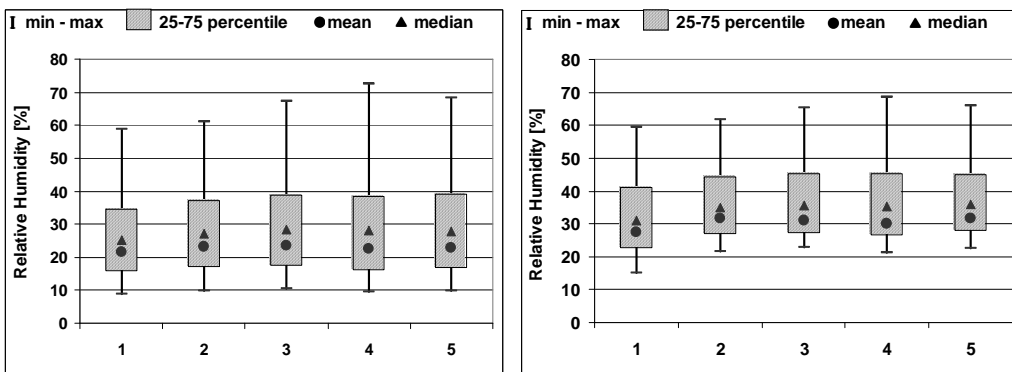


Figure 4.4.4. Indoor relative humidity during the cold week for both ventilation systems  
 (a) Constant ventilation rate (b) RHS ventilation

As shown in Figure 4.4.5, the impact of ventilation systems is much smaller in the mild period. The spread of RH values is still smaller and the minimum values higher for RHS ventilation. However, the differences are very small, approximately 2 to 3 % of RH. Both Figure 4.4.5 and Figure 4.4.6 illustrate the influence of moisture buffering on the indoor RH. When some hygroscopic surfaces are in contact with the indoor air, the amplitude of RH variations is much lower; it goes drops approximately 50% to approximately 20%. This was confirmed by run D, presented in Figure 4.4.7, where the participants proposed some hygroscopic materials associated with RHS ventilation. In this case the amplitude was less than 20%; and 50% of values were within an interval of 8%, considered very stable. Tools 2 and 5 used wood to reduce very efficiently RH variations. Indeed the amplitude was then approximately 13% for the tool 2 and 9% for tool 5. In tool 4, gypsum board surface was enlarged, and in tool 1, concrete was used to buffer humidity variations.

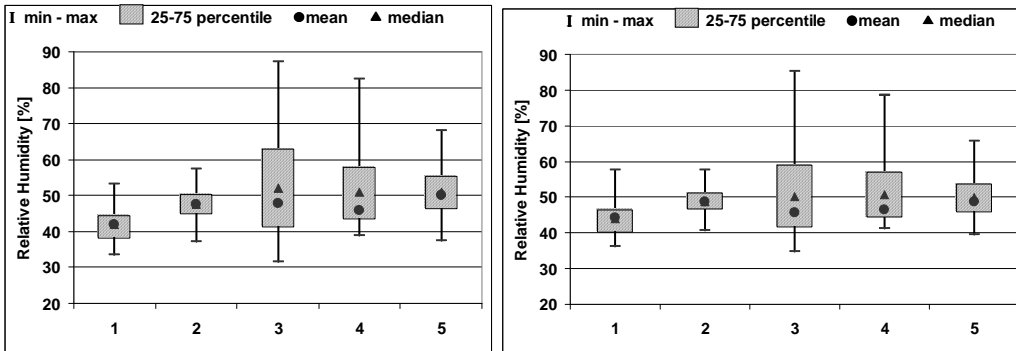


Figure 4.4.5. Indoor relative humidity during the mild week for both ventilation systems (tools 1, 2 and 5 include hygroscopic materials and tools 3 and 4 do not)  
 (a) Constant ventilation rate (b) RHS ventilation

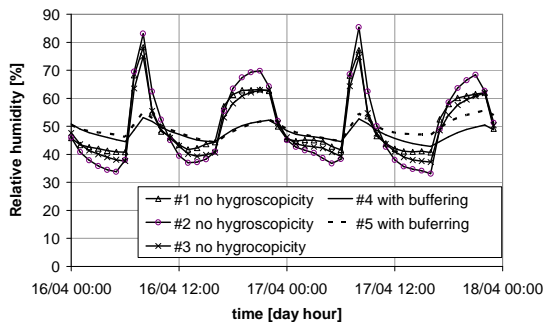


Figure 4.4.6. Indoor relative humidity in mild period with and without hygroscopic materials (constant ventilation)

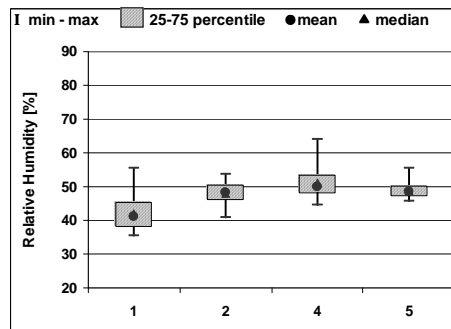


Figure 4.4.7. Indoor relative humidity in mild period with RHS ventilation and hygroscopic materials proposed by the participant

4.4.4.2 Impact on energy use

Ventilation air flows are contrasted in Figure 4.4.8. During the cold week the average value of the airflow was approximately 58% of the constant ventilation air flow. The differences are much less significant for the mild period, where both mean ventilation rates are very similar. Very good agreement between all tools on both average and amplitude values can be seen in Figure 4.4.8a for the cold period with no hygroscopic materials. The spread between values computed by different tools is much higher for the mild period (Figure 4.4.8b). This is partly explained by the fact that hygroscopic materials were differently represented in all tools.

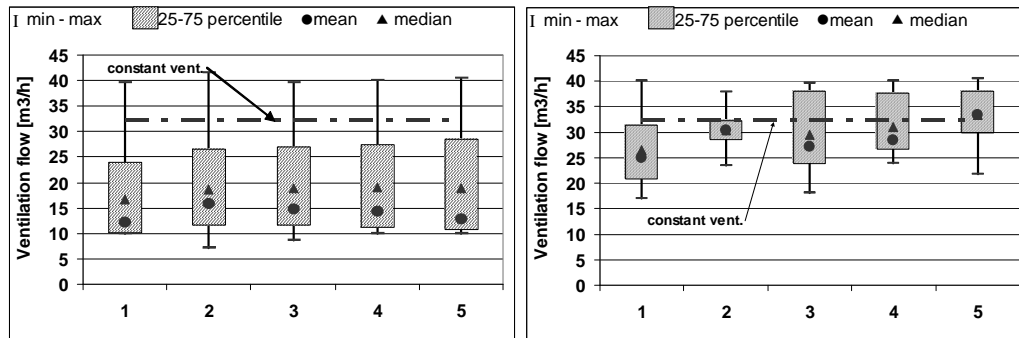


Figure 4.4.8. Ventilation airflow as computed by all the tools  
(a) Cold period (b) Mild period

Energy demand is presented in Figure 4.4.9. Ventilation systems are compared for both average values (representing energy use) and maximum values (representing heating power to be installed). During the cold season (see Figure 4.4.9a) we can clearly see the reduction in energy use in the case of RHS ventilation. The energy savings computed by all tools are between 14 and 20% of energy use. This is directly correlated with the reduction of the average value of fresh air flowing into the room. However, most of the simulations predict higher peak power (rise of as much as 9%) in case of RHS ventilation. This is easily explained by the sudden rise of air change when vapour release starts. Outdoor air is very cold; therefore a higher heating power is needed in order to maintain constant temperature. In the reality situation might be somewhat different, because most vapour sources are associated with heat release (physical activity, cooking, shower...).

For mild periods the difference in energy use by both ventilation systems is much lower (between 0 and 6%). It confirms values from Figure 4.4.8b where the average airflow values for RHS ventilation are very similar to the constant ventilation rate.

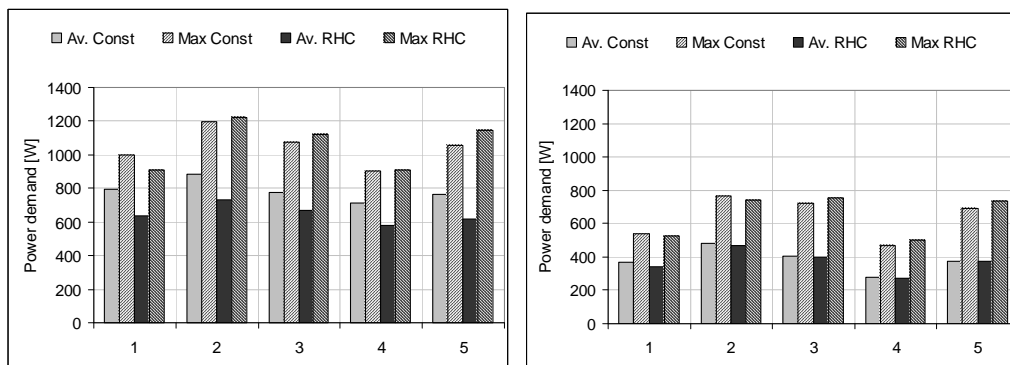


Figure 4.4.9. Power demand as computed by all the tools (no hygroscopic materials)  
(a) Cold period (b) Mild period

#### 4.4.5 Original ideas

One of the goals of this common exercise was to encourage participants to test new ideas. Therefore, in runs D and E the initiative was left to the participants to choose the ventilation systems and hygroscopic materials.

.For example, Steeman (2007) using TRNSYS proposed to adapt RHS ventilation to the outdoor climate. Indeed, run B confirmed that the indoor RH in the test room was often below 40% because of the dry outside air in winter. For Steps 2 and 3 the indoor RH never dropped under 25%, and thus the lowest air flow rate (10 m<sup>3</sup>/h) was almost never applied. The suggestion was to increase this lower limit to decrease the ventilation rate in low RH regions. Finally, the most stable indoor RH was achieved for the following schemes:

- Step 1 (cold): if the indoor RH < 40%, the flow is set to 10m<sup>3</sup>/h, if RH > 50%, the air flow is set to 40m<sup>3</sup>/h; in between the flow is linearly interpolated. In this case the humidity outside was quite low and no buffering occurred. Not much difference in indoor RH was noticed when applying another ventilation scheme.
- Step 2 (cold): if the indoor RH < 40%, the flow is set to 10m<sup>3</sup>/h, if RH > 50%, the air flow is set to 20 m<sup>3</sup>/h; in between the flow is linearly interpolated. In this case the maximum ventilation rate could be decreased because there is moisture buffering and the outdoor air is still quite dry.
- Step 3 (mild): if the indoor RH < 40%, the flow is set to 10 m<sup>3</sup>/h, if RH > 50%, the air flow is set to 50 m<sup>3</sup>/h; in between the flow is linearly interpolated. Here we chose again to increase the maximum flow rate, because of the higher indoor humidity caused by the higher humidity in the outdoor air.

It must be noted that the ventilation schemes were adapted for every time period. Similar reduction of ventilation flow for Step 2 was proposed by Abadie (2007) from Brazil.

Additional simulations were performed by Steeman (2007), where all surfaces (walls + ceiling + floor) consisted of the same material: 15 cm concrete, 25 mm wood or 12.5 mm gypsum board. For all three steps simulations using concrete, the most stable climate was obtained.

Abadie (2007) performed additional tests by increasing the wall surface area for moisture only and keeping the thermal characteristics of the envelope constant (there was no additional material included in the thermal calculation). Using TRNSYS, this was achieved by increasing the convective moisture-transfer coefficient between the wall surface layer and the zone. Ten simulations have been run for Step 3, doubling the wall surface area each time. RH and heating energy evolutions are presented in Figure 4.4.10 demonstrate that the "class A" RH zone [40;50] can not be reached by increasing the surface area only, and that additional materials (with adapted properties) have to be included in the zone.

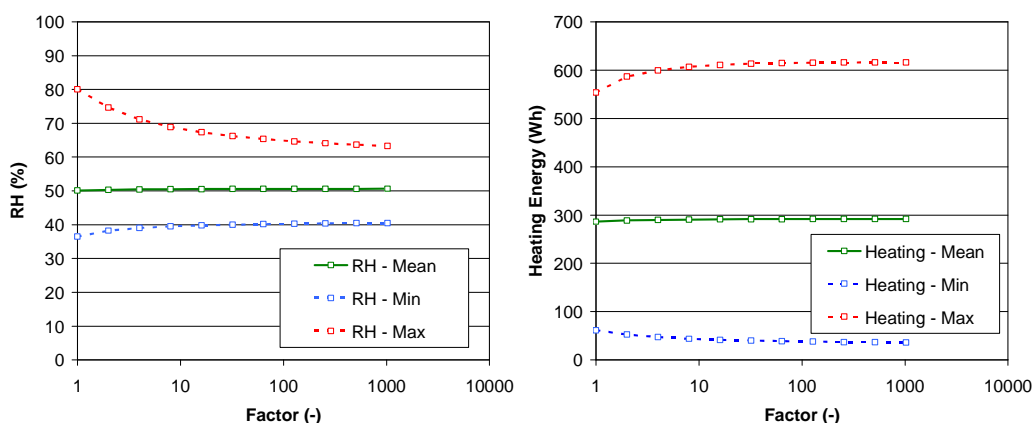


Figure 4.4.10: RH and heating energy as a function of the wall surface area (=Factor\*Sstep3).

Kalamees (2007), used IDA-ICE to include the effect of indoor CO<sub>2</sub> on both indoor air-quality estimations and on controlling ventilation rate. Indeed, reducing energy used for ventilation of buildings should be made without compromising the indoor air quality. Indoor CO<sub>2</sub> levels can be used as an indicator of the presence of human body odour and also are often employed as an indicator to control the performance of a ventilation system. In Run C, the ventilation systems with the airflow controlled by carbon dioxide (CO<sub>2</sub>) adapt the airflow to changes in the indoor CO<sub>2</sub>:

- when CO<sub>2</sub> < 600ppm, the flow is set to the minimum value of Q<sub>min</sub> = 10 m<sup>3</sup>/h
- when CO<sub>2</sub> > 1500ppm, the flow is set to the maximum value of Q<sub>max</sub> = 40 m<sup>3</sup>/h
- when CO<sub>2</sub> is between the minimum and the maximum, the airflow rate is linearly interpolated

The diurnal CO<sub>2</sub> and humidity production pattern used in the simulation tool is shown in Figure 4.4.11. CO<sub>2</sub> was calculated based on metabolic activity rate 0.8 met during the night and 1.2 met during peaks in the morning and the afternoon.

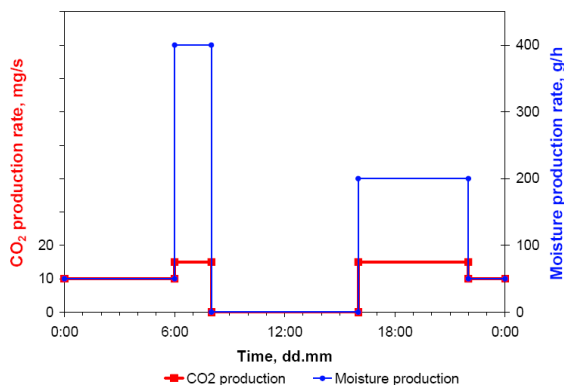


Figure 4.4.11. Diurnal CO<sub>2</sub> and humidity production pattern

Table 4.4.4. Percent of the time, when the indoor climate parameters were over and under acceptable RH (25 and 60%) and CO<sub>2</sub> (1200ppm) limit values.

	Step 1 (17.01...2.02)			Step 2 (14.02...19.03)			Step 3 (28.03...21.04)		
	<1200ppm	<RH25%	>RH60%	<1200ppm	<RH25%	>RH60%	<1200ppm	<RH25%	>RH60%
Run A: CE3 T Constant mass flow Aluminium foil	0	39	5	0	20	1	0	0	10
Run B: CE4 T RH controlled vent. system Gypsum board	33	13	4	35	0	1	1	0	6
Run C: CE4 T <sub>v</sub> CO <sub>2</sub> controlled vent. system Gypsum board	0	20	6	0	3	3	0	0	31
Run D: CE4 T <sub>m</sub> RH controlled vent. system Wood fibreboard	33	13	4	45	0	0	0	0	0
Run E: CE4 T <sub>v+m</sub> CO <sub>2</sub> controlled vent. system Wood fibreboard	0	20	6	0	0	0	0	0	5

The main results from this study, presented in Table 4.4.4, were:

In the case of continuous ventilation there was the lowest CO<sub>2</sub> level but also the highest energy consumption and RH deviation

- There was similar energy consumption in the case of CO<sub>2</sub> controlled and RH controlled ventilation systems, especially during cold period (Steps 1 and 2)
- Hygroscopic indoor surface materials (wood fibreboard compared to gypsum board) damped fluctuation of indoor RH in cases of all ventilation systems

- During cold period, in the case of RH controlled ventilation, there were the longest periods when the CO<sub>2</sub> was >1200ppm
- During cold period, in the case of continuous ventilation, there was the longest period when the RH < 25%
- During warm period (Step 3), in the case of CO<sub>2</sub> controlled ventilation there was the longest period when the RH > 60%.

We should also mention here the study presented by Koronthalyova (2006) which served as an inspiration for this Common Exercise. Koronthalyova evaluated by numerical simulation the effect of the different surface coating of indoor hygroscopic plasters on the indoor relative humidity amplitude reduction. The simulations were done for the ventilation regime with constant air change and with air change correlated with water vapour production. The ventilation regime correlated with the vapour production regime enables significant reduction of indoor humidity amplitude.

#### 4.4.6 Conclusions

Six solutions were provided by six participants from different countries. Even if some differences in results were noticed, a generally good agreement was found for the different simulations and similar trends emerged. The results demonstrate that RHS ventilation reduces the spread between the minimum and the maximum values of relative humidity. In this case it was also found that the use of a RHS system could reduce the mean ventilation rate of 30 - 40% in the cold period and generate 12 - 17% of energy savings. It should be stressed that the energy savings are realized with keeping the peak RH values at the same level, therefore without raising the risk of condensation. However, during the mild period the savings are much lower (only about 2%), mainly because of much higher moisture content outside.

A more general conclusion is that humidity sensitive ventilation is a good way of reducing building energy demand. This is directly related to the reduction of mean ventilation rate. Advantage of this type of demand controlled-ventilation is that relative humidity maximum values are still kept at a correct level. However one should also check that other pollutants (such as CO<sub>2</sub>) are within correct limits.

This study also confirmed that the use of moisture buffering materials is a very efficient way to reduce the amplitude of daily moisture variations (see Figure 4.4.6 and Figure 4.4.7). It was even possible, by the combined effect of ventilation and wood as buffering material (Figure 4.4.7 - tool 5) to keep the indoor RH at a very stable level, between 46 – 56%.

The deviation of results within a reasonable range gives some more confidence in the tools. Also, all codes, with rather different HAM models, proved their performance in HAM modelling of whole buildings.

## 4.5 Common Exercise X

Hugo Hens

K.U.-Leuven, Department of Civil Engineering, Laboratory of Building Physics, B-3001 Leuven (Belgium)

### 4.5.1 Introduction

With exercise X, a practice-related case was introduced within the Annex 41 chain of common exercises. First, we sketch the case as it was handled in reality. Then its translation into a common exercise is explained, to end with the reference solution and a comparison with results from the participants.

### 4.5.2 The case

The case concerns a low income estate of 48 two story houses built in the 1970-ties (Anon. 1981) (Hens et al, 2003) (figure 1). The only difference between the 48 dwellings was the orientation of the main façade: 9 NW, 4 NNW, 16 NE, 5 E, 5 SE and 8 SW. All had a non insulated floor on grade, non insulated cavity walls, double glazed aluminium windows on the ground floor, single glazed aluminium windows on the first floor and a cathedralized ceiling composed of (from the inside to the outside) (1) gypsum boards with open joints, (2) 6 cm glass-fibre bats with a vapour retarder at the underside, (3) an un-vented air space and (4) corrugated fibre cement plates as roof cover (figure 2). The two floors were linked by an open staircase in the living room. Dwelling ventilation was adventitious with peak ventilation provided by open windows.



Figure 1 The dwellings considered

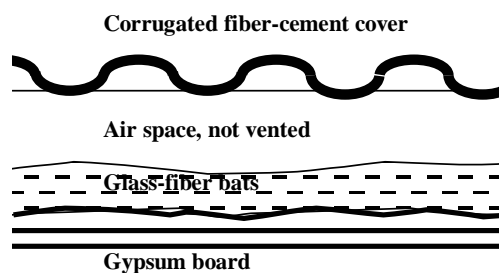


Figure 2 Roof section

85% of the dwellings showed traces of moisture on the cathedralized ceiling internal lining, while a large number of inhabitants complained about dripping moisture in the sleeping rooms during winter after cold nights. A detailed inspection of some roofs revealed poor installation of the glass-fibre bats, abundant traces of condensation on the corrugated fibre-cement plates, the rafters and the backside of the inside lining and mould on the rafters.

In a first step, a multiple correlation was sought between the severity of the complaints and the average number of inhabitants, well or no cooking hood in the kitchen, the average annual heating consumption and the orientation of the main façade. Annual heating consumption explained most of the differences, giving 128 GJ/a on the average in dwellings with severe damage and 164 GJ/a on the average in dwellings with moderate damage. In these, people apparently heated better or/and ventilated more. The other three parameters had hardly any impact. Logic for the orientation, as all dwellings looked to dominant wind directions.

In a second step, during the winter 1981-1982, inside temperature and relative humidity was followed in two dwellings with severe (2 and 3) and one dwelling with moderate complaints (1). Beforehand, house 2 got a PE air and vapour retarder mounted below the existing gypsum board lining, with all

joints and overlaps carefully sealed. At the same time two roof models, one 'as built' and the other as 'the solution', were constructed at the laboratory and tested in a hot box rig for horizontal assemblies. The roof called 'the solution' had following composition (from inside to outside): gypsum board, air cavity, PE air and vapour retarder, 17 cm of mineral fibre fully filling the air space between the rafters, vapour permeable underlay, battens, corrugated plates.

*Table 4.5.1 Weekly mean inside temperature and vapor pressure excess as a function of the weekly mean outside temperature (dwelling 2 got the air and vapour retarder installed)*

Dwelling	Parents sleeping room		Children sleeping room		Bathroom	
	Inside temperature °C	Inside vapour pressure excess Pa	Inside temperature °C	Inside vapour pressure excess Pa	Inside temperature °C	Inside vapour pressure excess Pa
1	13.6+0.42θ <sub>e</sub>	196-1.23θ <sub>e</sub>	14.1+0.42θ <sub>e</sub>	159-0.9θ <sub>e</sub>		
2	13.1+0.32θ <sub>e</sub>	373-14.7θ <sub>e</sub>	13.9+0.26θ <sub>e</sub>	237+2.5θ <sub>e</sub>	14.3+0.21θ <sub>e</sub>	457-17.7θ <sub>e</sub>
3	11.7+0.48θ <sub>e</sub>	324-10.8θ <sub>e</sub>	15.6+0.06θ <sub>e</sub>	411-34θ <sub>e</sub>	17.7+0.25θ <sub>e</sub>	395-19.4θ <sub>e</sub>

Table 4.5.1 gives the results of the inside climate readings. Dwelling 2 and 3 experience higher vapour pressure excesses and lower temperatures than dwelling 1. A higher excess is by definition negative in terms of condensation deposit. To control the consequences, we calculated the vapour diffusion thickness of the poorly installed mineral fibre bats with vapour retarding paper back from a condensation test in the hot box rig on the roof 'as built' (40 days between 2.7°C, 557 Pa and 23.6°C, 2165 Pa). 0.23 m was measured instead of the wet cup's 5.2 m, measured on samples of the paper back. Poor workmanship clearly killed vapour retarding quality. That, however, did not explain dripping. In fact, the calculated accumulation by diffusion never passed the 2 l/m<sup>2</sup> the corrugated fibre-cement could buffer.

Instead, adventitious ventilation with air exfiltration through the roof fully explained the case. An air permeance measurement on the test roof as built gave a poor  $3.3 \cdot 10^{-4} \text{ P}0.66$ , i.e. very air leaky. House 2 offered additional evidence as the PE air and vapour retarder effectively solved the condensation problem. A particle board sample, glued against the corrugated fibre-cement, remained drier in that roof than in the roof of house 3. Also not a single complaint of moisture dripping on the retarder was noted. A roof control early February 1982 revealed a perfectly dry assembly. In the house 3, instead, severe dripping happened after a cold spell in January 1982 while a roof control early February 1982 showed abundant moisture deposit at the backside of the corrugated fibre cement. The hot box test on the better solution confirmed that evidence: no condensation as long as the PE air and vapour retarder was leakage-free. Yet, once deliberately perforated a couple of weeks before the end of the test, abundant condensation appeared against the underlay.

The solution advised was: (1) retrofit the roof in accordance to the better solution; (2) upgrade the overall poor insulation quality of the dwellings; (3) equip the dwellings with a purpose designed ventilation system.

### 4.5.3 The exercise

#### 4.5.3.1 Objective

Objective of the exercise was not comparing software-based solutions, but evaluating if the annex 41 participants could solve an engineering problem using simplified approaches. For that reason, the exercise was kept steady state, looking to a cold week. For Flanders, such week was defined by (Janssens, 1998), when proposing a methodology to distinguish problematic from non problematic response for lightweight roof systems facing advective heat and vapour flow: see

Table 4.5.2.

*Table 4.5.2. The cold week considered*

Temperature °C	Rel. hum. %	Radiant exchanges, hor. W/m <sup>2</sup>	Mean wind velocity m/s	Wind direction
-2.5	98	-30	3.8	NE

The exercise was split in three successive steps:

- Step 1: ground floor and first floor heated, daily vapour release constant over the week, air leakage through the façade distributed proportional to the surface
- Step 2: ground floor heated, first floor not, vapour release on both floors given on an hourly basis, air buffering only, air leakage through the façade distributed proportional to the window perimeter lengths
- Step 3: as step 2 plus moisture buffering by the fabric included

#### 4.5.3.2 Common data

##### Floors and section

See figure 2. The ground floor has a height of 2.5 m. The same height is found in the first floor at the façade wall. The roof contains two pitches, a longer one with a slope of 17° and a shorter one with a slope of 10°. The open staircase couples the living room and kitchen to the sleeping and bathroom on the first floor.

##### n50-value

The n50-value of the dwellings varied between 6 and 14 h<sup>-1</sup> with an average of 10 h<sup>-1</sup> (compared to the gross volume). That number includes the leaks in the cathedralized ceiling, represented by an average air flow rate of  $3.3 \cdot 10^{-4} \cdot P^{0.66}$  kg/(m<sup>2</sup>·s).

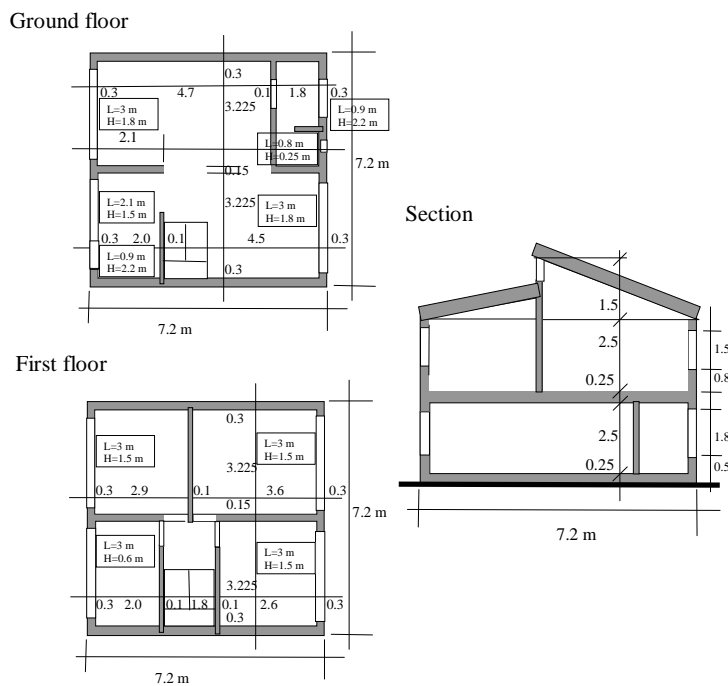


Figure 2 Floors and section

##### Envelope assemblies

Façade walls, from inside to outside	<ul style="list-style-type: none"> <li>– Inside leaf, 14 cm, rendered at the inside with a 1.5 cm thick gypsum plaster. Mortar joint to stone ratio 0.098/0.902</li> <li>– Cavity, 6 cm, unfilled</li> <li>– Brick veneer, 9 cm, mortar joint to stone ratio 0.18/0.82</li> </ul>
Roof, from inside to outside	<ul style="list-style-type: none"> <li>– Gypsum board, d=9.5 mm, mounted with open joints perpendicular to the slope</li> </ul>

	<ul style="list-style-type: none"> <li>- Battens 50 x30 mm, parallel to the slope, 47 cm from each</li> <li>- Girders 24x8 cm perpendicular to the slope, 80 to 110 cm from each.</li> <li>Mineral wool bats, 60 mm thick, vapour retarding paper back, draped in between. Flanges not overlapping.</li> <li>- Corrugated fibre cement plates, 6 mm.</li> </ul>
Floor on grade, from inside to outside	<ul style="list-style-type: none"> <li>- Flooring</li> <li>- Sand/cement screed, thickness 6 cm</li> <li>- Concrete slab, 14 cm</li> </ul>
Floor between both stocks, top down	<ul style="list-style-type: none"> <li>- Flooring</li> <li>- Sand/cement screed, thickness 6 cm</li> <li>- Concrete slab, 14 cm, rendered at the underside with 1 cm gypsum</li> </ul>
Windows	Aluminium without thermal break, double glazing on the ground floor, single glass on the first floor
Roof window	See figure 3

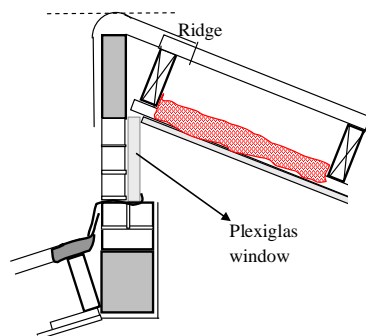


Figure 3 Detail of the roof window

### Volume, surfaces and material properties

With lifted small pitch to get a common ridge with the large pitch, the gross volume of the dwelling is 344.9 m<sup>3</sup> (exterior dimensions), of which 149.0 m<sup>3</sup> belongs to the first floor. For the surfaces, see Table 4.5.3.

Table 4.5.3 Surfaces

Envelope part		Surface (m <sup>2</sup> )
Floor on grade		51.84
Cavity wall	Sidewall 1	45.75
	Sidewall 2	45.75
	Front	26.68
	Back	24.30
Roof	Large pitch	29.74
	Small pitch	24.96
Windows	Front door	1.98
	Toilet	0.20
	Living room, front	5.40
	Living room, back	5.40
	Kitchen	5.13
	Sleeping room 1	4.50
	Sleeping room 2	4.50
	Sleeping room 3	4.50
	Bathroom	1.80

Table 4.5.4 gives the material property values used. Window frames cover 20% of the window area and have a U-value 5.9 W/(m<sup>2</sup>.K). For single glass U is 5.7 W/(m<sup>2</sup>.K), while for double glass it is 2.7 W/(m<sup>2</sup>.K). The double glass edges add a linear thermal transmittance of 0.02 W/(m.K). Each window is divided in three equally large parts, filled with a glass pane. The inside surface film coefficient totals 7.7 W/(m<sup>2</sup>.K) for the walls, 6 W/(m<sup>2</sup>.K) for the floor on grade and 10 W/(m<sup>2</sup>.K) for the roof. The outside value is 25 W/(m<sup>2</sup>.K) for walls and ground surfaces and 17 W/(m<sup>2</sup>.K) for the roof. Thermal bridging is not considered.

Table 4.5.4 Material property values

Envelope part Layer	Thickness m	Density kg/m <sup>3</sup>	$\lambda$ -value W/(m.K)	R-value m <sup>2</sup> .K/W	$\delta_s$ /d-value kg/(m <sup>2</sup> .s.Pa)
Floor on grade					
Concrete	0.14	2300	2.3		
Screed	0.06	1800	1.0		
Tiles	0.01	2300	1.3		
Cavity wall					
Veneer, bricks	0.09	1800	0.9	0.17	
Cavity	0.06				
Inside leaf, blocks	0.14	1400	0.5		
Mortar		1800	1.0		
Inside render	0.015	900	0.3		
Roof					
Corrugated plates	0.006	1800	0.95	0.17	1.2E-10
Air space					0
Girders	0.24	450	0.14		
Thermal insulation	0.06	12	0.04	0.17	2.6E-9
Vapor retarder	-	-	-		8.0E-10
Air space, battens	0.04				0
Gypsum board	0.009	700	0.21		1.5E-9

## Wind

Wind velocity in table 2 is the value measured in the open field. The estate creates a closed landscape with an effective terrain roughness of 1 m and a friction velocity of 0.47 m/s. Velocity there is given by  $1.121 \ln(z+1)$  (m/s) with z height above grade. Wind pressure is calculated as  $0.6C_v^2$  (Pa) with the pressure coefficient C taken from (Liddament, 1996):

Location	Wind Angle								
	0°	45°	90°	135°	180°	225°	270°	315°	
Face 1	0.2	0.05	-0.25	-0.3	-0.25	-0.3	-0.25	0.05	
Face 2	-0.25	-0.3	-0.25	0.05	0.2	0.05	-0.25	-0.3	
Face 3	-0.25	0.05	0.2	0.05	-0.25	-0.3	-0.25	-0.3	
Face 4	-0.25	-0.3	-0.25	-0.3	-0.25	0.05	0.2	0.05	
Roof <10°	Front	-0.5	-0.5	-0.4	-0.5	-0.5	-0.5	-0.4	-0.5
	Rear	-0.5	-0.5	-0.4	-0.5	-0.5	-0.5	-0.4	-0.5
Average	-0.5	-0.5	-0.4	-0.5	-0.5	-0.5	-0.4	-0.5	
Roof 11-30°	-0.3	-0.4	-0.5	-0.4	-0.3	-0.4	-0.5	-0.4	
Average	-0.3	-0.4	-0.5	-0.4	-0.3	-0.4	-0.5	-0.4	
Roof >30°		0.25	-0.3	-0.5	-0.3	-0.4	-0.3	-0.5	-0.3
		-0.4	-0.3	-0.5	-0.3	0.25	-0.3	-0.5	-0.3
Average	-0.08	-0.3	-0.5	-0.3	-0.08	-0.3	-0.5	-0.3	

### 4.5.3.3 Specific data per step

#### Step 1

Temperature on both floors 18°C, vapour release totalling 13.5 kg/day.

**Step 2**

Ground floor heated at 20°C, first floor unheated. Hourly vapour release at both floors as in table 5

*Table 4.5.5. Hourly vapour release*

Time	Ground floor g/h	First floor g/h
0	0	350
1	0	350
2	0	350
3	0	350
4	0	350
5	0	350
6	0	350
7	890	1000
8	300	210
9	120	0
10	120	0
11	360	0
12	800	0
13	480	0
14	240	0
15	240	0
16	360	210
17	720	210
18	1400	210
19	1400	0
20	150	210
21	150	210
22	150	210
23	0	700

**Step 3**

See step 2. Gypsum plaster unpainted. Vapour permeance considered constant (see table with material properties), specific moisture content 66.7 kg/m<sup>3</sup> for the plaster and 10 kg/m<sup>3</sup> for masonry (relative humidity on a scale from 0 to 1). Furniture not taken into account.

## 4.5.3.4 Questions posed

In each step, following question had to be answered:

1. Air in- and outflow, ventilation flow?
2. Partial water vapour pressure and relative humidity on both floors? Surface condensation?
3. Interstitial condensation in the cathedralized ceiling?
4. Impact of air outflow across the ceiling on net energy demand during that one week?

**4.5.4 Methodology applied**

## 4.5.4.1 Air balances in the dwelling

The dwelling is assumed behaving as a three nodes air flow system (Hens, 2005). Nodes are located on the ground floor, 1 m above floor level, on the first floor, 2.75 m above node 1, and in the space created by the two cathedralized roof pitches, 2.25 m above node 2. Each node is linked to two outside nodes, one at the front and one at the back of the dwelling. Ground and first floor are connected by the open staircase. First floor and roof space form one volume. Inside doors are assumed open day and night. In the three nodes, mass equilibrium imposes a sum of air flows zero, or:  $\sum G_a = 0$ . Airflow between nodes at the same height is given by:

$$G_a = aA [P_{a,x} - P_{a,y}]^b \quad (1)$$

For nodes at different heights that equation changes into:

$$G_a = aA \left[ \left( P_{a,x} - \frac{gP_a}{R_a} z_x \left( \frac{1}{T_x} - \frac{1}{T_e} \right) \right) - \left( P_{a,y} - \frac{gP_a}{R_a} z_y \left( \frac{1}{T_y} - \frac{1}{T_e} \right) \right) \right]^b \quad (2)$$

In both,  $a$  is the air permeance coefficient,  $b$  the air permeance exponent (set 0.67 except for the stair case and the space between nodes 2 and 3, where 0.5 is a better value),  $A$  in- and outflow section (surface),  $g$  acceleration by gravity ( $9.81 \text{ m/s}^2$ ),  $P_a$  atmospheric pressure,  $R_a$  specific gas constant for air ( $287 \text{ Pa}\cdot\text{m}^3/(\text{kg}\cdot\text{K})$ ),  $z_x$  and  $z_y$  height and  $T_x$  and  $T_y$  temperatures in the nodes considered (K),  $T_e$  outside temperature (K),  $P_{a,x}$  air pressure excess compared to atmospheric in node  $x$ ,  $P_{a,y}$  air pressure excess compared to atmospheric in node  $y$  (all in SI-units). The term  $gP_a/R_a$  hardly differs from  $3462 \text{ Pa}\cdot\text{K}/\text{m}$ , simplifying equation (2) to:

$$G_a = a \left[ P_{a,x} - P_{a,y} - 3462 \left( \frac{z_x}{T_x} + \frac{z_y}{T_y} - \frac{z_x + z_y}{T_e} \right) \right]^b \quad (3)$$

The result is a system of 3 equations with as unknowns air pressure excess  $P_{a,x}$  in each node:

*Node 1*

$$a_{e1,1} A_{e1} [P_{a,e1} - P_{a,x1}]^{0.67} + a_{e2,1} A_{e2} [P_{a,e2} - P_{a,x1}]^{0.67} + a_{2,1} A_{2,1} \left[ P_{a,x2} - 3462 h_2 \left( \frac{1}{T_i} - \frac{1}{T_e} \right) - P_{a,x1} \right]^{0.5} = 0$$

*Node 2*

$$a_{e3,2} A_{e3} [P_{a,e3} - P_{a,x2}]^{0.67} + a_{e4,2} A_{e4} [P_{a,e4} - P_{a,x2}]^{0.67} + a_{1,2} A_{1,2} \left[ P_{a,x1} - P_{a,x2} + 3462 h_2 \left( \frac{1}{T_i} - \frac{1}{T_e} \right) \right]^{0.5} \\ + a_{3,2} A_{3,2} \left[ P_{a,x3} - P_{a,x2} - 3462 \left( \frac{1}{T_i} - \frac{1}{T_e} \right) (h_3 - h_2) \right]^{0.5} = 0$$

*Node 3*

$$a_{e5,3} A_{e5} [P_{a,e5} - P_{a,x3}]^{0.67} + a_{e6,3} A_{e6} [P_{a,e6} - P_{a,x3}]^{0.67} \\ + a_{2,3} A_{2,3} \left[ P_{a,x2} - P_{a,x3} - 3462 \left( \frac{1}{T_i} - \frac{1}{T_i} \right) (h_2 - h_3) \right]^{0.5} = 0$$

Solving the system, demands linearization, followed by a split between known and unknown terms. Result is following matrix equation:

$$\begin{bmatrix} C_{11} & C_{12} & C_{13} \\ C_{21} & C_{22} & C_{23} \\ C_{31} & C_{32} & C_{33} \end{bmatrix} \begin{bmatrix} P_{a,x1} \\ P_{a,x3} \\ P_{a,x3} \end{bmatrix} = \begin{bmatrix} F_1 \\ F_2 \\ F_3 \end{bmatrix} \quad (4)$$

with the  $C$ 's and  $F$ 's function of air pressure excess between and temperatures in neighbouring nodes. To solve the system, known pressures excesses and temperatures are filled in together with a first guess for  $P_{a,x1}$ ,  $P_{a,x2}$  and  $P_{a,x3}$ . That allows calculating the  $C$ 's and  $F$ 's and solving the system. With the three new nodal pressure excesses generated, the  $C$ 's and  $F$ 's are recalculated and the system solved again. Iterating that way goes on until the most probable error between the actual and previous pressure excesses becomes smaller than preset.

#### 4.5.4.2 Vapour balances in the dwelling

In step 1, the dwelling behaves as one node. Balance equation (diffusion not considered):

$$p_i = \frac{p_e + \frac{RT_i}{V} \left( G_{v,P} + \sum_{j=1}^3 \beta A_j p_{s,sat,j} \right)}{1 + \frac{RT_i}{V} \sum_{j=1}^3 \beta A_j} \quad (5)$$

with  $\dot{V}$  ventilation flow in m<sup>3</sup>/s,  $\square$  surface film coefficient for diffusion at all condensation surfaces (2.59 10<sup>-8</sup> s/m), in the case being the aluminium window frames, the single glass and the double glazing,  $A_j$  the respective surfaces, 6.68 m<sup>2</sup> for the frame, 12.24 m<sup>2</sup> for single glass and 14.49 m<sup>2</sup> for double glass (included the entrance door,  $p_{s,sat,j}$  (partial water) vapour saturation pressure at the respective surfaces, 2.9°C and 752 Pa for the aluminium frame, 3.4°C and 780 Pa for single glass and 11.1°C and 1322 Pa for double glass,  $R$  specific gas constant for water vapour (462 Pa.m<sup>3</sup>/(kg.K)),  $G_{v,P}$  average vapour release in kg/s,  $T_i$  inside temperature in °C and  $p_e$  vapour pressure outside in Pa.

In step 2, that one balance is replaced by a balance for the ground and the first floor. Both write as ODE's of first order (diffusion not considered) (Hens, 2006):

$$\rho_a V_1 \frac{dp_{i,1}}{dt} + p_{i,1} \left( G_{a,12} + \frac{\sum_{j=1}^3 \beta A_{1,j}}{6.21 \cdot 10^{-6}} \right) = p_e G_{a,e1} + \frac{G_{v,P1}(t) + \sum_{j=1}^3 \beta A_{1,j} p_{s,sat,j}}{6.21 \cdot 10^{-6}} \quad (6)$$

$$\rho_a V_2 \frac{dp_{i,2}}{dt} + p_{i,2} \left( G_{a,2e} + \frac{\sum_{j=1}^3 \beta A_{2,j}}{6.21 \cdot 10^{-6}} \right) = p_{i,1} G_{a,12} + p_e G_{a,e2} + \frac{G_{v,P2}(t) + \sum_{j=1}^3 \beta A_{2,j} p_{s,sat,j}}{6.21 \cdot 10^{-6}} \quad (7)$$

with  $G_{a,xy}$  ventilation flow in kg/s,  $x$  for the outflow and  $y$  for the inflow zone,  $p_{s,sat,j}$  vapour saturation pressure at the respective condensation surfaces (781 Pa for the frames on the ground floor, 619 Pa for the frames on the first floor, 12.4°C and 1443 Pa for the double glass on the ground floor and 0.4°C and 631 Pa for the single glass on the first floor) and  $G_{v,P1}(t)$ ,  $G_{v,P2}(t)$  vapour release in kg/s on ground and first floor.

In step 3, the active thickness model is used to include moisture buffering in the fabric, transposing the two first order ODE's of step 2 in two second order ODE's, which are solved numerically.

#### 4.5.4.3 Interstitial condensation in the roof

Condensation in the roof relates to advection, the combination of air outflow, water vapour diffusion and heat transmission. Governing equations are:

##### Temperatures

$$\theta_x = \theta_i - (\theta_i - \theta_e^*) \frac{1 - \exp(-c_a g_a R_i^x)}{1 - \exp(-c_a g_a R_a)} \quad (8)$$

with  $R_i^x$  thermal resistance between the inside and the interface  $x$ ,  $R_a$  total thermal resistance across the roof,  $c_a$  specific heat of air (1008 J/(kg.K)) and  $g_a$  air outflow density in kg/(m<sup>2</sup>.s).

##### Vapour saturation pressures

Known once temperature in all interfaces is known

##### Partial water vapour pressures

$$p_x = p_i - (p_i - p_e) \frac{1 - \exp(a_H Z_i^x)}{1 - \exp(a_H Z_a)} \quad (9)$$

with  $a_H = -6.2110^{-6} g_a$ ,  $Z_i^x$  the water vapour resistance between the inside and the interface x and  $Z_a$  total water vapour resistance across the roof.

#### Condition for condensation

Interstitial condensation will appear when the vapour pressure at the underside of the roof cover passes the vapour saturation pressure at that spot. Undercooling of course may also induce condensation on top of the roof cover, as is the case here.

#### Condensation deposit

Calculated as:

$$g_c = \frac{a_H}{1 - \exp(a_H Z_i^c)} [p_i \exp(a_H Z_i^c) - p_{\text{sat},c}] - \frac{a_H}{1 - \exp(a_H Z_c^{\text{se}})} [p_c \exp(a_H Z_c^{\text{se}}) - p_{\text{s,e,sat}}] \quad (10)$$

For high densities of air outflow, the formula simplifies to:  $g_c = a_H [p_i - p_{\text{sat},c}]$

#### 4.5.4.4 Weekly net energy demand with and without outflow through the ceiling

The weekly net energy demand is calculated according to the European standard EN ISO 13790.

### 4.5.5 Reference Solution

#### 4.5.5.1 Step 1

##### Airflows

Take  $n_{50}=10 \text{ h}^{-1}$  and the front façade NE. The roof has an air permeance coefficient  $2.75 \cdot 10^{-4} \text{ m}^3/(\text{m}^2 \cdot \text{s} \cdot \text{Pa})$ . A ventilation rate  $10 \text{ h}^{-1}$  at  $50 \text{ Pa}$  for a gross volume of  $331.6 \text{ m}^3$  means airflow at  $1 \text{ Pa}$  of  $0.067 \text{ m}^3/\text{s}$ . Of that flow  $0.013 \text{ m}^3/\text{s}$  passes through the roof leaving  $0.054 \text{ m}^3/\text{s}$  for front and back façade. With a façade surface of  $66 \text{ m}^2$  the flow per  $\text{m}^2$  at  $1 \text{ Pa}$  thus becomes  $1.03 \cdot 10^{-3} \text{ m}^3/\text{s}$ . Each quarter façade so represents a total permeance of  $1.68 \cdot 10^{-2} \text{ m}^3/(\text{s} \cdot \text{Pa})$ . Stack pressures are (undercooling of the roof drops the sol-air temperature there to  $-3.9^\circ\text{C}$ ):

	Height m	Outside Pa	Inside Pa	Difference Pa
Ground floor	0	0	0	0
First floor	2.75	-35.18	-32.7	-2.48
Roof	5	-64.28	-59.45	-4.83

Wind pressures at the front, the back and the two roof pitches are:

	Wind pressure, Pa	
	Front	Back
Ground floor	0.072	-0.090
First floor	0.365	-0.457
Roof	-1.425	-1.425

Solving the system of equations gives as air flows (+ for inflow, - for outflow)

$n_{50} (\text{h}^{-1})$	Air flows, $\text{m}^3/\text{h}$					
	Ground floor		First floor		Roof space	
	Front	Back	Front	Back	Large pitch	Small pitch
10	82.3	78.2	3.7	-41.7	-66.6	-55.9

Ventilation thus totals  $164.2 \text{ m}^3/\text{h}$ . With the net volume as reference ( $248.3 \text{ m}^3$ ), that flow gives a ventilation rate of  $0.66 \text{ h}^{-1}$ , i.e. better than  $0.5 \text{ h}^{-1}$ , the IAQ-requirement. Compared to the gross volume ( $331.6 \text{ m}^3$ ), the rate drops to  $0.5 \text{ h}^{-1}$ . For the other  $n_{50}$ -ties, air flows became:

$n_{50}$ ( $\text{h}^{-1}$ )	Air flows, $\text{m}^3/\text{h}$					
	Floor 1		Floor 2		Roof space	
	Front	Back	Front	Back	Large pitch	Small pitch
6	49.3	47.4	18.8	-6.5	-59.3	-49.7
8	66.0	63.0	14.2	-25.2	-64.2	-53.8
12	99.3	94.1	-11.9	-56.8	-67.8	-56.9
14	115.1	108.8	-24.0	-73.2	-68.9	-57.8

resulting in the following ventilation flows and rates:

$n_{50}$ ( $\text{h}^{-1}$ )	Ventilation flow $\text{m}^3/\text{h}$	Ventilation rate (net volume) $\text{h}^{-1}$	Ventilation rate (gross volume) $\text{h}^{-1}$
6	115.5	0.47	0.35
8	143.1	0.58	0.43
12	193.4	0.80	0.58
14	223.9	0.90	0.68

Figure 4 shows the divider needed to calculate the effective ventilation rate from the  $n_{50}$ -value. Figure 2 lists the outflow through the roof as a function of  $n_{50}$ . The divider lays between 17 and 21, where an average of 20 is typically used for hand calculations. The outflow increases a little with higher  $n_{50}$ -value. It in fact should stop once the roof is the only leak left. Of course, thermal stack over the roof's height may then change it into an inflow/outflow system with inflow through the lower and outflow through the higher half of the pitches.

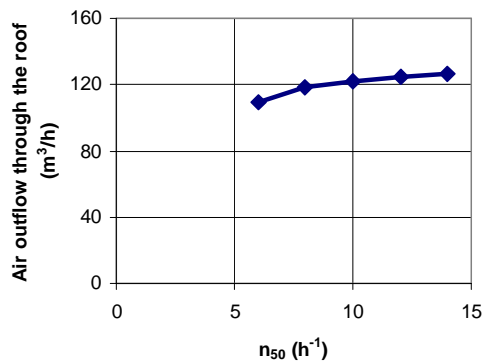
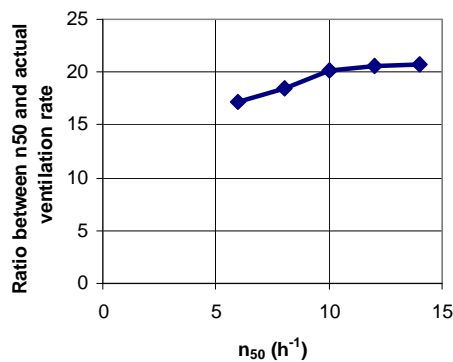


Figure 4 Ratio between  $n_{50}$  and the actual ventilation rate

Figure 5 Air outflow through the roof

#### Partial water vapour pressure and surface condensation indoors

Calculation for an average vapour release of 13.5 kg/day gives:

$n_{50}$ ( $\text{h}^{-1}$ )	Ventilation flow $\text{m}^3/\text{h}$	Surface condensation?		Inside vapour pressure Pa	$\Delta p_{ie}$ ( $p_e=496$ Pa) Pa
		Where?	Amount kg/week		
6	115.5	On aluminium and the single glass	37.0	895	399
8	143.1		28.4	866	370
10	164.2		22.7	847	351
12	193.4		15.7	823	327
14	223.9		9.3	801	305

Figure 6 shows the excess as function of ventilation flow. More ventilation not only lowers the excess but also the condensation deposit on window frames and single glass. This is positive as abundant condensate on the frames may damage the window reveals.

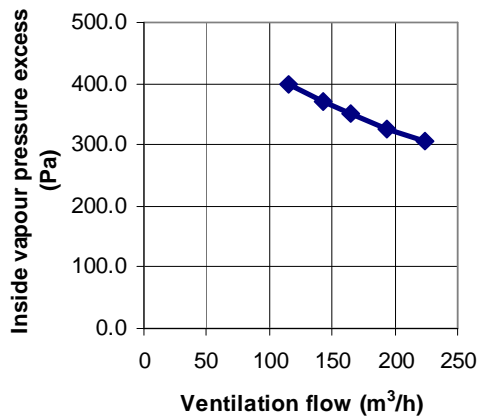


Figure 6 Inside vapour pressure excess as a function of the ventilation flow

### Interstitial condensation in the cathedralized ceiling

Calculated results for a ventilation rate at 50 Pa of  $10 \text{ h}^{-1}$ :

Interface	Temperature °C	Saturation pressure Pa	Vapor pressure Pa	$p > p_{\text{sat}}$ ?
Inside	18.0		846.5	
Inside surface	17.6	2016	846.5	
Gypsum/air layer	17.4	1993	846.5	
Air layer/paper backing	16.6	1894	846.5	
Paper backing/insulation	16.6	1894	846.5	
Insulation/air layer	1.0	656	846.5	YES
Air layer/roof cover	-2.4	499	846.5	YES
Outside surface	-2.6	494	509.4	
Outside	-3.9		496.3	

Clearly, interstitial condensation below the roof cover is a fact. Using formula (10), the deposit during that one cold week amounts to  $1.12 \text{ kg/m}^2$  or  $53.8 \text{ kg}$  for the whole roof. The simplified formula gives identical results. However, as temperature in the interface, where condensation deposits, is below zero, vapour condenses as ice. As long as freezing persists, no dripping may happen. In reality, a weekly mean includes night lows and day highs with the sun warming the roof to temperatures above zero. The ice will thus melt during daytime, which may cause dripping!

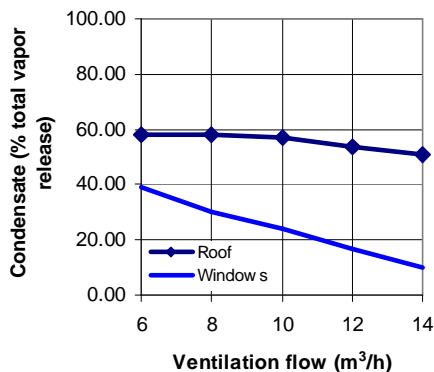


Figure 7 Condensate as a percentage of total vapor release

Calculation for all  $n_{50}$ -values gives the condensation deposits in percent of total vapour release of figure 4. The figure also contains the percentage surface condensate on window frames and single glass represents. While these quickly decrease with better ventilation, deposit in the roof hardly changes, a result of two opposing facts: decreasing inside partial water vapour pressure but increasing outflow across the roof with increasing ventilation flow! Diffusion only for  $n_{50}=10 \text{ h}^{-1}$  should have given a deposit below  $4.7 \text{ kg/week}$ , i.e. only 4.9% of the vapour released.

**Weekly net energy demand***Without outflow across the roof*

In that case, ventilation should be fully accounted for in the energy balance.

## Transmission

	Surfaces m <sup>2</sup>	U-factor W/(m <sup>2</sup> .K)	UA W/K	$\Delta\theta$ °C	UA $\Delta\theta$ W
<b>Ground floor</b>					
Front façade	13.1	1.35	17.7	20.5	362
Back façade	16.5	1.35	22.2	20.5	454
Sidewall	22.1	1.35	29.8	20.5	611
Floor grade	51.8	0.70	36.2	20.5	741
Door	2.0	3.00	5.9	20.5	122
Window T	0.2	3.55	0.7	20.5	15
Window 1	5.4	3.40	18.4	20.5	377
Window 2	5.4	3.40	18.4	20.5	377
Window K	3.2	3.42	10.8	20.5	221
Door K	2.0	3.00	5.9	20.5	122
			<b>Total</b>		<b>3401</b>
<b>First floor</b>					
Front façade	12.0	1.35	16.2	20.5	332
Back façade	14.7	1.35	19.8	20.5	406
Sidewall	26.4	1.35	35.6	20.5	729
Roof 1	30.4	0.49	15.0	21.9	328
Roof 2	25.8	0.49	12.7	21.9	278
Window 1	4.5	5.74	25.8	20.5	530
Window 2	4.5	5.74	25.8	20.5	530
Window 2	4.5	5.74	25.8	20.5	530
Window BR	1.8	5.74	10.3	20.5	212
			<b>Total</b>		<b>3873</b>

## Ventilation

$N_{50}$ h <sup>-1</sup>	$c_a$ J/(kg.K)	$\rho_a$ kg/m <sup>3</sup>	$c_a \rho_a \dot{V}$ W/K	$\theta$ °C	$c_a \rho_a \dot{V} \theta$ W
6	1008	1.21	39.2	20.5	803
8			48.6		995
10			55.7		1142
12			65.6		1346
14			76.0		1552

## Net energy demand

$N_{50}$	Net energy demand MJ/week
6	4885
8	5002
10	5090
12	5213
14	5341

*With outflow across the roof*

Exfiltration changes the conduction losses at roof level. The fictive inside U-factor and the net energy demand so become:

$n_{50}$	Fictive U-value roof W/(m <sup>2</sup> .K)	Net energy demand MJ/week	Decrease in %, compared to no exfiltration
6	0.20	4667	-4.46
8	0.18	4772	-4.59
10	0.18	4855	-4.62
12	0.17	4925	-4.56
14	0.17	5101	-4.50

#### 4.5.5.2 Step 2

##### Airflows

Take  $n_{50}=10 \text{ h}^{-1}$  and the front façade NE. As the flow over front and back at the ground and first floor has to be distributed proportional to the whole window perimeter, flows at 1 Pa pressure difference become:

	Front m <sup>3</sup> /(s.Pa)	Back m <sup>3</sup> /(s.Pa)
Ground floor	$1.28 \cdot 10^{-2}$	$1.65 \cdot 10^{-2}$
First floor	$1.29 \cdot 10^{-2}$	$1.16 \cdot 10^{-2}$

Stack pressures are:

	Height m	Outside Pa	Inside Pa	Difference Pa
First floor	0	0	0	0
Second floor	2.75	-35.18	$-\left(19.19 + \frac{3395}{T_{a,2}}\right)$	?
Roof	5	-64.28	$-\frac{17313}{T_{a,2}}$	?

Wind pressures at the front, the back and the roof pitches do not change, compared to step 1. Solving the system of equations gives as air flows and temperature on the first floor (+ for inflow, - for outflow)

Air temp. first floor °C	Air flows, m <sup>3</sup> /h					
	Ground floor		First floor		Roof space	
	Front	Back	Front	Back	Large pitch	Small pitch
7.7	71.0	60.5	1.9	-51.7	-44.5	-37.3

Ventilation thus totals 133 m<sup>3</sup>/h, less than the 164 m<sup>3</sup>/h found for the dwelling heated at 18°C! Clearly, not heating the second floor diminishes thermal stack and decreases adventitious ventilation. With the net volume as reference (248.3 m<sup>3</sup>), ventilation rate becomes 0.54 h<sup>-1</sup>, i.e. still better than 0.5 h<sup>-1</sup>, the IAQ-requirement. Compared to gross volume (331.6 m<sup>3</sup>), the rate drops to 0.40 h<sup>-1</sup>. The conclusion is that  $n_{50}=10 \text{ h}^{-1}$  guarantees sufficient adventitious ventilation from an IAQ point of view. That conclusion fits with the  $n_{50}$ -interval for adventitious ventilation, given in (Liddament, 1996):  $8 \leq n_{50} \leq 15 \text{ h}^{-1}$ .

Temperature on the first floor does not account for the internal heat gains as these were not given. These included gives 9°C. This is acceptable for sleeping rooms at night but too cold for daytime use. Some heating will be necessary.

##### Partial water vapour pressure and surface condensation indoors

Calculation for the instantaneous vapour releases gave the indoor vapour pressures and condensation deposit on the aluminium frames, single glass, double glass and opaque façade walls of figure 8 and 9.

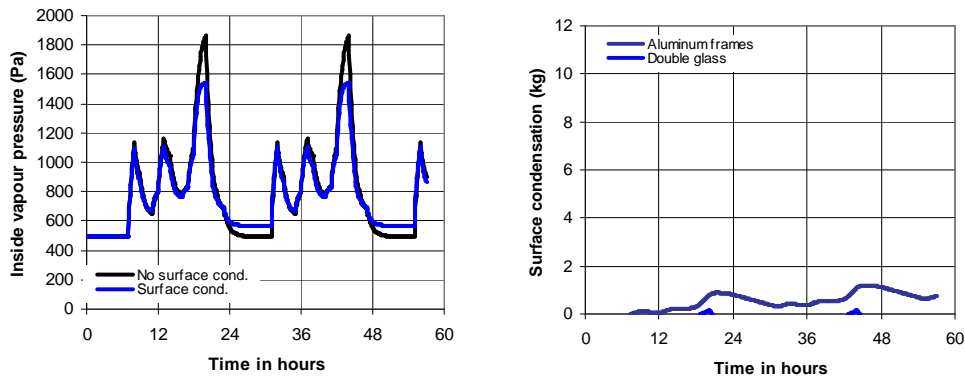


Figure 8 Ground floor: partial water vapour pressure and condensation deposit on the aluminium frames and the double glass

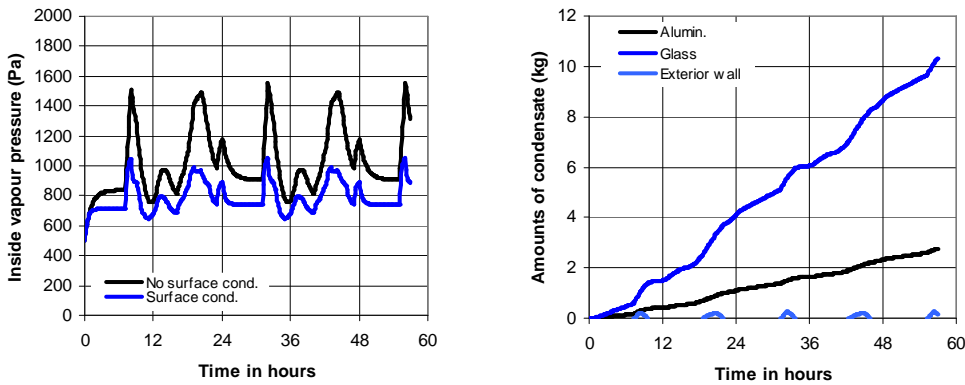


Figure 9 First floor: partial water vapour pressure and condensation deposit on the aluminium frames, the single glass and the façade walls

Surface condensation clearly lowers the average vapour pressure and cuts the peaks. On the ground floor, decrease is tempered by the high inside temperature and less condensing surface. On the first floor, the decrease in average and peak values is very pronounced as more condensing surfaces are available and the air temperature is low. Some condensate even deposits on the opaque façade walls!

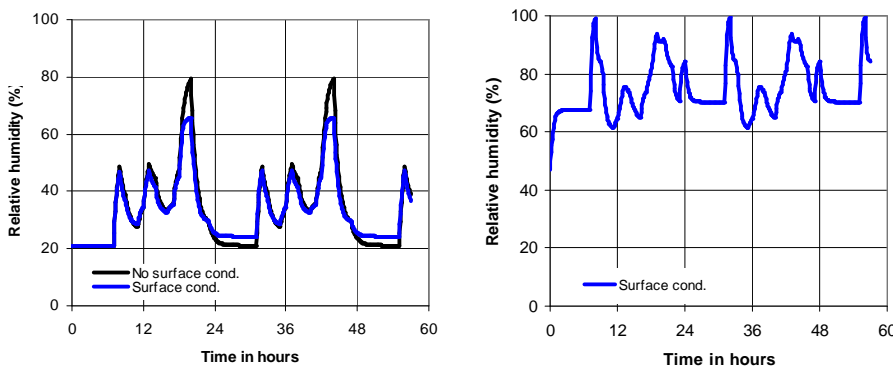


Figure 10 Ground and first floor: relative humidity

Figure 10 shows relative humidity over time. On the ground floor, peaks touch 65%, while the lows near 25%. On the first floor instead, the vapour coming from the ground floor, the important quantities released, the low temperatures and surface condensation result in a relative humidity oscillating between 50 and 99%, with mould as a most likely consequence.

### Interstitial condensation in the cathedralized ceiling

As in step 1, interstitial condensation is a fact. At the peaks in inside vapour pressure, little moisture even condenses against the gypsum board, the paper back of the insulation and the insulation. Over time anyhow, most is deposited as ice below the cover, see figure 11. As the weekly mean combines night lows with day highs, that ice may melt during daytime! The line in black on the figure gives the amount that remains stick against the cover. Only the surplus drips. That way, condensate is periodically removed, keeping the maximum in the roof close to the line. Drainage to the outside through the overlaps between the corrugated plates could also help in stabilizing the maximum, if these overlaps were not sealed as was the case here. Sealing was done after the first winter, when the inhabitants believed the roofs leaked.

After 7 days, a total of 33.1 kg of vapour should have condensed in the roof, which is less than the amount predicted in CEX1 (53.8 kg/week). The main reason for that is the decrease in outflow across the roof (81.8 m<sup>3</sup>/h versus 122.5 m<sup>3</sup>/h).

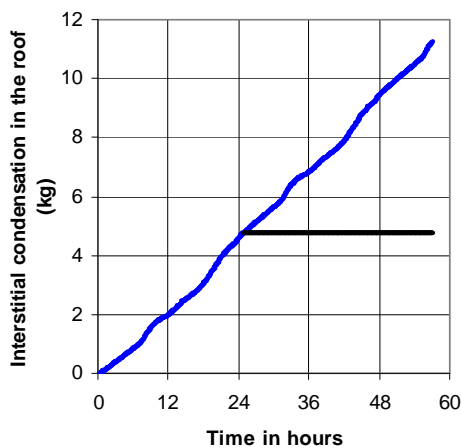


Figure 11 Condensation deposit at the backside of the roof cover

### Weekly net energy demand

#### *Without outflow across the roof*

Without outflow, the temperature on the second floor drops to 7.3°C, while the in- and outgoing airflows hardly change. For  $n_{50}=10 \text{ h}^{-1}$ , the transmission losses at the ground floor attain 5049 W, which is an increase with 48.5% compared to step 1. The first floor, however, has zero transmission loss. Ventilation loss touches 985 W. Both together results in a net energy demand of 3649 MJ/week, 25% lower than in step 1

#### *With outflow across the roof*

Outflow reduces the transmission losses at the ground floor a little, from 5049 W down to 4999 W. Transmission loss stays zero at the first floor, while ventilation loss increases somewhat to 994 W. Both together results in a net energy demand of 3625 MJ/week, hardly different from the situation without outflow.

#### 4.5.5.3 Step 3

Airflows and ventilation do not change, compared to step 2. Buffering, however, dampens ups and downs in inside partial water vapour pressure much more effectively than surface condensation does, as figure 12 shows for the ground floor. That turns condensation deposit on the aluminium frames to a marginal phenomenon, see figure 13. Also relative humidity is stabilised. Interstitial condensation in the cathedralized ceiling finally remained close to what was found in step 2. This is logic, as buffering hardly changed the average inside vapour pressure on the first floor.

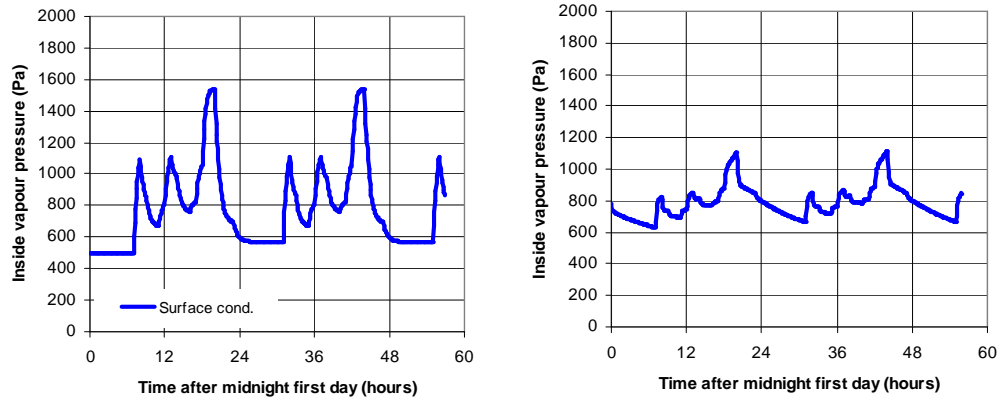


Figure 12 Ground floor: on the left vapour pressure without moisture buffering, on the right vapour pressure with moisture buffering

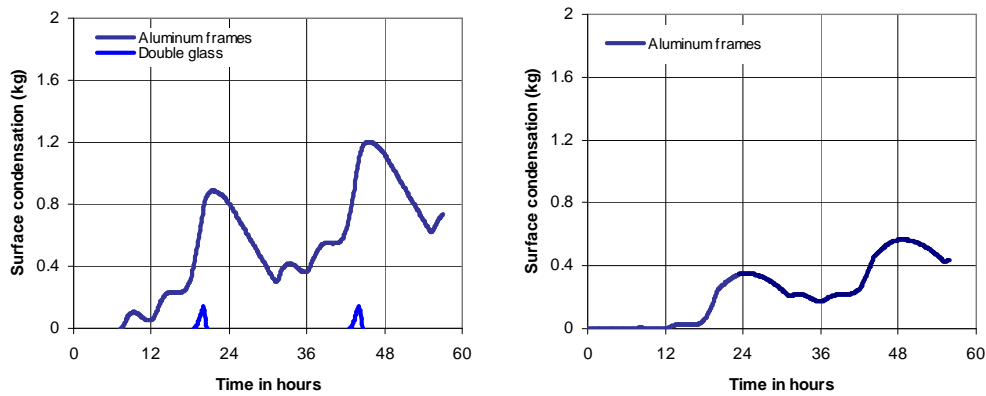


Figure 13 Ground floor: on the left surface condensation on double glass and aluminium frames without moisture buffering, on the right surface condensation on the aluminium frames with moisture buffering

#### 4.5.6 Solutions introduced

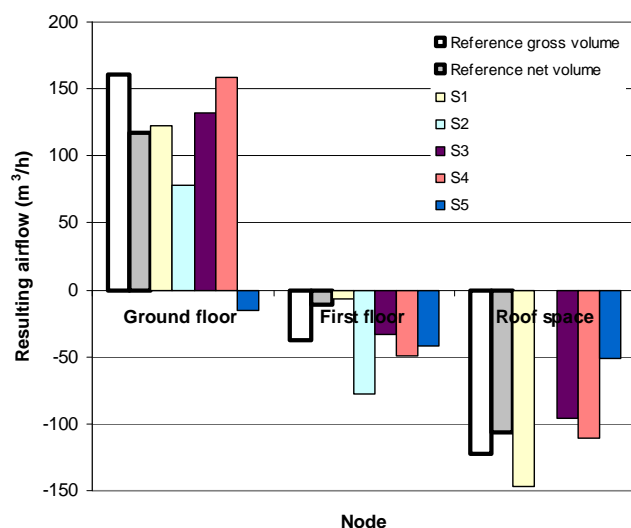
##### 4.5.6.1 Step 1

Four participating countries introduced solutions (FIB,2005)( Kwiatkowski et al, 2005)( Hameury, 2005)(Ridly et al, 2005)(Van Schijndel, 2005). We restrict comparing the results with the reference to the main façade oriented NE.

##### Air flows

$n_{50}=10h^{-1}$	Air flows, $m^3/h$					
	Ground floor		First floor		Roof space	
	Total		Total	Back	Large pitch	Small pitch
Reference						
NE (gross)	82.3	78.2	3.7	-41.7	-66.6	-55.9
NE (net)	60.1	57.4	12.4	-23.4	-57.9	-48.6
S1						
NE	123.0		-6.6		-72.7	-74.0
S2						
NE	117.0	-38.7	39.0	-117.0	53.4	-54
S3						
NE	132.0		-33.0		-96.0	
S4						

NE	159.1		-48.8		-110.3	
S5						
NE	-14.8		-42.0		-50.9	



S1, S2 and S3 took the net volume as reference for  $n_{50}$  where the exercise stated using the gross volume. What troubles more in S1 is the air balance at dwelling level: not zero! S2 heavily exaggerates wind effect. In fact, no reduction was applied between the open field velocity at 10 m and the velocity in the estate. S3 and S4 give results pretty close to the reference solution. S5 finally forwards physically wrong results as the air balances at floor and dwelling level are all negative!

#### Vapour balance and condensation deposits

Orientation Main Façade	Surface Condensation on window frames and glas kg/(m².week)		Condensation in the roof kg/(m².week)
	Single glas, window frame	Double glazing	
<b>Reference solution</b>			
NE (exterior)	22.7	0	53.8
NE (interior)	31.4	0	52.9
<b>S1</b>			
NE	28.6	0	39.5
<b>S2</b>			
	No results		24.4
<b>S3</b>			
	No results		0
<b>S4</b>			
NE	27.6	0	50.7
<b>S5</b>			
	No results		

S1 and S4 give results quite close to the reference. S2 underestimates interstitial condensation in the roof. S3 concludes there is no condensation which does not match with the field evidence, while S5 gives no answer at all. None of the participants evaluated the amounts of surface condensation on window frames and glass.

### Net energy demand during that one cold week

Orientation Main Façade	Net energy demand MJ/week	
	Exfiltration roof not considered	Exfiltration roof considered
<b>Reference solution</b>		
NE (exterior)	5090	4855
NE (interior)	4762	4582
<b>S1</b>		
NE		4873
<b>S2</b>		
NE		867
<b>S3</b>		
NE		617
<b>S4</b>		
NE		4766
<b>S5</b>		
NE		3871

S1 and S4 give results close to the reference. However, in none of the two outflow was correctly accounted for. S2 and S3 are far away from the reference, while S5 give results that differ quite substantially from the reference. The reason why is not clear. A possibility is that the conduction losses have been calculated using the interior dimensions.

#### 4.5.6.2 Step 2 and 3

Only one participating country solved the exercise for step 1, step 2 and step 3 together (De Wit, 2006). The methodology differed somewhat from the reference, as more zones were considered for the air balance. Conclusions and numerical results, however, were very close:

- Very high relative humidity in the sleeping rooms with abundant surface condensation on the aluminium windows with single glass
- Moisture buffering dampens relative humidity oscillations effectively but has no impact on the mean values
- Abundant interstitial condensation in the cathedralized ceiling, independent of moisture buffering or not, although buffering makes condensation more steady state
- Hardly any impact of outflow across the roof on net energy demand.

#### 4.5.7 Conclusions

The exercise proved that solving real life problems, using simplified methods, is not as simple as one could expect. One has to know a lot about what could happen before starting modelling and calculating. The simple models used should be physically correct. Mass balances should fit, etc.

#### References

- Anon. (1981), Warotveld Estate, Winksele (near Leuven), Moisture Problems in the Roofs, Laboratory of Building Physics, Report 81.12 (In Dutch)
- FiB, 2005, Common exercise x, step 1
- Hens H., Zheng R., Janssens A., (2003), Does Performance Based Design Impacts Traditional Solutions: Metal Roofs as an Example, Proceedings of the 2nd International Building Physics Conference, Leuven
- Hens H., 2005, Common exercise x, first step, Paper IEA, EXCO ECBCS, Annex 41, Montreal meeting
- Hens H., 2006, Common exercise x, second step, Paper IEA, EXCO ECBCS, Annex 41, Kyoto meeting
- Janssens A, 1998, Reliable control of interstitial condensation in lightweight roof systems, Doctoral Thesis K.U.Leuven, 217 pp
- Kwiatkowski J, Woloszyn M, 2005, Common exercise1, report
- Liddament M.W. (1996), A Guide to Energy Efficient Ventilation, AIVC, Coventry, 254 p.
- Hameury S., 2005, Common exercise x, step 1
- Ridley I, Davies M., 2005, Common exercise x
- van Schijndel J, 2005, Common exercise 1, step 1, using MatLab, revision 1, including stack pressures
- De Wit, 2006, CEX

## 5 Some indicators for Whole Building HAM Modelling

Models are created to represent some parts of the reality, with the objective to get a better understanding of this reality or to predict the behaviour of the represented system. Therefore a model is always a simplified vision of the reality. The confidence in model results depends on the quality of the model. The focus here is on the question: what can be called a "good quality model" in the context of Whole Building Heat Air and Moisture context? Without being exhaustive, the ambition was to collect common experience of Annex 41 participants, and to address some relevant points. Some of the following may appear fairly naïve, but these ideas were pointed out by several contributors, beginning researchers but also experienced participants.

First and foremost, the modelling objective should be defined in terms of the outputs from the model that are considered necessary. Then analysing involved physical processes, available information and eventual constraints (such as computational time, availability of existing tools, expertise...) adequate modelling process should be chosen. The modelling process includes the choice of granularity (mainly the size of control volume, as discussed in 2.5.) and number and level of detail of physical phenomena. For example: should liquid transfer in the envelope elements be represented? should radiation transfer coefficients be used or exact view factors calculated while modelling radiation? should moisture impact on air density be considered? etc. The complexity of the model must be adapted to required results. For example CFD calculation (complex to use and demanding very precise input data) is not needed to estimate mean annual variations. On the other hand moisture field in the room air can not be predicted by multizone calculations (such model gives correct mean values, but local values may not be correct). It is very important to know the limits of the models. These choices are crucial and need some time and expertise. Some indications, far from being exhaustive, can be found in chapter 2.

There is another essential concern about model complexity. There is a belief that more complex the model is, better the results are. It is not so simple. Results issued from some very complex calculations, requiring very precise and numerous input data and hours or days of project definition and simulations, can excessively outlay experimental measurements. At the same time simplified model programmed in a spreadsheet can give a very realistic estimate of mean values. Both complex and simplified models require some additional analysis, there are in general very sensitive to the choice of some crucial parameters, such as thickness of the humidity buffering layer for EMPD-type models, or turbulence model for CFD. Existing programs must be carefully used and computer can not replace analysis and expertise.

A correct balance between different phenomena that interact on each other must be ensured. For example there is no point on performing detailed 2D calculations of liquid and vapour transfers in the envelope if the temperature fields are not represented.

Once these questions addressed, the modelling process starts. The final model can be built by connecting some existing modules, writing your own modules to express additional physical laws or by any combination of both. Be careful! Check if you understand well what you are doing and be aware of model limits. Once the model completed, make sure that all the parameters and inputs are set to correct values. It is very useful to first check the model in some known situations to make sure that it gives correct or at least plausible outputs.

There is a very large difference of time constants for airflow, energy and moisture. Airflow's dynamic is very rapid, moisture's is very slow, and energy's is in between. This impacts directly the choice of the initial state, numerical method and time-step. Any problems of numerical divergence must be avoided, for example mesh must be adapted for both moisture and energy. A useful verification is to change moderately time step and/or mesh and check if the results remain constant.

And last and not least, when whole building HAM modelling is applied it is important to review the results critically and perform sensitivity studies, with a dual objective. First, very important point is to help the validation of the results. Second, they can also reveal the effect of changes in one parameter at the time. Simulation results are strongly dependent of the

input data and thus the results will never be better than the supplied input data. Therefore also the uncertainty of the input data must be known and used to evaluate the output data.

The task seems hard, but is achievable, as attest many interesting and "good" results from common exercises!

## 6 Challenges for the future

*The challenges are somehow different for different approaches (CFD, WB, simplified..)*

The following text will present in a short form some detached impressions given from the work in Annex 41's Modelling subtask, as to what seems the most pertinent requirements for further work to be done in order to further develop the ideas seeded in Annex 41.

- Consolidate these recent developments. Know better where the pitfalls are. Don't believe tools to predict the truth, but understand how they can be very valuable tools anyway to predict interactions so sensitivity studies can be made etc.
- Validation of models, possibly as a comparison with measurement data, sensitivity studies
- Carry out sensitivity studies
- Detailed investigation and validation of moisture interaction air/material (coupling or developing CFD)
- Consider the effect of the air flow in
  - rooms and microenvironments
  - the building envelope, including ventilated cavities
- Effect of multidimensional transports
- Equipment/system modelling
- How to model the effect of indoor furnishing: Furniture, books, textiles... ?
- Coping with discontinuities and contact resistances
- Liquid migration and sorption isotherms at high RH (>0.99)
- Including rain as a boundary condition
- Considering hysteresis
- Temperature effects on moisture properties,
- Reduce computer run time for simulation of whole buildings
- Provide reliable database of material properties
- Durability modelling and ageing
- Extended assessment of the importance of convective mass transport coefficients.
- Relative small attention has been given to problems of not well mixed air, specification of the cases when it is or is not negligible in real building. Also the influence of possible 2D or 3D HAM transfer through the envelope parts, possible space and time surface film coefficients variability effects have not been discussed
- End user issues: Are these kinds of models amenable for building designers and other members of the professional community? Does it require particular experience/training to be able to overlook all these interacting phenomena?
- For detailed modelling (HAM in whole building combined with CFD technique), we should decompose the whole problem into each object, such as walls and rooms. We can't calculate whole space in the building by mm order grid, which should be used in transport in the material. So, the multi-grid method becomes significant
- More need for comparison with experiences from practice and field tests.
- Extend the models further, e.g. to predict other indoor pollutants and mass transfers than moisture.
- Use the tools to harvest on the energy benefit while maintaining good IAQ.

- Develop distributed calculations. Rather than having one tool that calculates everything, a suite of separate, specialized tool should be able to work together synchronously.

## 7 Conclusion and Perspectives

An overall ambition of IEA Annex 41 has been to stimulate the development of information and analytical tools about how a whole building works in terms of its hygrothermal building physics conditions. This involves several physical processes: Flows of heat, air and moisture (HAM). And it involves different building elements at various levels: Its spaces, the building envelope with its materials, the interior building structures and furnishing, the system for heating, ventilating and air conditioning, occupants and equipment, and finally the exposure to the exterior environment. The actual challenge in whole building Heat, Air and Moisture modelling is to ensure a good balance between the many different physical phenomena which interact on each other, rather than to develop models that focus too much on mainly one phenomenon. For example in most of the existing programs, if moisture is well modelled, then the energy model is rather simple; or if energy is rather well calculated, then moisture behaviour is treated in a simplified way - if not neglected. In this field a lot of progress has been made and encouraging results are seen from Common Exercises.

Concerning some general principles about the impact of moisture on whole building energy response, different researchers agree that the first and essential step is to represent correctly the moisture balance, including vapour absorption and desorption from hygroscopic surfaces. In some practical applications, when only an estimation of the moisture in the indoor climate is of interest, this can be done using simplified lumped models (Hens, 2005, Hokoi, 2005, Woloszyn et al. 2005). However when moisture level in constructions is needed the investigations require use of coupled heat and mass transfer models to describe complex physics in walls. Encouraging fact is that different potentials for moisture transfer can be successfully used (relative humidity, moisture ratio by volume, etc.). However, correct estimation of the initial conditions and good choice of mesh size and of time step size seem to have significant impacts on the predicted solutions (Hagentoft 2006, Abadie et al, 2005). When a detailed field of moisture in the air or in the construction is needed, CFD can help to get a precise response (Steehan et al. 2005), however they require an experienced user and a detailed description of the room.

The experience from the Common Exercises, as well as some parameter study performed and some of the free papers tell that there is still a lot to do. There is a need to execute more validation cases, possibly as a comparison with measurement data. Some other aspects have to be considered as well, e.g. adding furniture and considering the air flows. Detailed consideration of the airflow should be done with detailed representation of HAM transfers in building elements: To link whole building behaviour with condensation problems behind a piece of furniture some adapted approach should be studied – such as for example multi-scale, reduced order or zonal models.

## References

- Abadie, M., J.P. Deblois and N. Mendes. 2005. A comparison exercise for calculating heat and moisture transfers using TRNSYS and PowerDomus. Paper presented at IEA-Annex 41 working meeting in Trondheim, A41-T1-Br-05-2.
- Abadie M.O., Mendes, N. 2006 "Comparative Analysis of Response-factor and Finite-volume based Methods for predicting Heat and Moisture Transfer through Porous Building Materials". *Journal of Building Physics*, 30(1): 7-37.
- Abadie, M., Deblois, J.P., Mendes, N. 2005. A comparison exercise for calculation heat and moisture transfers using TRNSYS and PowerDomus. IEA Annex 41 working meeting. Trondheim (Norway), October 2005.
- Abadie M. 2007. Report from Subtask 1: Common Exercise 4: `Moisture management` PUCPR participation using TRNSYS.
- ABAQUS 2007. [www.simulia.com](http://www.simulia.com)
- Achermann, M. 2000. Validation of IDA ICE, Version 2.11.06 With IEA Task 12 - Envelope BESTEST. Hochschule Technik+Architektur Luzern. HLK Engineering
- AIVC Technical notes 44
- Akinyemi, olukayode ; Mendes, N. . Numerical and Experimental Determination of Surface Temperature and Moisture Evolution of a Field Soil. *Journal Of Geophysics And Engineering*, Reino Unido, v. 4, p. 7-17, 2007.
- Allard F. and Y. Utsumi. *Airflow through large openings*. Energy and Buildings. 1992. Vol 18, pp. 133-145.
- ASHRAE. 2004. Standard Method of Test for the Evaluation of Building Energy Analysis Computer Programs. ANSI/ASHRAE Standard 140-2004. Atlanta, GA: American Society of Heating, Refrigerating and Air-Conditioning Engineers, Inc.
- Barbosa R.M., N. Mendes, 2007, Combined simulation of central HVAC systems with a whole-building hygrothermal model, *Energy & Buildings*
- Blocken, B. Airflow patterns around a building. The reference will be completed. Breesch H. 2006. "Natural night ventilation in office buildings." PhD - thesis. Ghent University, Belgium.
- Bonneau D., F.X. Rongere, D. Covalet and B. Gauthier. *Clim2000 : Modular software for energy simulation in buildings*. In : Proceedings of IBPSA 93. Adelaide, Australia. 1993.
- Brown W. G. and K. R. Solvason. *Natural convection through rectangular openings in partitions. I. Vertical openings*. *Int. J. Heat Mass Transfer*. 1962. Vol 5, pp. 859-868.
- Building Energy and Environmental Systems Laboratory at Syracuse University. 2007. Coupled Heat, Air, Moisture and Pollutant Simulation (CHAMPS). <http://beesl.syr.edu/champs.htm> (January 15, 2007)
- Burchiu, S. *Etude de l'influence d'un système de chauffage sur l'état thermique et aéraulique des bâtiments multizones avec prise en compte de la stratification thermique*. PhD thesis. Institut National des Sciences Appliquées de Lyon. 1998. 162 p.
- CD-adapco. 2007. STAR-CD. <http://www.cd-adapco.com/> (January 15, 2007)
- Clarke J A (1985) Energy simulation in building design Adam Hilger, Bristol and Boston.
- COMSOL. 2007. [www.comsol.com](http://www.comsol.com)
- COSMOS. 2007. [www.cosmosm.com](http://www.cosmosm.com)
- Crawley D. B., J.W. Hand, M. Kummert, B.T. Griffith. 2005 "Contrasting the capabilities of building energy performance simulation programs". Version 1.0.
- Crawley D.B., L. K. Lawrie, C. O. Pedersen, F.C. Winkelmann, EnergyPlus: An Update. In Proc. SimBuild 2004, Building Sustainability and Performance Through Simulation, August 4-6, 2004, Boulder, CO, USA LBNL-55518
- Crawley, D.B., Lawrie, L.K, Pedersen, C.O., Winkelmann, F.C. 2000. EnergyPlus: Energy Simulation Program, in *ASHRAE Journal*, Vol. 42, No. 4 (April), pp. 49-56
- Cunningham, M.J. 2003. The building volume with hygroscopic materials: an analytical study of a classical building physics problem. *Building and Environment* 38, p.329-337.
- Duforestel, T. and P. Dalicieux. 1994. A model of hygroscopic buffer to simulate the indoor air humidity behaviour in transient conditions. In : Proceedings of European Conference on Energy Performance and Indoor Climate in buildings. Lyon, France. Vol 3, pp. 791-797.

- Ellinger 2004. Feuchtepufferwirkung von Holzinneinraumverkleidungen. University of applied science Rosenheim. Thesis.
- Emmel, M.G.; Abadie, M O; Mendes, N. . New External Convective Heat Transfer Coefficient Correlations for Isolated Low-Rise Buildings. *Energy and Buildings, USA*, v. 9, p. 335-342, 2006.
- Erriguible, A., P. Bernada, et al. (2005). Modeling of heat and mass transfer at the boundary between a porous medium and its surroundings. *Drying Technology* 23(3): 455-472.
- Eyglunent, B. 1997. Manuel de thermique (Handbook of heat transfer, in French), ed. Hermes, Paris (France), 2e ed. 374 p.
- Feustel H.E. and al. *Fundamentals of the multizone airflow model COMIS*. Technical note AIVC 29. 1990. 115 p.
- FLUENT. 2007. FLUENT Flow Modeling Software. <http://www.fluent.com/> (January 15, 2007)
- Fraunhofer Institut für Bauphysik. 2007. WUFI-2D PC-Program for calculating the coupled heat and moisture transfer in building components. [http://www.hoki.ibp.fhg.de/wufi/wufi\\_frame\\_e.html](http://www.hoki.ibp.fhg.de/wufi/wufi_frame_e.html) (January 15, 2007).
- Grunewald J., Ruisinger, U., Häupl, P., 2006. The Rijksmuseum Amsterdam - Hygrothermal analysis and dimensioning of thermal insulation, 3rd International Building Physics/ Science Conference, Montreal 2006, Balkema Publishers, Rotterdam, Netherlands, ISBN 0-415-41675-2, S. 345-352
- Grunewald J. 2000. Documentation of the Numerical Simulation Program DIM3.1, Volume 1: Theoretical Fundamentals. Delphin4 program installation available on the ftp-server of the Institute of Building Climatology: <http://bauklimatik-dresden.de/software.html>
- Grunewald, J: 1996. Diffusiver und konvektiver Stoff- und Energietransport in kapillarporösen Baustoffen. Dissertation TU Dresden, Fakultät Bauingenieurwesen.
- Hagendoorn, C-E, Sasic Kalagasidis, A., Adl-Zarrabi, B., Roels, S., Carmeliet, J., Hens, H., Grunewald, J., Funk, M., Becker, R., Shamir, D., Adan, O., Brocken, H., Kumaran, K., Djebbar, R. 2004. Assessment Method of Numerical Prediction Models for Combined Heat, Air and Moisture Transfer in Building Components. Benchmarks for One-dimensional Cases. *Journal of Thermal Envelope and Building Science*, Vol. 27, No. 4/ April.
- Hartmann et al. 2001. Feuchteschäden und Schimmelpilzbefall in Wohnungen. *Bundesbaublatt Jg. 53, Nr. 3, page 38-42*.
- Häupl P., H. Fechner, 2003. The calculation of the moisture and temperature field in the sandstone cupola of the „Church of Our Lady“ in Dresden, proceedings Conference “Structural Studies, Repair and Maintenance of Heritage Architecture VIII”, Halkidiki, May 5th-6th 2003, 231-240
- Häupl, P., H. Fechner, H. Petzold, 2004. Interior Retrofit of a Masonry Wall to Reduce Energy and Eliminate Moisture Damages: Comparison of Modeling and Field Performance, Proceedings Buildings IX Conference, Clearwater Beach, Florida, ISBN 1-931862-60-5, ASHRAE Publisher, Publications
- Hedegaard, L., M. Woloszyn & G. Rusaouen. 2004. Moisture interactions between air and constructions modelled with CFD. IEA Annex 41 2nd working meeting. Glasgow (United Kingdom), October 2004.
- Henninger, R.H., Witte, M.J Crawley, D.B., 2004. Analytical and Comparative Testing of EnergyPlus using IEA HVAC BESTEST E100-E200 Test Suite, pp 855-863, *Energy and Buildings*, 36:8
- Hens, H. 1991. Modelling: hygric aspects. Chapter in ‘Condensation and Energy: Source book’ IEA-Annex 14. Acco, Leuven.
- Hens, H. 2002. Technical Synthesis Report on Heat, Air and Moisture Transfer in Highly Insulated Building Envelopes. UK, Faber Maunsell Ltd..
- Hens, H. 2005. Impact of hygric inertia on indoor climate: simple models. Paper presented at IEA-Annex 41 working meeting in Trondheim, A41-T1-B-05-6.
- Hohota R. 2003. Moisture modeling in a CFD code (low velocity in large enclosure). Comparison with experiments. (in French) PhD thesis, Laboratoire CETHIL INSA de Lyon, France

- Hohota, R., M. Woloszyn & L. Hedegaard. 2004. CFD modeling of moisture transport and condensation. IEA Annex 41 1st working meeting. Zurich (Switzerland), 12-14 may 2004. 11/04/2007 Outline of A41 S1 report 27
- Hokoi, S. 2005. Simplified method for evaluating moisture buffering effect. Paper presented at IEA-Annex 41 working meeting in Trondheim, A41-T1-J-05-10.
- Holm, A., H.M. Künzle, & K. Sedlbauer. 2003. The Hygrothermal Behaviour of Rooms: Combining Thermal Building Simulation and Hygrothermal Envelope Calculation. 8th IBPSA Conf. Eindhoven.
- Holm A., Radon J., Künzle H, Sedlbauer K. 2004. Description of the IBP holistic hygrothermal model. IEA Annex 41 1st working meeting. Zurich (Switzerland), 12-14 may 2004.
- Hong, S.H., Ridley, I., Oreszczyn, T. A Hygrothermal Monitoring and Modelling of a Historic Roof. *Proceedings Eighth International IBPSA Conference*. Vol 1, pp 515-522. Eindhoven, Netherlands August 2003. ISBN 90-386-15663. International Building Performance Simulation Association
- International Energy Agency. Energy Conservation in Buildings and Community Systems Programme. Annex 20 : Air flow patterns within buildings. Subtask 2 : Air flow between zones. *Air flow through large openings in buildings*. Ed. J. van der Maas. 1992.
- Iwamae, A., H. Hanibuchi, T. Chikada 1999. A Windows-based PC-software to design thermal environment in residential houses, *Proceedings of Building Simulation'99*, Volume 3: 1325-1330.
- Iwamae, A. 2004. A Development Of Pc Software To Calculate Temperature And Humidity Variations In Residential Houses, Presentation for IEA Annex 41 meeting, Glasgow, October 2004, A41-T1-J-04-1.pdf
- Janssen, H. 2002. The influence of soil moisture transfer on building heat loss via the ground. Doctoral thesis. KU Leuven.
- Janssen, H. and S. Roels. 2007. The hygric inertia of building zones: characterisation and application. Paper presented at IEA-Annex 41 working meeting in Florianopolis, A41-T4-Dk-07-1.
- Janssens, A. and M; De Paepe. 2005. Effect of moisture inertia models on the predicted indoor humidity in a room. *Proceedings of the 26<sup>th</sup> AIVC-Conference 'Ventilation in Relation to the Energy Performance of Buildings'*, Brussels, ISBN 2-9600355-8-5, INIVE EEIG, 287-294.
- Judkoff, R. and J. Neymark. 1995. Building energy simulation test (BESTEST) and diagnostic method. NREL/TP-472-6231. Golden, Colo.: National Renewable Energy Laboratory.
- Kalamees, T. 2004. IDA ICE: the simulation tool for making the whole building energy and HAM analysis. IEA Annex 41 1st working meeting. Zurich (Switzerland), 12-14 may 2004.
- Klein, S.A., Beckman, W.A., Mitchell, J.W., Duffie, J.A., Duffie, N.A., Freeman, T.L., Mitchell, J.C., Brau, J.E., Evans, B.L., Kummer, J.P., Urban, R.E., Fiksel, A., Thornton, J.W., Blair, N.J., Williams, P.M., Bradley, D.E., McDowell, T.P., Kummert, M. (2004). TRNSYS 16 – A TRaNsient System Simulation program, User manual. Solar Energy Laboratory. Madison: University of Wisconsin-Madison.
- Kalamees T. 2007. Influence of different ventilation strategies on indoor climate. Report A41-T1-EE-07-01
- Karagiozis, A. and L. Gu. 2004. The EMPD-model. Paper presented at IEA-Annex 41 working meeting in Glasgow, A41-T1-US-04-5.
- Koronthályová, O. 2006. Determination of moisture buffer ability of 1-zone space. In *Building Research Journal* 2006, vol 54, No.3-4, pp. 221 - 232
- Koronthályová, O. Mihálka, P. 2006. Calculation of heating energy consumption and resultant indoor climate in 1-zone object by integrated simulation model. In: *Budovy a prostredie*, ISBN 80-227-2518-8, STU, Bratislava 2006, pp. 79-82
- Koronthályová O Mihálka P Matiašovský P. 2004a. Model for complex simulation of HAM-transfer in a single thermal zone building. In: *Building Research Journal*, 2004, vol 52, no.4, pp. 199 – 217.

- Koronthalyova O., Mihalka P., Matiasovsky P. 2004b. Model for whole HAM-transfer simulation in room. IEA Annex 41 1st working meeting. Zurich (Switzerland), 12-14 may 2004. Annex 41 report A41-T1-SI-04-1
- Koronthályová, O. 1998. Non-steady Model for Calculation of Indoor Air Relative Humidity. Building Research Journal 46, pp. 201-211. (application of NPI only)
- Koronthalyova O. 2006. The coupled effect of hygroscopic materials and ventilation regime on indoor humidity. Report A41-T1-SI-06-1.
- Kropf, S., Zweifel, G. Validation of the Building Simulation Program IDA ICE According to CEN 13791 „Thermal Performance of Buildings - Calculation of Internal Temperatures of a Room in Summer Without Mechanical Cooling – General Criteria and Validation Procedures“. Hochschule Technik+Architektur Luzern. HLK Engineering
- Künzel, H. M. 1994. Simultaneous Heat and Moisture Transport in Building. Components. Dissertation. Stuttgart: University of Stuttgart, Download: [www.building-physics.com](http://www.building-physics.com)
- Kurnitski, J., T. Kalamees, J. Palonen<sup>1</sup>, L. Eskola, O. Seppänen 2006 Potential effects of permeable and hygroscopic lightweight structures on thermal comfort and perceived IAQ in a cold climate. Indoor Air 2007; 17: 37–49
- Kurnitski, J., Vuolle, M. 2000. Simultaneous calculation of heat, moisture, and air transport in a modular simulation environment; Proceedings of the Estonian Academy of Sciences Engineering, Vol. 6/1 March 2000, pp 25–47
- Kwiatkowski, J., Feret, K., Woloszyn, M., Predicting indoor relative humidity using building energy simulation tools. To be presented in IAQVEC conference, October 2007, Sendai, Japan
- Lane-Serff G.F., P.F. Linden and J.E. Simpson. *Transient flow through doorways produced by temperature differences*. in Proceedings of Roomvent'87. Session 2. Stockholm, Sweden. 10-12 June 1987.
- Lawrence Berkeley National Laboratory. 2007. COMIS Multi-zone Air Flow Model. Energy Performance of Buildings Group. <http://epb.lbl.gov/comis/> (January 15, 2007)
- Lengsfeld, K. 2006. Results of the complete Common Exercise 3. Presentation for IEA Annex 41 meeting, Kyoto, April 2006. A41-T1/D/06/01.pdf
- Lenz, K. & Holm, A. 2005. Annex 41 Subtask1. Common Exercise 3: Whole building heat and moisture analysis.
- Lomas, K.J. et al. 1997. Empirical Validation of Building Energy Simulation Programs. Energy and Buildings, vol 26, p 253-275.
- Mattsson, B. 2007, PhD thesis, Chalmers University of Technology, Sweden. The reference will be completed.
- McAdams W.H. Heat Transmission. New York: McGraw-Hill, 1954.
- Mendes, N. Philippi, P. C. 2005. A Method for Predicting Heat and Moisture Transfer through Multilayered Walls Based on Temperature and Moisture Content Gradients. International Journal of Heat and Mass Transfer, v. 48, p. 37-51, 2005.
- Mendes, N., Winkelmann, F.C., Lamberts, R. and Philippi, P.C. (2003a) "Moisture Effects on Conduction Loads". Energy and Buildings, 35(7): 631-644.
- Mendes, N., Oliveira, R.C.L.F. and Santos, G.H.dos. (2003b) "Domus 2.0: A Whole-Building Hygrothermal Simulation Program". Proceedings of the 8th International Building Performance Simulation Association (IBPSA), 1, Eindhoven – Netherlands.
- Mendes, N., Philippi, P.C. and Lamberts, R. (2002) "A New Mathematical Method to Solve Highly Coupled Equations of Heat and Mass Transfer in Porous Media". International Journal of Heat and Mass Transfer, 45: 509-518.
- Mendonça K.C., E. Wurtz, C. Inard, 2005, Predicting temperature and moisture distribution in conditioned spaces using the zonal approach, IBPSA Conference, Montréal, Canada, 763-768, 2005
- Mitamura, T. & Hasegawa, K. & Yoshino, H. & Mastumoto, S. & Takahashi, N. 2004. *Experiment for Moisture Buffering and Effects of Ventilation Rate, Volume Rate of the Hygrothermal Materials*. 5th International Conference of Indoor Air Quality, Ventilation and Energy Conservation, Toronto.

- Mora L., E. Wurtz, K.C. Mendonça, C. Inard, 2004. Effects of coupled heat and moisture transfers through walls upon indoor environment predictions, *International Journal of Ventilation* (3)3: 227 - 234,
- National Institute of Standards and Technology. 2007. CONTAM airflow and contaminant transport analysis software. Building and Fire Research Laboratory. <http://www.bfrl.nist.gov/IAQanalysis/CONTAM/index.htm> (January 15, 2007)
- Pedersen, C.R. Impact of Latent Heat Transfer on the Thermal Performance of Constructions Having Vapor Permeable Insulation. 2nd Nordic Symposium on Building Physics, Trondheim, August 1990.
- Perschke, A. 2000. Gebäude-Anlagen-Simulation unter Berücksichtigung der hygrischen Prozesse in den Gebäudewänden. Dissertation TU Dresden.
- Perschke, A., Meinhold, U.: Ein Modell zur hygrisch-thermischen Gebäudesimulation mit Hilfe der Kopplung von Zonen- und Feldmodell. *Bauphysik 1/2007* & Sohn Verlag, Berlin, ISBN 0171-5445, S. 55-62
- Plathner P. and M. Woloszyn. 2002. Interzonal air and moisture transport in a test house. Experiment and modelling. *Buildings and Environment*, vol. 37/2, 189-199.
- Ramos, N.M.M., de Freitas, V.P., Delgado, J.P.Q. 2005. Hygroscopic inertia of a room. Evaluation of finishing materials contribution. Paper presented at IEA-Annex 41 working meeting in Montreal, A41-T2-P-05-2.
- Ridley, I. Fox J, Oreszczyn, T. Controllable Background Ventilation in Dwellings – The Equivalent Opening Area Needed to achieve Appropriate Indoor Air Quality. *International Journal of Ventilation*, Volume 3 No 2, Sep 2004 pp 147-154. ISSN 1473-3315. Veetech Ltd
- Rode, C. & K. Grau. 2003. Whole Building Hygrothermal Simulation Model. ASHRAE Transactions, V. 109, Pt. 1. Atlanta, GA: American Society of Heating, Refrigerating and Air-Conditioning Engineers. pp. 572-582. 2003.
- Rode C., Grau K. 2004b. Calculation Tool for Whole Building Hygrothermal Analysis Building Simulation 2000. IEA Annex 41 1st working meeting. Zurich (Switzerland), 12-14 may 2004.
- Rode, C. 2004 "Whole-Building Hygrothermal Analysis" in: *Simulationenmethoden bei der Planung von Neubauten und Instandsetzungen*. WTA-Schriftenreihe, Heft 24, pp. 63-80. WTA-Publications, München. 2004.
- Rode, C., Peuhkuri, R., Hansen, K.K., Time, B., Svennberg, K., Arfvidsson, J. and Ojanen, T. 2005. Moisture buffer value of materials in buildings. In *Proceedings of the 7th Symposium on Building Physics in the Nordic Countries*, June 13-15 2005. Reykjavik Iceland, Vol. 1, pp. 108-115.
- Rode, C. and Peuhkuri, R. 2006 Modelling the Hygrothermal Interaction Between Materials and the Indoor Climate. Paper for WTA Kolloquium "Bauinstandsetzen + Bauphysik III". WTA Wissenschaftlich-Technische Arbeitsgemeinschaft für e.V. Bauwerkserhaltung und Denkmalpflege, HAWK Hildesheim Germany. March 10, 2006.
- Roels, S. and H. Janssen. 2005. Is the moisture buffer value a reliable material property to characterize the hygric buffering capacities of building materials? Paper presented at IEA-Annex 41 working meeting in Trondheim, A41-T2-B-05-7.
- Sahlin P., L. Eriksson, P. Grozman, H. Johnsson, A. Shapovalov and M. Vuolle 2004 Whole-building simulation with symbolic DAE equations and general purpose solvers. *Building and Environment*. Volume 39, Issue 8, Pages 949-958.
- Sahlin, P., 1996. Modelling and Simulation Methods for Modular Continuous Systems in Buildings. Doctoral Dissertation KTH Stockholm Sweden.
- Santos, G.H.; Mendes, N. . Simultaneous Heat and Moisture Transfer in Soils Combined with Building Simulation. *Energy and Buildings*, USA, v. 8, n. 4, p. 303-314, 2006.
- Sasic Kalagasidis, A. 2007a. Hygrothermal response of a house with dynamical insulation in the roof. Case study: Test house from CE 1B, IEA Annex 41. IEA Annex 41 working meeting, Florianopolis, 2007.
- Sasic Kalagasidis, A.. 2007b. Simulations as the way of bridging the gaps between desired and actual hygrothermal performance of buildings. 10th International Building Performance Simulation Association (IBPSA) Conference. Beijing, China, September 2007.

Sasic Kalagasidis, A., Karlsson, H., Hagentoft, C-E. 2005. A simulation tool for temperature and moisture dependent transport of VOC's in buildings. Proceedings of the 7th Symposium on Building Physics in the Nordic Countries, Reykjavik, Island, June 2005.

Sasic Kalagasidis, A. 2004a. The whole model validation for HAM-Tools. Case study: hygro-thermal conditions in the cold attic under different ventilation regimes. The 9th International Conference on Performance of the Exterior Envelopes of Whole Buildings. Clearwater Beach, Florida.

Sasic Kalagasidis A 2004b. HAM-Tools. An Integrated Simulation Tool for Heat, Air and Moisture Transfer Analyses in Building Physics. Doctoral thesis. Chalmers University of Technology, Gothenburg, Sweden

Schijndel, A.W.M. van, 2007. Integrated Heat Air & Moisture Modeling and Simulation, PhD thesis, Eindhoven University of Technology, ISBN 978-90-6814-604-2

Schijndel A.W.M. 2005. van Integrated heat, air and moisture modeling and simulation in HAMLAB. IEA Annex 41 working meeting, Montreal, May 2005.

Schijndel A.W.M. van, Wit M.H., de 1999. A Building Physics Toolbox in MATLAB, 5<sup>th</sup> Building Physics in the Nordic Countries Conference, Goteborg, August 24-26, 1999, pp. 81-88

Sedlbauer, K.: *Prediction of mould fungus formation on the surface of and inside building components*. Dissertation. University of Stuttgart 2001, Download: [www.buildingphysics.com](http://www.buildingphysics.com).

Skelboe S. and P. Stangerup. *A minicomputer based network analysis program*. In Proc. Africorn '83, IEEE-Region 8: E2.3.1-E.2.3.5. Nairobi, Kenya. 1983.

Solar Energy Laboratory. *TRNSYS a Transient System Simulation Program*. University of Wisconsin-Madison. 1994.

Steehan H.J., A. Janssens & M. De Paepe. 2005. How accurate are traditional models for air moisture transport in rooms: a comparison of CFD and lumped models. IEA Annex 41 working meeting, Montreal, May 2005.

Steehan. M. 2007. Report from Subtask 1: Common Exercise 4: `Moisture management` University of Ghent participation using TRNSYS.

Stovall, T. K., Karagiozis, A., "Airflow in the Ventilation Space Behind a Rain Screen Wall," Performance of Exterior Envelopes of Whole Buildings IX International Conference, ASHRAE, December, 2004

Voit, P., Th. Lechner, M. Schuler, 1994. "Common EC validation procedure for dynamic simulation programs – application with TRNSYS", TRANSSOLAR GmbH, Conference of international simulation societies 94, Zürich.

Tariku, F.; Kumaran, M.K.; Fazio, P. 2006. Whole building heat and moisture analysis. IEA Annex 41 working meeting, Lyon (France), 25-27 October 2006. 18 p.

Versteeg H.K., Malalasekera W., 1995. An introduction to computational fluid dynamics, the finite volume method. John Wiley & Sons Inc., New York.

Walton, G.N. *A computer algorithm for predicting infiltration and inter-room airflows*. ASHRAE Transactions. Vol 95, part 2. pp 611-620. 1984.

Wit, M.H. de, 2006. Hambase, Heat, Air and Moisture Model for Building and Systems Evaluation, Eindhoven University of Technology, ISBN 90-6814-601-7

Wit M.H. de 2004. WAVO, A model for the simulation of thermal and hygric performance of building and systems. <http://sts.bwk.tue.nl/hamlab/>

Witte, M.J., Henninger, R.H., Crawley, D.B., 2004. Experience Testing EnergyPlus with the ASHRAE 1052-RP Building Fabric Analytical Tests, in *Proceedings of the SimBuild 2004 Conference*, 4-6 August 2004, Boulder, Colorado. IBPSA-USA

Woloszyn, M., J. Shen, A. Mordelet, J. Brau. 2005. Numerical simulations of energy performance of a ventilation system controlled by relative humidity. In proceedings of 26th AIVC Conference; Bruxelles (Belgique), 21-23 September 2005. 295-300.

Woloszyn, M. G. Rusaouen, D. Covalet. 2004. Whole building simulation tools: Clim2000. IEA Annexe 41 working meeting, Zurich (Switzerland), 13-15 May 2004. 15 p.

Woloszyn, M., G. Rusaouën, G. Fraisse, J-L. Hubert. 2000. Predicting indoor climate using electric analogy. Estimations of condensation potential. Proceedings of Healthy Building. Espoo (Finland) : SIY Indoor Air Information Oy, vol 3, p 165-170.

- Wilson D. J. and Kiel D. E. *Gravity driven Counterflow Through an Open Door in a Sealed Room*. Buildings and Environment. Vol 25, n°4 pp. 379-388 . 1990.
- Woloszyn, M., J. Shen, A. Mordelet and J. Brau. 2005. Numerical simulations of energy performance of a ventilation system controlled by relative humidity. Paper presented at IEA-Annex 41 working meeting in Trondheim, A41-T1-F-05-1.
- Wurtz E., F. Haghighat, L. Mora, K.C. Mendonca, C. Maalouf, H.Zhao, P. Bourdoukan, 2006. An integrated zonal model to predict transient indoor humidity distribution, ASHRAE Transactions (112)2: 175-186, 2006
- Wurtz E., C. Maalouf, L. Mora, F. Allard, 2005, Parametric analysis of a solar assisted desiccant cooling system using the SimSPARK environment, In proceedings of Building Simulation 2005, Montréal, Canada, 1369-1376.
- Zhai, Z. (2006). Applications of Computational Fluid Dynamics in Building Design: Aspects and Trends. Indoor and Built Environment 15(4): 305-313.

## Addenda – digital edition

- List of free papers
- Documentation of CEs
- Documentation of models
- Some points from the participants' "motivations"